Master's thesis

NTNU
Norwegian University of Science and Technology
Faculty of Natural Sciences
Department of Chemistry

Thomas Walmsley

Studies of environmental footprint in Brøggerdalen after rocket launching in Ny-Ålesund

Master's thesis in MSENVITOX
Supervisor: Øyvind Mikkelsen
August 2022

NTNU
Norwegian University of
Science and Technology

Thomas Walmsley

Studies of environmental footprint in Brøggerdalen after rocket launching in Ny-Ålesund

Master's thesis in MSENVITOX
Supervisor: Øyvind Mikkelsen
August 2022

Norwegian University of Science and Technology
Faculty of Natural Sciences
Department of Chemistry

NTNU
Norwegian University of
Science and Technology

Abstract

In this master thesis levels of selected trace metals and polychlorinated biphenyls (PCBs) were determined in sediment samples from Brøggerdalen, Ny-Ålesund, Svalbard. Sampling was conducted in August 2021. The aim of this thesis was to identify possible pollution in connection with recent rocket activity in the area. The selected trace elements were cadmium (Cd), iron (Fe), lead (Pb), arsenic (As), aluminium (Al), titanium (Ti), lithium (Li), copper (Cu), zinc (Zn), tin (Sn), cobalt (Co), magnesium (Mg) and beryllium (Be), and the selected PCBs were PCB-28, PCB-52, PCB-101, PCB-118, PCB-138, PCB-153 and PCB-180. For trace element analysis the samples were freeze-dried, treated with microwave-assisted acid digestion and analysed in inductively coupled plasma-mass spectrometry (ICP-MS), and for PCB analysis the samples were air-dried, extracted with accelerated solvent extraction (ASE), concentrated, and analysed with gas chromatography-mass spectrometry (GC-MS).

The samples connected to booster impact area A (78°54.59' N 11°49.41 E) showed significantly higher levels of Fe, Pb, As, Li, Zn and Co, while the samples connected to booster impact area B (78°55.33' N 11°49.43' E) showed significantly higher levels of Cd, Sn and Mg. The levels of Fe and Li can be connected to the crustal composition, the levels of As, Fe, Pb, Zn and Co can be connected to the vicinity of old mining sites, the levels of Mg can be connected to the sedimentary rocks, and the levels of Cd and Sn can be connected to trace element contamination in birds. Two samples, 20 and 23, showed elevated levels of Cu (437.9 μg/g), Zn (229.0 μg/g) and Sn (0.9280 μg/g), and Cd (123.4 μg/g) respectively. These outliers can be connected to metal fragments, and there was no indication of these elevated levels in other, nearby samples. PCA shows that the crustal composition contributes to PC1, the geological difference between Vestre and Austre Brøggerdalen and vicinity to old coal mines contribute to PC2 and the outlier, sample 20, contributes to PC3 for 47%, 13% and 10% of the variance respectively.

None of the PCBs were detected above the limit of detection.

Sammendrag

I denne masteroppgåva blei nivå av eit utval sporelement og polyklorerte bifenyl (PCB) målt i sedimentprøver frå Brøggerdalen, Ny-Ålesund, Svalbard. Prøvetaking vart gjennomført i august 2021. Målet med denne oppgåva var å identifisera mogleg forureining i forbindelse med nyleg rakettaktivitet i området. Dei utvalde sporelementa var kadmium (Cd), jern (Fe), bly (Pb), arsenikk (As), aluminium (Al), titan (Ti), litium (Li), kopar (Cu), sink (Zn), tinn (Sn), kobalt (Co), magnesium (Mg) og beryllium (Be), og dei utvalde PCB var PCB-28, PCB-52, PCB-101, PCB-118, PCB-138, PCB-153 og PCB-180. For sporelementanalyse vart prøvane frysetørka, behandla med mikrobølgeassistert syrefordøying og analysert med induktivt koblet plasmamassespektrometri (ICP-MS), og for PCB-analyse vart prøvane lufttørka, ekstrahert med akselert løysingsekstraksjon (ASE), konsentrert, og analysert med gasskromatografi-massespektrometri (GC-MS).

Prøvane forbundne med boosterlandingssona A (78°54.59' N 11°49.41 E) viste signifikant høgare nivå av Fe, Pb, As, Li, Zn og Co, medan prøvane forbundne med boosterlandingssona B (78°55.33' N 11°49.43' E) viste signifikant høgare nivå av Cd, Sn og Mg. Nivåa av Fe og Li kan vera knytta til jordskorpekomposisjonen, nivåa av As, Fe, Pb, Zn og Co kan vera knytta til nærleik til gamle gruveområde, nivåa av Mg kan vera knytta til sedimentære bergartar, og nivåa av Cd og Sn kan vera knytta til sporelementforureining i fuglar. To prøvar, 20 og 23, viste forhøgde nivå av Cu (437.9 μg/g), Zn (229.0 μg/g) og Sn (0.9280 μg/g), og Cd (123.4 μg/g) respektivt. Desse ser ut til å vera knytta til metallfragment og det var ingen indikasjon på forhøgde nivå i andre, nærliggande prøver. PCA viser at jordskorpekomposisjonen bidreg til PC1, geologiske forskjeller mellom Vestre og Austre Brøggerdalen og nærleik til gamle kullgruver bidreg til PC2 og prøve 20 bidreg til PC3 for 47%, 13% and 10% av den totale variansen respektivt.

Ingen PCB blei målt over deteksjonsgrensa.

Acknowledgements

I would like to extend a massive thank you to my supervisor Øyvind Mikkelsen for his guidance throughout this thesis work. Thank you to Kyyas Seyitmuhammedov and Anica Simic for help with UltraCLAVE and for the ICP-MS analysis and to Susana Villa Gonzalez for the GC-MS analysis.

Thank you to Forskningsrådet for providing financial support through the Arctic Field Grant, and thank you to the Norwegian Polar Institute for accomodation in Ny-Ålesund.

Thank you to my friends and family for their support. Thank you to my classmates for valuable discussions and long evenings. I would like to thank every fellow student who I've had the pleasure of meeting during my years at NTNU. A special thank you goes to Volvox & Alkymisten, Studentorchesteret Dei Taktlause and Lyche. Lastly, I would like to give a heartfelt thank you to Hovmestermafiaen.

Contents

List of Figures

List of Tables

1 Introduction

The Arctic region is viewed as a pristine, remote environment, although it in reality is a highly sensitive ecosystem affected by global pollution. The polluting compounds have both local and global sources, and the pathways of these compounds within and to the Arctic region mainly occur in the atmospheric, terrestrial/freshwater, and marine compartments [1]. Compounds of particular concern in the Arctic include trace elements and persistent organic pollutants (POPs) like polychlorinated biphenyls (PCBs) [1]. PCBs and the other POPs are a particular risk for the Arctic region and the indigenous communities due to biomagnification and contamination of their traditional foods [2, 3]. PCBs have historically been applied in protective coatings, coolant or dielectric for transformers and capacitors, heat transfer fluids, and fire retardants. [4, 5, 6, 7]. Production and new use of PCBs have been banned by all members of the Stockholm Convention, and existing products containing PCBs can be used until 2025 [2]. Trace elements occur at varying concentrations depending on the local geology, and are also connected to anthropogenic sources at local and global levels. Some large anthropogenic sources include fossil fuel combustion, non-ferrous metal production, and waste incineration [8]. Both POPs and trace elements can be transported to the Arctic through long-range transportation [1, 9, 10].

Commercial space flight is becoming increasingly available, and with follows an increased number of space launches. The environmental impact of space flight activity occur in several phases, from launch to the impact of rocket debris with the ground below [11, 12]. The Grand Challenge Initiative (GCI) is an international collaboration which aims to advance specific, fundamental issues in space and Earth science [13]. In 2019-2021 American, Japanese and Norwegian universities and space agencies worked on the CGI Cusp project. The aim of this project was to advance the understanding of the cusp region space physics through use of ground based instruments, modeling, sounding rocket investigations, and satellite based instruments [14]. In all 9 missions were planned, where 4 of these were conducted in Ny-Ålesund, Svalbard, namely VISIONS-2 (December 2018), ICI-5 (November/December 2019), CHI (November-December 2019), and JAXA-SS-520-3 (4th November 2021) [14]. A sampling campaign was conducted to monitor the area were the launches were conducted. One sample found elevated cadmium and

PCB-138 levels, with a possible cause of contamination being booster rocket debris [15].

2 Background

2.1 Arctic environment

The arctic region is often defined as the area north of the Arctic Circle at 66°32'N, which is also the Southern border of the midnight sun [1]. There are however other definitions which take into account physical, geographical and/or ecological characteristics. One of these definitions is the the area north of the 10°C July isotherm which is where the mean July temperature is 10°C. Another definition is north of the treeline which is the northern limit of where trees can grow. And a third definition is the boundary of cool, less saline surface water from the Arctic Ocean and warmer, saltier waters from more southern oceans. Typical for the polar areas are low air temperatures, less than 500 mm of annual precipitation, foggy conditions, winds and open terrains [1].

2.2 Bayelva

Bayelva is a river located around 79°N, 12°E outside of Ny-Ålesund, Svalbard as shown in figure 2.1. The Bayelva drainage basin contains Austre and Vestre Brøggerbreen.

Figure 2.1: Map of the Bayleva in relation to Ny-Ålesund. Map courtesy of the Norwegian Polar Institute [16].

The Bayelva basin is heterogeneous, the bedrock of Bayelva is sedimentary and consists of limestone, shale, and sandstone. The areas around contain minerals such as quartz, mica, chlorite, talc, feldspar, garnet, kyanite, staurolite, amphibole, kaolin, montmorillonite, illite, and coal and sedimentary rocks like limestones, dolostones, phyllites, quartzite, schist, conglomerate, and shales [17, 18, 19]. The chemical composition of these minerals and sedimentary rocks is shown in table 2.1.

2.3 Overbank sediment

Rivers are flowing waters gathered in complex systems called drainage basins [23]. Drainage basins are areas surrounded by a continuous topographic divide in which runoffs combine to a single stream and which then continues downstream until the divide is crossed [24]. Sediments are fine-grained materials from different local sources like erosion, weathering and deposition of minerals and rocks, consisting of river borne clay, silt, sand, organic material and a mixture of other materials [25]. Overbank sediments are sediments that are deposited on the floodplain surface during flooding of a river [26, 27]. The bank of a river is determined by Nunnally to start at the point where the inundation of floodplains first occur [26]. During a flowing river, coarse gravel is deposited in the stream channel, natural levees are formed by sand and fine gravel along banks, while silt and clay are deposited on

Table 2.1: Chemical composition of a selection of minerals and sedimentary rock found in Brøggerdalen.

Name	Chemical composition
Amphibole	$(Mg,Fe,Ca,Na)_{2-3}(Mg,Fe,Al)_5(Si,Al)_8O_{22}OH_2$[20]
Chlorite	$M_{4-6}T_4O_{10}(OH,O)_8$ where M = Al, Fe^{3+}, Fe^{2+}, Li, Mn^{2+}, Cr, Ni and Zn, and T = Si, Al, Fe^{3+}, Be and B [20]
Coal	C, O and H, N, S (Anthracite and bituminous coal) [20]
Feldspar	$NaAlSi_3O_8$, $KAlSi_3O_8$, and $CaAl_2Si_2O_8$ [20]
Garnet	$Ca_3Al_2(SiO_4)_3$ [20]
Illite	$K_{0.65}Al_2(OH)_2Al_{0.65}Si_{3.35}O_{10}$ [20]
Kaolin	$Al_4Si_4O_{10}(OH)_8$ [20]
Kyanite	Al_2SiO_5 [20]
Mica	$I_2M_{4-6}\ \square_{2-0}T_8O_{20}A_4$, where I = mainly K or Na, can also be Cs NH_4, Rb, Ca, Ba and other cations; M = Mg, Fe^{2+}, Fe^{3+}, Al, Li, but also Ti, Mn, Zn, Cr, V and other cations; $\square$ = vacant site; T = mainly Si or Al, can also be Fe^{3+}; A = mainly OH, F, but also Cl, O, S [21]
Montmorillonite	$(Na,\ Ca)_{0.3}(Al,\ Mg)_2Si_4O_{10}(OH)_2 \cdot nH_2O$ [22]
Quartz	SiO_2 [20]
Staurolite	$Fe_2Al_9O_7(OH)(SiO_4)_4$ [20]
Talc	$3MgO,\ 4SiO_2H_2O$ [20]
Argillite	Lithified mud and oozes [20]
Conglomerate	Clasts of preexisting rocks and minerals within fine-grained matrix [20]
Dolostone	Predominantly dolomite (calciumemagnesium carbonate) $\pm$ silica
Limestone	Mainly calcite and aragonite, skeletal fragments of marine organism (coral and foraminifera), and silica (chert and flint) [20]
Phyllite	Quartz, sericite, mica, and chlorite [20]
Quartzite	Monomineralic and dominantly of quartz [20]
Schist	Micas, chlorite, talc, quartz, feldspar, garnet, kyanite, staurolite [20]

the floodplain [24]. Sediments transported along a river will be deposited during flooding onto floodplains and levees, thus overbank deposits will consist of nearly horizontal strata of sediments, in which the upper layers will be younger than the layers further down [28, 29]. These sediments have a widespread origin, and by sampling layers of strata a great variety of sources from different times can be analysed [28].

Common contaminants in rivers, and thus, sediments, include organic contaminants like pathogens, PAHs and PCBs, and inorganic contaminants like trace elements and radioactive isotopes. These contaminants come from a variety of sources including agricultural cropland, mine sites, atmospheric deposition and industrial and municipal discharges. Chemical contaminants in the river occur primarily as either dissolved or attached to suspended sediment in the water column, and dissolved contaminants are thought to be more bioavailable and thus pose a larger risk to human and ecosystem health [30]. Sediments are considered sinks for reactive, hydrophobic contaminants like trace elements and through properties like size, abundance crystallinity and mineralogy sediments can affect the concentration of aqueous species in surface waters. The grain-size, shape, specific gravity and surface area are some of the dimensions that differ between various sediments, and both the chemical and physical composition reflect the underlying geology of the drainage basin. Of these properties, a general trend of increase in surface area and enhancement of trace element concentration can be found, and finer-grained sediments have larger surface area per mass and thus a decrease in grain-size also shows an increase in trace element concentration. Trace elements dissolved can accumulate on particle surfaces through precipitation, ion exchange and adsorption [31].

Sediments are composed of a variety of materials and the composition depends on the underlying geographical units, weathering and transport processes. The main components of sand-sized and coarser particles are quartz, feldspars and carbonates, which are all inert. The less abundant materials are thus the materials that provide trace element accumulating capacity. These less abundant materials include clay minerals, organic materials, organically coated materials, and Fe and Mn oxides and hydroxides. Their reactivity stems from a high surface charge distributed over a large surface area, as well as high cation exchange properties.

Fifield & Haines define speciation as "the different forms of an element which together comprise its total concentration in a given sample" [25]. These different forms will have different chemical properties which will affect its interaction with mediums, its bioavailability, and its toxicity. The speciation of trace elements will depend on the environment in which it is located. Trace elements can occur in ion pairs or complexes, also called inner- and outer-sphere complexes. These complexes form with an ion of opposite charge in the case of ion pairs, or with covalent bonds between a metal ion and an electron-donating ligand. Metal ions can form inner- and outer-sphere complexes with both inorganic ligands like OH^-, HCO_3^-, and NH_3, and organic ligands like glycine and oxalic acid [32, 31, 33]. All metal ions in water form aquo complexes and exchange reactions occur where ligands are substituted for the water molecules. For divalent metal ions and monodentate ligands, the formation of complexes can be expressed by equation 2.1 as follows:

$$M^{2+} + nL^- \rightleftharpoons ML^{(2-n)+} \tag{2.1}$$

where M is the metal ion, L is the ligand and n is the number of ligands. For precipitation to occur the solubility product, K_S of the reaction must be exceeded. The reaction of a divalent metal ion and a divalent ligand to give a solid phase, can be expressed as equation 2.2:

$$M^{2+} + L^{2-} \rightleftharpoons ML \tag{2.2}$$

and K_S can be expressed as equation 2.3,

$$[M^{2+}][L^{2-}] = K_S \tag{2.3}$$

where $[M^{2+}]$ and $[L^{2-}]$ are the concentrations of M^{2+} and L^{2-}.

Ion exchange is a process of exchanging ions between a liquid and a solid phase [34]. Ion exchange occurs when a cation is exchanged for another on a surface with constant charge. Pure ion exchange or adsorption seldom occur in nature, as it normally occurs as a mix of the two [34]. Adsorption is a process of transferring components from a liquid phase to the surface of a solid phase and creates a concentration difference of a solute between the surface and bulk phase [34, 35]. Sorption of heavy metal ions is increased by the presence of organic particles and finer mineral grains [36]. Clay minerals are important natural ion exchange materials and are generally coated in metal

oxides and organic matter which have surface characteristics important for ion exchange. The adsorption on the surface depends on pH due to the surface chemistry. OH-groups cover the surface of metal and metalloid hydrous oxides, and proton transfers on this surface result in amphoteric properties as shown in equations 2.4 and 2.5:

$$\equiv S - OH_2^+ \rightleftharpoons \equiv S - OH + H^+ \tag{2.4}$$

$$\equiv S - OH \rightleftharpoons \equiv S - O^- + H^+ \tag{2.5}$$

A reaction between this kind of surface and a divalent metal ion can be represented by equation 2.6:

$$\equiv S - OH + M^{2+} \rightleftharpoons \equiv S - OM^+ + H^+ \tag{2.6}$$

Reactions between the surface of metal and metalloid hydrous oxides and protons and metal ions are similar in humic and other organic matter on particle surfaces [31, 37].

Of the 118 elements, 90 are naturally occuring on earth [25]. There are several different ways of grouping the elements. One way of doing this in biological systems is by grouping them into three categories, the major elements (C, H, N and O), the minor elements (Ca, Cl, Mg, P, K and Na), and the remainders are grouped together as trace elements [25]. The trace elements can be subdivided into essential, non-essential and toxic. The essential elements are those that cannot be substituted by others in their biochemical roles which influence the organism. The non-essential elements are elements found in tissues and fluids, but are not proven to be essential and can be toxic at high levels. Toxic elements are so classed because they are toxic even at low levels [25]. There are several different sources of trace elements found in nature, some anthropogenic and some natural. The primordial source of trace elements is the earth's crust as various rocks are subjected to different chemical and geological processes [25]. Weathering occurs both as a mechanical and chemical process. The weathering process is slow, continuous and affects all substances exposed to the atmosphere [38]. Examples of mechanical weathering include temperature changes, freeze-thaw processes and root growth [38, 39]. Chemical weathering includes ionic dissociation, water and carbon dioxide addition, hydrolysis and oxidation [39]. An example of this

is the calcium carbonate ($CaCO_3$), which is also called limestone, and its equilibrium represented in equations 2.7 through 2.12 [39].

In a strong acid $CaCO_3$ dissolves as shown in equation 2.7:

$$CaCO_3 + 2H^+ \longrightarrow Ca^{2+} + H_2O + CO_2 \tag{2.7}$$

In a weak acid however, the dissolution is represented through equation 2.8:

$$CaCO_3 + H^+ \longrightarrow Ca^{2+} + HCO_3^- \tag{2.8}$$

In a basic environment the process can be reversed as represented in equation 2.9:

$$Ca^{2+} + HCO_3^- + OH^- \longrightarrow CaCO_3 + H_2O \tag{2.9}$$

In nature the acids involved are usually weak, and an example of the overall process of limestone dissolved with carbonic acid (H_2CO_3) can be represented as in equation 2.10:

$$CaCO_3 + H_2CO_3 \rightleftharpoons Ca^{2+} + 2HCO_3^- \tag{2.10}$$

The concentration of H_2CO_3 is dependent on the pressure of CO_2 above the solution as represented in equation 2.11

$$H_2CO_3 \rightleftharpoons H_2O + CO_2 \tag{2.11}$$

As shown in the equations 2.7 through 2.11, this reaction is both dependent on the CO_2 pressure and pH. In addition, these reactions are also temperature-dependent as the solubility of $CaCO_3$, as opposed to most salts, decreases with a temperature increase due to the solubility of CO_2 decreasing at higher temperatures. Precipitation of $CaCO_3$ can be caused by green plants removing CO_2 from the water through photosynthesis. Through hydrolysis $CaCO_3$ can be somewhat soluble in water without CO_2 as represented in equation 2.12:

$$CaCO_3 + H_2O \rightleftharpoons Ca^{2+} + HCO_3^- + OH^- \tag{2.12}$$

Through activities such as rivers, volcanic activity and forest fires trace elements are transported globally [25]. Plants can bioaccumulate trace elements which also leads trace metals into the food chain of animals and humans. Anthropogenic sources such as mining, industrial processing, agriculture, and

transport lead to increased levels of trace metals[25, 8]. In the earth's crust these are found as simple salts, cationic constituents in aluminosilicates, insoluble carbonate or sulphates, oxides, or sulphides [25]. In waters, on the other hand, trace elements are mainly present as suspended colloids or fixed by organic and mineral substances, as shown in table 2.2.

Table 2.2: Species of Pb in fresh water [32].

Size	State	Speciation	Examples
< 5 nm	Dissolved	Free metal ion	Pb^{2+}
		Ion pair	$PbHCO_3$
		Organic complex	Pb^{2+}/EDTA
	Suspended	Natural acid complex	Pb^{2+}/fulvic acid
< 100 μm	Colloids	Ions adsorbed on colloids	$Pb^{2+}/Fe(OH)_3$
> 100 μm	Solid particles	Metal in dispersed organic material	Pb in organic soil
		Ions in particles	Pb^{2+} bound in clay, $PbCO_3$

In sediments, the main trace elements are Cd, Co, Cr, Cu, Fe, Mn, Mo, Ni, and Pb. Most of these occur as sorbed on to clays and Mn(IV) or Fe(III) hydrous oxides, or low soluble organic complexes [25]. Conditions that can affect the speciation of trace elements in sediments include bacteria in the top sediment-water interaction, pH, redox conditions, and other ligands. Trace elements occur within all components of the environment, and pollution refers to levels of trace elements above the natural occurrence of these [25]. Pollution in different environments occurs in different forms and thus carry with them different problems.

Air pollutants are generally related to gaseous emissions, and trace element contamination occurs through atmospheric particles and particulates. Maximum air pollution normally occurs within kilometres of the emission source, although small particulate and aerosol pollutants can be transported to all areas of earth [25].

Trace elements from fossil fuels, ores and industrial products can evaporate, partially or completely, through incineration, high-temperature production of

goods and fossil fuel combustion, thus being released with exhaust gases [40]. The volatility of trace elements can be used to roughly divide the trace elements into three groups, where group three consists of the most volatile trace elements. Group one consists of elements like Mn, Ba, Ce and Cs, group two consists of elements like As, Cd, Cu, Pb and Zn, while group three consists of elements like Hg, F and Cl [41] [42]. When volatilised, the trace elements can undergo long-range atmospheric transport through the "grasshopper" effect, where the compounds undergo a complete deposition/volatilisation cycle [9, 10]. Metal particulates can play a role in oxidation of sulphur dioxide to form acidic aerosols which are a component in acid rain. Metal ions, such as Fe(II), Cu(II) and Pb(II), catalyse the reaction represented by equation 2.13:

$$2SO_2 + 2H_2O + O \longrightarrow 2H_2SO_4 \tag{2.13}$$

Trace elements like Fe, V, Ca, Pb, Br and Cl also contribute to the formation of photochemical smog [25].

In aquatic environments anthropogenic trace element contamination occurs primarily through industrial processes. Depending on the magnitude and duration of input, as well as the chemical and physical form of the trace elements, the impact in extent and toxicity will vary. Through bioaccumulation input into the aquatic environment can cause problems for humans and animals. In sediments, increased industry and agriculture as well as long-range transport and interactions in the water-sediment interface are the main sources of trace element pollution. These trace elements normally accumulate in the upper layers of the soil profile due to the soil organic horizon which is rich in humic substances and organic acids which have high affinity to elemental ions. Many trace elements are considered necessary for plants, animals and humans, but at excessive levels they can be directly related to diseases and toxic responses, while others are known to be toxic, even in small quantities. The toxicity of trace elements depends on magnitude, chemical form and the "cocktail effect". The "cocktail effect" describes the effect of interelement interactions where the combination of chemicals can lead to more severe consequences than the exposure of a trace element by itself [25].

2.4 PCBs

Polychlorinated biphenyls (PCBs) are, as the name suggests, biphenyl ring systems with one to ten Cl attached to it. The general structure of PCBs are given in figure 2.2.

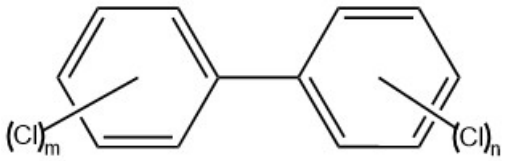

Figure 2.2: The general structure of PCBs, where m and n are integers between 1 and 5.

There exist 209 discrete chemical compounds in the class of PCBs, called congeners, which are known to have general stability and inertness, as well as having excellent dielectric properties [5, 7]. A common way of grouping PCBs is grouping PCB-28, -52, -101, -118, -138, -153 and -180 together as seven indicator PCBs [7, 43]. PCBs have been used in many ways including as protective coatings, coolant or dielectric for transformers and capacitors, heat transfer fluids, and fire retardants. [4, 5, 6, 7]. Leakage from equipment containing PCBs and PCB-manufacture are two main sources of PCB pollution [6]. To determine the environmental fate of chemicals the bioconcentration factor, K_B can be utilised, which is represented by equation 2.14:

$$K_B = \frac{C_B}{C_M} \tag{2.14}$$

where C_B is the biotic concentration and C_M is the medium concentration. With water as the medium, the octanol-water partition coefficient, K_{OW}, can be used as a correlating quantity, expressed through equation 2.15:

$$K_{OW} = \frac{C_O}{C_M} \tag{2.15}$$

where C_O is the octanol concentration. Thus, K_B and K_{OW} correlate well [44]. Similarly, the water-to-air partitioning can be represented in equation 2.16 as:

$$K_{AW} = \frac{C_A}{C_M} \tag{2.16}$$

where C_A is the air concentration, and thus the octanol-to-air partition can be represented as K_OA as represented in equation 2.17:

$$K_{OA} = \frac{K_{OW}}{K_{AW}} \tag{2.17}$$

to indicate susceptibility of a chemical to global fractionation [45]. PCBs have high log K_{OA} [45] and log K_{OW} [7] which indicate hydrophobicity and lower volatilisation. The log K_{OW} and log K_{OA} for common PCBs are given in table 2.3. Due to high lipophility, PCBs are commonly found in soils, however, they can also be found atmospherically transported due to volatilisation from sources like spills, road oils, and land fills [46, 10]. Due to the lipid solubility and resistance to degradation PCBs accumulate in the food chain and thus humans are exposed [47, 5].

Table 2.3: Table of common PCBs, their log K_{OW}s, and log K_{OA}s. The values of log K_{OW} and log K_{OA} are given for 25°C [48].

PCB	$LogK_{OW}$	$LogK_{OA}$
PCB-28	5.66	7.85
PCB-52	5.91	8.22
PCB-101	6.33	8.73
PCB-118	6.69	9.36
PCB-138	7.22	9.66
PCB-153	6.87	9.44
PCB-180	7.16	10.16

PCBs can cause yellow atrophy of liver, dermatitis and fatty degeneration of the liver in humans, and has also been linked with various toxicological responses like effects on egg-hatching ability in aquatic species. It can also cause liver change, altered reproduction cycles, reduced growth, and hepatocellular carcinoma in terrestrial species [5, 7, 6].

2.5 Rocket engines

There are two main propulsion systems in rockets, solid rocket motors (SRMs) and liquid rocket engines (LREs) [11]. In SRMs the most common propel-

lant is solid aluminium fuel with ammonium perchlorate (NH_4ClO_4) as an oxidiser, some modern SRMs will also contain hydroxyl-terminated polybutandiene (HTPD). LREs, on the other hand, primarily use three different liquid fuel combinations as propellants. The first of these uses kerosene (RP-1) as fuel and liquid oxygen as the oxidiser, the second uses liquid hydrogen as fuel and liquid oxygen as the oxidiser, and the third uses unsymmetrical dimethylhydrazine (UDMH) as fuel and dinitrogen tetroxide as the oxidiser.

These propellants have different advantages and disadvantages in terms of practical use and environmental impact. In terms of environmental impact the exhaust of the SRM propellant contains hydrochloric acid (HCl) and alumina (Al_2O_3) which has known damaging properties in local environments [49]. The environmental impact of the first LRE propellant, RP-1 with liquid oxygen, occurs mostly in the form of CO_2 and soot particles. For the second LRE propellant, liquid hydrogen and liquid oxygen, the exhaust consists mainly of water vapour, so the environmental impact is low. In the case of the third propellant, UDMH with liquid oxygen, it consists of nitric acid, which is highly corrosive, and UDMH, which is highly toxic, and is therefore sometimes referred to as the "Devil's Venom". In addition to this impact, nitrous oxide is formed during combustion of any propellant [11].

SRMs and LREs with RP-1 and UDMH are typically used in the first stages of rocket launches, while LRE with liquid hydrogen and liquid oxygen is more suited for the later stages of the rocket launch due to higher specific impulse.

In rockets different metals and alloys are used in parts like printed circuit boards, thrust chambers, nozzles and structure. In printed circuit boards a large amount of metals can be utilised, including Cu, Al, Pb, Zn, Fe, Sn, Cd, Ti, Co and In [50]. Thrust chambers are designed to absorb heat from hot gases as well as not adding any unnecessary weight to the rocket. These are typically composed of either copper or an alloy of aluminium, steel or nickel [51]. Nozzles have to built to endure thermal stress and typically are composed of tungsten, steel, metal oxides like alumina, magnesia and zirconia, carbon, and graphite [51]. Rocket structures are built to withstand the load of a rocket to deal with temperature variations, thus typical materials used for this purpose are aluminium, titanium, magnesium, beryllium and epoxies of aramid, glass, Kevlar or graphite [52].

Rockets and their components have been connected with adverse environmental effects in the vicinity of their rocket activity sites. In Brazil, high levels of Cd, Hg, and Pb, in addition to the first reporting of Rb in nurse sharks were potentially linked to a rocket base explosion [53]. Military training activity with mortars, artillery, and rockets uses metal components consisting of Sb, As, Cu, Pb, W, Al, Ba, Be, Cd, Cr, Co, Fe, Mg, Mn, Hg, Ni, Se and more. These elements are to a varying degree deposited in the local environment within the activity range [54]. In Russia, kerosene was shown to cause significant changes in vegetation at a load of 25g/kg [55]. In the US, depositional material from rocket motors were shown to have elevated chloride levels and corrosive properties on steel [56]. Cl and Al_2O_3 are connected with ozone depletion, Cl in the form of the radical catalyst Cl_x, and Al_2O_3 through particle surface chemical reactions [11]. Shrimps bioaccumulate Al at all pHs and Al_2O_3 combined with low pH was shown to impact enzymatic activity through neurotoxicity and reduced detoxification capacity [57]. Inhaled Al_2O_3 can cause Shaver's disease which symptoms are laboured breathing and dry cough, and can lead to right heart failure [49].

2.6 Quality Assurance and Quality Control

Quality assurance (QA) is composed of the development, validation, recording of the procedure, and regular performance monitoring [25]. This is done to ensure that the samples are representative and have integrity, and analytical results can be viewed as reliable and accurate [58]. Quality control (QC) is composed of the actions that monitor and measure the effectiveness of the QA procedures based on defined objectives [58].

ISO, the international organisation of standardisation, is an independent non-governmental organisation which develops international standards. These international standards are documents that detail practical information and the best practice, and is used to make products compatible, identify safety issues, and share solutions [59].

The ISO standards, and other standards, are a way of ensuring that sampling, storage, pre-treatment and analysis is conducted in accordance within accepted guidelines [59, 60, 61, 62, 63, 64, 65, 66, 67, 68, 69]. To check the performance of a given method, a standard reference material is used. The standard used can be established within the laboratory, and should have a

known composition and should resemble the analyte, both in concentration and matrix. There are two standard methods, an external and an internal. For the external standard method, the calibration curve for the analyte in question is created by plotting the concentration of a standard analyte against the signal (i.e. area or peak height) of the standard analyte. For the internal standard method a known amount of a known compound is added to the samples and a calibration curve is made. The internal standard should be distinguishable from the analyte, with similar chemical properties. The concentration of the analyte divided by the concentration of the internal standard is plotted against the signal ratio between the analyte and the internal standard [70]. A reference, on the other hand, must be made for others, and accepted nationally and internationally. Standard reference materials are available from different bodies worldwide [25].

Blanks are a tool used to assess the amount of signal stemming from the analyte itself or other causes. Reagent blanks are used to assess the signal impact of the analytical procedure, while sample blanks are used to assess the signal impact of the sample matrix [71].

The limit of detection (LOD) and limit of quantification (LOQ) are detection boundaries. The LOD is the lowest concentration of the analyte that can be detected at a specific level of confidence [71] and can be represented through equation 2.18:

$$\text{LOD} = \frac{3.3\sigma}{m} \tag{2.18}$$

where σ is the standard deviation of the response and m is the slope of the calibration curve [72]. The LOQ is the lowest concentration of the analyte at which the performance is deemed acceptable for a typical application [71] and can be represented through equation 2.19:

$$\text{LOQ} = \frac{10\sigma}{m} \tag{2.19}$$

where σ is the standard deviation of the response and m is the slope of the calibration curve [72].

When transferring analytes between matrixes some loss of the analyte can occur [73]. Recovery is a validation method defined as "the relative amount of analyte measured in the final extract compared to the amount in the

original sample" [70]. There are two forms of recovery, absolute ($R_{abs.}$) and relative ($R_{rel.}$). Some samples have standards added before the extraction, called spiked samples (SP), and some have standards added after the extraction procedure, called matrix match samples (MM), and together with the method blanks (MB) the recoveries can be calculated through equations 2.20 and 2.21 [74, 75],

$$R_{abs.} = \frac{\text{Area}_{A;SP} - \text{Area}_{A;MB}}{\text{Area}_{A;MM} - \text{Area}_{A;MB}} \cdot 100\% \tag{2.20}$$

$$R_{rel.} = \frac{\frac{\text{Area}_{A;SP}}{\text{Area}_{IS;SP}} - \frac{\text{Area}_{A;MB}}{\text{Area}_{IS;MB}}}{\frac{\text{Area}_{A;MM}}{\text{Area}_{IS;MM}} - \frac{\text{Area}_{A;MB}}{\text{Area}_{IS;MB}}} \cdot 100\% \tag{2.21}$$

where the subscript Area indicates the peak area, and the subscripts A and IS denote the analyte and internal standard [74, 75].

2.6.1 Sampling

Sampling is a method of collecting a sample that is thought to be representative of the total material to be analysed[76]. There are several different sampling designs, including simple random sampling, stratified random sampling, systematic sampling, fixed transect. Simple random sampling is a method most effective for homogeneous areas and is utilised such that all possible samples have equal probability of being selected. Stratified random sampling is similar to simple random sampling, but it takes a heterogeneous area and divides it into homogeneous subareas. Systematic sampling is conducted by sampling at constant intervals between sampling sites, while fixed transect does not use constant intervals [77]. It is thought that the bulk of errors occur during sampling, and it is thus important to take steps to minimise this occurrence [77]. Errors in sampling include contamination, and alteration of sample properties and composition [76]. For quality assurance of the sample, one of the main problems is guaranteeing biological, ecological, and geographical representativeness [76]. In addition, the weather conditions should be noted as this can affect the reproducibility of results [76]. The number of samples taken is also an important factor, as it relates to the statistical representativeness of the sample group [76]. Packaging, storing, and transport can all lead to contamination of the samples [76]. When planning sampling, standards, like ISO, are utilised in every step to ensure quality of sampling [60].

2.6.2 Sample preparation

Freeze-drying is a method of removing ice and other frozen solvents from a sample through sublimination, and removing bound water through desorption. The samples are frozen before freeze-drying to avoid expansion of the sample while under vacuum. While frozen, the samples are placed under vacuum below the triple point of water, which lies at 4.58 torr and 0.0098°C. Heat energy is then applied to cause the sublimation of ice. When the ice and other frozen solvents have undergone sublimation, the temperature is raised further so that the bound water undergoes desorption [78].

Sample wet digestion is a sample preparation method that converts components of a matrix into simple chemical forms. This is conducted through energy, such as heat, use of a chemical reagent, like an acid, or through a combination. Due to the conditions of this method, the equipment used must be chosen to withstand these conditions without introducing contamination. Microwave-assisted acid digestion uses microwaves as the energy source, and one of the most common acids used for digestion is nitric acid (HNO_3) due to its commercial availability [79].

Accelerated solvent extraction (ASE) is an extraction method for extracts from solid and semi-solid matrices and utilises elevated temperature and pressure, and liquid solvents to achieve the extraction [80, 81]. The principles of the extraction of an analyte from a semisolid or solid sample can be described in five steps. First, the sample is moistened with extraction solvent. Second, the desorption of compounds from the matrix occurs, followed by the third step where compound solvation in the extraction solvent occurs. Fourth, the compounds are dispersed out of the matrix, and fifth, diffusion through the solvent layer around the matrix into the bulk solvent [82, 83]. The cell, within which the sample is located and solvent is pushed through, is made of stainless steel or zirconium. In addition to this resins can be layered in the extraction cell, in a process called in-cell cleanup [80]. ASE achieves enhanced mass transfer rates for the solvent, while the surface tension and viscosity are decreased and analyte solubility is increased. These changes in physiochemical properties occur through high temperature and pressure, while keeping the conditions below the critical point of the solvent, keeping it liquid [82]. The efficiency of the extraction is dependent on kinetic and thermodynamic parameters, and is thus influenced by matrix

effects, mass transfer, and solubility. These features are limited by different factors, including flow rate, temperature, pressure, and extraction duration. Chemical species can form bound residues in a matrices, such as plants and soils, which have previously been non-extractable. The conditions of ASE introduce high energy through temperature and pressure can separate these species from the matrices [84]. Changes in physiochemical properties can affect other compounds in the matrix - e.g., an increase in the temperature can lead to an increase in the solubility of other compounds than the target analyte in the matrix, thus making the ASE less selective [82]. Too high a flow-rate can lead to dilution above the levels sought, and lead to the samples being too diluted for analysis [82]. Use of an acid or a base to change the pH of the medium is useful for breaking down non-covalent bonds between the analyte and matrix, but can also break down covalent bonds in the analyte [82]. ASE can be used to extract chemicals like organic contaminants, pesticides, mycotoxins, metal and organometallic species and antibiotics [82].

2.6.3 Analytical methods

Inductively coupled plasma mass spectrometry (ICP-MS) is an analytical method used to detect trace levels of elements. The instrument consists of six compartments, the sample introduction system, inductively coupled plasma, interface, ion optics, mass analyser and detector. Liquid samples are nebulised and transferred to argon plasma. Thus, samples are atomised and ions are extracted through the interface into electrostatic lenses called ion optics, where an ion beam is focused and lead through to the quadropole mass analyser which separates ions based on the mass-charge ratio before being detected [85].

Gas chromatography-mass spectrometry (GC-MS) is an analytical method of separating analytes based on adsorption and partition chromatography before detection. In GC the mobile phase is an inert gas, and the stationary phase can be a liquid or a solid. The gas chromatograph consists of a gas flask with carrier gas, reduction valve, injection system, column oven, and detector. In GC there are several detection methods that can be utilised, one of these is the mass spectrometer (MS). The MS consists of an ionising unit, a mass/charge separation unit, and an ion detector [70].

ICP-MS interference can be classified as spectroscopic or non-spectroscopic.

Spectroscopic interferences include isobaric elements, double-charged ions, polyatomic ions, and tailing interference. Non-spectroscopic interferances can be divided into matrix effects and instrument drift [85]. Signal interferences due to extraneous species in the matrix are called matrix effects, and include sample introduction effects, plasma effects, and space-charge effects [86, 85]. Sample introduction effects occurs with changes in physical and chemical properties which affect aerosol characteristics, like viscosity, vapour pressure, surface tension, ionic strength, and acidity. Plasma effects occur if the levels of easily-ionised elements is high which decreases instrument signal, or carbon is present, which will enhance analyte ionisation of elements with high ionisation potential. Effects in the interface and ion optics are called space-charge effects and occur "through mutual electrostatic repulsion between positively charged ions in the ion beam" [85]. Instrument drift occurs when dissolved solids deposit on the nebuliser or interface cones and thus lower suppressing signals [85]. To reduce sample-specific matrix effects and potential for nebuliser blockage in ICP-MS, the amount of total dissolved solids is recommended to be below 2 g/L and samples are usually diluted, either in acids or alkali [85]. Reduction and elimination spectroscopic interferences can be employed in the pre-analytical, analytical, or post-analytical stages. Sample pre-treatment, matrix removal, isotope selection, correction equation, optimisation of instrument settings, high-resolution ICP-MS, collision and reaction gases, and tandem MS can be utilised to achieve reduction or elimination. For non-spectroscopic interference reduction and elimination dilution and matrix-analyte separation can be utilised [85].

There are several factors in GC-analysis which all have small, potential sources of error, and which can accumulate through analysis and affect different parameters. Poor reproducibility of parameters such as oven temperature, detector temperature, and injection, can lead to uncertainty in the data returned to the user, like peak height and width, and retention time. Factors that affect sample introduction include split ratios and column temperature. Low split ratios can affect the mixing of the sample and the carrier gas, while low column temperature can lead to sample recondensation. Per °C the column temperature can affect the retention time, and thus the peak width up to 3%. For concentration-dependent detectors decreased flow-rate leads to increased peak width, and thus peak area, while for mass flow detection systems the response is inversely proportional to the flow-rate, and thus will affect the peak height [87].

2.7 Statistics

The mean is a measure of location designed to find the numerical average of the sample data, and is represented by equation 2.22,

$$\bar{x} = \sum_{i=1}^{n} \frac{x_i}{n} = \frac{x_1 + x_2 + ... + x_n}{n} \tag{2.22}$$

where x_i represents sample number i and n is the total number of samples in the data.

The median is another measure of location which reflects the central tendency of data without being influenced by outliers, and is represented by equation 2.23,

$$\tilde{x} = \begin{cases} x_{(n+1)/2}, & \text{if } n \text{ is odd,} \\ \frac{1}{2}(x_{n/2} + x_{n/2+1}, & \text{if } n \text{ is even.} \end{cases} \tag{2.23}$$

where n is the total number of samples in the data.

Standard deviation is a measure of spread of a population, and when looking at a sample it is represented by equation 2.24,

$$s = \sqrt{\sum_{i=1}^{n} \frac{(x_i - \bar{x})^2}{n-1}} \tag{2.24}$$

where x_i represents sample number i and n is the total number of samples in the data.

The normal distribution is a continuous probability distribution with a graph called the normal curve. The normal curve is bell-shaped with the mean as its maximum and is symmetric about the vertical axis at the mean. Chebyshev's theorem states that a random variable X has a probability of at least $1 - \frac{1}{k^2}$ of falling within k standard deviations of the mean, as represented in equation 2.25,

$$P(\mu - k\sigma < X < \mu + k\sigma) \geq 1 - \frac{1}{k^2} \tag{2.25}$$

where P is the probability, μ is the mean, σ is the standard deviation, X is the random variable and k is the number of standard deviations. Following

equation 2.25 at least 88.89% of the sample data will fall within 3 standard deviations of the mean.

A statistical hypothesis is defined by Walpole et al. as "an assertion or conjecture concerning one or more populations" [88]. The null hypothesis, H_0, is the hypothesis tested and the alternative hypothesis, H_1, is the logical complement [88]. The Shapiro Wilk test is a test for the normality, it checks the observed data to check if it is normally distributed [89]. If the data set is normally distributed, it can be compared to another normally distributed, independent data set through the t-test [90]. For three or more normally distributed, independent data sets, the one-way analysis of variance (ANOVA) may be used [91]. One-way ANOVA is an omnibus test statistic, and thus cannot indicate which specific groups are significantly different from each other, only if at least two groups are. Through post-hoc tests the difference between groups can be tested [92].

When two independent, non-normally distributed groups are to be tested,the Wilcoxon rank-sum test, also called the Mann-Whitney U test, can be used. For three or more independent, non-normally distributed groups the Kruskal-Wallis test can be used [88, 93].

The box-and-whisker plot is a way of displaying the data at hand. It consists of a box that encloses the data in the range from the 25th percentile to the 75th percentile, called the interquartile range, with a dividing line representing the median. The whiskers enclose the data outside the interquartile range, in addition to outliers being placed outside these whiskers. The definition of an outlier is commonly decided as a multiple of the interquartile range.

Linear regression for two variables is based on a linear equation with one independent variable, represented in equation 2.26:

$$y = mx + b \tag{2.26}$$

where m and b are constant numbers, x is the independent variable, and y is the dependent variable [94]. This gives rise to the correlation coefficient, R, and the coefficient of determination, R^2, which, when represented in percent, represents the percentage of variance in y explained by the variation in x using the regression line.

Multivariate statistical analysis is defined as "the simultaneous statistical analysis of a collection of random variables" [95]. It extends univariate analysis, wherein a single variable is analysed, by conducting the analysis of several variables simultaneously. It also improves upon univariate analysis by incorporating information of the relationships between the variables [95]. Principal component analysis (PCA) is a multivariate technique that aims to describe the variation of set of multivariate data through the use of uncorrelated variables. These uncorrelated variables are linear combinations of the original variables [96]. The data used in PCA can be represented as an **X** matrix with n objects and p variables (n x p matrix) [97]. The data is centred around the means of each variable to ensure that the data is centred around the principal components (PCs) [98]. Each PC describes a certain amount of the variance in the data, and the PCs are a linear combination of the original variables. The first PC can be viewed as an axis of maximum variance direction in the original data, or as an axis that minimises the sum of squared distances from each sample point to the axis [97]. The first PC, y_1, can be represented as the linear combination as shown in equation 2.27:

$$y_1 = a_{11}x_1 + a_{12}x_2 + ... + a_{1p}x_p \tag{2.27}$$

with the criteria of maximum variance or least squares fit as described above. y_1 can grow as large as wanted by choosing large values for $a_{11}, a_{12}, ..., a_{1p}$, therefore a constraint of setting the sum of squares of these are set to 1 as shown in equation 2.28:

$$a_{11}^2 + a_{12}^2 + ... + a_{1p}^2 = 1 \tag{2.28}$$

The coefficients $a_{11}, a_{12}, ..., a_{1p}$ can also be expressed as the vector $\mathbf{a}_1$ and thus equation 2.29 follows:

$$\mathbf{a}_1{}'\mathbf{a}_1 = 1 \tag{2.29}$$

The second PC is given in equation 2.30:

$$y_2 = a_{21}x_1 + a_{22}x_2 + ... + a_{2p}x_p = \mathbf{a'}_2\mathbf{x} \tag{2.30}$$

with two stipulations as expressed in equations 2.31 and 2.32:

$$\mathbf{a}_2{}'\mathbf{a}_2 = 1 \tag{2.31}$$

$$\mathbf{a}_2{}'\mathbf{a}_1 = 0 \tag{2.32}$$

where equation 2.32 ensures that y_1 and y_2 are uncorrelated. Extrapolated, this gives that the jth PC, $y_j = \mathbf{a'}_j\mathbf{x}$ with the following conditions given in equations 2.33 and 2.34:

$$\mathbf{a}_j{}'\mathbf{a}_j = 1 \tag{2.33}$$

$$\mathbf{a}_j{}'\mathbf{a}_i = 0, i < j \tag{2.34}$$

When deriving the PCs, this can be performed with eigenvalues and eigenvectors of the covariance matrix $\mathbf{S}$, but it is more common to extract the components as the eigenvectors from the correlation matrix $\mathbf{R}$ [96]. Equations 2.35 and 2.36 show the formulas for covariance and correlations between two variables x and y.

$$\text{cov}(x, y) = \frac{\sum_{i=1}^{n}(x_i - \bar{x})(y_i - \bar{y})}{n - 1} \tag{2.35}$$

$$r = \frac{\text{cov}(x, y)}{s_x s_y} \tag{2.36}$$

The reason for using $\mathbf{R}$ over $\mathbf{S}$ is that it will behave as if the PCs have been calculated from the original variables after having been standardised to have unit variance and thus avoid the problem of different units for each variable [96]. The maximum number of PCs is limited to the smaller of n and p in the $\mathbf{X}$ matrix. The coefficients represented by the vector $\mathbf{a}_j$ are also called loadings [97]. The linear combination for each PC contains p loadings and the loadings for each PC constitutes the $\mathbf{P}$ matrix which can be viewed as a transformation matrix between the original variable space and the PC space. Thus, the loadings give information about the relationship between the original p variables and the PCs. By taking an object i in $\mathbf{X}$ and projecting onto the PC space object i will have a coordinate for each PC. The coordinate for a given object i for a given PC is called a score. The scores for all objects projected onto each PC can be arranged in a $\mathbf{T}$ matrix called the score matrix [97]. For determining the number of PCs to be used, a variety of selection criteria can be utilised. Usually, the number of PCs is chosen to explain 70 to 90% of the total variance, although this value might be lower for large n or p [96]. Variable selection criteria can be based on criteria such as the size of the loadings, the size of the correlation between the variables and PCs, the conditional covariance or correlation matrices for the removed variables given the retained variables, looking at the clusters of variables [99]. It is also possible to utilise a scree plot, in which the

sample eigenvalues are plotted against their order numbers, wherein a break, or elbow, will differentiate the variables that account for a large amount of variance from the small variables [95]. Kaiser's rule is another method of determining the numbers of PCs in which PCs with eigenvalues above one are retained. A modified version of Kaiser's rule suggests a cut-off of 0.7 [95, 96]. PCs that explain a large amount of variance are said to describe the structure, or underlying phenomena, in the data, while the PCs that account for a small amount of the variance are said to describe the noise [97]. The plots of the scores and loading are usually represented with two PCs at a time, with the PC that accounts for the largest variance along the x-axis. The loading plot is useful for revealing the underlying phenomena by interpreting the context of the data. By looking at the PC-coordinates for the loadings it can be determined how large the influence of the variable is on the PC. If a variable p is located on the x-axis and far up on the y-axis the variable p does not contribute to the PC in the x direction, but contributes strongly to the PC in the y direction. The further a coordinate is from 0 relative to the other variables, the more important it is for the PC being described. Variables clustered together and on a straight line through the origin covary. If they are on opposite sides of the origin they are negatively correlated, while they are positively correlated if they are on the same side [97]. Outliers can influence the composition of the PCs, in particular the PCs that describe less of the variance, at is thus important to make decision on whether to include outliers with known sources or not [97]. A problem that occurs when choosing which PCs to retain is truncation. Truncation is the loss of information that occurs when a linear combination consisting of some loadings close to 0 are replaced by loadings equal to exactly 0. Use of multiple correlation coefficients and regressing the the PCs of subsets of variables are possible solutions [100]. Using too many PCs will lead to including noise in the model, while including too few PCs will lead to loss of information [97].

3 Material and methods

3.1 Sampling locations

The sampling was conducted in Ny-Ålesund, Svalbard from 16th August to 22nd August 2021 and the temperature and weather conditions were around 4°C and light rain at times, but mostly clear. The main sampling was conducted in Brøggerdalen, Ny-Ålesund, Svalbard at two locations. These locations were selected as they where the booster impact areas (BIAs) of rockets launched by NASA. The coordinates of these two BIAs were 78°54.59' N 11°49.41 E for BIA A and 78°55.33' N 11°49.43' E for BIA B as shown in the figure 3.1.

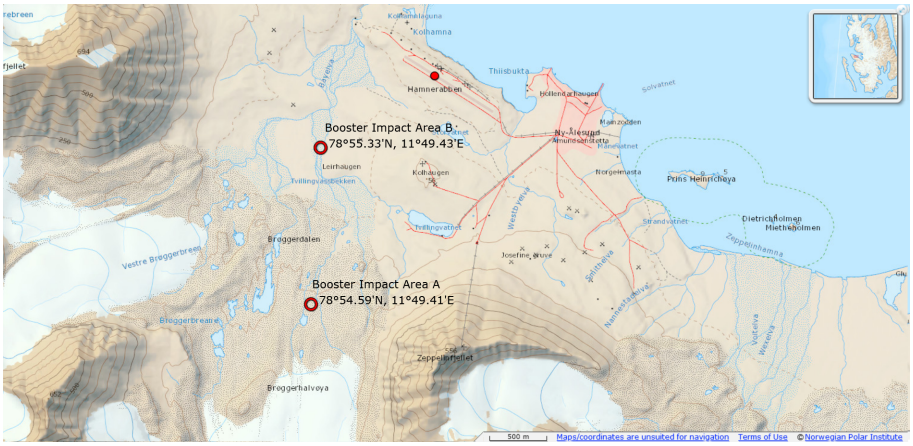

Figure 3.1: Map of the BIAs in relation to Ny-Ålesund. Map courtesy of the Norwegian Polar Institute [16].

In addition, background sampling was conducted next to a river close to Midtre Lofvenbreen at the coordinates 78°54.32' N 12°04.47 E, shown in figure 3.2 and on the Ossian Sars mountain, shown in figure 3.3.

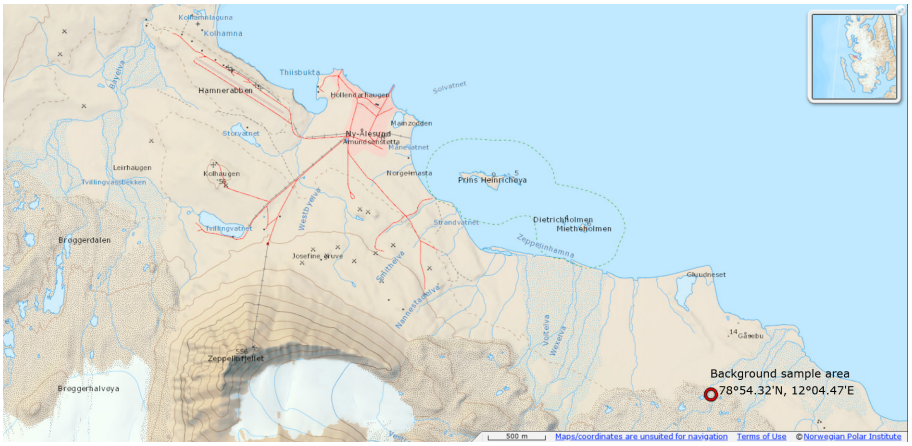

Figure 3.2: Map of the background sample area by Midtre Lofvenbreen in relation to Ny-Ålesund. Map courtesy of the Norwegian Polar Institute [16].

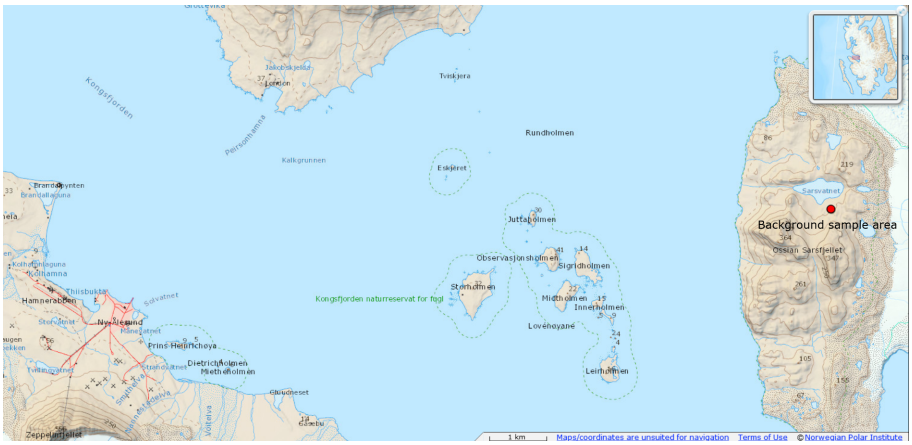

Figure 3.3: Map of the background sample area by Ossian Sars mountain in relation to Ny-Ålesund. Map courtesy of the Norwegian Polar Institute [16].

From the BIAs sampling for trace element analysis was conducted by taking 10 samples from the epicentre of the BIA, within 25m of the BIA, and in 25m intervals for 200m in the direction of the Ny-Ålesund airport, Hamnerabben, where the launches were conducted [15]. An exception was made for the sample point of BIA A + 50m, which was changed to + 44m due to an object of interest being located at this point. Three parallels of

six samples were collected from the sampling area by Midtre Lofvenbreen and two samples were collected from the Ossian Sars mountain. These background samples were not used due to more relevant background data being found. For the PCB analysis the interval was 50m for 200m, with an extra sample location at 25m from the BIA. Three sample parallels were collected from the sampling area by Midtre Lofvenbreen, but were not used. For both analysises three sample collection parallels were conducted outside of the epicentre, yielding a total of 68 samples for trace element analysis, and 20 samples for PCB analysis. An overview of these samples can be seen in tables A.1 and A.2.

3.2 Sampling

The samples intended for trace element analysis were collected and stored in polystyrene sample cups with polyethylene lids (Coulter®). The sampling was conducted by scraping the top few millimetres of the overbank sediment at each point with the polystyrene cups (Coulter®) while wearing nitrile gloves (VWR Chemicals Radnor, PA, US) to avoid contamination, and a conscious effort was made to avoid larger stones.

The samples intended for PCB analysis were collected in low-density polyethylene plastic bags by scooping the top few millimetres of overbank sediment with polystyrene cups (Coulter®) and transfering it to the plastic bags.

The sampling and sample collection planning was based on ISO 18400-104 *Soil quality — Sampling — Part 104: Strategies*, ISO 18400-202 *Soil quality — Sampling — Part 202: Preliminary investigations*, and ISO 18400-203 *Soil quality — Sampling — Part 203: Investigation of potentially contaminated sites* [60, 61, 62].

3.3 Sample preparation

The samples for trace element analysis were freeze-dried in Alpha 1-4 LD plus (Martin Christ Gefriertrocknungsanlagen GmbH, Osterode am Harz, Germany) under vacuum at 0.94 mbar and -21°C for 48 hours, and finished of at 0.090 mbar and -43°C for 20 minutes. When dried, the samples were homogenised with mortar and pestle. Freeze-drying was conducted in accordance with ISO 16720:2005 titled *Soil quality - Pretreatment of samples by*

freeze-drying for subsequent analysis [63]. The samples were then weighed out to 250-350 mg in Teflon tubes, 9 ml of 50% w/v HNO_3 (Ultra Pure grade, distilled by Milestone SubPur unit) before microwave digestion in Milestone UltraCLAVE (UltraClave, Milestone GmbH, Leutkirch, Germany). In addition to the samples collected, method blanks and certified reference materials for river sediment, MODAS-2 Bottom Sediment (Nicolaus Copernicus University, Toruń, Poland), originating from the Vistula River near Włocławek, Poland and marine sediment, MESS-4 Marine Sediment (Canada Centre for Mineral and Energy Technology, Ottawa, Canada), originating from Beufort Sea in Arctic Canada, were prepared [101, 102, 103]. After digestion the samples were diluted to between 109.33g and 117.22g with ultra-pure type I water from an ELGA Purelabs Chorus water purification system, and the overview is shown in table B.1. Then, 15 mL of the diluted sample was transferred to metal-free, polypropylene tubes (VWR Chemicals, Radnor, PA, US) for ICP-MS analysis. This method was based on NS-EN 16173:2012 titled *Sludge, treated biowaste and soil - Digestion of nitric acid soluble fractions of elements* [69].

The samples intended for PCB analysis were stored in low-density polyethylene plastic bags during travel and transferred to aluminium boxes at the laboratory. The samples were air-dried until the weight of three selected samples changed by less than 5% after a week. The samples were then homogenised with a mortar and pestle. The samples for PCB analysis were pretreated using ASE in accordance with a method by Pintado-Herrera et al. modified by Sylvia Weging [104, 75]. The chemicals and materials used in ASE and Turbovap can be seen in table 3.1.

Table 3.1: Overview of the chemicals and materials used in ASE, their use, specifications, and provider.

Chemicals/materials	Use	Specifications	Provider
Dichloromethane	Extraction	GC-capillary grade	VWR Chemicals (Radnor, PA, US)
Ethylacetate	Dilution	Analytical grade	VWR Chemicals (Radnor, PA, US)
Acetone	Cleaning	Technical grade	VWR Chemicals (Radnor, PA, US)

Ottawa sand	Extraction	General purpose grade	Fisher Scientific (Loughborough, UK)
Al_2O_3 (activated)	Extraction	Basic brockmann I, standard grade, ca. 150 mesh	Sigma-Aldrich (St. Louis, MO, US)
Cu	Extraction	<425 μm, 99.5% trace metals basis	Sigma-Aldrich (St. Louis, MO, US)
Diatomaceous earth	Extraction		Sigma-Aldrich (St. Louis, MO, US)
ASE extraction filters (cellulose)	Extraction	For 1, 5, 10, 22 mL Dionex™ ASE 350/150 extraction cell	Thermo Scientific (Waltham, MA, US)
Nylon syringe filter	Filtration	0.45 μm pore diameter	VWR Chemicals (Radnor, PA, US)
PCB Congeners in Soil SQC068	Extraction	Certified reference material	Sigma-Aldrich (St. Louis, MO, US)
3'-F-PCB-28	Extraction	100 μg/mL in isooctane, internal standard	CHIRON AS (Trondheim, NO)
5'-F-PCB-28	Extraction	10 μg/mL in isooctane, internal standard	CHIRON AS (Trondheim, NO)
Dutch seven PCBs	Extraction	100 μg/mL in isooctane of PCBs 28, 52, 101, 118, 138, 153, and 180. ISO10382 multicomponent stock solution	CHIRON AS (Trondheim, NO)

Before extraction, Ottawa sand and diatomaceous earth were purified in accordance with the U.S. EPA method 3545A [105] by heating in a shallow tray at 400°C for 4 hours in an oven (Carbolite ELF 11/6). A stainless steel 22 mL cell with two caps was tightened at one end and the components of the cell were layered. First, two cellulose filters were placed in the bottom, followed by 2g of Cu, followed by a cellulose filter and 2g alumina (Al_2O_3)

and a cellulose filter. 2g of diatomaceous earth was mixed with 50 μL of the two internal standards. For some extractions 50 or 100 μL of the external standard, 0.5 $\pm$0.02g of a sample, mixed sample (containing a mix of all 12 samples) or the reference material were mixed in with the diatomaceous earth and standards. The composition of the samples can be seen in table 3.3. Finally, the cell was topped with Ottawa sand and closed. The internal standards used were 1 μ g/mL 3'-F-PCB-28 and 1 μg/mL 5'-F-PCB-118 and were attained by dilution with ethyl acetate, the external standard used was 1 μ g/mL Dutch seven [68] and was attained by dilution with ethyl acetate, and the reference material used was PCB Congeners in Soil SQC068.

In table 3.3 M in the sample name denotes method blank, S denotes sample, Rec denotes recovery, RefM denotes reference material and MM denoted matrix match. For the sample column s denotes samples, ms denotes mix of all 12 samples, and ref denotes reference material. In the IS and ES columns pre denotes standard added pre-extraction, while post denotes standard added post-extraction, and the number is the amount added in μL.

The ASE was conducted with a Dionex™ (Sunnyvale, CA, US) ASE 150 accelerated solvent extractor and the samples were collected in 60 mL amber vials and stored in a freezer at below -18 °C. When the sample type was changed, the extractor was rinsed three times with an extraction cell only filled with resins. The extraction parameters are shown in table 3.2 as conducted by Weging [75].

Table 3.2: Overview of ASE system parameters.

System parameter	Value
Oven temperature	100 °C
System pressure	1500 psi
Cell size	22 mL
Solvent	Dichloromethane
Time per run	24 min
Solvent per sample	∼35 mL

After ASE, the samples, along with 4 blanks were concentrated with the Biotage TurboVap Classic LV evaporator (Biotage, Charlotte NC, US) from 35 mL to 2mL in the 60 mL amber vials in a water bath at 35°C with 5 psi gas stream of N_2. The walls of the vials were rinsed with 10 mL ethyl acetate

Table 3.3: Overview of the procedure for analysis of each sample.

Sample name	Sample	IS	ES
M1	-	pre50	-
M2	-	pre50	-
M3	-	pre50	-
S1	s	pre50	-
S2	s	pre50	-
S3	s	pre50	-
S4	s	pre50	-
S5	s	pre50	-
S6	s	pre50	-
S7	s	pre50	-
S8	s	pre50	-
S9	s	pre50	-
S10	s	pre50	-
S11	s	pre50	-
S12	s	pre50	-
M4	-	pre50	-
M5	-	pre50	-
Rec1	ms	pre50	-
Rec2	ms	pre50	-
Rec3	ms	pre50	pre50
Rec4	ms	pre50	pre50
Rec5	ms	pre50	pre100
Rec6	ms	pre50	pre100
RefM1	ref	pre50	-
RefM2	ref	pre50	-
RefM3	ref	pre50	-
MM1	ms	post50	post50
MM2	ms	post50	post50
MM3	ms	post50	post100
MM4	ms	post50	post100

and the solution filtered through a 0.22 μm nylon syringe filter. The solution was then concentrated to 1 mL and for the matrix match samples IS and ES were added.

3.4 Chemical analysis

The ICP-MS analysis of trace elements was conducted on an Agilent 8800 Triple Quadropole ICP-MS (Agilent Technologies, Santa Clara, California, US) instrument equipped with prepFAST M5 autosampler (ESI, USA) for 52 elements. The tuning parameters can be found table B.5 and the system parameters in table 3.4. The analysis was performed based on NS-EN 16171:2016 titled *Sludge, treated biowaste and soil - Determination of elements using inductively coupled plasma mass spectrometry (ICP-MS)* and ISO/TS 16965:2013 titled *Soil quality — Determination of trace elements using inductively coupled plasma mass spectrometry (ICP-MS)* [65, 64].

Table 3.4: Parameters of the system for the ICP-MS analysis

General parameters	
RF Power	1550 W
Nebulizer gas	0.80 L/min
Makeup gas	0.38 L/min
Sample depth	8.0 mm
Ion lenses	X-lens
H_2 mode	
H_2 gas flow	4.5 mL/min
He gas flow	1.0 mL/min
O_2 mode	
O_2 gas flow	0.525 mL/min

The GC-MS analysis of PCBs was conducted on an Agilent 7890A gas chromatograph equipped with a GC Pal autosampler (CTC Analytics, Zwingen, CH) coupled to an Agilent 5975 single quadrupole mass spectrometer. The column used was a Thermo Scientific™ TraceGOLD™ TG-5MS GC Column (5% diphenyl/95% dimethyl polysiloxane, 30 m x 0.25 mm inner diameter x 0.5 μm film thickness), with helium as the carrier gas at 1 mL/min. The temperatures of the transfer line and injection port were set to 290°C.

Table 3.5 shows the temperature programme.

Table 3.5: Overview of the GC temperature programme.

Temperature	Duration
50°C	2 min
+25°C/min	8 min
250°C	1 min
+3°C/min	12 min
286°C	3 min
+8°C/min	2 min 45 sec
308°C	1 min
+1°C/min	2 min
310°C	3 min

The injection was run in splitless mode, the injection volume was 1 μL, and the selected ion monitoring mode was used for the mass detector with electron impact ionisation. A calibration curve with concentrations of 0.5 to 100 ng/mL of the ES Dutch seven was run together with the samples, as well as blanks and a number of the ES sample for 10 ng/mL. The analysis was performed based on ISO 16703:2004 titled *Soil quality - Determination of content of hydrocarbon in the range C10 to C40 by gas chromatography* and ISO-13876:2013 titled *Determination of polychlorinated biphenyls (PCB) by gas chromatography with mass selective detection (GC-MS) and gas chromatography with electron-capture detection (GC-ECD)* [66, 67].

3.5 Statistical analysis

When analysing the ICP-MS data, a preliminary check for extreme outliers and their possible source was performed. Then, the data sets were checked for normality through the use of the Shapiro-Wilk test. If normal, a one-way ANOVA was performed on the data from BIA A and B, in addition to background data from 2015 supplied by Kveli [106]. After which, a t-test was performed as a post-hoc analysis. If one or more of the groups did not display normality, the Kruskal-Wallis test was performed, and the Mann-Whitney U test was performed as a post-hoc analysis. For the GC-MS data, calibration curves based on the external standards were made, and retention times for the external standards were compared to the retention times given

for the samples. LODs and LOQs were found for the external standards and compared to the concentrations of PCBs in the samples. Absolute and relative recovery for the PCBs were also calculated. PCA score- and loading-plots were made for BIA A, BIA B, and relevant background data from Kveli [106].

4 Results and discussion

Table 4.1 shows relevant data from BIA A and B for trace elements of interest. The results in table 4.1 were calculated from the raw data in table B.2. Overarching causes of differences between data from BIA A and BIA B and the background data include methodical and instrumental differences, other anthropogenic activity not related to rocket activity, and geological changes over time. The background data is used to statistically compare the means of the trace elements analysed. The concentrations of all PCBs monitored were below the limit of detection.

4.1 Trace elements

4.1.1 PCA

The PCA score-plots for PC1 and PC2 (figure 4.1) and PC1 and PC3 (figure4.2), and loading-plots for PC1 and PC2 (figure 4.3) and PC1 and PC3 (figure 4.4) show that PC1, PC2 and PC3 account for 47%, 13% and 10% of the variance respectively, for a total of 70% of the variance. In the PCA score-plots in figures 4.1 and 4.2 A denotes BIA A and B denotes BIA B. In the PCA loading-plots in figures 4.3 and 4.4 the points are marked with the chemical symbols of the trace elements analysed.

The sample areas are not distinctly divided along PC1, and the major difference between the sample areas can be explained through PC2. PC1 explains some of the difference within BIA A and BIA B. The largest contributors to PC1 are Al, Ba, Tl, V, Fe, Na, Cr, Co, La, Ti, Ni, B, P, Pb, Mn, Sr, K, Li and Be, with S, Bi and Ca negatively correlating with the aforementioned elements. PC1 appears to be connected to the underlying geology of the sampling area [17, 18, 19]. For PC2 the largest contributors are Mg, Ca, Si and Sr with As negatively correlating with these trace elements. PC2 appears to be connected to the Carboniferous and Permian sedimentary rock in the western sector of the Bayelva basin, Vestre Brøggerdalen and the western sector of Austre Brøggerdalen as Mg and Ca positively correlate with this PC [17]. PC2 also appears to be connected to the vicinity of old mining sites in the Ny-Ålesund area as the loadings with negative PC2-coordinates are connected to coal mining [107, 108]. Importantly, rocket debris does not appear to significantly influence the two largest PCs. While sample 20 dom-

Table 4.1: The means, medians, maximum and minimum concentration values in μg/g as well as the variance of selected trace elements measured from the samples of BIA A (n = 34) and BIA B (n = 33).

Trace element	Area	Mean	Median	Max.	Min.	Variance
Cd	BIA A	3.718	0.0915	123.4	0.0568	447.2
	BIA B	0.1340	0.1258	0.2230	0.0866	0.001205
Fe	BIA A	22443	22077	26984	18895	4685831
	BIA B	19579	19327	23652	15297	5441082
Pb	BIA A	12.64	12.33	16.93	10.22	2.904
	BIA B	10.60	10.72	13.32	8.122	1.999
As	BIA A	4.199	4.022	6.058	3.046	0.5466
	BIA B	2.698	2.756	4.018	1.507	0.2742
Al	BIA A	22774	22267	31864	15788	17402952
	BIA B	20469	19100	29031	14148	18463934
Ti	BIA A	521.9	527.6	697.1	390.9	6078
	BIA B	490.1	490.7	623.2	313.6	6349
Li	BIA A	17.12	16.84	22.07	13.42	5.531
	BIA B	14.58	14.13	19.29	10.26	6.781
Cu	BIA A	26.11	13.42	437.9	10.65	5297
	BIA B	13.04	12.70	18.14	10.08	3.598
Zn	BIA A	49.46	45.30	229.0	33.78	1030
	BIA B	38.20	37.52	50.31	29.73	31.75
Sn	BIA A	0.4179	0.4056	0.9280	0.3097	0.009522
	BIA B	0.4390	0.4281	0.5326	0.3517	0.003338
Co	BIA A	9.864	9.867	11.86	8.197	0.9002
	BIA B	8.289	8.348	10.13	6.851	0.8456
Mg	BIA A	9791	9761	12300	7657	1720713
	BIA B	14708	14498	22433	10829	7015737
Be	BIA A	1.079	1.055	1.570	0.6632	0.06720
	BIA B	1.042	0.9804	1.461	0.4447	0.06554

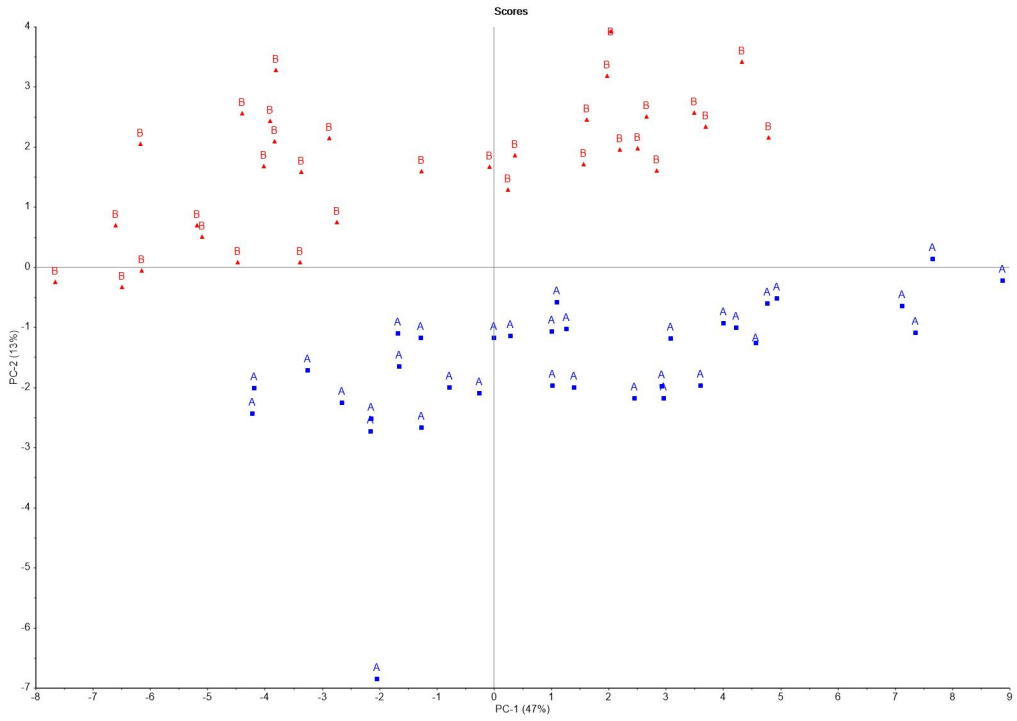

Figure 4.1: The PCA score-plot for PC1 and PC2 of the samples from BIA A (blue) and BIA B (red).

inates PC3 as an extreme outlier with large values of Zn, Sn and Cu there are no other samples with levels close to these which would suggest that the contamination of trace elements is highly local. Tin-zinc and tin-copper alloys have been used as engine bearings in the aerospace industry [109]. Thus, a possible contamination source can be a metal fragment in the immediate vicinity of this sample. It is important to note that 30% of the total variance remains unexplained with this selection of PCs, and thus it is not possible to rule out the existense of other underlying phenomena not immediately visible to the naked eye. In PC2, Cd and Cu, along with Zn, Sn and Sb show weak correlation, and for Cd and Cu there is a weak negative correlation with PC1, while Zn, Sn and Sb show a weak positive correlation with PC1. Arsenic shows a clear negative correlation with PC2, while Co, Pb, Fe, Al and Ti show a clear positive correlation with PC1, and Mg and Ca show a clear positive correlation with PC2. Further, Ca and Mg are perpendicular to the group where Co, Pb, Fe, Al and Ti reside, and thus, there is minimal

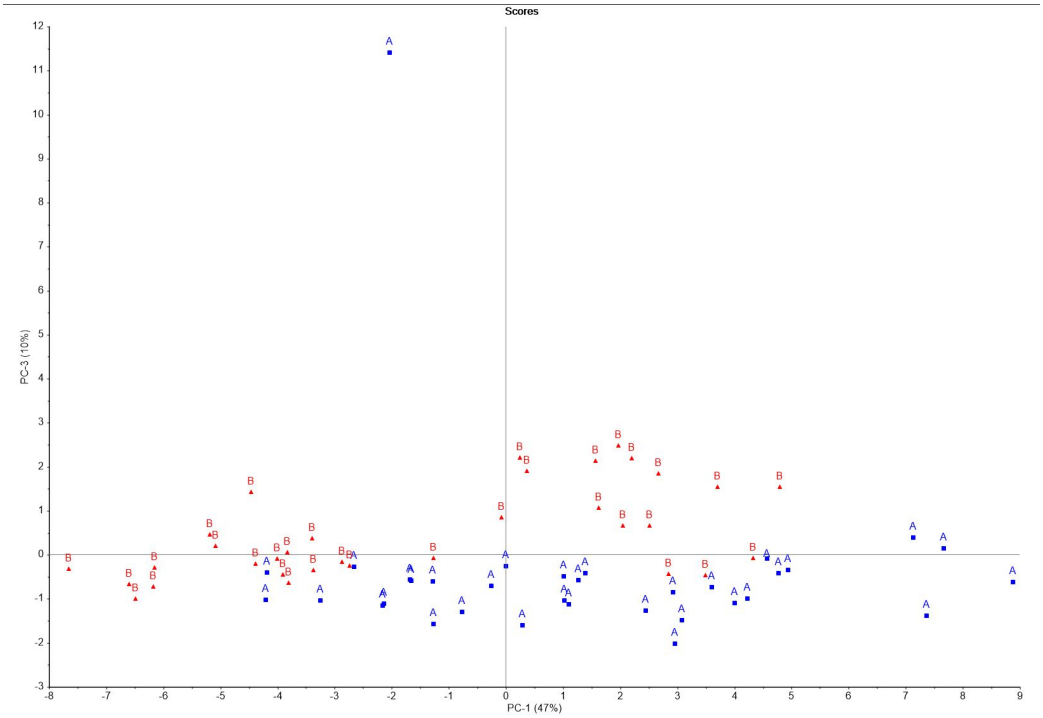

Figure 4.2: The PCA score-plot for PC1 and PC3 of the samples from BIA A (blue) and BIA B (red).

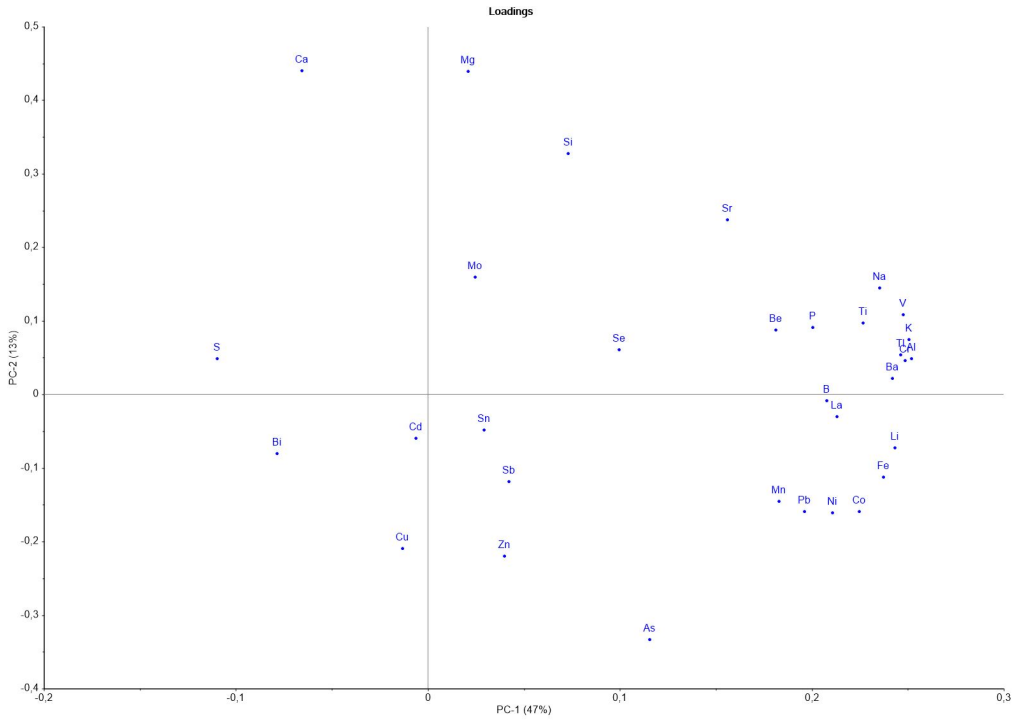

Figure 4.3: The PCA loading-plot for PC1 and PC2 of the samples from BIA A and BIA B.

correlation between these groups. Cu and Cd correlate negatively with Mg, while Ca correlates negatively with Zn, Sb and Sn.

The PCA score- and loading-plot together shows that samples from BIA A associate with As, Cd, Cu, Zn and Sb through their near-zero and negative PC2-values. At the same time, samples from BIA A do not associate with Ca and Mg as their PC2-values have opposite signs, while the samples from BIA B associate with Ca and Mg.

In the following sections closer attention is given to a selection of trace elements, chosen due to their presence in rocket materials and general toxicological interest in the region. The null hypothesis (H_0) in the statistical tests conducted was that the means of the sample groups were not significantly different.

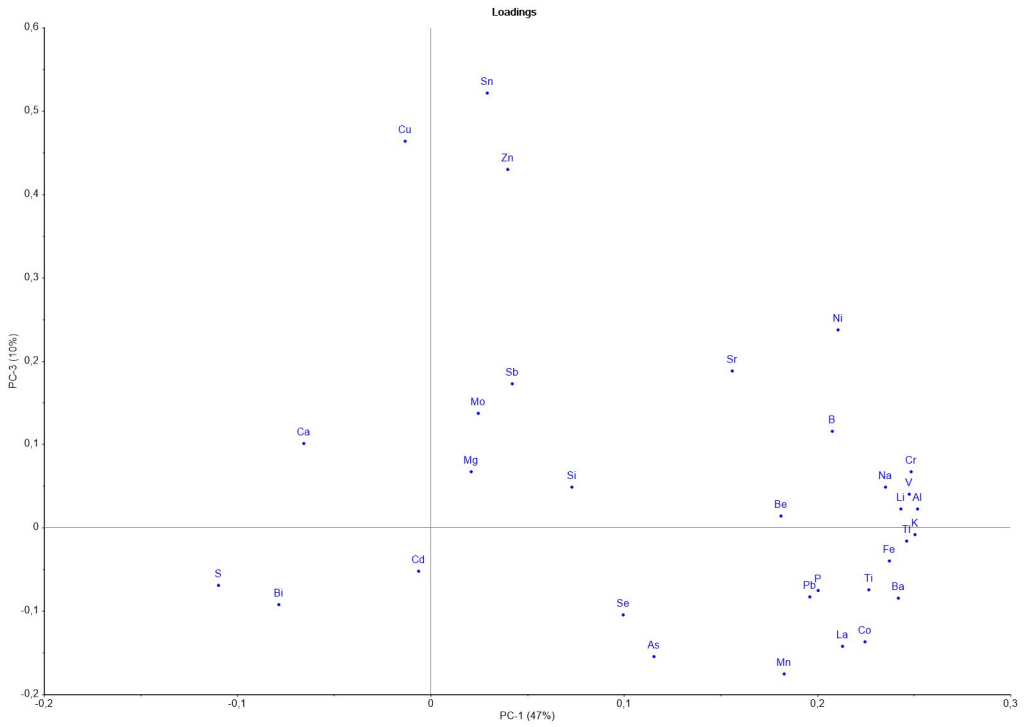

Figure 4.4: The PCA loading-plot for PC1 and PC3 of the samples from BIA A and BIA B.

4.1.2 Cadmium

Sample 23 taken at 44m from the epicentre of BIA A was omitted from the boxplot and statistical testing due to being an extreme deviation with a value of 123.4 μg/g. The sample was collected from under a metal fragment, which is a probable cause for the deviation. The source likely being due to being sampled from under a metal fragment and thus, having a known reason for deviation. H_0 is rejected for all the tests (table 4.2), and thus the means of the groups are significantly different from each other and there is less than 5% probability that the difference in means is insignificant. As sample 23 with a large Cd spike was around 950x larger than the next highest sample from the BIA A, sample 28 at 0.1304 μg/g, and given the small variation in the rest of the Cd data from BIA A, it appears that trace element pollution from metal fragments is highly localised. When comparing sample 23 to samples 7 and 15, at Cd levels of 0.0901 μg/g and 0.0716 μg/g respectively, which were both taken at 50m from BIA A, it supports the claim that Cd pollution from metal fragments occurs in the immediate vicinity of the fragment itself. In BIA A the highest single concentration is found, but when excluding the outlier of sample 23 the mean of BIA A goes from 3.718 μg/g to 0.1304 μg/g and is significantly lower than the means of BIA B of 0.1340 μg/g and the background data of 0.1815 μg/g, as seen in figure 4.5. Cadmium appears to correlate with Cu in the PCA. The analysed Cd levels can stem from long-range atmospheric deposition and from local pollution sources like fossil fuels, coal mining, research stations and tourist shipping [110, 111, 112]. In addition a potential secondary source of increased Cd can be melting glaciers [113]. Higher levels of Cd in BIA B compared to BIA A can be explained by BIA B being closer to Stuphallet were birds with accumulated Cd are more abundant [114].

Table 4.2: Results from the statistical tests applied to the Cd data, where groups A, B and K denote BIA A, BIA B and the relevant background data from Kveli [106] respectively.

Statistical test	Groups	N	Significance	Conclusion
Kruskal-Wallis	A, B, K	33/33/11	.001	Reject H_0
Mann-Whitney U	A, B	33/33	.00001	Reject H_0
Mann-Whitney U	A, K	33/11	.00001	Reject H_0
Mann-Whitney U	B, K	33/11	.02144	Reject H_0

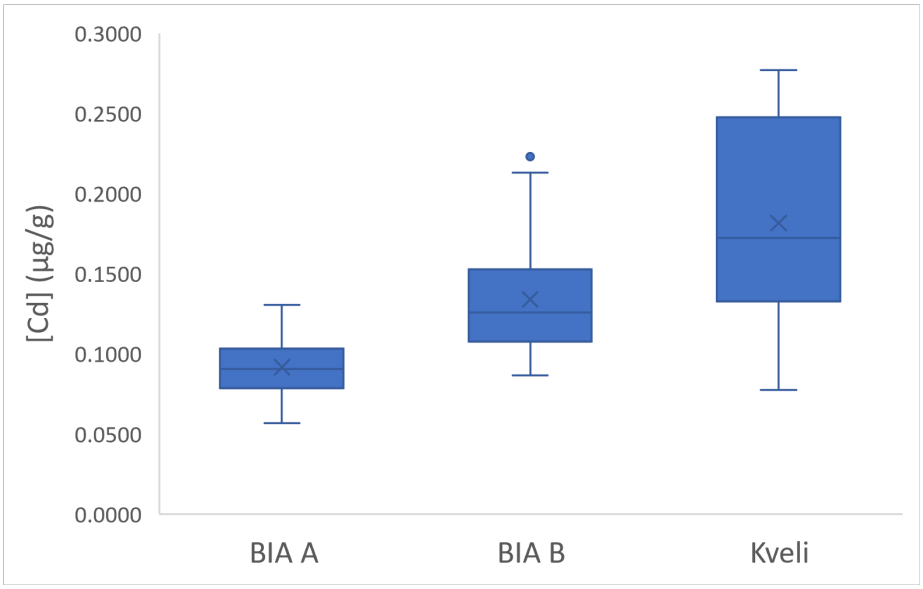

Figure 4.5: Concentrations in μg/g of Cd from BIA A, BIA B, and relevant background data from Kveli [106].

4.1.3 Iron

Table 4.3 shows that H_0 is rejected for the ANOVA-test, and the t-tests between BIA A and BIA B, and between BIA A and the background data, while H_0 is retained for the t-test between BIA B and the background data. Thus, the mean of BIA A of 22443 μg/g is significantly different from the means of BIA B of 19327 μg/g and the background data of 18973 μg/g, while the means of BIA B and the background data do not significantly differ. Figure 4.6 helps illustrate that the mean of BIA A is significantly higher than the means of BIA B and the background data. The spread of the background data can be explained through the large sampling area the background data covers. Iron is a large contributor to PC1, and contributes somewhat to PC2. The significant difference between BIA A and BIA B appears to be attributed to the underlying geological differences and vicinity to coal mines as seen in the Pb-loading PC1- PC2-coordinates [110, 17, 108].

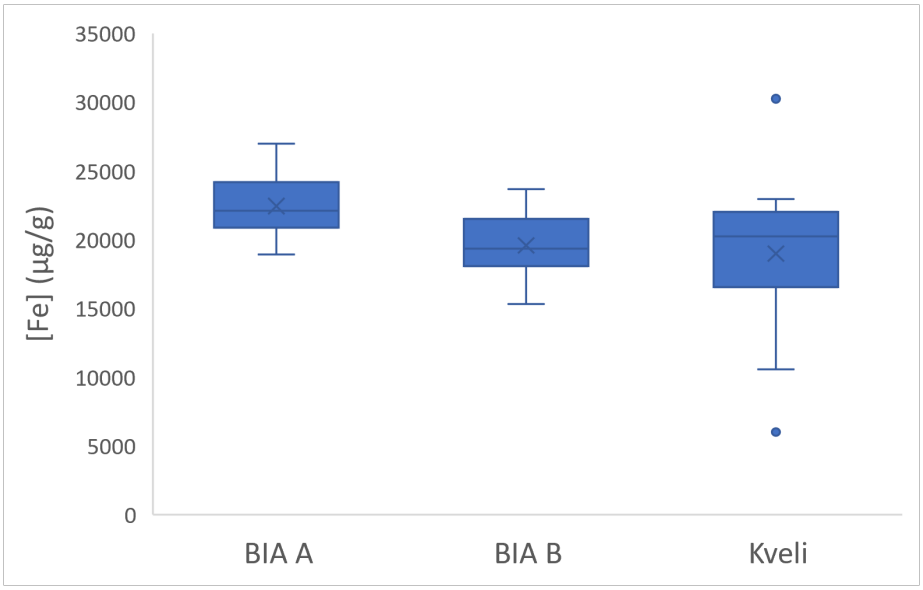

Figure 4.6: Concentrations in μg/g of Fe from BIA A, BIA B, and relevant background data from Kveli [106].

Table 4.3: Results from the statistical tests applied to the Fe data, where groups A, B and K denote BIA A, BIA B and the relevant background data from Kveli [106] respectively.

Statistical test	Groups	N	Significance	Conclusion
ANOVA	A, B, K	34/33/11	.000313	Reject H_0
t-test	A, B	34/33	.00001	Reject H_0
t-test	A, K	34/11	.004236	Reject H_0
t-test	B, K	33/11	.321789	Retain H_0

4.1.4 Lead

The statistical results in table 4.4 show that H_0 is rejected for the ANOVA-test, and the t-tests between BIA A and BIA B, and between BIA A and the background data, while H_0 is retained for the t-test between BIA B and the background data. Thus, the mean of BIA A of 12.64 μg/g is significantly different from the means of BIA B of 10.60 μg/g and the background data of 10.71 μg/g, while the means of BIA B and the background data do not significantly differ. The mean of BIA A is significantly higher than the means of BIA B and the background data (figure 4.7. This difference can be connected to the vicinity of BIA A to the old mining sites compared to BIA B [107, 108].

Table 4.4: Results from the statistical tests applied to the Pb data, where groups A, B and K denote BIA A, BIA B and the relevant background data from Kveli [106] respectively.

Statistical test	Groups	N	Significance	Conclusion
ANOVA	A, B, K	34/33/11	.000692	Reject H_0
t-test	A, B	34/33	.00001	Reject H_0
t-test	A, K	34/11	.020422	Reject H_0
t-test	B, K	33/11	.450239	Retain H_0

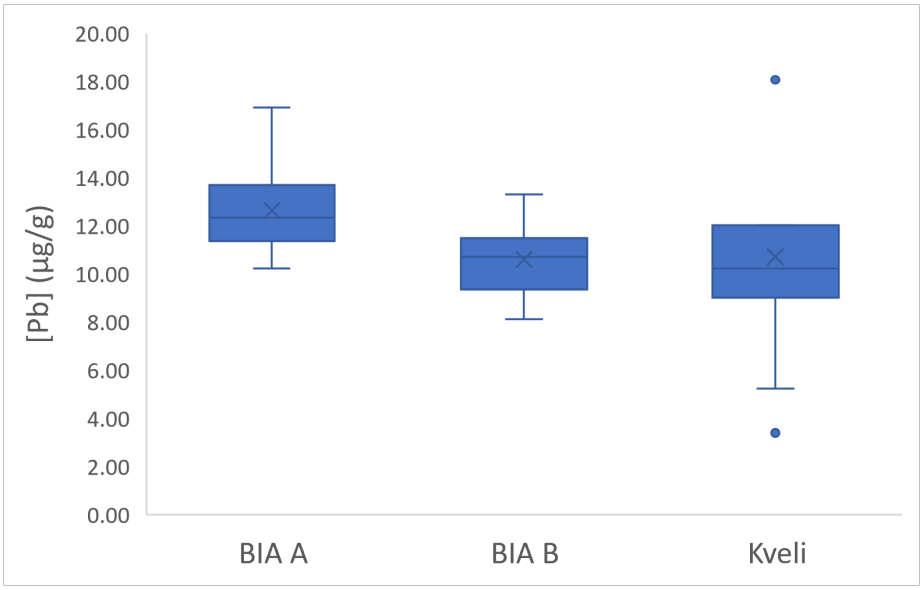

Figure 4.7: Concentrations in μg/g of Pb from BIA A, BIA B, and relevant background data from Kveli [106].

4.1.5 Arsenic

H_0 is rejected for all the statistical tests, as seen in table 4.5, and thus the means of BIA A of 4.199 μg/g, BIA B of 2.698 μg/g and the background data of 3.617 μg/g are significantly different to each other. Figure 4.8 illustrates that the levels of As is significantly higher in BIA A than BIA B, while the levels reported in the background data fall between the two. This significant difference in As-concentration is mainly down to BIA A being closer to the old mining sites than BIA B, as substantiated by the composition of PC2 [107, 108].

Table 4.5: Results from the statistical tests applied to the As data, where groups A, B and K denote BIA A, BIA B and the relevant background data from Kveli [106] respectively.

Statistical test	Groups	N	Significance	Conclusion
ANOVA	A, B, K	34/33/11	.00001	Reject H_0
t-test	A, B	34/33	.00001	Reject H_0
t-test	A, K	34/11	.012944	Reject H_0
t-test	B, K	33/11	.000017	Reject H_0

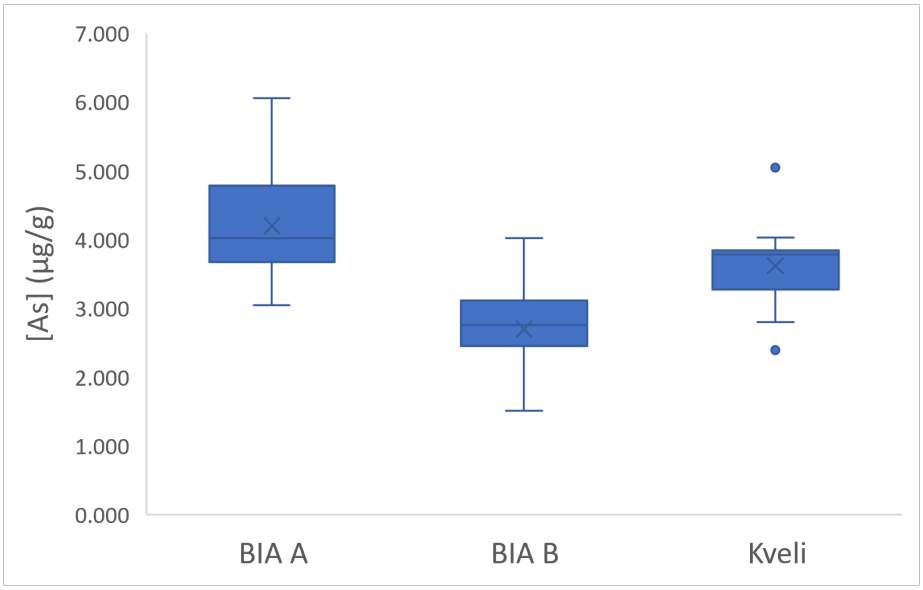

Figure 4.8: Concentrations in μg/g of As from BIA A, BIA B, and relevant background data from Kveli [106].

4.1.6 Aluminium

For Al, the means of BIA A of 22774 μg/g, BIA B of 20469 μg/g and the background data of 21849 μg/g were not significantly different as H_0 was retained for all the statistical tests, as shown in table 4.6. The levels of Al across the three sample data sets are similarly distributed, as seen in figure 4.9. As seen in the PCA-plot for PC1 and PC2, Al is primarily attributed to the underlying geology [17, 110, 112].

Table 4.6: Results from the statistical tests applied to the Al data, where groups A, B and K denote BIA A, BIA B and the relevant background data from Kveli [106] respectively.

Statistical test	Groups	N	Significance	Conclusion
Kruskal-Wallis	A, B, K	34/33/11	.197	Retain H_0
Mann-Whitney U	A, B	34/33	.0536	Retain H_0
Mann-Whitney U	A, K	34/11	.62414	Retain H_0
Mann-Whitney U	B, K	33/11	.88866	Retain H_0

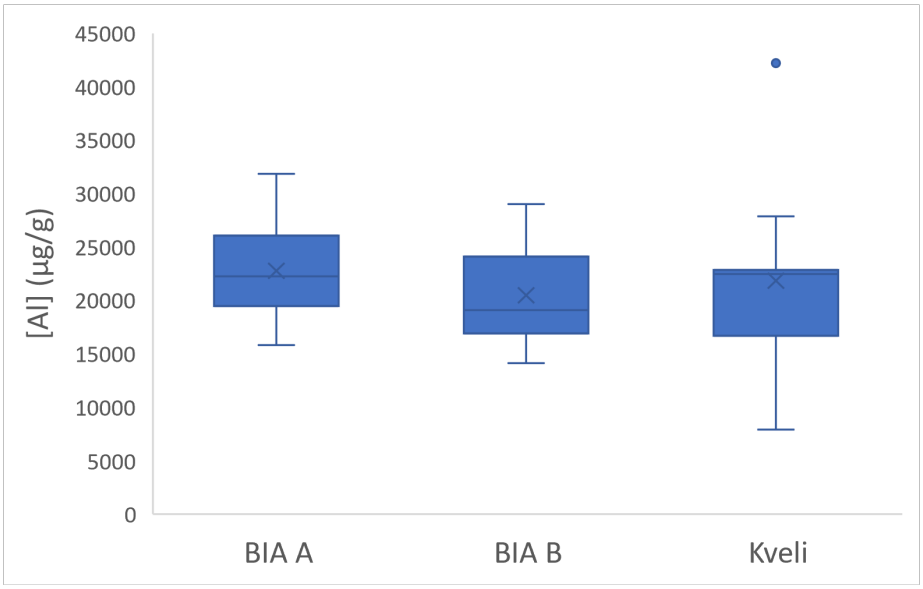

Figure 4.9: Concentrations in μg/g of Al from BIA A, BIA B, and relevant background data from Kveli [106].

4.1.7 Titanium

For Ti, the statistical means of BIA A of 521.9 μg/g, BIA B of 490.1 μg/g and the background data of 465.4 μg/g were not significantly different as H_0 was retained for all the statistical tests, as shown in table 4.7. Figure 4.10 shows that the levels of Ti for BIA A and BIA B are similarly distributed, while the background data has more variance. The primary source of Ti in the samples is likely crustal composition, which coincides with the composition of PC1 [112].

Table 4.7: Results from the statistical tests applied to the Ti data, where groups A, B and K denote BIA A, BIA B and the relevant background data from Kveli [106] respectively.

Statistical test	Groups	N	Significance	Conclusion
ANOVA	A, B, K	34/33/11	.207537	Retain H_0
t-test	A, B	34/33	.05174	Retain H_0
t-test	A, K	34/11	.080416	Retain H_0
t-test	B, K	33/11	.271689	Retain H_0

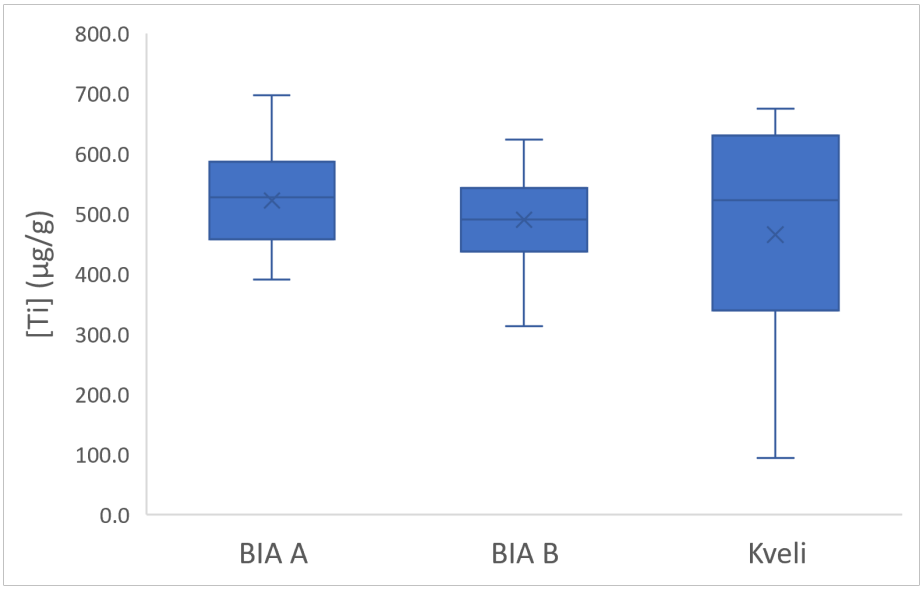

Figure 4.10: Concentrations in μg/g of Ti from BIA A, BIA B, and relevant background data from Kveli [106].

4.1.8 Lithium

As shown in table 4.8 the t-test between BIA A and BIA B concludes with a rejection of H_0 which indicates that the mean of BIA A of 17.12 μg/g is significantly different from the mean of BIA B of 14.58 μg/g. The means of BIA A and BIA B are not respectively significantly different from the mean of the background data of 17.65 μg/g. The Li levels are higher in BIA A than BIA B, while the range of the background data covers the ranges of both BIAs. The PCA-plot indicates that the difference in Li levels between BIA A and BIA B can be attributed to the underlying geology as the composition differs between the two sampling areas [115, 17].

Table 4.8: Results from the statistical tests applied to the Li data, where groups A, B and K denote BIA A, BIA B and the relevant background data from Kveli [106] respectively.

Statistical test	Groups	N	Significance	Conclusion
Kruskal-Wallis	A, B, K	34/33/11	.002	Reject H_0
Mann-Whitney U	A, B	34/33	.00044	Reject H_0
Mann-Whitney U	A, K	34/11	.40654	Retain H_0
Mann-Whitney U	B, K	33/11	.15854	Retain H_0

4.1.9 Copper

Sample 20, taken at BIA A at 125m from the epicentre, was omitted from the statistical tests due to being an extreme deviation with a value of 437.9 μg/g. This sample is the main contributor to PC3 as seen in figures 4.2 and 4.4. The mean of Cu in BIA A with the outlier was 26.11 μg/g, compared to 13.63 μg/g when the outlier was removed. This sample coincides with higher levels of Zn and Sn. A possible explanation is that it has been affected by a nearby metal fragment although no fragment was found [109, 15]. No similar levels are found in sample 4 (13.94 μg/g) and 12 (15.08 μg/g) which were also taken 125m from the epicentre of BIA A. Table 4.9 shows that H_0 is rejected for the statistical tests between BIA A and the background data, and between BIA B and the background data respectively. This indicates that the means of BIA A of 13.63 μg/g and BIA B of 13.04 μg/g are each

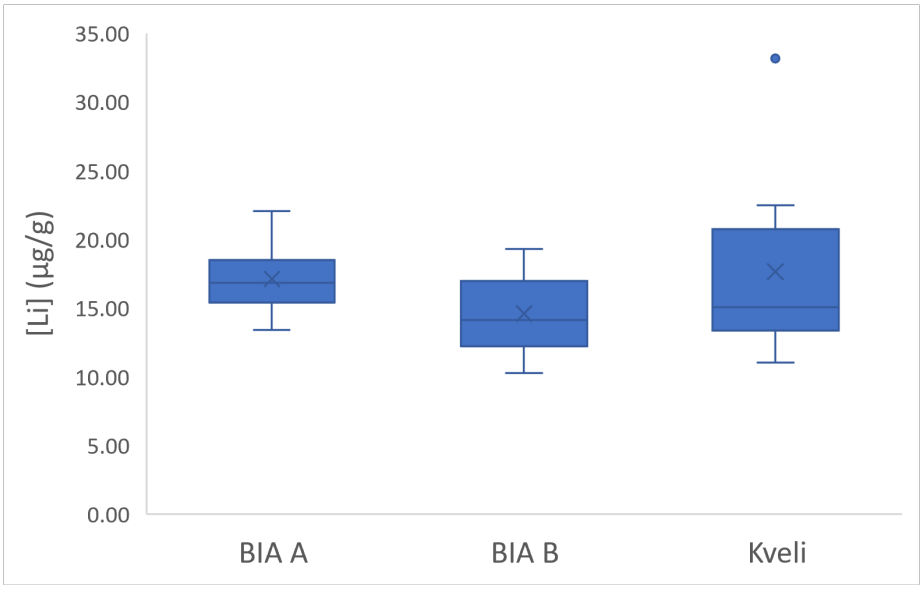

Figure 4.11: Concentrations in μg/g of Li from BIA A, BIA B, and relevant background data from Kveli [106].

significantly different from the mean of the background data of 10.08 μg/g. As figure 4.12 shows, the levels in both BIA A and B are higher than in the background data which can indicate a recent increase in Cu levels. The primary source of increased copper levels can be anthropogenic sources like coal mining and long-range atmospheric deposition [108, 111].

Table 4.9: Results from the statistical tests applied to the Cu data, where groups A, B and K denote BIA A, BIA B and the relevant background data from Kveli [106] respectively.

Statistical test	Groups	N	Significance	Conclusion
Kruskal-Wallis	A, B, K	33/33/11	.001	Reject H_0
Mann-Whitney U	A, B	33/33	.06432	Retain H_0
Mann-Whitney U	A, K	33/11	.00034	Reject H_0
Mann-Whitney U	B, K	33/11	.00124	Reject H_0

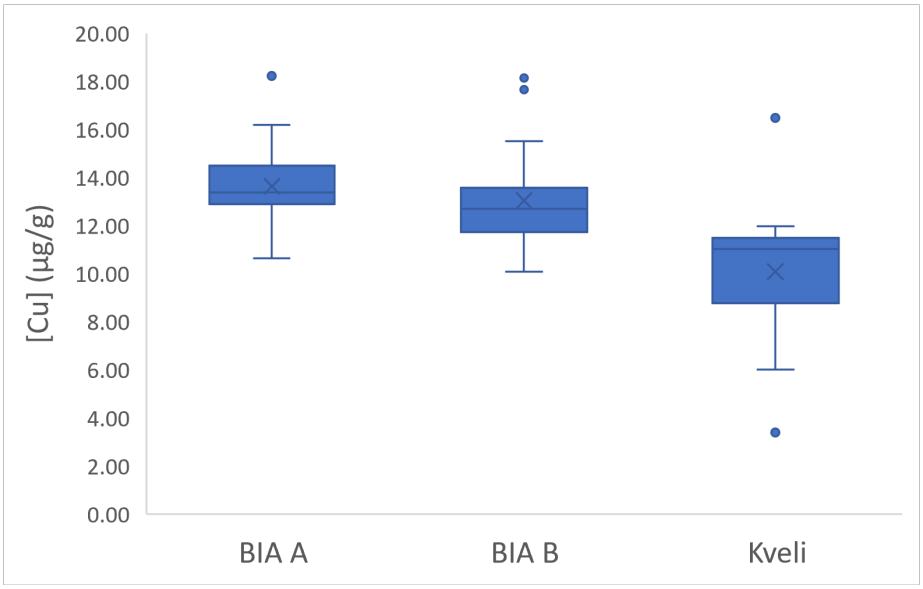

Figure 4.12: Concentrations in μg/g of Cu from BIA A, BIA B, and relevant background data from Kveli [106].

4.1.10 Zinc

Sample 20, taken at BIA A at 125m from the impact area, was omitted from the statistical tests due to being an extreme deviation with a value of 229.0 μg/g. The mean of Zn in BIA A with the outlier was 49.46 μg/g, compared to 44.02 μg/g when the outlier was removed. No similar levels are found in sample 4 (49.44 μg/g) and 12 (46.11 μg/g) which were also taken 125m from the epicentre of BIA A. Table 4.10 shows that H_0 is rejected for the test between BIA A and BIA B, and retained for the tests between BIA A and the background data, and between BIA B and the background data respectively. Thus, the means of BIA A of 44.02 μg/g and of BIA B of 38.20 μg/g are significantly different to each other, but not with the mean of the background data of of 40.92 μg/g. In figure 4.13 the Zn levels are generally higher in BIA A than BIA B, while the range of the background data covers the ranges of both BIAs, thus the source of increase in BIA A compared to BIA B is likely not related to anthropogenic activity over the last couple of years. The significant difference between BIA A and BIA B can be down to the vicinity of old mining cites as association with PC2 indicates [108].

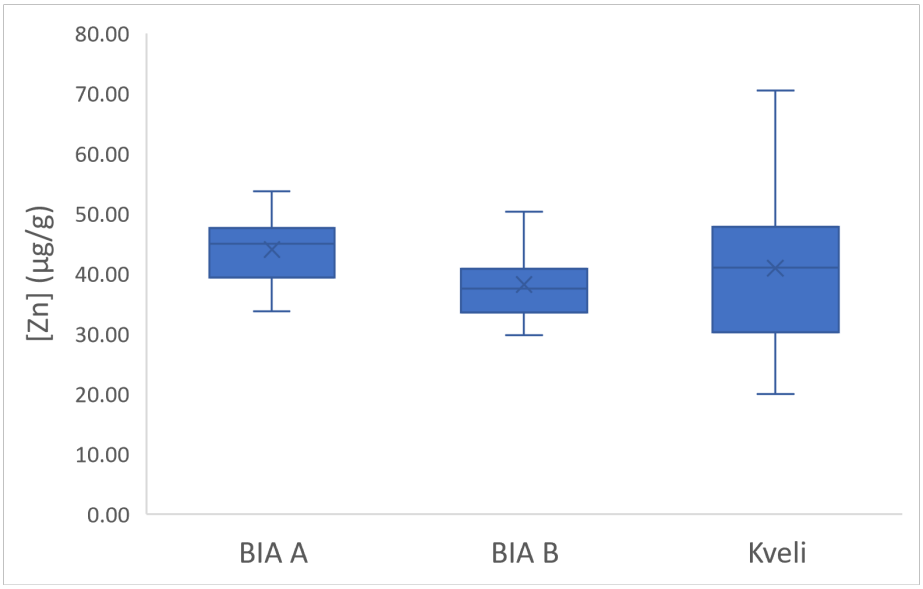

Figure 4.13: Concentrations in μg/g of Zn from BIA A, BIA B, and relevant background data from Kveli [106].

Table 4.10: Results from the statistical tests applied to the Zn data, where groups A, B and K denote BIA A, BIA B and the relevant background data from Kveli [106] respectively.

Statistical test	Groups	N	Significance	Conclusion
Kruskal-Wallis	A, B, K	33/33/11	.001	Reject H_0
Mann-Whitney U	A, B	33/33	.00012	Reject H_0
Mann-Whitney U	A, K	33/11	.28914	Retain H_0
Mann-Whitney U	B, K	33/11	.4654	Retain H_0

4.1.11 Tin

Sample 20, taken at BIA A at 125m from the epicentre, was omitted from the statistical tests due to being an extreme deviation with a value of 0.9280 μg/g. The mean of Zn in BIA A with the outlier was 0.4179 μg/g, compared to 0.4024 μg/g when the outlier was removed. No similar levels are found in sample 4 (0.4179 μg/g) and 12 (0.3811 μg/g) which were also taken 125m from the epicentre of BIA A. In table 4.11 H_0 is rejected for the test between BIA A and BIA B, and retained for the tests between BIA A and the background data, and between BIA B and the background data. This indicates that the means of BIA A of 0.4024 μg/g and BIA B of 0.4390 μg/g are significantly different with each other, but not with the background data of 0.4053 μg/g. In figure 4.14 the levels of Sn in BIA B are higher than in BIA A. The significant difference in Sn may be connected to bioaccumulation in fish, which in turn leads to biomagnification and contamination from guano [116].

Table 4.11: Results from the statistical tests applied to the Sn data, where groups A, B and K denote BIA A, BIA B and the relevant background data from Kveli [106] respectively.

Statistical test	Groups	N	Significance	Conclusion
Kruskal-Wallis	A, B, K	33/33/11	.039	Reject H_0
Mann-Whitney U	A, B	33/33	.01046	Reject H_0
Mann-Whitney U	A, K	33/11	.3843	Retain H_0
Mann-Whitney U	B, K	33/11	.42952	Retain H_0

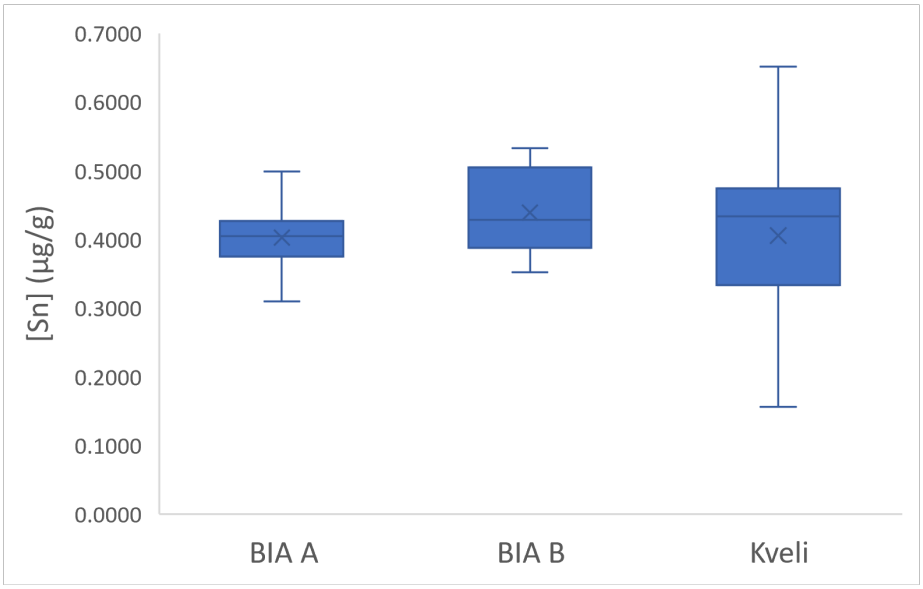

Figure 4.14: Concentrations in μg/g of Sn from BIA A, BIA B, and relevant background data from Kveli [106].

4.1.12 Cobalt

All the statistical tests for Co concluded with rejections of H_0 (table 4.12 and thus the means of BIA A of 9.864 μg/g, BIA B of 8.289 μg/g, and the background data of 7.723 μg/g are all significantly different to each other. The Co levels, seen in figure 4.15, are significantly higher in BIA A than in BIA B and the background data, and this could be tied to BIA A being closer to the old mining sites [107, 108].

Table 4.12: Results from the statistical tests applied to the Co data, where groups A, B and K denote BIA A, BIA B and the relevant background data from Kveli [106] respectively.

Statistical test	Groups	N	Significance	Conclusion
ANOVA	A, B, K	34/33/11	.00001	Reject H_0
t-test	A, B	34/33	.00001	Reject H_0
t-test	A, K	34/11	.00001	Reject H_0
t-test	B, K	33/11	.029603	Reject H_0

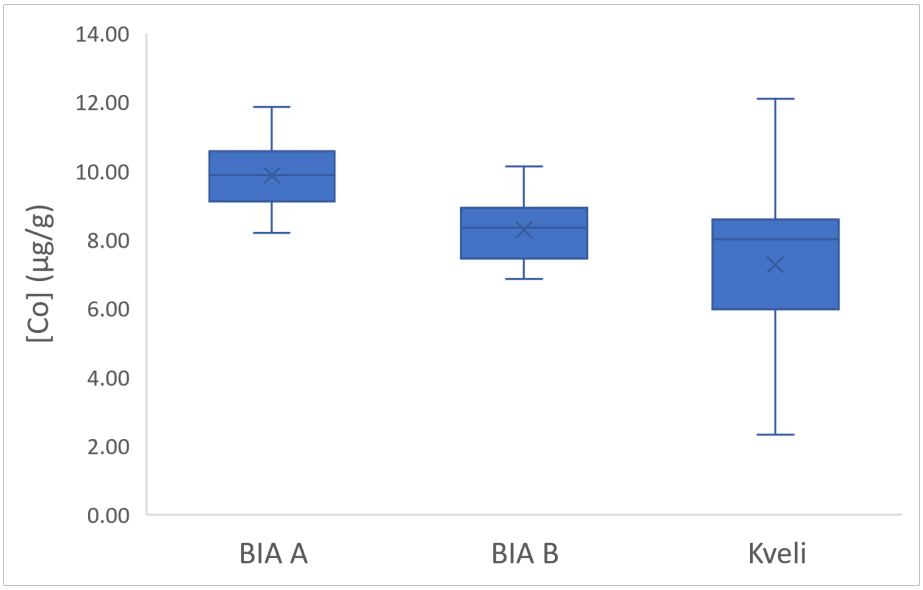

Figure 4.15: Concentrations in μg/g of Co from BIA A, BIA B, and relevant background data from Kveli [106].

4.1.13 Magnesium

The means of BIA A of 9791 μg/g, BIA B of 14708 μg/g, and the background data of 28509 μg/g are all significantly different from each other as shown in table 4.13. The levels of Mg are generally lower in the BIAs than the background data, as illustrated in figure 4.16, and thus it does not appear that these levels have increased over the recent years. The significant difference between BIA A and BIA B can be attributed to the underlying geological differences between Vestre and Austre Brøggerdalen [17].

Table 4.13: Results from the statistical tests applied to the Mg data, where groups A, B and K denote BIA A, BIA B and the relevant background data from Kveli [106] respectively.

Statistical test	Groups	N	Significance	Conclusion
Kruskal-Wallis	A, B, K	34/33/11	.001	Reject H_0
Mann-Whitney U	A, B	34/33	.00001	Reject H_0
Mann-Whitney U	A, K	34/11	.00001	Reject H_0
Mann-Whitney U	B, K	33/11	.0018	Reject H_0

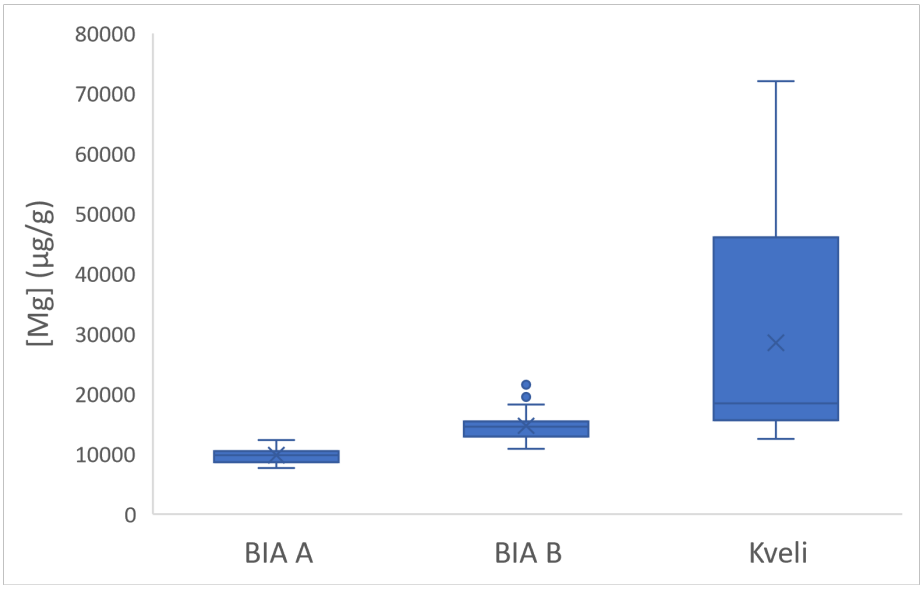

Figure 4.16: Concentrations in μg/g of Mg from BIA A, BIA B, and relevant background data from Kveli [106].

4.1.14 Beryllium

For Be, the statistical means of BIA A of 1.079 μg/g, BIA B of 1.042 μg/g and the background data of 0.9286 μg/g were not significantly different as H_0 was retained for all the statistical tests, as shown in table 4.14. As can be seen in figure 4.17 the levels of Be in BIA A and BIA B and the means of all three data sets are not significantly different, thus the levels of Al are therefore likely not tied to recent anthropogenic activity.

Table 4.14: Results from the statistical tests applied to the Be data, where groups A, B and K denote BIA A, BIA B and the relevant background data from Kveli [106] respectively.

Statistical test	Groups	N	Significance	Conclusion
Kruskal-Wallis	A, B, K	34/33/11	.352	Retain H_0
Mann-Whitney U	A, B	34/33	.90448	Retain H_0
Mann-Whitney U	A, K	34/11	.20054	Retain H_0
Mann-Whitney U	B, K	33/11	.16758	Retain H_0

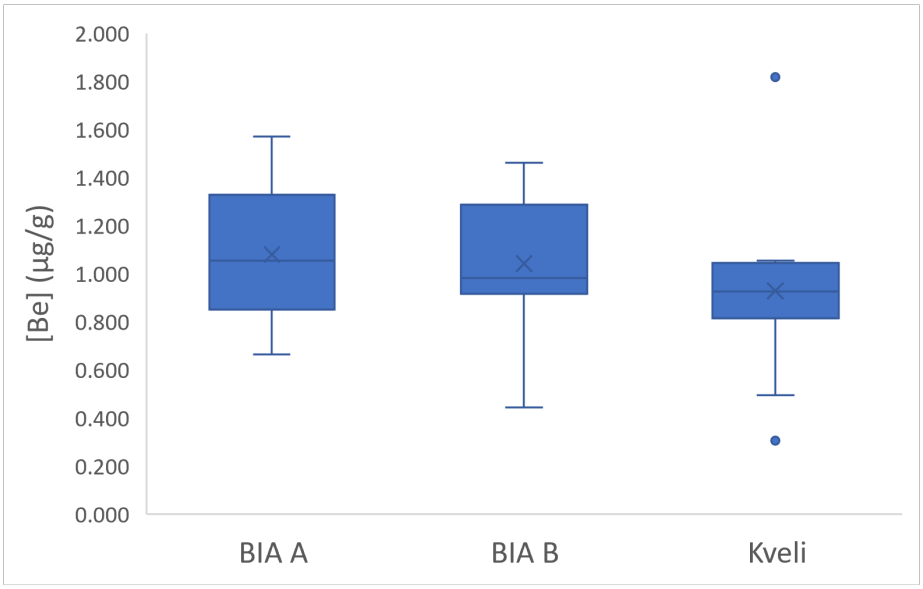

Figure 4.17: Concentrations in μg/g of Be from BIA A, BIA B, and relevant background data from Kveli [106].

4.2 PCB analysis

No samples showed any concentrations over LOD for any of the seven PCBs analysed (table 4.15). The chromatograms for the calibration curve (figures C.1-C.6), samples (figures C.7-C.18 and the calibration curves for the seven PCBs (figures D.1-D.7) can be found in appendices C and D. If there had been PCBs present as a result of rocket activity sampling should reveal increased levels, due to the high K_{OA} and thus, the affinity of PCBs to organic matter, over air and water. This affinity however, could also lead to highly localised PCB pollution. It is therefore possible that the sampling did not cover a potentially contaminated area. Previously reported concentrations of the PCBs of interest in the Brøggerdalen area indicated that all levels were below the detection limit [75]. It should also be noted that PCB-138 and PCB-153 had overlapping retention times and could thus not be adequately separated in GC-MS, which is also reflected in recoveries in figure 4.18 and table 4.16. For the other PCBs, the recovery testing shows that the analysis should be suitable for PCB detection in samples, and that the method has not suffered large losses.

Table 4.15: Concentrations in ng/g of the PCBs analysed.

Sample	[PCB-28]	[PCB-52]	[PCB-101]	[PCB-118]	[PCB-138]	[PCB-153]	[PCB-180]
1	<LOD	<LOD	<LOD	<LOD	<LOD	<LOD	<LOD
2	<LOD	<LOD	<LOD	<LOD	<LOD	<LOD	<LOD
3	<LOD	<LOD	<LOD	<LOD	<LOD	<LOD	<LOD
4	<LOD	<LOD	<LOD	<LOD	<LOD	<LOD	<LOD
5	<LOD	<LOD	<LOD	<LOD	<LOD	<LOD	<LOD
6	<LOD	<LOD	<LOD	<LOD	<LOD	<LOD	<LOD
7	<LOD	<LOD	<LOD	<LOD	<LOD	<LOD	<LOD
8	<LOD	<LOD	<LOD	<LOD	<LOD	<LOD	<LOD
9	<LOD	<LOD	<LOD	<LOD	<LOD	<LOD	<LOD
10	<LOD	<LOD	<LOD	<LOD	<LOD	<LOD	<LOD
11	<LOD	<LOD	<LOD	<LOD	<LOD	<LOD	<LOD
12	<LOD	<LOD	<LOD	<LOD	<LOD	<LOD	<LOD

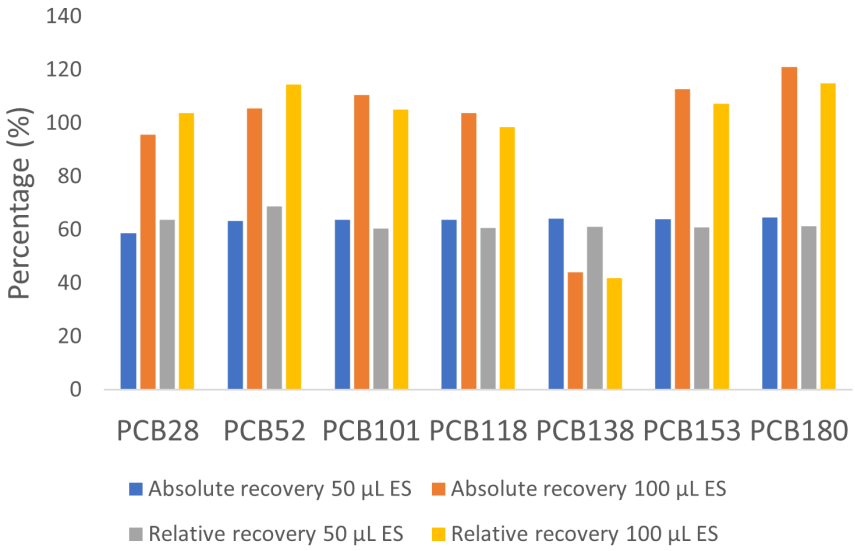

Figure 4.18: Absolute and relative recoveries of the analysed PCBs with different amounts of external standard (ES) added.

Table 4.16: LOD and LOQ in ng/g of the PCBs analysed.

PCB	LOD (ng/g)	LOQ (ng/g)
PCB-28	38.77	117.5
PCB-52	38.69	117.2
PCB-101	39.14	118.6
PCB-118	38.13	115.5
PCB-138	39.05	118.3
PCB-153	40.13	121.6
PCB-180	34.47	104.5

5 Conclusion

Two sample sites in Brøggerdalen, Ny-Ålesund, Svalbard were analysed in connection with rocket launch activity in the area. Trace elements and PCBs were analysed from overbank sediments from the Bayelva river. The levels of the PCBs of interest were below the limit of detection in both areas. The samples connected to BIA A showed significantly higher levels of Fe, Pb, As, Li, Zn and Co, while the samples connect to BIA B showed significantly higher levels of Cd, Sn and Mg. The levels of Fe and Li can be connected to the crustal composition, the levels of As, Fe, Pb, Zn and Co can be connected to the vicinity of old mining sites, the levels of Mg can be connected to the sedimentary rocks, and the levels of Cd and Sn can be connected to trace element contamination in birds. Of note are samples 20 and 23 which showed elevated levels of Cu, Zn and Sn, and Cd respectively. These outliers may be attributed to metal fragments, and there was no indication of these elevated levels in other, nearby samples.

The composition of the PCs appear to unveil some hidden phenomena in the sample data. The main contributors to PC1 are elements associated with the underlying crustal composition. PC1 explains 47% of the total variance in the data. The main contributors to PC2 are elements associated with differences in sedimentary rock composition between Vestre and Austre Brøggerdalen and the vicinity to the old coal mines in the Ny-Ålesund area. PC2 explains 13% of the total variance in the data. PC3 is mainly influenced by sample 20 with the increased Cu, Zn and Sn levels and explains 10% of the total variance in the data.

To conclude, contamination with a plausible connection to the rocket activity in the area appeared to stem from metal fragments and did not contribute to the overall levels of trace elements and PCBs in the sampling area.

References

[1] Arctic Monitoring and Assessment Programme (AMAP), ed. *AMAP assessment report: Arctic pollution issues*. Oslo, Norway: The Programme, 1998. 859 pp. ISBN: 978-82-7655-061-0.

[2] Secretariat of the Stockholm Convention. *The 12 Initial POPs*. 2001. URL: http://chm.pops.int/TheConvention/ThePOPs/The12InitialPOPs/tabid/296/Default.aspx (visited on 04/22/2022).

[3] UNECE. *Protocol on Persistent Organic Pollutants (POPs)*. 2014. URL: https://unece.org/environment-policy/air/protocol-persistent-organic-pollutants-pops (visited on 07/30/2022).

[4] Chester H. Penning. "Physical Characteristics and Commercial Possibilities of Chlorinated Diphenyl". In: *Industrial & Engineering Chemistry* 22.11 (Nov. 1930), pp. 1180–1182. ISSN: 0019-7866, 1541-5724. DOI: 10.1021/ie50251a020. URL: https://pubs.acs.org/doi/abs/10.1021/ie50251a020.

[5] O Hutzinger, S Safe, and V Zitko. *The chemistry of PCB's*. OCLC: 1145897547. 2018. ISBN: 978-1-315-89149-1.

[6] National Research Council (U.S.), ed. *Polychlorinated biphenyls: a report*. Washington: National Academy of Sciences, 1979. 182 pp. ISBN: 978-0-309-02885-1.

[7] Mitchell D. Erickson. *Analytical chemistry of PCBs*. 2nd ed. Boca Raton, Fla: CRC/Lewis Publ, 1997. 667 pp. ISBN: 978-0-87371-923-0.

[8] Arctic Monitoring and Assessment Programme (AMAP). *AMAP Assessment 2002: Heavy Metals in the Arctic.* Accepted: 2015-07-14T11:18:34Z. Arctic Monitoring and Assessment Programme (AMAP), June 1, 2005. ISBN: 978-82-7971-018-9. URL: https://oaarchive.arctic-council.org/handle/11374/706.

[9] E. Steinnes, R. O. Allen, H. M. Petersen, J. P. Rambæk, and P. Varskog. "Evidence of large scale heavy-metal contamination of natural surface soils in Norway from long-range atmospheric transport". In: *Science of The Total Environment* 205.2 (Oct. 20, 1997), pp. 255–266. ISSN: 0048-9697. DOI: 10.1016/S0048-9697(97)00209-X. URL: https://www.sciencedirect.com/science/article/pii/S004896979700209X.

[10] T. Gouin, D. Mackay, K. C. Jones, T. Harner, and S. N. Meijer. "Evidence for the "grasshopper" effect and fractionation during long-range atmospheric transport of organic contaminants". In: *Environmental Pollution*. Persistant Organic Pollutants 128.1 (Mar. 1, 2004), pp. 139–148. ISSN: 0269-7491. DOI: 10.1016/j.envpol.2003.08.025. URL: https://www.sciencedirect.com/science/article/pii/S0269749103003385.

[11] J. A. Dallas, S. Raval, J. P. Alvarez Gaitan, S. Saydam, and A. G. Dempster. "The environmental impact of emissions from space launches: A comprehensive review". In: *Journal of Cleaner Production* 255 (May 10, 2020), p. 120209. ISSN: 0959-6526. DOI: 10.1016/j.jclepro.2020.120209. URL: https://www.sciencedirect.com/science/article/pii/S0959652620302560.

[12] P. P. Krechetov, V. V. Neronov, T. V. Koroleva, and O. V. Chernistova. "Transformation of the soil-vegetation cover in carrier rocket first-stage impact areas". In: *Arid Ecosystems* 1.1 (Jan. 2011), pp. 59–64. ISSN: 2079-0961, 2079-0988. DOI: 10.1134/S2079096111010045. URL: http://link.springer.com/10.1134/S2079096111010045.

[13] The Grand Challenge Initiative. *Forsiden*. GCI. Aug. 26, 2019. URL: https://www.grandchallenge.no/ (visited on 07/30/2022).

[14] The Grand Challenge Initiative. *Project CUSP*. GCI. Aug. 27, 2019. URL: https://www.grandchallenge.no/project-cusp/ (visited on 07/30/2022).

[15] Wenche Aas, Jean-Charles Gallet, Anne Karine Halse, Ove Hermansen, Øyvind Mikkelsen, Christina A Pedersen, Andrea Spolaor, Kjersti Tørnkvist, and Hilde Uggerud. *Effects of rocket launches in Ny-Ålesund, 2018 - 2019*. Apr. 13, 2021, p. 53.

[16] *TopoSvalbard - Norsk Polarinstitutt*. URL: https://toposvalbard.npolar.no/ (visited on 06/11/2022).

[17] Wiesława Ewa Krawczyk, Bernard Lefauconnier, and Lars-Evan Pettersson. "Chemical denudation rates in the Bayelva Catchment, Svalbard, in the Fall of 2000". In: *Physics and Chemistry of the Earth, Parts A/B/C*. The changing physical environment of Ny-Alesund Svalbard 28.28 (Jan. 1, 2003), pp. 1257–1271. ISSN: 1474-7065. DOI: 10.1016/j.pce.2003.08.054. URL: https://www.sciencedirect.com/science/article/pii/S1474706503002043.

[18] John E. Brittain, Jim Bogen, Ludmila G. Khokhlova, Kjetil Melvold, Angelina S. Stenina, Gisli M. Gislason, Sturla Brørs, Sergej K. Kochanov, Jon S. Olafsson, Vasily I. Ponomarev, Arne J. Jensen, Alexander V. Kokovkin, and Lars-Evan Pettersson. *Arctic rivers*. Accepted: 2021-01-13T12:11:46Z Publication Title: 337-379. Academic Press, 2009. ISBN: 978-0-12-369449-2. URL: https://nve.brage.unit.no/nve-xmlui/handle/11250/2722767.

[19] Audun Hjelle. *Geology of Svalbard*. Polarhåndbok 7. Oslo: Norsk Polarinst, 1993. 162 pp. ISBN: 978-82-7666-057-9.

[20] S. K. Haldar. *Introduction to mineralogy and petrology*. Amsterdam: Elsevier, 2014. 338 pp. ISBN: 978-0-12-408133-8.

[21] W. A. Deer, Robert A. Howie, and Jack Zussman. *An introduction to the rock-forming minerals*. 3. ed. London: The Minerological Society, 2013. 498 pp. ISBN: 978-0-903056-27-4.

[22] John W. Anthony, Richard A. Bideaux, Kenneth W. Bladh, and Monte C. Nichols, eds. *Handbook of Mineralogy*. Chantilly, VA 20151-1110, USA: Mineralogical Society of America. URL: http://www.handbookofmineralogy.org/.

[23] Deborah V Chapman, Unesco, World Health Organization, and United Nations Environment Programme. *Water quality assessments: a guide to the use of biota, sediments, and water in environmental monitoring*. OCLC: 69243714. Place of publication not identified: Taylor & Francis e-Library, 2003. ISBN: 978-0-203-47671-0. URL: http://engnetbase.com/ejournals/books/book_summary/summary.asp?id=2685.

[24] C. W. Fetter. *Applied hydrogeology*. Fourth edition, new international edition. Pearson custom library. Harlow, Essex: Pearson Education, 2014. 612 pp. ISBN: 978-1-292-02290-1.

[25] F. W. Fifield and P. J. Haines, eds. *Environmental analytical chemistry*. 2nd ed. Oxford ; Malden, MA: Blackwell Science, 2000. 490 pp. ISBN: 978-0-632-05383-4.

[26] Nelson R. Nunnally. "Definition and Identification of Channel and Overbank Deposits and Their Respective Roles In Flood Plain Formation". In: *The Professional Geographer* 19.1 (Jan. 1967), pp. 1–4. ISSN: 0033-0124, 1467-9272. DOI: 10.1111/j.0033-0124.1967.00001.x.

URL: http://www.tandfonline.com/doi/abs/10.1111/j.0033-0124.1967.00001.x.

[27] *Overbank-sediments — Norges Geologiske Undersøkelse*. URL: https://www.ngu.no/en/topic/overbank-sediments (visited on 04/26/2022).

[28] R. T. Ottesen, J. Bogen, B. Bølviken, and T. Volden. "Overbank sediment: a representative sample medium for regional geochemical mapping". In: *Journal of Geochemical Exploration*. 12th International Geochemical Exploration Symposium and the 4th Symposium on Methods of Geochemical Prospecting 32.1 (Apr. 1, 1989), pp. 257–277. ISSN: 0375-6742. DOI: 10.1016/0375-6742(89)90061-7. URL: https://www.sciencedirect.com/science/article/pii/0375674289900617.

[29] B. Bølviken, J. Bogen, M. Jartun, M. Langedal, R. T. Ottesen, and T. Volden. "Overbank sediments : a natural bed blending sampling medium for large—scale geochemical mapping". In: *Chemometrics and Intelligent Laboratory Systems*. Special Issue: 50 years of Pierre Gy's Theory of Sampling Proceedings: First World Conference on Sampling and Blending (WCSB1) Tutorials on sampling: Theory and Practice 74.1 (Nov. 28, 2004), pp. 183–199. ISSN: 0169-7439. DOI: 10.1016/j.chemolab.2004.06.006. URL: https://www.sciencedirect.com/science/article/pii/S0169743904001698.

[30] Wim Salomons and Ulrich Förstner. "Sediments and the Transport of Metals". In: *Metals in the Hydrocycle*. Berlin, Heidelberg: Springer Berlin Heidelberg, 1984, pp. 63–98. ISBN: 978-3-642-69327-4. DOI: 10.1007/978-3-642-69325-0_3. URL: http://link.springer.com/10.1007/978-3-642-69325-0_3.

[31] Herbert E. Allen. "The significance of trace metal speciation for water, sediment and soil quality criteria and standards". In: *Science of The Total Environment*. Proceedings of the 2nd European Conference on Ecotoxicology 134 (Jan. 1, 1993), pp. 23–45. ISSN: 0048-9697. DOI: 10.1016/S0048-9697(05)80004-X. URL: https://www.sciencedirect.com/science/article/pii/S004896970580004X.

[32] Werner Stumm and James J. Morgan. *Aquatic chemistry: chemical equilibria and rates in natural waters*. 3rd ed. Environmental science and technology. New York: Wiley, 1996. 1022 pp. ISBN: 978-0-471-51184-7.

[33] James F Pankow. *Aquatic chemistry concepts*. OCLC: 1032375133. 2018. ISBN: 978-0-87371-150-0. URL: https://search.ebscohost.com/login.aspx?direct=true&scope=site&db=nlebk&db=nlabk&AN=1797587.

[34] Sven Erik Jørgensen. "Chapter 4 - Adsorption and Ion Exchange". In: *Developments in Environmental Modelling*. Ed. by S. E. Jørgensen and M. J. Gromiec. Vol. 14. Mathematical Submodels in Water Quality Systems. Elsevier, Jan. 1, 1989, pp. 65–81. DOI: 10.1016/B978-0-444-88030-7.50003-2. URL: https://www.sciencedirect.com/science/article/pii/B9780444880307500032.

[35] H. Yıldırım Erbil. *Surface chemistry of solid and liquid interfaces*. Oxford, UK ; Malden, MA: Blackwell Pub, 2006. 352 pp. ISBN: 978-1-4051-1968-9.

[36] S. Ramamoorthy and B. R. Rust. "Heavy metal exchange processes in sediment-water systems". In: *Environmental Geology* 2.3 (May 1978), pp. 165–172. ISSN: 0943-0105, 1432-0495. DOI: 10.1007/BF02430670. URL: http://link.springer.com/10.1007/BF02430670.

[37] Werner Stumm, Herbert Hohl, and Felix Dalang. "Interaction of Metal Ions with Hydrous Oxide Surfaces". In: (1976), p. 14.

[38] Siegfried Siegesmund, T. Weiss, Axel Vollbrecht, and Geological Society of London, eds. *Natural stone, weathering phenomena, conservation strategies, and case studies*. Geological Society special publication no. 205. OCLC: ocm51870529. London: Geological Society, 2002. 448 pp. ISBN: 978-1-86239-123-9.

[39] Konrad B. Krauskopf. *Introduction to geochemistry*. 2d ed. McGraw-Hill international series in the earth and planetary sciences. New York: McGraw-Hill, 1979. 617 pp. ISBN: 978-0-07-035447-0.

[40] J M Pacyna and E G Pacyna. "An assessment of global and regional emissions of trace metals to the atmosphere from anthropogenic sources worldwide". In: *Environmental Reviews* 9.4 (Dec. 1, 2001), pp. 269–298. ISSN: 1181-8700, 1208-6053. DOI: 10.1139/a01-012. URL: http://www.nrcresearchpress.com/doi/10.1139/a01-012.

[41] Lawrence A. Ruth. "Energy from municipal solid waste: A comparison with coal combustion technology". In: *Progress in Energy and Combustion Science* 24.6 (Jan. 1, 1998), pp. 545–564. ISSN: 0360-1285. DOI: 10.1016/S0360-1285(98)00011-2. URL: https://www.sciencedirect.com/science/article/pii/S0360128598000112.

[42] David H. Klein, Anders W. Andren, Joel A. Carter, Jeul F. Emery, Cyrus Feldman, William Fulkerson, William S. Lyon, Jack C. Ogle, and Yair Talmi. "Pathways of thirty-seven trace elements through coal-fired power plant". In: *Environmental Science & Technology* 9.10 (Oct. 1975), pp. 973–979. ISSN: 0013-936X, 1520-5851. DOI: 10.1021/es60108a007. URL: https://pubs.acs.org/doi/abs/10.1021/es60108a007.

[43] L. Webster; L. Roose; P. Bersuder; M. Kotterman; M. Haarich; K. Vorkamp. "Determination of polychlorianted biphenyls (PCBs) in sediment and biota". In: (2013). Publisher: ICES. DOI: 10.17895/ICES.PUB.5078. URL: https://ices-library.figshare.com/articles/_/18627050.

[44] Donald. Mackay. "Correlation of bioconcentration factors". In: *Environmental Science & Technology* 16.5 (May 1982), pp. 274–278. ISSN: 0013-936X, 1520-5851. DOI: 10.1021/es00099a008. URL: https://pubs.acs.org/doi/abs/10.1021/es00099a008.

[45] Tom. Harner and Don. Mackay. "Measurement of Octanol-Air Partition Coefficients for Chlorobenzenes, PCBs, and DDT". In: *Environmental Science & Technology* 29.6 (June 1995), pp. 1599–1606. ISSN: 0013-936X, 1520-5851. DOI: 10.1021/es00006a025. URL: https://pubs.acs.org/doi/abs/10.1021/es00006a025.

[46] Curtis C Travis and Sheri T Hester. "Global chemical pollution". In: (May 1, 1991), p. 6. DOI: 10.1021/es00017a001.

[47] S. Jensen, A. G. Johnels, M. Olsson, and G. Otterlind. "DDT and PCB in Marine Animals from Swedish Waters". In: *Nature* 224.5216 (Oct. 1969). Number: 5216 Publisher: Nature Publishing Group, pp. 247–250. ISSN: 1476-4687. DOI: 10.1038/224247a0. URL: https://www.nature.com/articles/224247a0.

[48] Nanqin Li, Frank Wania, Ying D. Lei, and Gillian L. Daly. "A Comprehensive and Critical Compilation, Evaluation, and Selection of Physical–Chemical Property Data for Selected Polychlorinated Biphenyls". In: *Journal of Physical and Chemical Reference Data* 32.4 (Dec. 2003), pp. 1545–1590. ISSN: 0047-2689, 1529-7845. DOI: 10.1063/1.1562632. URL: http://aip.scitation.org/doi/10.1063/1.1562632.

[49] R. J. Cicerone, D. H. Stedman, R. S. Stolarski, A. N. Dingle, and R. A. Cellarius. *Assessment of possible environmental effects of space shuttle operations*. June 1973.

[50] Waldir A. Bizzo, Renata A. Figueiredo, and Valdelis F. de Andrade. "Characterization of Printed Circuit Boards for Metal and Energy Recovery after Milling and Mechanical Separation". In: *Materials* 7.6 (June 16, 2014), pp. 4555–4566. ISSN: 1996-1944. DOI: 10.3390/ma7064555. URL: https://www.ncbi.nlm.nih.gov/pmc/articles/PMC5455934/.

[51] George Paul Sutton and Donald M. Ross. *Rocket propulsion elements: an introduction to the engineering of rockets*. 4. ed. A Wiley-Interscience publication. New York: Wiley, 1976. 557 pp. ISBN: 978-0-471-83836-4.

[52] Tetsuo Yasaka and Junjiro Onoda. "Spacecraft Structures". In: *Encyclopedia of Physical Science and Technology*. Elsevier, 2003, pp. 449–461. ISBN: 978-0-12-227410-7. DOI: 10.1016/B0-12-227410-5/00899-1. URL: https://linkinghub.elsevier.com/retrieve/pii/B0122274105008991.

[53] Natascha Wosnick, Ana Paula Chaves, Renata Daldin Leite, Jorge Luiz Silva Nunes, Tatiana Dillenburg Saint'Pierre, Isabel Quental Willmer, and Rachel Ann Hauser-Davis. "Nurse sharks, space rockets and cargo ships: Metals and oxidative stress in a benthic, resident and large-sized mesopredator, Ginglymostoma cirratum". In: *Environmental Pollution* 288 (Nov. 1, 2021), p. 117784. ISSN: 0269-7491. DOI: 10.1016/j.envpol.2021.117784. URL: https://www.sciencedirect.com/science/article/pii/S026974912101366X.

[54] Amanda J. Barker, Jay L. Clausen, Thomas A. Douglas, Anthony J. Bednar, Christopher S. Griggs, and William A. Martin. "Environmental impact of metals resulting from military training activities: A review". In: *Chemosphere* 265 (Feb. 1, 2021), p. 129110. ISSN: 0045-6535.

DOI: 10.1016/j.chemosphere.2020.129110. URL: https://www.sciencedirect.com/science/article/pii/S0045653520333075.

[55] Sergey A. Lednev, Ivan N. Semenkov, Galya V. Klink, Pavel P. Krechetov, Anna V. Sharapova, and Tatyana V. Koroleva. "Impact of kerosene pollution on ground vegetation of southern taiga in the Amur Region, Russia". In: *Science of The Total Environment* 772 (June 10, 2021), p. 144965. ISSN: 0048-9697. DOI: 10.1016/j.scitotenv.2021.144965. URL: https://www.sciencedirect.com/science/article/pii/S0048969721000310.

[56] William J. Doucette, Laurie S. McNeill, Scout Mendenhall, Paul V. Hancock, Jason E. Wells, Kevin J. Thackeray, and David P. Gosen. "The sky is falling: Chemical characterization and corrosion evaluation of deposition produced during the static testing of solid rocket motors". In: *Science of The Total Environment* 447 (Mar. 1, 2013), pp. 390–395. ISSN: 0048-9697. DOI: 10.1016/j.scitotenv.2013.01.013. URL: https://www.sciencedirect.com/science/article/pii/S0048969713000223.

[57] Georgina A. Rivera-Ingraham, Madalena Andrade, Regis Vigouroux, Montserrat Solé, Katherina Brokordt, Jehan-Hervé Lignot, and Rosa Freitas. "Are we neglecting earth while conquering space? Effects of aluminized solid rocket fuel combustion on the physiology of a tropical freshwater invertebrate". In: *Chemosphere* 268 (Apr. 1, 2021), p. 128820. ISSN: 0045-6535. DOI: 10.1016/j.chemosphere.2020.128820. URL: https://www.sciencedirect.com/science/article/pii/S0045653520330186.

[58] G. E Batley. "Quality Assurance in Environmental Monitoring". In: *Marine Pollution Bulletin* 39.1 (Jan. 1, 1999), pp. 23–31. ISSN: 0025-326X. DOI: 10.1016/S0025-326X(99)00016-8. URL: https://www.sciencedirect.com/science/article/pii/S0025326X99000168.

[59] International Organization for Standardization. *ISO in brief*. URL: https://www.iso.org/files/live/sites/isoorg/files/store/en/PUB100007.pdf (visited on 06/04/2022).

[60] International Organization for Standardization. *ISO 18400-104 Soil quality — Sampling — Part 104: Strategies*. 2018. URL: https://www.standard.no/no/Nettbutikk/produktkatalogen/Produktpresentasjon/?ProductID=998926.

[61] International Organization for Standardization. *ISO 18400-202 Soil quality — Sampling — Part 202: Preliminary investigations*. 2018. URL: https://www.standard.no/no/Nettbutikk/produktkatalogen/Produktpresentasjon/?ProductID=1000434.

[62] International Organization for Standardization. *ISO 18400-203 Soil quality — Sampling — Part 203: Investigation of potentially contaminated sites*. 2018. URL: https://www.standard.no/no/Nettbutikk/produktkatalogen/Produktpresentasjon/?ProductID=998932.

[63] International Organization for Standardization. *ISO 16720 Soil quality — Pretreatment of samples by freeze-drying for subsequent analysis*. 2005. URL: https://www.standard.no/no/Nettbutikk/produktkatalogen/Produktpresentasjon/?ProductID=117086.

[64] International Organization for Standardization. *ISO/TS 16965 Soil quality — Determination of trace elements using inductively coupled plasma mass spectrometry (ICP-MS)*. 2013. URL: https://www.standard.no/no/Nettbutikk/produktkatalogen/Produktpresentasjon/?ProductID=654064.

[65] Standard Norge. *NS-EN 16171 Sludge, treated biowaste and soil Determination of elements using inductively coupled plasma mass spectrometry (ICP-MS)*. 2016. URL: https://www.standard.no/no/Nettbutikk/produktkatalogen/Produktpresentasjon/?ProductID=871048.

[66] International Organization for Standardization. *ISO 16703 Soil quality — Determination of content of hydrocarbon in the range C10 to C40 by gas chromatography*. 2004. URL: https://www.standard.no/no/Nettbutikk/produktkatalogen/Produktpresentasjon/?ProductID=117084.

[67] International Organization for Standardization. *ISO 13876 Soil quality — Determination of polychlorinated biphenyls (PCB) by gas chromatography with mass selective detection (GC-MS) and gas chromatography with electron- capture detection (GC-ECD)*. 2013. URL: https://www.standard.no/no/Nettbutikk/produktkatalogen/Produktpresentasjon/?ProductID=668205.

[68] International Organization for Standardization. *ISO 10382 Soil quality — Determination of organochlorine pesticides and polychlorinated biphenyls — Gas- chromatographic method with electron capture detection*. 2002. URL: https://www.standard.no/no/Nettbutikk/produktkatalogen/Produktpresentasjon/?ProductID=113055.

[69] Standard Norge. *NS-EN 16173 - Sludge, treated biowaste and soil Digestion of nitric acid soluble fractions of elements*. 2012. URL: https://www.standard.no/nettbutikk/sokeresultater/?search=NS-EN+16173%3a2012&subscr=1.

[70] Elsa Lundanes, Léon Reubsaet, and Tyge Greibrokk. *Chromatography: basic principles, sample preparations and related methods*. OCLC: ocn869358059. Weinheim, Germany: Wiley-VCH Verlag GmbH & Co. KGaA, 2014. 207 pp. ISBN: 978-3-527-33620-3.

[71] B. Magnusson and U. Örnemark, eds. *Eurachem Guide: The Fitness for Purpose of Analytical Methods – A Laboratory Guide to Method Validation and Related Topics*. OCLC: 1039221699. 2014. ISBN: 978-91-87461-59-0. URL: https://www.eurachem.org/images/stories/Guides/pdf/MV_guide_2nd_ed_EN.pdf.

[72] "International Conference On Harmonisation Of Technical Requirements For Registration Of Pharmaceuticals For Human Use". In: *Handbook of Transnational Economic Governance Regimes*. Ed. by Christian Tietje and Alan Brouder. Brill — Nijhoff, Jan. 1, 2010, pp. 1041–1053. ISBN: 978-90-04-16330-0. DOI: 10.1163/ej.9789004163300.i-1081.897. URL: https://brill.com/view/book/edcoll/9789004181564/Bej.9789004163300.i-1081_085.xml.

[73] Michael Thompson, Steven L. R. Ellison, Aleš Fajgelj, Paul Willetts, and Roger Wood. *Harmonised guidelines for the use of recovery information in analytical measurement (Technical Report)*. 1996. URL: https://www.eurachem.org/images/stories/Guides/pdf/recovery.pdf.

[74] Alexandros G. Asimakopoulos, Lei Wang, Nikolaos S. Thomaidis, and Kurunthachalam Kannan. "A multi-class bioanalytical methodology for the determination of bisphenol A diglycidyl ethers, p-hydroxybenzoic acid esters, benzophenone-type ultraviolet filters, triclosan, and triclocarban in human urine by liquid chromatography–tandem mass spectrometry". In: *Journal of Chromatography A* 1324 (Jan. 10, 2014),

pp. 141–148. ISSN: 0021-9673. DOI: 10.1016/j.chroma.2013.11.031. URL: https://www.sciencedirect.com/science/article/pii/S0021967313018025.

[75] Sylvia Weging. "Study of trace elements, natural organic matter and selected environmental toxicants in soil at Mitrahalvøya, to establish bias correction for studies of long-range atmospheric transported pollutants in Ny-Ålesund". Master. NTNU, June 2021.

[76] G Wagner. "Basic approaches and methods for quality assurance and quality control in sample collection and storage for environmental monitoring". In: *Science of The Total Environment* 176.1 (Dec. 22, 1995), pp. 63–71. ISSN: 00489697. DOI: 10.1016/0048-9697(95)04830-8. URL: https://linkinghub.elsevier.com/retrieve/pii/0048969795048308.

[77] AJ Horowitz. "A primer on sediment-trace element chemistry, 2nd edition". In: (1991), p. 142. DOI: https://doi.org/10.3133/ofr9176.

[78] John Barley. *Freeze Drying / Lyophilization Information: Basic Principles*. URL: https://www.spscientific.com/freeze-drying-lyophilization-basics/.

[79] Zoltan Mester and Ralph E Sturgeon. *Sample Preparation for Trace Element Analysis*. OCLC: 476075577. Burlington: Elsevier, 2003. ISBN: 978-0-08-054548-6. URL: http://www.123library.org/book_details/?id=39093.

[80] Aaron Kettle. "Use of Accelerated Solvent Extraction with In-Cell Cleanup to Eliminate Sample Cleanup During Sample Preparation". In: *Thermo Fisher Scientific White Paper 70632* (2013), p. 7.

[81] Bruce E. Richter, Brian A. Jones, John L. Ezzell, Nathan L. Porter, Nebojsa Avdalovic, and Chris Pohl. "Accelerated Solvent Extraction: A Technique for Sample Preparation". In: *Analytical Chemistry* 68.6 (Jan. 1, 1996), pp. 1033–1039. ISSN: 0003-2700, 1520-6882. DOI: 10.1021/ac9508199. URL: https://pubs.acs.org/doi/10.1021/ac9508199.

[82] Gerardo Alvarez-Rivera, Monica Bueno, Diego Ballesteros-Vivas, Jose A. Mendiola, and Elena Ibañez. "Pressurized Liquid Extraction". In: *Liquid-Phase Extraction*. Elsevier, 2020, pp. 375–398. ISBN: 978-0-12-

816911-7. DOI: 10.1016/B978-0-12-816911-7.00013-X. URL: https://linkinghub.elsevier.com/retrieve/pii/B978012816911700013X.

[83] J. Pawliszyn. "Theory of Extraction". In: *Comprehensive Sampling and Sample Preparation*. Elsevier, 2012, pp. 1–25. ISBN: 978-0-12-381374-9. DOI: 10.1016/B978-0-12-381373-2.00149-6. URL: https://linkinghub.elsevier.com/retrieve/pii/B9780123813732001496.

[84] A. Hubert, K.-D. Wenzel, W. Engewald, and G. Schüürmann. "Accelerated Solvent Extraction - More Efficient Extraction of POPs and PAHs from Real Contaminated Plant and Soil Samples". In: *Reviews in Analytical Chemistry* 20.2 (Jan. 2001). ISSN: 2191-0189, 0793-0135. DOI: 10.1515/REVAC.2001.20.2.101. URL: https://www.degruyter.com/document/doi/10.1515/REVAC.2001.20.2.101/html.

[85] Scott C Wilschefski and Matthew R Baxter. "Inductively Coupled Plasma Mass Spectrometry: Introduction to Analytical Aspects". In: *The Clinical Biochemist Reviews* 40.3 (Aug. 2019), pp. 115–133. ISSN: 0159-8090. DOI: 10.33176/AACB-19-00024. URL: https://www.ncbi.nlm.nih.gov/pmc/articles/PMC6719745/.

[86] Douglas A. Skoog, Donald Markham West, F. James Holler, and Stanley R. Crouch, eds. *Fundamentals of analytical chemistry*. 9. ed., International ed. Melbourne: Brooks/Cole, Cengage Learning, 2014. ISBN: 978-0-495-55828-6.

[87] Vicki J. Barwick. "Sources of uncertainty in gas chromatography and high-performance liquid chromatography". In: *Journal of Chromatography A* 849.1 (July 1999), pp. 13–33. ISSN: 00219673. DOI: 10.1016/S0021-9673(99)00537-3. URL: https://linkinghub.elsevier.com/retrieve/pii/S0021967399005373.

[88] Ronald E. Walpole, Raymond H. Myers, Jackie DeShannon, and Keying Ye. *Probability & statistics for engineers & scientists*. Ninth edition, global edition. Boston Columbus Hoboken [und 22 weitere]: Pearson Education Limited, 2016. 811 pp. ISBN: 978-1-292-16136-5.

[89] *Shapiro Wilk Test*. URL: https://www.statskingdom.com/doc_shapiro_wilk.html (visited on 06/05/2022).

[90] *T-Test Calculator for 2 Independent Means*. URL: https://www.socscistatistics.com/tests/studentttest/default.aspx (visited on 06/05/2022).

[91] *One-way ANOVA - An introduction to when you should run this test and the test hypothesis — Laerd Statistics*. URL: https://statistics.laerd.com/statistical-guides/one-way-anova-statistical-guide.php (visited on 06/05/2022).

[92] *One-way ANOVA in SPSS Statistics - Step-by-step procedure including testing of assumptions*. URL: https://statistics.laerd.com/spss-tutorials/one-way-anova-using-spss-statistics.php (visited on 06/05/2022).

[93] *Mann-Whitney U Test guide*. URL: https://www.statskingdom.com/test_mann_whitney.html (visited on 06/05/2022).

[94] Barbara Illowsky, Susan L Dean, Barbara Illowsky, and OpenStax (Nonprofit organization). *Introductory statistics*. OCLC: 1045798958. 2018. ISBN: 978-1-5066-9823-6.

[95] Alan J. Izenman. *Modern Multivariate Statistical Techniques*. Red. by G. Casella, S. Fienberg, and I. Olkin. Springer Texts in Statistics. New York, NY: Springer New York, 2008. ISBN: 978-0-387-78188-4. DOI: 10.1007/978-0-387-78189-1. URL: http://link.springer.com/10.1007/978-0-387-78189-1.

[96] Brian Everitt and Graham Dunn. *Applied multivariate data analysis*. Chichester: Wiley, 2001. 342 pp. ISBN: 978-0-470-71117-0.

[97] Kim H. Esbensen. *Multivariate data analysis - in practice: an introduction to multivariate data analysis and experimental design*. 5th ed., repr. Oslo: CAMO, 2012. 598 pp. ISBN: 978-82-993330-3-0.

[98] Steven M. Holland. *Principal components analysis (PCA)*. May 2008.

[99] Noriah M. Al-Kandari and Ian T. Jolliffe. "Variable selection and interpretation in correlation principal components". In: *Environmetrics* 16.6 (Sept. 2005), pp. 659–672. ISSN: 1180-4009, 1099-095X. DOI: 10.1002/env.728. URL: https://onlinelibrary.wiley.com/doi/10.1002/env.728.

[100] Jorge Cadima and Ian T. Jolliffe. "Loading and correlations in the interpretation of principle compenents". In: *Journal of Applied Statistics* 22.2 (Jan. 1995), pp. 203–214. ISSN: 0266-4763, 1360-0532. DOI: 10.1080/757584614. URL: http://www.tandfonline.com/doi/abs/10.1080/757584614.

[101] Ewa Bulska, Agnieszka Krata, Mateusz Kałabun, and Marcin Wojciechowski. "On the use of certified reference materials for assuring the quality of results for the determination of mercury in environmental samples". In: *Environmental Science and Pollution Research International* 24.9 (2017), pp. 7889–7897. ISSN: 0944-1344. DOI: 10.1007/s11356-016-7262-4. URL: https://www.ncbi.nlm.nih.gov/pmc/articles/PMC5384953/.

[102] *POLISH CERTIFIED REFERENCE MATERIAL (CRM) FOR MULTIELEMENT TRACE ANALYSIS WITH RECOMMENDED AND INFORMATION VALUES FOR SELECTED RADIONUCLIDES MODAS–2 Bottom Sediment (M–2 BotSed)*. URL: https://assets.lgcstandards.com/sys-master%2Fpdfs%2Fh27%2Fh54%2F10137839403038%2FCOA_MODAS-2_ST-WB-CERT-2507848-1-1-1.PDF (visited on 06/15/2022).

[103] *MESS-4 Marine Sediment Certified Reference Material for total and extractable metal content*. URL: https://nrc-digital-repository.canada.ca/eng/view/crt/?id=8a3fd39a-c068-4ce0-820c-d08cf742a20a&dsl=en (visited on 06/15/2022).

[104] Marina G. Pintado-Herrera, Eduardo González-Mazo, and Pablo A. Lara-Martín. "In-cell clean-up pressurized liquid extraction and gas chromatography–tandem mass spectrometry determination of hydrophobic persistent and emerging organic pollutants in coastal sediments". In: *Journal of Chromatography A* 1429 (Jan. 15, 2016), pp. 107–118. ISSN: 0021-9673. DOI: 10.1016/j.chroma.2015.12.040. URL: https://www.sciencedirect.com/science/article/pii/S002196731501835X.

[105] U.S. EPA. *3545a (SW-846) PRESSURIZED FLUID EXTRACTION (PFE)*. 2007. URL: https://www.epa.gov/sites/default/files/2015-12/documents/3545a.pdf (visited on 06/11/2022).

[106] Sigrid Myhr Kveli. "Studie av totalt organisk materiale, kvikksølv og andre sporelementer i sedimenter/elveavsetninger i Bayelva og andre elver i Ny Ålesund (Svalbard)". Master. NTNU, 2015.

[107] Per Kyrre Reymert. *Ny-Ålesund*. The Governor of Svalbard and Department for Environment Protection with Kings Bay AS., 2016. 40 pp. ISBN: 978-82-91850-46-7.

[108] Anna Abramova, Ivan Semenkov, Sergey Chernyanskii, and Stanislav Ogorodov. "CONCENTRATION OF TRACE ELEMENTS IN SOILS HISTORICALLY AFFECTED BY COAL MINING IN SVALBARD". In: 18th International Multidisciplinary Scientific GeoConference SGEM2018. June 2018. DOI: DOI:10.5593/sgem2018/5.2/S20.033.

[109] F.C. Walsh and C.T.J. Low. "A review of developments in the electrodeposition of tin-copper alloys". In: *Surface and Coatings Technology* 304 (Oct. 2016), pp. 246–262. ISSN: 02578972. DOI: 10.1016/j.surfcoat.2016.06.065. URL: https://linkinghub.elsevier.com/retrieve/pii/S0257897216305576.

[110] Shazia N. Aslam, Carolin Huber, Alexandros G. Asimakopoulos, Eiliv Steinnes, and Øyvind Mikkelsen. "Trace elements and polychlorinated biphenyls (PCBs) in terrestrial compartments of Svalbard, Norwegian Arctic". In: *Science of The Total Environment* 685 (Oct. 1, 2019), pp. 1127–1138. ISSN: 0048-9697. DOI: 10.1016/j.scitotenv.2019.06.060. URL: https://www.sciencedirect.com/science/article/pii/S0048969719326282.

[111] Zhongkang Yang, Linxi Yuan, Zhouqing Xie, Jun Wang, Zhaolei Li, Luyao Tu, and Liguang Sun. "Historical records and contamination assessment of potential toxic elements (PTEs) over the past 100 years in Ny-Ålesund, Svalbard". In: *Environmental Pollution* 266 (Nov. 1, 2020), p. 115205. ISSN: 0269-7491. DOI: 10.1016/j.envpol.2020.115205. URL: https://www.sciencedirect.com/science/article/pii/S0269749120313178.

[112] Jozef M. Pacyna and Brynjulf Ottar. "Transport and chemical composition of the summer aerosol in the Norwegian Arctic". In: *Atmospheric Environment (1967)* 19.12 (Jan. 1, 1985), pp. 2109–2120. ISSN: 0004-6981. DOI: 10.1016/0004-6981(85)90118-0. URL: https://www.sciencedirect.com/science/article/pii/0004698185901180.

[113] Agata Zaborska, Agnieszka Beszczyńska-Möller, and Maria Włodarska-Kowalczuk. "History of heavy metal accumulation in the Svalbard area: Distribution, origin and transport pathways". In: *Environmental Pollution* 231 (Dec. 1, 2017), pp. 437–450. ISSN: 0269-7491. DOI: 10.

1016/j.envpol.2017.08.042. URL: https://www.sciencedirect.com/science/article/pii/S0269749117315579.

[114] Sigrid Bergseng Lakså. "The role of migratory birds in the transport of pollutants to the Arctic". Master. NTNU, July 2021.

[115] Eiliv Steinnes, Hilde Uggerud, Torunn Berg, and Katrine Aspmo Pfaffhuber. *Atmosfærisk nedfall av tungmetaller i Norge. Landsomfattende undersøkelse i 2010*. Klima- og forurensningsdirektoratet, 2011. 38 pp. ISBN: 978-82-425-2457-7.

[116] Alina Kabata-Pendias and Barbara Szteke. *Trace elements in abiotic and biotic environments*. OCLC: ocn900179575. Boca Raton: CRC Press, Taylor & Francis Group, 2015. 440 pp. ISBN: 978-1-4822-1279-2.

A Sample data

Table A.1: Sampling information for the samples intended for ICP-MS analysis. ML indicates the Midtre Lofvenbreen sampling area and Sars indicates the Ossian Sars background area.

Sample	Area	Meters from BIA	ICP-MS	Not used
1	BIA A	200	X	
2	BIA A	175	X	
3	BIA A	150	X	
4	BIA A	125	X	
5	BIA A	100	X	
6	BIA A	75	X	
7	BIA A	50	X	
8	BIA A	25	X	
9	BIA A	200	X	
10	BIA A	175	X	
11	BIA A	150	X	
12	BIA A	125	X	
13	BIA A	100	X	
14	BIA A	75	X	
15	BIA A	50	X	
16	BIA A	25	X	
17	BIA A	200	X	
18	BIA A	175	X	
19	BIA A	150	X	
20	BIA A	125	X	
21	BIA A	100	X	
22	BIA A	75	X	
23	BIA A	50	X	
24	BIA A	25	X	
25	BIA A	0	X	
26	BIA A	0	X	
27	BIA A	0	X	
28	BIA A	0	X	
29	BIA A	0	X	

30	BIA A	0	X
31	BIA A	0	X
32	BIA A	0	X
33	BIA A	0	X
34	BIA A	0	X
35	BIA B	200	X
36	BIA B	175	X
37	BIA B	150	X
38	BIA B	125	X
39	BIA B	100	X
40	BIA B	75	X
41	BIA B	50	X
42	BIA B	25	X
43	BIA B	200	X
44	BIA B	175	X
45	BIA B	150	X
46	BIA B	125	X
47	BIA B	100	X
48	BIA B	75	X
49	BIA B	50	X
50	BIA B	25	X
51	BIA B	200	X
52	BIA B	175	X
53	BIA B	150	X
54	BIA B	125	X
55	BIA B	100	X
56	BIA B	75	X
57	BIA B	50	X
58	BIA B	25	X
59	BIA B	0	X
60	BIA B	0	X
61	BIA B	0	X
62	BIA B	0	X
63	BIA B	0	X
64	BIA B	0	X
65	BIA B	0	X
66	BIA B	0	X
67	BIA B	0	X

68	BIA B	0	X
B1 2	ML	-	X
B1 3	ML	-	X
B1 4	ML	-	X
B1 5	ML	-	X
B1 6	ML	-	X
B1 7	ML	-	X
B2 2	ML	-	X
B2 3	ML	-	X
B2 4	ML	-	X
B2 5	ML	-	X
B2 6	ML	-	X
B2 7	ML	-	X
B3 2	ML	-	X
B3 3	ML	-	X
B3 4	ML	-	X
B3 5	ML	-	X
B3 6	ML	-	X
B3 7	ML	-	X
Sars 1	Sars	-	X
Sars 2	Sars	-	X

Table A.2: Sampling information for the samples intended for GC-MS analysis. ML indicates the Midtre Lofvenbreen sampling area and Sars indicates the Ossian Sars background area.

Sample	Area	Meters from BIA	GC-MS	Not used
P1	BIA A	200	X	
P2	BIA A	150	X	
P3	BIA A	100		X
P4	BIA A	50		X
P5	BIA A	25		X
P6	BIA A	0		X
P7	BIA A	0	X	
P8	BIA A	0	X	
P9	BIA A	0	X	
P10	BIA A	0	X	
P11	BIA B	200	X	
P12	BIA B	150	X	
P13	BIA B	100		X
P14	BIA B	50		X
P15	BIA B	25		X
P16	BIA B	0		X
P17	BIA B	0	X	
P18	BIA B	0	X	
P19	BIA B	0	X	
P20	BIA B	0	X	
B1 1	ML	-		X
B2 1	ML	-		X
B3 1	ML	-		X

B Trace element raw data

Table B.1: Overview of weights of the samples before and after dilution during the UltraCLAVE sample preparation.

Sample	UC sample weight (mg)	Diluted sample weight (mg)	Diluted sample (mL)
Blank 1	0	110220	108.4095603
Blank 2	0	109590	107.7899085
Blank 3	0	110020	108.2128455
Ref. marine 1	263.4	117220	115.2945805
Ref. marine 2	329.8	109620	107.8194158
Ref. river 1	294.5	109990	108.1833383
Ref. river 2	278.8	109750	107.9472804
1	313.5	112010	110.1701584
2	314.9	109910	108.1046523
2	314.9	109910	108.1046523
3	306.4	109570	107.770237
4	324.8	109800	107.9964591
5	302.5	109900	108.0948166
6	281.9	109830	108.0259664
7	284.2	109900	108.0948166
8	304.3	109820	108.0161306
9	308.3	110730	108.9111832
10	276.5	109860	108.0554736
11	315.3	110840	109.0193764
12	333.3	109890	108.0849808
13	325.3	109820	108.0161306
14	268.7	110110	108.3013672
15	261.8	109820	108.0161306
16	296.9	110840	109.0193764
17	295	110670	108.8521688
18	315.4	109990	108.1833383
19	278.9	109750	107.9472804
20	330	109860	108.0554736
21	263.6	109840	108.0358021

22	306.3	109840	108.0358021
23	281.6	110100	108.2915314
24	343.3	110910	109.0882266
25	268	109900	108.0948166
26	288	109860	108.0554736
27	260.3	109740	107.9374447
28	316	109800	107.9964591
29	265	109840	108.0358021
30	250.9	109750	107.9472804
31	307.8	109800	107.9964591
32	281.1	109680	107.8784302
33	284.7	110360	108.5472607
34	262.1	109760	107.9571162
35	301.3	109730	107.9276089
35	301.3	109730	107.9276089
36	279.2	109610	107.80958
37	284	109550	107.7505656
38	276.6	109470	107.6718796
39	327.7	113940	112.0684568
40	270.4	109620	107.8194158
41	272.4	109330	107.5341792
42	313.3	109500	107.7013868
43	252.1	109630	107.8292515
44	302.1	110370	108.5570965
45	269.1	112280	110.4357234
46	275.8	109630	107.8292515
Blank 4	0	109880	108.0751451
Blank 5	0	109750	107.9472804
Blank 6	0	109800	107.9964591
Ref. marine 3	251.6	109600	107.7997443
Ref. marine 4	269.3	110080	108.2718599
Ref. river 3	329.8	110910	109.0882266
Ref. river 4	257.1	109740	107.9374447
47	259.6	110470	108.6554539
48	259.6	109490	107.6915511
49	265.2	109760	107.9571162
50	279.8	109590	107.7899085
51 rep1	257.6	109650	107.848923

51 rep2	257.6	109650	107.848923
53	270.4	109530	107.7308941
54	292.1	109520	107.7210583
55	267.3	109490	107.6915511
56	275.8	109630	107.8292515
57	250.7	109390	107.5931937
58	274	111560	109.7275499
59	329	110000	108.193174
60	280.2	111560	109.7275499
61	283.8	109560	107.7604013
62	289.9	109410	107.6128652
63	278.3	109470	107.6718796
64	269.1	109820	108.0161306
65	260.7	109810	108.0062949
66	268.1	110430	108.6161109
Blank 7	0	112340	110.4947379
Blank 8	0	110170	108.3603816
Blank 9	0	109750	107.9472804
Ref. marine 5	255.4	110150	108.3407101
Ref. marine 6	263.4	110170	108.3603816
Ref. river 5	257.8	110300	108.4882463
Ref. river 6	265	109970	108.1636668
52	268.8	110570	108.7538114
67	304.4	109890	108.0849808
B1 2-1	336.2	110860	109.0390479
B1 3-1	275.3	109810	108.0062949
B1 4	265.4	109660	107.8587587
B1 5-1	255.6	110130	108.3210387
B1 6	344.7	110680	108.8620045
B1 7	270.7	110430	108.6161109
B2 2-1	283.2	110000	108.193174
B2 3-1	345	109690	107.888266
B2 4	268.5	110320	108.5079178
B2 5 rep1	298.4	109430	107.6325366
B2 5 rep2	298.4	109430	107.6325366
B2 6	304.4	109450	107.6522081
B3 2	250.7	110140	108.3308744
B3 3	257.9	109430	107.6325366

B3 4	274.6	110510	108.6947969
B3 5	269.6	109850	108.0456378
B3 6	288.4	110290	108.4784105
B3 7	283.5	110200	108.3898889
Sars 1-1	311.8	110120	108.3112029
Sars 2-1	315.8	110680	108.8620045

Table B.2: Results from the ICP-MS analysis.

Sample			7 -> 7 Li [No Gas]		9 -> 9 Be [H2]		11 -> 11 B [O2]		23 -> 23 Na [O2]		24 -> 24 Mg [O2]		27 -> 27 Al [H2]		28 -> 44 Si [O2]		31 -> 47 P [O2]		32 -> 48 S [O2]	
Acq. Date-Time	Sample Name	Comment	Conc. [ug/l]	Conc. RSD	Conc. [ug/l]	Conc. RSD	Conc. [ug/l]	Conc. RSD	Conc. [ug/l]	Conc. RSD	Conc. [ug/l]	Conc. RSD	Conc. [ug/l]	Conc. RSD	Conc. [ug/l]	Conc. RSD	Conc. [ug/l]	Conc. RSD	Conc. [ug/l]	Conc. RSD
14/03/2022 14:41	1	Blank 1	<0.0026	N/A	0.00	173.2	<0.047	N/A	<0.26	N/A	<0.078	6.2	0.11	4.0	0.16	17.3	<0.014	73.7	<0.22	N/A
14/03/2022 14:45	2	Blank 2	<0.0026	N/A	0.00	N/A	<0.047	N/A	<0.26	N/A	0.079	21.5	0.083	1.5	0.17	12.6	0.017	68.4	<0.22	N/A
14/03/2022 14:49	3	Blank 3	<0.0026	N/A	0.00	N/A	<0.047	N/A	<0.26	N/A	<0.078	2.1	0.32	100.6	0.16	9.0	<0.014	1072.3	<0.22	N/A
14/03/2022 14:52	4	Ref. marine 1	128.00	0.9	2.62	17.0	256.77	3.6	18839.91	1.8	28499.26	2.7	120061.16	1.2	6640.28	0.6	1936.85	2.1	3149.91	3.2
14/03/2022 14:56	5	Ref. marine 2	161.80	0.4	4.38	35.1	318.72	7.2	23267.50	4.0	34624.67	3.3	146158.32	1.2	7289.76	2.3	2351.47	4.9	3907.20	4.2
14/03/2022 14:59	6	Ref. river 1	63.33	0.7	2.09	40.3	81.90	3.9	1156.44	2.7	15007.78	1.0	64755.14	0.1	7400.57	2.8	4724.62	2.2	7671.39	2.3
14/03/2022 15:03	7	Ref. river 2	59.73	0.6	2.32	28.7	73.19	5.0	1100.04	3.2	13844.88	1.3	60989.26	0.7	8362.09	1.7	4375.19	0.8	7073.14	1.0
14/03/2022 15:07	8	1	60.35	1.7	3.55	26.3	72.47	1.3	1399.87	2.3	28997.46	1.2	79674.74	0.3	5538.42	0.5	1163.42	2.3	1081.43	2.2
14/03/2022 14:31	9	2	60.44	0.4	4.46	9.5	78.12	2.3	1605.83	2.0	33619.47	0.3	88798.60	1.3	5964.79	0.6	1555.78	0.9	1177.13	1.8
14/03/2022 15:10	9 rep2	2	62.44	2.1	3.90	25.4	78.32	1.7	1566.78	1.9	32569.13	1.9	86425.41	0.8	5835.62	0.4	1491.17	1.2	1127.75	2.7
14/03/2022 15:14	10	3	54.36	0.9	3.89	30.1	64.56	1.2	1179.45	2.1	29434.33	2.8	74378.24	1.4	6216.95	1.4	1415.30	2.3	2026.27	2.9
14/03/2022 15:17	11	4	58.75	0.2	4.72	11.1	67.66	4.0	1332.53	2.1	34713.87	0.7	82452.79	1.5	5833.23	1.0	1521.78	2.2	1439.46	2.1
14/03/2022 15:21	12	5	51.60	1.0	3.41	41.8	55.84	1.9	1130.40	1.4	28711.60	0.6	72752.81	0.3	5951.58	1.3	1234.67	0.7	971.75	1.3
14/03/2022 15:24	13	6	57.09	2.2	3.95	10.9	73.87	3.9	1437.78	2.0	32098.17	1.8	79986.71	0.9	6072.79	1.2	1480.64	2.0	1139.94	2.4
14/03/2022 15:28	14	7	58.02	1.2	3.74	21.8	73.87	4.0	1427.96	1.8	31946.12	0.7	83775.54	2.8	6299.63	0.3	1466.64	1.8	1207.48	2.1
14/03/2022 15:31	15	8	52.51	1.3	2.81	45.2	57.02	3.0	1024.81	1.1	27848.34	1.0	65396.03	0.4	5921.00	0.6	1402.21	1.6	2132.37	0.4
14/03/2022 15:35	16	9	39.36	0.9	2.38	26.1	46.56	6.5	772.09	1.4	21675.69	1.3	50788.96	1.2	5231.16	0.9	1037.25	2.3	1310.66	1.9
14/03/2022 15:38	17	10	40.27	0.8	3.28	45.3	45.25	13.1	866.68	1.0	21781.32	0.9	57503.17	0.8	6073.44	0.2	1173.41	1.2	1283.65	2.4
14/03/2022 15:42	18	11	50.18	0.3	3.49	34.2	56.71	5.2	1112.01	1.3	26938.91	1.1	70205.85	1.4	6798.28	0.2	1292.00	1.4	1211.39	2.0
14/03/2022 15:45	19	12	55.66	2.3	2.83	15.1	65.13	3.7	1293.34	3.0	33743.07	1.3	75179.92	0.7	8883.76	0.7	1881.41	1.8	1951.16	1.6
14/03/2022 15:49	20	13	46.31	0.3	3.25	17.2	45.74	6.4	780.26	0.5	23600.45	0.7	57396.99	1.7	6336.38	0.6	1128.14	0.8	1408.71	1.9
14/03/2022 15:53	21	14	38.73	0.6	2.17	40.1	46.98	6.6	815.78	2.8	21091.69	0.8	52526.00	2.5	5969.43	1.2	937.17	0.9	1356.50	1.1
14/03/2022 15:56	22	15	36.35	1.3	2.58	15.2	38.87	4.3	703.87	1.0	19706.23	1.9	47406.21	1.0	5960.99	0.1	1006.54	0.4	1382.52	1.3
14/03/2022 16:00	23	16	45.37	0.1	2.44	36.8	54.08	9.0	985.59	3.2	24394.02	2.1	55444.65	2.2	6443.57	2.5	1120.86	0.9	1054.78	1.4
14/03/2022 16:03	24	17	46.92	1.7	2.48	25.8	60.81	5.0	1121.80	2.1	24836.47	1.5	63867.48	3.5	6821.82	0.9	1184.27	2.8	1074.47	2.1
14/03/2022 16:07	25	18	52.67	0.3	3.18	4.9	52.33	0.5	1042.49	1.8	27026.97	1.9	67932.50	0.8	6256.66	1.0	1497.65	1.8	1708.00	2.4
14/03/2022 16:10	26	19	47.42	1.9	3.51	2.7	59.76	5.5	1125.38	0.4	29723.84	2.4	69155.12	1.3	7054.38	0.9	1427.40	2.5	1396.31	2.4
14/03/2022 16:14	27	20	46.94	2.2	2.44	26.0	50.12	2.1	837.16	2.9	23484.75	3.1	55172.97	0.7	5760.40	1.7	1066.24	1.2	1483.92	1.7
14/03/2022 16:35	28	21	44.92	0.5	3.25	59.4	48.80	5.0	897.06	1.9	22843.33	1.2	58472.53	1.5	6761.87	0.6	1223.33	1.6	1389.30	0.3
14/03/2022 16:39	29	22	43.41	0.5	2.31	21.1	48.12	2.5	776.69	1.2	23662.50	1.6	54106.75	0.8	5413.79	0.8	1061.42	1.5	1609.29	1.2
14/03/2022 16:42	30	23	40.48	0.8	3.62	19.3	46.13	4.0	744.34	1.9	25452.54	1.7	51091.06	1.1	5295.97	0.7	1065.42	3.3	1475.10	2.9
14/03/2022 16:46	31	24	45.52	0.8	2.73	20.3	49.00	3.7	890.38	3.9	30403.25	1.8	59142.37	2.0	5716.80	1.2	1547.96	2.3	2374.97	1.2
14/03/2022 16:49	32	25	33.82	1.2	2.04	27.5	35.34	5.3	615.39	1.4	25495.78	1.1	42905.41	1.3	5438.11	0.5	917.38	0.5	1867.47	1.6
14/03/2022 16:53	33	26	41.11	0.6	2.79	24.6	47.77	9.4	817.38	4.8	27300.58	3.7	54002.23	0.7	6145.41	2.0	1499.42	1.4	2465.08	2.9
14/03/2022 16:56	34	27	41.04	2.9	1.60	25.5	42.03	10.9	823.83	4.3	26190.69	2.7	55124.08	0.3	6691.90	2.4	1110.86	1.6	1753.43	1.5
14/03/2022 17:00	35	28	58.87	0.7	3.22	39.2	70.95	3.3	1365.33	3.6	35317.98	2.2	84539.15	1.1	6720.32	1.4	1818.46	1.3	1624.75	2.0
14/03/2022 17:03	36	29	39.88	0.9	1.98	12.9	45.15	6.2	766.41	1.3	24797.06	1.4	51597.21	0.4	6044.84	2.3	1325.46	1.2	1576.98	1.4
14/03/2022 17:07	37	30	40.21	1.6	3.09	31.6	41.08	9.7	728.26	0.4	22623.21	0.9	51279.96	1.9	6019.49	0.0	1001.03	1.4	1000.68	1.0
14/03/2022 17:11	38	31	38.23	0.6	2.03	20.1	43.83	8.2	638.11	2.4	23304.23	2.4	44998.32	0.5	5247.41	1.5	1113.56	2.2	2621.44	2.8
14/03/2022 17:14	39	32	42.48	3.2	2.23	40.2	50.41	4.3	846.04	1.2	22605.44	1.4	54121.11	0.6	6388.61	0.7	1049.76	0.7	1296.38	0.8
14/03/2022 17:18	40	33	37.23	0.7	2.07	21.0	39.72	1.5	720.25	0.9	25003.95	0.5	45988.81	1.8	5040.24	0.8	1110.20	1.9	2213.36	1.0
14/03/2022 17:21	48	34	39.44	1.2	2.39	24.6	45.50	4.3	806.97	1.5	25092.15	1.8	52492.53	0.9	5762.13	0.7	1184.75	3.0	1712.68	1.8
14/03/2022 17:25	49 rep1	35	44.52	1.9	2.93	39.7	72.14	8.1	1146.08	1.9	36022.29	0.7	61874.13	1.1	7754.44	0.4	1205.25	0.4	1432.77	1.1
14/03/2022 17:28	49 rep2	35	48.94	1.5	3.35	20.1	74.03	3.1	1132.66	3.7	36534.46	1.3	66734.78	2.4	7915.82	2.5	1225.24	1.8	1446.18	2.3
14/03/2022 17:32	50	36	37.35	2.2	2.28	39.6	53.06	4.1	763.29	0.1	29282.87	0.1	47356.68	0.6	4937.81	0.4	826.26	2.0	1130.09	1.4
14/03/2022 17:35	51	37	34.95	0.8	2.47	24.8	29.58	1.7	825.33	1.8	48048.33	1.9	46104.16	1.5	6999.68	0.9	1055.24	1.5	2292.22	2.6
14/03/2022 17:39	52	38	34.64	0.6	3.21	2.9	49.82	8.2	675.36	0.9	32795.81	1.5	43245.79	1.3	5382.20	0.6	839.61	2.9	2036.18	2.1
14/03/2022 17:43	53	39	41.31	0.2	2.55	4.5	45.70	1.0	908.82	1.9	37399.05	0.8	53735.22	1.2	5840.98	0.7	1262.86	1.8	2485.56	2.5
14/03/2022 17:46	54	40	40.74	1.2	3.19	7.8	63.27	3.0	957.92	0.9	33349.94	0.3	56156.09	2.3	6500.83	0.8	1111.35	2.0	1134.80	1.4
14/03/2022 17:50	55	41	45.00	2.1	2.79	40.6	54.80	5.3	1208.20	1.5	56826.71	1.4	64678.16	1.0	7242.51	1.1	1262.26	2.8	1052.19	2.3
14/03/2022 17:53	56	42	30.06	0.6	2.02	36.9	23.16	11.0	762.44	1.9	39498.32	1.8	43280.59	0.6	5995.87	1.3	1410.77	2.0	2840.25	2.1
14/03/2022 17:57	57	43	31.94	1.7	2.54	24.0	36.89	7.5	653.36	1.6	28456.15	2.3	42254.78	1.5	6267.45	1.1	955.71	2.8	3453.17	2.6
14/03/2022 18:00	58	44	46.70	0.6	4.03	26.1	43.82	8.5	1223.24	0.3	46272.90	1.6	66885.28	1.2	6885.96	1.2	1403.12	2.0	1122.10	2.7
14/03/2022 18:04	59	45	32.12	0.7	2.17	35.6	32.26	8.8	803.30	1.9	36736.57	2.0	46542.39	0.7	6307.16	1.4	1117.61	0.5	2781.53	2.4
14/03/2022 18:07	60	46	33.19	1.3	2.75	56.3	27.19	4.4	803.28	1.4	38235.58	2.2	46949.65	3.0	6196.19	0.6	1021.39	3.0	2009.44	1.4

Sample			39 -> 39 K [O2]		40 -> 40 Ca [H2]		45 -> 61 Sc [O2]		47 -> 63 Ti [O2]		51 -> 67 V [O2]		52 -> 52 Cr [O2]		55 -> 55 Mn [O2]		56 -> 56 Fe [H2]		59 -> 59 Co [O2]	
Acq. Date-Time	Sample Name	Comment	Conc. [ug/l]	Conc. RSD	Conc. [ug/l]	Conc. RSD	Conc. [ug/l]	Conc. RSD	Conc. [ug/l]	Conc. RSD	Conc. [ug/l]	Conc. RSD	Conc. [ug/l]	Conc. RSD	Conc. [ug/l]	Conc. RSD	Conc. [ug/l]	Conc. RSD	Conc. [ug/l]	Conc. RSD
14/03/2022 14:41	1	Blank 1	<0.11	N/A	<0.0044	113.4	<0.00072	N/A	0.0045	15.2	<0.0013	N/A	<0.0043	23.0	<0.017	N/A	0.048	4.4	<0.00079	N/A
14/03/2022 14:45	2	Blank 2	<0.11	3.5	0.34	1.5	<0.00072	N/A	0.024	22.1	<0.0013	N/A	<0.0043	77.5	<0.017	N/A	0.036	1.7	<0.00079	N/A
14/03/2022 14:49	3	Blank 3	<0.11	N/A	1.13	131.1	<0.00072	N/A	0.0058	11.3	<0.0013	N/A	<0.0043	67.0	<0.017	N/A	0.25	125.4	<0.00079	N/A
14/03/2022 14:52	4	Ref. marine 1	38105.06	0.8	24421.89	0.8	24.40	1.9	344.29	1.3	365.14	1.6	163.36	1.2	556.78	1.4	68859.36	1.0	24.67	2.5
14/03/2022 14:56	5	Ref. marine 2	45295.82	3.8	30725.87	0.5	29.41	1.3	372.52	3.4	439.60	2.8	196.64	2.9	678.14	2.8	86426.83	0.6	30.58	2.2
14/03/2022 14:59	6	Ref. river 1	16906.11	1.2	160205.33	1.2	15.77	1.8	629.64	0.7	199.93	1.7	177.05	1.6	2806.41	0.8	67302.32	0.8	21.00	1.0
14/03/2022 15:03	7	Ref. river 2	15959.87	0.4	148310.80	1.2	14.61	0.8	663.11	1.5	187.23	1.0	160.52	0.7	2594.94	0.7	63085.44	1.3	19.45	0.6
14/03/2022 15:07	8	1	31087.54	1.1	47061.23	0.6	19.07	2.8	1606.71	1.0	116.90	1.0	99.48	1.2	1063.10	1.8	68345.12	0.7	28.74	1.5
14/03/2022 14:31	9	2	35187.63	1.0	54633.15	1.1	21.41	0.8	1720.69	0.4	129.57	0.4	112.34	0.2	1114.61	0.9	72558.30	0.3	31.02	0.9
14/03/2022 15:10	9 rep2	2	33817.10	1.0	53234.35	2.2	20.89	1.2	1663.14	0.8	124.97	1.2	108.34	0.8	1088.14	1.0	71348.65	1.0	29.90	1.4
14/03/2022 15:14	10	3	27926.01	1.4	52045.50	0.8	18.45	1.2	1527.33	1.7	112.87	1.9	95.94	2.2	1000.24	2.2	71664.93	2.3	31.06	1.2
14/03/2022 15:17	11	4	31548.76	1.2	59388.38	1.0	19.97	1.4	1763.17	1.0	122.83	1.0	102.80	1.0	1074.74	1.3	75311.43	1.1	31.58	0.2
14/03/2022 15:21	12	5	29900.16	0.8	43793.66	0.7	18.64	1.5	1580.44	0.7	111.32	1.2	92.15	0.8	1071.83	0.4	64947.90	0.1	29.39	1.0
14/03/2022 15:24	13	6	31742.18	1.6	50889.81	1.0	19.41	3.0	1668.13	1.6	118.46	1.3	100.11	1.5	981.07	0.7	67638.39	0.7	28.08	2.3
14/03/2022 15:28	14	7	33769.03	0.6	44629.70	0.9	20.78	0.4	1833.45	1.0	124.12	0.6	106.71	0.4	1020.92	0.6	70946.24	1.1	30.33	0.5
14/03/2022 15:31	15	8	26386.90	0.2	46032.99	1.9	17.67	0.8	1697.92	0.3	109.19	0.9	90.81	0.7	991.38	0.4	70735.18	1.3	31.04	0.6
14/03/2022 15:35	16	9	18885.04	0.5	43252.18	0.6	12.85	1.0	1107.16	0.7	81.08	0.7	66.13	1.5	835.42	0.3	53486.97	0.8	23.25	1.1
14/03/2022 15:38	17	10	22670.11	0.8	35408.74	0.6	14.67	1.2	1258.76	1.2	88.80	0.7	72.92	1.4	920.93	0.2	56554.53	1.0	24.52	0.5
14/03/2022 15:42	18	11	28160.89	0.5	42206.80	0.3	17.72	1.2	1565.85	1.4	106.20	0.2	87.43	1.5	1082.19	1.5	65640.33	0.7	30.38	0.8
14/03/2022 15:45	19	12	31429.91	1.7	51387.53	0.8	19.90	1.6	1743.59	2.2	119.20	1.4	102.82	1.5	1169.16	0.8	69969.67	1.3	33.76	1.7
14/03/2022 15:49	20	13	22682.57	1.0	43021.53	1.3	15.27	0.4	1386.09	0.6	92.55	0.7	72.53	0.9	981.59	0.5	60466.50	1.5	29.20	0.6
14/03/2022 15:53	21	14	20373.13	0.7	37638.37	1.9	13.28	0.7	1188.06	0.8	82.90	0.5	67.35	0.7	774.77	1.1	50634.49	1.4	21.96	1.0
14/03/2022 15:56	22	15	18515.61	0.6	38783.52	0.7	12.70	1.5	1094.14	1.5	77.25	0.7	64.99	1.5	799.30	0.3	50625.84	1.0	21.35	0.9
14/03/2022 16:00	23	16	22286.46	2.6	41519.25	1.6	14.54	0.7	1170.64	1.4	87.83	1.9	71.28	1.6	858.12	2.5	51764.45	1.2	22.82	2.8
14/03/2022 16:03	24	17	24293.97	1.7	43673.29	1.3	15.61	1.0	1310.72	2.0	95.83	1.2	80.81	1.1	925.91	1.2	59337.77	1.7	27.54	2.6
14/03/2022 16:07	25	18	27675.31	1.6	38776.01	0.5	17.72	1.0	1715.79	1.1	108.12	0.9	90.63	1.6	976.77	1.2	69504.51	1.1	29.98	1.0
14/03/2022 16:10	26	19	27484.39	2.5	48249.52	1.4	17.23	0.5	1603.63	2.0	106.55	1.4	90.23	1.4	934.99	1.4	63797.06	1.2	27.86	1.7
14/03/2022 16:14	27	20	20805.54	1.6	44979.81	0.9	14.01	1.9	1221.99	0.3	88.94	1.5	81.23	1.2	971.78	2.1	60482.39	0.6	25.04	0.7
14/03/2022 16:35	28	21	23253.29	1.5	35536.02	1.1	14.81	0.9	1439.66	0.3	92.28	0.3	75.83	0.2	863.57	1.4	57797.07	1.9	25.73	1.2
14/03/2022 16:39	29	22	20839.32	0.5	43023.14	1.5	14.41	2.9	1275.11	0.6	88.94	0.6	71.67	0.9	921.54	1.4	59355.28	1.6	27.76	0.9
14/03/2022 16:42	30	23	20626.12	1.8	48090.18	1.0	14.14	3.0	1247.49	2.3	86.04	1.4	71.94	2.1	852.88	1.5	55017.24	0.8	23.54	1.8
14/03/2022 16:46	31	24	23572.52	1.3	54445.65	1.6	16.35	2.0	1523.30	1.8	99.33	1.3	80.62	1.3	1094.51	0.9	65365.74	0.9	30.18	0.5
14/03/2022 16:49	32	25	17243.18	0.6	46292.60	1.0	12.27	2.9	1031.71	1.0	74.61	1.7	57.92	1.8	887.81	2.8	51884.00	1.9	22.63	0.6
14/03/2022 16:53	33	26	20880.15	1.7	52837.19	1.1	14.22	2.8	1253.93	1.2	88.59	1.2	79.89	1.5	914.27	1.2	58776.09	0.6	24.39	2.3
14/03/2022 16:56	34	27	22702.22	0.7	49471.12	0.8	14.80	2.7	1397.48	2.1	88.45	2.1	73.57	1.5	881.85	1.7	54426.60	0.5	24.57	3.5
14/03/2022 17:00	35	28	34362.49	1.4	55745.95	0.4	21.69	1.5	1881.36	1.3	127.88	1.4	108.45	2.0	1195.88	0.6	76461.37	0.3	34.70	1.9
14/03/2022 17:03	36	29	20780.10	1.4	50336.17	0.2	13.99	2.3	1274.61	1.4	87.51	1.1	72.35	0.5	835.55	1.5	56022.91	1.0	21.53	2.0
14/03/2022 17:07	37	30	20724.57	1.0	38050.03	2.4	12.82	0.3	1218.06	0.7	78.94	1.3	63.84	0.7	800.96	1.5	51177.13	1.8	22.38	0.7
14/03/2022 17:11	38	31	17284.83	1.3	47247.94	0.5	12.71	1.2	1140.70	0.8	80.44	1.4	64.12	1.4	922.92	1.6	56651.66	0.4	24.88	2.2
14/03/2022 17:14	39	32	22622.76	0.2	36631.24	1.5	14.58	0.8	1385.34	0.3	90.18	0.6	72.51	0.3	899.37	0.7	54421.65	1.4	24.59	1.2
14/03/2022 17:18	40	33	18632.21	0.8	49343.71	1.2	12.86	0.9	1152.65	0.3	81.25	0.9	73.51	1.0	871.42	0.7	52335.03	1.3	24.05	0.9
14/03/2022 17:21	48	34	21557.90	1.0	44577.09	0.7	13.95	1.1	1309.30	1.0	86.98	0.9	74.56	0.8	869.53	0.6	53082.10	0.4	24.14	0.8
14/03/2022 17:25	49 rep1	35	24723.49	0.8	74690.23	0.8	15.98	0.8	1187.97	0.6	99.80	0.7	83.61	0.5	783.64	1.0	54691.05	0.5	24.43	0.6
14/03/2022 17:28	49 rep2	35	24934.42	1.5	81264.06	2.1	16.24	1.7	1201.92	1.3	100.88	0.8	84.90	1.7	797.05	2.1	59434.54	2.1	24.78	0.2
14/03/2022 17:32	50	36	19087.47	0.7	68207.54	1.3	12.55	0.4	981.29	0.4	79.04	0.9	61.92	0.3	670.83	1.1	47562.87	0.1	18.69	0.6
14/03/2022 17:35	51	37	19440.16	1.8	107198.35	1.5	13.41	2.6	1241.35	0.7	77.51	0.8	59.20	1.6	841.54	1.3	47606.95	1.1	20.44	1.3
14/03/2022 17:39	52	38	17003.72	0.7	69838.87	0.3	11.41	0.6	897.16	1.2	75.70	1.1	56.89	0.5	599.05	2.6	47588.44	0.7	19.34	2.2
14/03/2022 17:43	53	39	21127.08	1.5	81268.30	1.0	14.76	2.7	1316.16	0.5	89.28	1.1	70.53	0.8	844.90	0.7	57336.52	0.9	22.32	0.6
14/03/2022 17:46	54	40	21800.29	0.9	70367.89	1.1	14.32	1.1	1160.61	0.5	91.31	0.8	75.39	0.7	687.75	2.2	52709.32	1.3	21.32	2.5
14/03/2022 17:50	55	41	28522.06	1.6	96976.46	0.8	17.98	1.6	1579.42	1.2	109.71	1.4	91.11	2.0	990.57	2.3	54747.21	0.7	25.66	2.2
14/03/2022 17:53	56	42	17883.08	0.6	96775.86	0.3	14.01	2.3	1371.38	0.4	75.54	0.6	52.59	1.6	866.42	0.9	49511.21	0.9	20.47	1.6
14/03/2022 17:57	57	43	16270.37	1.6	66097.40	1.0	11.76	2.0	980.55	2.0	73.08	1.8	59.98	1.6	676.91	1.8	50130.86	0.9	20.65	0.6
14/03/2022 18:00	58	44	27151.63	1.4	81918.23	3.2	18.18	0.6	1529.65	1.9	107.60	1.1	87.09	2.2	1005.88	3.2	59744.50	1.2	25.94	2.3
14/03/2022 18:04	59	45	19219.41	1.2	82156.96	1.5	13.12	1.4	1223.22	1.7	75.94	1.9	57.52	1.5	740.78	1.0	46222.28	1.2	19.76	0.7
14/03/2022 18:07	60	46	19250.53	0.5	87045.74	2.2	12.92	2.3	1255.83	0.8	76.67	0.9	57.39	1.7	741.56	0.8	46453.89	1.2	18.74	0.8

Sample			60 -> 60 Ni [O2]		63 -> 63 Cu [O2]		66 -> 66 Zn [H2]		71 -> 71 Ga [H2]		75 -> 91 As [O2]		78 -> 78 Se [H2]		85 -> 85 Rb [O2]		88 -> 88 Sr [H2]		89 -> 105 Y [O2]	
Acq. Date-Time	Sample Name	Comment	Conc. [ug/l]	Conc. RSD	Conc. [ug/l]	Conc. RSD	Conc. [ug/l]	Conc. RSD	Conc. [ug/l]	Conc. RSD	Conc. [ug/l]	Conc. RSD	Conc. [ug/l]	Conc. RSD	Conc. [ug/l]	Conc. RSD	Conc. [ug/l]	Conc. RSD	Conc. [ug/l]	Conc. RSD
14/03/2022 14:41	1	Blank 1	<0.0016	N/A	<0.019	N/A	<0.011	N/A	<0.00039	177.1	<0.0023	N/A	<0.0069	9924.1	<0.0025	N/A	<0.0010	N/A	<0.00022	188.7
14/03/2022 14:45	2	Blank 2	<0.0016	N/A	<0.019	N/A	<0.011	142.0	<0.00039	68.9	<0.0023	0.0	<0.0069	127.7	<0.0025	N/A	<0.0010	N/A	<0.00022	32.0
14/03/2022 14:49	3	Blank 3	<0.0016	N/A	<0.019	N/A	0.098	147.6	0.00096	140.5	<0.0023	0.0	<0.0069	184.1	<0.0025	N/A	0.098	145.5	<0.00022	N/A
14/03/2022 14:52	4	Ref. marine 1	81.24	1.5	59.97	1.0	289.03	2.7	33.05	0.5	39.74	1.2	2.78	14.4	229.48	1.0	201.10	0.7	28.52	1.8
14/03/2022 14:56	5	Ref. marine 2	98.71	3.7	79.50	2.9	374.30	0.3	41.28	1.0	49.39	6.0	3.34	16.1	270.64	3.3	242.28	0.0	35.05	3.1
14/03/2022 14:59	6	Ref. river 1	100.18	2.0	87.82	1.3	808.50	1.0	21.76	2.3	20.42	2.0	5.57	17.8	127.37	1.1	457.69	0.6	36.10	0.9
14/03/2022 15:03	7	Ref. river 2	93.22	2.3	100.41	0.5	771.39	1.8	20.64	2.5	17.95	4.2	5.35	10.6	119.68	0.1	428.76	1.4	32.61	0.4
14/03/2022 15:07	8	1	58.61	1.5	37.99	2.1	140.06	0.5	29.54	2.6	10.12	3.9	2.97	12.2	177.72	0.7	122.14	0.1	46.79	1.2
14/03/2022 14:31	9	2	63.17	0.8	38.69	3.5	133.04	1.3	32.28	1.1	10.37	3.1	2.69	27.0	193.45	0.2	141.76	0.6	57.84	0.6
14/03/2022 15:10	9 rep2	2	60.16	1.3	36.55	0.7	132.37	1.2	32.10	2.0	9.61	4.8	3.34	41.8	186.43	1.2	140.55	1.3	56.09	1.3
14/03/2022 15:14	10	3	57.44	2.9	40.80	0.8	133.90	1.5	29.04	0.9	12.84	5.5	4.20	16.6	160.29	1.5	124.88	1.4	53.05	2.0
14/03/2022 15:17	11	4	61.39	1.6	41.94	0.3	148.70	1.0	31.76	2.2	11.04	3.1	3.60	38.7	181.59	1.2	129.73	1.0	52.17	0.5
14/03/2022 15:21	12	5	55.47	1.6	40.89	1.2	134.21	2.5	27.14	1.6	13.90	2.1	2.61	36.3	169.86	0.4	104.78	0.2	45.45	1.0
14/03/2022 15:24	13	6	57.25	1.2	34.71	2.7	127.88	1.1	29.56	1.4	8.62	4.2	3.10	28.9	178.98	1.5	126.46	1.3	48.35	0.9
14/03/2022 15:28	14	7	59.67	1.7	37.75	1.0	141.16	0.5	31.53	1.6	9.64	3.7	3.14	36.3	192.41	0.8	120.85	1.0	51.97	1.3
14/03/2022 15:31	15	8	54.96	1.0	44.64	0.5	129.67	3.1	26.40	3.2	13.69	8.9	2.79	12.8	154.48	0.3	106.32	1.9	51.27	1.6
14/03/2022 15:35	16	9	44.24	0.9	31.87	0.2	95.65	2.5	19.52	2.1	8.62	10.0	2.51	21.3	109.57	0.7	90.55	0.3	33.57	1.2
14/03/2022 15:38	17	10	46.26	2.4	35.14	1.2	107.99	0.8	22.72	2.0	12.90	3.6	2.32	9.3	129.62	0.6	92.30	1.0	42.62	0.9
14/03/2022 15:42	18	11	54.93	1.7	43.45	1.3	133.62	2.0	27.00	2.0	15.50	4.6	2.64	39.1	161.06	0.7	99.80	0.5	46.91	1.2
14/03/2022 15:45	19	12	62.46	2.0	46.51	0.3	142.20	1.6	28.49	0.5	13.71	3.6	2.61	19.3	178.05	1.5	118.39	0.6	55.59	1.4
14/03/2022 15:49	20	13	49.77	1.0	40.03	1.1	126.86	2.3	23.07	1.6	14.81	5.3	2.20	36.0	132.27	0.3	88.50	1.5	41.61	0.4
14/03/2022 15:53	21	14	42.90	1.2	30.80	1.0	92.79	1.4	19.89	3.0	10.03	3.1	2.26	16.6	116.73	0.8	87.17	2.0	35.96	1.0
14/03/2022 15:56	22	15	40.60	0.7	33.39	0.5	94.18	3.1	18.98	2.2	10.51	4.3	2.04	32.5	105.74	0.8	77.88	0.9	38.27	0.4
14/03/2022 16:00	23	16	45.09	2.3	29.01	1.1	97.55	2.8	20.87	2.9	8.30	5.5	2.27	24.1	126.42	2.7	92.24	2.2	38.21	1.8
14/03/2022 16:03	24	17	49.61	1.0	36.29	2.3	105.23	1.2	23.70	3.5	10.09	4.0	2.25	13.5	137.94	1.6	105.68	1.7	40.43	1.5
14/03/2022 16:07	25	18	54.96	1.0	38.34	2.2	137.10	1.5	27.74	0.9	16.03	6.4	4.10	11.4	159.80	0.7	101.05	0.6	52.75	1.5
14/03/2022 16:10	26	19	52.77	2.4	35.24	1.7	127.98	2.1	26.12	1.0	11.82	6.4	2.17	33.6	155.73	1.2	109.88	0.4	45.71	1.1
14/03/2022 16:14	27	20	85.25	1.7	1337.34	0.7	699.26	0.5	21.74	1.3	9.90	7.4	2.54	35.2	122.11	1.0	98.69	1.0	37.11	0.9
14/03/2022 16:35	28	21	45.78	1.5	32.57	1.5	115.16	0.3	23.10	1.7	11.00	1.5	3.04	33.2	132.37	0.6	86.90	2.0	45.07	1.2
14/03/2022 16:39	29	22	49.28	1.8	40.11	0.5	110.97	2.0	21.60	1.9	11.00	5.8	2.47	4.1	122.86	0.6	90.36	0.6	38.86	0.4
14/03/2022 16:42	30	23	46.26	1.9	32.16	0.5	116.69	1.8	20.95	1.4	10.38	4.7	3.22	39.4	121.83	2.0	87.41	1.3	38.00	1.2
14/03/2022 16:46	31	24	54.03	0.8	40.78	2.0	136.67	2.5	24.11	0.9	15.92	5.1	2.67	17.4	139.85	1.3	99.56	0.3	49.88	1.5
14/03/2022 16:49	32	25	40.28	1.3	28.50	2.3	111.50	1.7	17.72	3.2	9.22	8.5	2.51	27.5	102.41	1.3	74.06	1.3	35.06	1.4
14/03/2022 16:53	33	26	46.34	1.6	40.63	1.9	107.29	1.3	21.55	1.4	10.67	6.8	2.04	29.4	119.53	0.5	102.56	0.4	44.28	1.6
14/03/2022 16:56	34	27	43.59	0.5	37.46	1.9	110.05	2.1	21.74	1.9	9.21	3.4	2.03	8.0	128.24	0.9	84.61	0.1	39.72	1.1
14/03/2022 17:00	35	28	64.17	0.8	53.36	0.4	152.08	1.4	32.30	1.2	13.31	7.7	3.27	24.7	196.11	0.9	124.64	1.0	59.29	1.4
14/03/2022 17:03	36	29	43.13	1.2	29.34	2.1	103.80	1.6	21.33	0.4	8.17	4.5	3.28	45.7	119.97	1.5	88.73	0.9	44.81	1.4
14/03/2022 17:07	37	30	42.35	1.1	30.04	1.0	115.48	2.1	19.86	3.2	9.77	6.3	2.10	30.0	120.85	0.5	70.39	1.5	34.83	0.9
14/03/2022 17:11	38	31	48.29	2.7	31.17	1.1	100.62	2.0	18.71	0.8	10.61	1.4	2.95	12.2	103.08	1.3	83.42	0.4	38.54	1.1
14/03/2022 17:14	39	32	47.36	0.1	33.53	1.5	103.33	0.6	20.90	2.3	12.41	7.3	1.93	11.9	129.86	0.9	82.33	0.7	37.99	0.1
14/03/2022 17:18	40	33	45.24	1.8	35.28	0.4	101.70	3.5	18.59	1.4	10.01	5.7	2.50	15.5	107.87	1.0	88.13	1.7	37.99	0.8
14/03/2022 17:21	48	34	45.03	3.6	39.31	1.9	106.06	1.0	20.52	1.1	14.71	3.3	3.27	22.5	121.23	1.2	84.81	0.5	40.66	1.5
14/03/2022 17:25	49 rep1	35	50.91	2.8	34.93	1.1	104.76	0.1	23.05	0.6	7.96	8.0	2.82	13.4	138.82	1.1	131.78	0.6	43.76	1.5
14/03/2022 17:28	49 rep2	35	51.67	0.7	35.07	0.8	111.90	1.7	25.05	3.0	8.48	1.6	2.41	28.6	139.16	1.1	142.66	1.2	44.14	1.3
14/03/2022 17:32	50	36	39.00	0.3	29.88	1.0	84.17	1.2	18.54	2.5	7.47	4.5	1.79	42.3	109.57	0.3	101.83	0.7	33.53	0.6
14/03/2022 17:35	51	37	38.34	1.0	30.59	0.5	101.58	4.1	19.29	1.3	5.31	8.5	3.20	21.3	113.69	1.8	101.82	0.6	42.14	1.0
14/03/2022 17:39	52	38	36.88	0.5	37.76	3.1	79.19	1.3	17.03	2.6	7.12	5.0	1.93	25.7	98.38	0.9	95.54	1.4	30.40	0.5
14/03/2022 17:43	53	39	44.34	1.6	36.17	1.5	107.93	0.2	21.68	1.7	11.75	1.7	2.42	13.5	122.42	1.1	115.18	0.8	43.93	1.3
14/03/2022 17:46	54	40	46.01	1.5	31.74	0.7	93.97	1.8	20.59	3.6	7.98	3.8	2.13	24.6	121.34	0.9	119.75	1.0	36.21	1.2
14/03/2022 17:50	55	41	54.46	1.1	33.67	0.9	127.46	2.0	24.29	1.2	7.49	6.8	2.62	45.1	156.11	1.4	100.08	0.9	43.75	1.2
14/03/2022 17:53	56	42	34.84	0.7	29.66	1.2	91.98	0.8	18.99	2.2	4.39	13.0	2.90	17.2	107.06	1.7	109.08	0.7	47.53	2.1
14/03/2022 17:57	57	43	36.93	2.8	31.56	1.3	81.60	1.9	17.52	3.1	7.55	3.3	3.02	12.0	96.13	1.7	87.75	1.1	35.77	1.5
14/03/2022 18:00	58	44	51.48	1.3	37.56	2.0	131.23	1.2	27.24	1.1	7.68	6.4	3.97	13.4	151.24	1.5	112.03	1.5	53.01	1.8
14/03/2022 18:04	59	45	35.15	2.0	31.81	1.4	96.88	1.6	19.21	3.1	6.01	1.6	2.71	34.5	113.04	1.9	89.09	1.5	41.07	1.0
14/03/2022 18:07	60	46	34.49	1.0	29.33	1.3	96.61	3.1	19.38	0.8	5.66	7.7	2.94	26.4	113.24	0.8	94.03	0.8	39.73	0.9

Sample			90 -> 106 Zr [O2]		93 -> 125 Nb [O2]		95 -> 127 Mo [O2]		111 -> 111 Cd [O2]		115 -> 115 In [O2]		118 -> 118 Sn [O2]		121 -> 137 Sb [O2]		133 -> 133 Cs [O2]		137 -> 137 Ba [O2]	
Acq. Date-Time	Sample Name	Comment	Conc. [ug/l]	Conc. RSD	Conc. [ug/l]	Conc. RSD	Conc. [ug/l]	Conc. RSD	Conc. [ug/l]	Conc. RSD	Conc. [ug/l]	Conc. RSD	Conc. [ug/l]	Conc. RSD	Conc. [ug/l]	Conc. RSD	Conc. [ug/l]	Conc. RSD	Conc. [ug/l]	Conc. RSD
14/03/2022 14:41	1	Blank 1	0.00072	41.2	<0.00012	N/A	0.0010	60.9	<0.00063	3100.9	<0.000035	137.2	<0.00086	214.5	<0.00076	N/A	<0.00053	N/A	<0.0023	N/A
14/03/2022 14:45	2	Blank 2	<0.00046	27.3	<0.00012	186.6	<0.00038	N/A	<0.00063	0.0	<0.000035	N/A	<0.00086	112.1	<0.00076	0.0	<0.00053	N/A	<0.0023	78.3
14/03/2022 14:49	3	Blank 3	<0.00046	170.2	<0.00012	N/A	<0.00038	N/A	<0.00063	1126.3	<0.000035	1310.5	<0.00086	N/A	<0.00076	0.0	<0.00053	N/A	<0.0023	212.9
14/03/2022 14:52	4	Ref. marine 1	31.43	1.1	0.033	19.0	1.87	4.6	0.40	19.9	0.19	16.4	1.35	6.4	0.090	46.1	14.73	1.5	1415.05	1.2
14/03/2022 14:56	5	Ref. marine 2	33.40	2.7	0.045	39.5	2.33	10.5	0.74	0.4	0.25	5.7	1.37	1.5	0.17	32.5	17.71	1.4	1682.48	2.2
14/03/2022 14:59	6	Ref. river 1	35.31	0.9	0.19	15.3	1.32	4.5	6.13	8.3	0.083	10.7	2.05	4.4	0.17	12.9	10.10	1.1	493.43	2.2
14/03/2022 15:03	7	Ref. river 2	33.65	2.5	0.17	8.3	1.25	8.8	5.40	4.1	0.082	11.4	2.10	7.3	0.35	43.8	9.32	2.6	462.74	1.3
14/03/2022 15:07	8	1	16.88	1.4	0.50	1.7	0.87	7.4	0.25	17.1	0.084	12.7	1.15	5.2	0.11	32.4	12.58	1.0	561.99	0.6
14/03/2022 14:31	9	2	18.50	1.7	0.58	6.7	0.81	17.5	0.34	8.3	0.11	12.4	1.33	4.5	0.17	22.7	13.51	1.1	644.95	0.8
14/03/2022 15:10	9 rep2	2	18.65	2.4	0.56	5.2	0.87	12.5	0.28	14.4	0.095	20.0	1.24	3.8	0.13	46.2	12.96	0.9	621.43	0.7
14/03/2022 15:14	10	3	19.55	3.4	0.48	0.9	1.21	3.0	0.28	29.4	0.091	14.2	1.16	3.1	0.063	44.4	10.95	1.2	502.17	1.6
14/03/2022 15:17	11	4	18.61	2.1	0.59	2.4	1.03	16.4	0.30	26.4	0.097	3.2	1.26	4.2	0.082	16.3	12.72	2.1	582.08	1.5
14/03/2022 15:21	12	5	16.81	0.8	0.54	10.8	0.90	7.2	0.23	21.3	0.088	17.8	1.17	3.6	0.11	30.7	11.22	1.3	588.10	1.1
14/03/2022 15:24	13	6	16.85	2.7	0.53	2.4	0.79	2.3	0.26	16.7	0.092	6.0	1.12	4.0	0.13	16.4	12.54	1.4	573.54	0.6
14/03/2022 15:28	14	7	19.08	0.3	0.52	5.4	0.77	6.1	0.24	29.4	0.097	13.9	1.07	9.8	0.073	45.9	13.55	2.1	639.73	0.6
14/03/2022 15:31	15	8	17.86	0.5	0.61	2.0	0.93	10.6	0.32	11.9	0.092	4.1	1.28	6.1	0.095	24.6	10.23	1.1	499.98	0.7
14/03/2022 15:35	16	9	11.96	0.3	0.49	3.9	0.78	6.5	0.23	15.5	0.067	12.1	1.12	2.4	0.12	68.2	7.33	1.5	325.91	2.0
14/03/2022 15:38	17	10	17.06	1.5	0.44	4.0	0.61	13.5	0.28	56.5	0.071	15.1	1.06	5.7	0.086	95.2	8.08	1.8	437.12	0.8
14/03/2022 15:42	18	11	18.55	0.8	0.49	1.6	0.73	7.6	0.31	12.5	0.085	9.5	1.13	9.6	0.087	49.3	10.61	1.2	526.83	1.2
14/03/2022 15:45	19	12	20.91	1.9	0.59	6.3	0.79	11.6	0.28	18.1	0.096	4.5	1.18	1.8	0.14	10.8	12.18	1.6	618.99	0.8
14/03/2022 15:49	20	13	15.51	1.5	0.55	3.8	0.97	3.9	0.29	13.4	0.076	8.2	1.15	5.1	0.088	18.0	7.63	2.0	401.22	0.3
14/03/2022 15:53	21	14	14.49	2.1	0.48	5.0	0.73	8.6	0.24	38.2	0.067	20.9	1.08	5.0	<0.00076	87.9	7.33	0.8	359.89	0.2
14/03/2022 15:56	22	15	14.65	1.0	0.49	6.1	0.56	8.4	0.17	12.4	0.060	10.6	1.05	6.4	0.074	47.3	6.11	0.5	323.21	1.0
14/03/2022 16:00	23	16	13.71	1.8	0.41	2.7	0.52	5.9	0.16	44.2	0.073	7.3	0.95	11.0	0.12	26.5	7.98	1.0	384.01	1.4
14/03/2022 16:03	24	17	14.82	2.8	0.46	3.0	0.57	12.9	0.24	13.6	0.067	12.9	1.01	5.3	0.092	44.8	9.00	2.5	417.16	1.8
14/03/2022 16:07	25	18	20.94	1.6	0.51	0.7	1.04	9.7	0.22	26.1	0.086	4.4	1.04	9.6	0.087	40.3	10.25	1.2	534.04	1.3
14/03/2022 16:10	26	19	17.34	0.9	0.47	6.5	0.85	10.4	0.29	3.6	0.081	5.4	1.10	7.6	0.11	21.9	10.63	1.0	514.14	0.8
14/03/2022 16:14	27	20	12.78	1.6	0.44	4.5	0.65	9.9	0.25	7.0	0.080	9.9	2.84	1.8	0.14	52.1	7.83	1.3	342.79	0.7
14/03/2022 16:35	28	21	17.62	0.6	0.47	5.8	0.61	12.8	0.16	22.1	0.073	7.6	0.99	7.3	0.051	81.9	8.49	1.5	443.71	1.8
14/03/2022 16:39	29	22	14.51	1.9	0.45	3.9	0.78	16.6	0.21	18.4	0.071	13.0	1.03	6.1	0.088	8.1	7.81	1.1	372.69	1.3
14/03/2022 16:42	30	23	14.44	4.1	0.44	4.4	0.65	7.4	320.87	1.8	0.071	17.1	0.97	4.8	0.094	44.4	7.24	2.8	361.39	0.8
14/03/2022 16:46	31	24	16.59	3.5	0.52	12.4	0.85	8.0	0.35	30.4	0.083	3.7	1.12	7.1	0.13	39.7	8.41	3.7	437.26	1.7
14/03/2022 16:49	32	25	11.47	2.2	0.31	5.5	0.65	16.2	0.23	11.7	0.061	3.5	0.92	5.1	0.080	20.3	5.69	1.8	301.02	0.8
14/03/2022 16:53	33	26	15.56	1.0	0.48	6.6	0.94	5.4	0.17	24.7	0.064	8.1	1.13	9.1	0.18	25.0	7.36	1.4	422.38	0.5
14/03/2022 16:56	34	27	14.35	2.8	0.40	7.7	0.62	10.3	0.23	23.9	0.073	11.6	0.94	6.8	0.047	94.0	7.48	1.4	477.85	1.7
14/03/2022 17:00	35	28	22.66	2.8	0.55	3.8	0.79	4.3	0.38	18.0	0.10	14.2	1.14	3.2	0.094	55.0	13.21	1.4	663.05	0.6
14/03/2022 17:03	36	29	17.30	3.7	0.47	0.7	0.91	8.4	0.27	30.4	0.073	6.1	1.12	9.8	0.14	16.7	6.92	1.0	376.16	1.6
14/03/2022 17:07	37	30	12.53	1.2	0.40	5.6	0.46	21.0	0.23	13.5	0.066	11.3	0.72	0.7	<0.00076	81.3	7.49	2.4	366.88	1.3
14/03/2022 17:11	38	31	12.48	0.8	0.43	2.4	0.96	7.0	0.26	9.6	0.065	6.4	1.08	9.1	0.12	43.6	5.92	0.8	300.38	0.9
14/03/2022 17:14	39	32	14.25	1.4	0.52	0.1	0.58	6.8	0.19	31.8	0.073	19.4	1.07	2.1	0.10	23.7	8.32	2.4	399.66	0.5
14/03/2022 17:18	40	33	13.90	1.7	0.58	8.1	0.81	20.2	0.20	29.0	0.071	5.7	1.19	9.5	0.18	34.9	6.36	2.6	352.06	0.8
14/03/2022 17:21	48	34	14.15	1.2	0.53	1.4	0.65	8.6	0.21	23.6	0.068	13.0	1.21	8.4	0.15	33.9	7.08	1.9	393.07	1.2
14/03/2022 17:25	49 rep1	35	13.87	2.2	0.32	5.1	1.07	9.5	0.43	25.4	0.074	3.4	0.98	5.2	0.12	13.0	9.47	1.9	361.65	0.1
14/03/2022 17:28	49 rep2	35	14.13	2.4	0.34	4.3	1.06	2.6	0.37	24.7	0.070	13.3	1.01	4.6	0.053	80.7	9.36	0.7	364.89	0.6
14/03/2022 17:32	50	36	10.51	1.9	0.39	10.3	1.27	4.1	0.30	39.0	0.058	14.7	1.18	4.4	0.12	28.5	6.66	1.6	254.12	0.5
14/03/2022 17:35	51	37	9.91	2.4	0.34	2.9	0.82	24.4	0.33	27.9	0.057	7.2	0.93	9.0	<0.00076	1.5	6.05	2.8	315.18	0.8
14/03/2022 17:39	52	38	9.32	1.8	0.29	5.2	0.81	8.3	0.27	23.2	0.055	20.2	0.91	5.2	0.086	32.3	5.92	2.1	270.00	1.4
14/03/2022 17:43	53	39	12.11	2.7	0.56	6.1	0.88	6.0	0.39	13.4	0.081	5.7	1.29	6.3	0.13	25.3	7.36	1.1	332.31	1.0
14/03/2022 17:46	54	40	12.50	2.3	0.51	4.8	1.12	13.7	0.34	11.9	0.061	20.1	1.29	5.3	0.16	18.2	8.50	1.3	334.41	0.4
14/03/2022 17:50	55	41	15.80	0.7	0.43	5.1	1.03	9.2	0.54	4.8	0.083	10.8	0.95	4.6	<0.00076	95.1	9.88	0.9	526.10	0.3
14/03/2022 17:53	56	42	8.89	1.4	0.51	11.4	0.82	8.1	0.30	27.3	0.069	4.0	1.21	6.4	<0.00076	106.8	5.21	3.1	305.30	1.3
14/03/2022 17:57	57	43	9.83	2.7	0.35	3.3	0.92	5.8	0.26	34.2	0.066	16.6	1.00	6.1	0.10	42.1	5.50	2.7	264.47	2.2
14/03/2022 18:00	58	44	15.86	2.2	0.38	2.5	0.98	8.3	0.41	15.8	0.095	9.4	1.19	10.3	0.083	81.8	8.93	0.6	511.76	0.5
14/03/2022 18:04	59	45	10.17	1.4	0.31	9.8	0.78	14.9	0.25	38.3	0.064	24.1	1.05	2.6	0.062	91.0	5.80	1.6	318.84	0.4
14/03/2022 18:07	60	46	9.59	0.7	0.35	6.8	0.63	20.5	0.26	42.5	0.065	11.5	1.01	8.9	<0.00076	65.6	6.02	1.4	321.79	0.9

Sample			139 -> 155 La [O2]		140 -> 156 Ce [O2]		141 -> 157 Pr [O2]		146 -> 162 Nd [O2]		153 -> 153 Eu [O2]		169 -> 185 Tm [O2]		175 -> 191 Lu [O2]		181 -> 213 Ta [O2]		182 -> 214 W [O2]	
Acq. Date-Time	Sample Name	Comment	Conc. [ug/l]	Conc. RSD	Conc. [ug/l]	Conc. RSD	Conc. [ug/l]	Conc. RSD	Conc. [ug/l]	Conc. RSD	Conc. [ug/l]	Conc. RSD	Conc. [ug/l]	Conc. RSD	Conc. [ug/l]	Conc. RSD	Conc. [ug/l]	Conc. RSD	Conc. [ug/l]	Conc. RSD
14/03/2022 14:41	1	Blank 1	<0.000078	N/A	<0.00015	37.4	<0.00043	N/A	<0.00017	229.7	<0.000056	N/A	<0.00028	N/A	<0.000043	N/A	<0.000028	N/A	<0.00026	218.8
14/03/2022 14:45	2	Blank 2	<0.000078	N/A	<0.00015	120.0	<0.00043	N/A	<0.00017	N/A	<0.000056	N/A	<0.00028	N/A	<0.000043	N/A	<0.000028	N/A	<0.00026	362.7
14/03/2022 14:49	3	Blank 3	<0.000078	N/A	<0.00015	N/A	<0.00043	N/A	<0.00017	N/A	<0.000056	N/A	<0.00028	0.0	<0.000043	N/A	<0.000028	N/A	<0.00026	231.8
14/03/2022 14:52	4	Ref. marine 1	50.58	0.1	102.25	1.0	12.31	1.0	46.71	0.9	2.16	1.3	0.34	4.7	0.28	3.2	<0.000028	N/A	<0.00026	N/A
14/03/2022 14:56	5	Ref. marine 2	56.95	2.1	115.83	1.9	13.92	3.1	54.03	2.9	2.47	4.1	0.40	6.3	0.36	15.2	<0.000028	1532.8	<0.00026	379.8
14/03/2022 14:59	6	Ref. river 1	79.25	2.0	169.88	2.2	19.53	1.9	74.48	1.4	1.94	2.0	0.44	2.4	0.42	1.7	<0.000028	N/A	0.22	2.9
14/03/2022 15:03	7	Ref. river 2	68.90	1.3	148.88	1.5	16.97	0.9	64.93	0.6	1.75	1.9	0.42	6.8	0.38	2.6	<0.000028	N/A	0.23	6.5
14/03/2022 15:07	8	1	84.92	0.9	183.27	1.1	21.32	0.6	81.75	0.2	2.83	0.7	0.59	2.2	0.48	4.0	<0.000028	N/A	0.066	10.9
14/03/2022 14:31	9	2	97.24	0.3	210.17	0.6	24.44	0.3	92.93	0.7	3.20	2.2	0.75	0.6	0.65	3.2	<0.000028	238.1	0.11	5.4
14/03/2022 15:10	9 rep2	2	93.62	0.6	202.27	0.7	23.40	0.9	90.05	0.5	3.14	0.7	0.70	4.6	0.62	5.3	<0.000028	289.9	0.11	20.1
14/03/2022 15:14	10	3	99.48	1.1	215.06	1.4	25.26	1.1	96.85	0.8	3.18	1.1	0.68	4.6	0.56	7.1	<0.000028	N/A	0.085	25.0
14/03/2022 15:17	11	4	95.28	0.6	206.54	1.3	24.12	1.1	92.19	0.7	3.14	4.5	0.67	0.5	0.54	9.1	<0.000028	N/A	0.085	18.7
14/03/2022 15:21	12	5	83.67	0.6	183.50	0.7	21.42	0.5	82.05	0.9	2.83	1.5	0.57	4.0	0.46	6.0	<0.000028	N/A	0.11	22.9
14/03/2022 15:24	13	6	86.64	1.5	186.79	0.9	21.86	2.2	83.67	2.1	2.86	3.2	0.62	2.5	0.50	4.5	<0.000028	N/A	0.079	20.5
14/03/2022 15:28	14	7	98.49	0.4	214.98	0.2	25.04	0.6	95.83	1.2	3.18	3.6	0.71	3.8	0.53	2.3	<0.000028	167.7	0.084	10.1
14/03/2022 15:31	15	8	93.87	0.4	202.81	0.5	23.65	0.4	90.24	0.4	3.07	2.6	0.68	3.8	0.57	9.2	<0.000028	N/A	0.15	20.9
14/03/2022 15:35	16	9	62.39	0.8	134.08	1.8	15.80	1.3	60.32	2.1	2.07	3.2	0.45	2.2	0.38	12.0	<0.000028	N/A	0.11	17.4
14/03/2022 15:38	17	10	82.27	0.9	179.40	0.7	21.02	0.3	80.67	1.0	2.70	1.4	0.55	3.8	0.47	6.2	<0.000028	N/A	0.081	18.0
14/03/2022 15:42	18	11	89.36	0.6	195.38	0.6	22.69	1.0	87.04	0.4	2.96	0.9	0.60	3.0	0.52	1.2	<0.000028	482.5	0.069	12.7
14/03/2022 15:45	19	12	108.35	0.3	236.51	0.6	27.54	0.3	106.30	0.7	3.65	1.6	0.74	1.9	0.62	8.8	<0.000028	N/A	0.12	28.7
14/03/2022 15:49	20	13	79.83	0.5	173.48	0.7	20.05	0.9	76.77	0.7	2.56	1.2	0.56	4.2	0.45	1.9	<0.000028	N/A	0.084	17.4
14/03/2022 15:53	21	14	65.26	0.2	140.90	0.1	16.40	1.5	63.54	1.1	2.12	3.5	0.47	1.5	0.41	6.1	<0.000028	33.9	0.069	30.8
14/03/2022 15:56	22	15	67.68	1.5	146.83	0.5	17.13	1.4	65.71	1.7	2.23	1.9	0.49	3.2	0.45	6.4	<0.000028	N/A	0.10	14.6
14/03/2022 16:00	23	16	71.02	1.0	153.38	0.7	17.87	0.8	68.77	0.2	2.37	1.0	0.49	4.2	0.42	8.9	<0.000028	N/A	0.065	29.3
14/03/2022 16:03	24	17	72.89	1.8	157.61	1.7	18.33	2.2	70.39	2.3	2.41	3.8	0.52	2.9	0.45	8.5	<0.000028	N/A	0.060	41.5
14/03/2022 16:07	25	18	105.33	1.2	228.73	1.8	26.81	0.9	103.14	2.4	3.49	1.1	0.68	1.5	0.54	5.3	<0.000028	N/A	0.10	12.5
14/03/2022 16:10	26	19	84.01	0.9	182.34	0.9	21.36	1.9	81.54	0.6	2.77	3.1	0.59	3.5	0.49	5.0	<0.000028	128.0	0.067	29.8
14/03/2022 16:14	27	20	69.88	0.5	152.19	1.1	17.82	1.3	68.32	1.3	2.32	2.4	0.49	5.8	0.41	8.0	<0.000028	N/A	0.082	22.8
14/03/2022 16:35	28	21	84.97	1.2	185.51	1.0	21.52	0.7	82.15	1.4	2.70	0.5	0.60	4.5	0.48	4.4	0.0020	53.3	0.067	3.3
14/03/2022 16:39	29	22	72.75	0.9	156.60	0.9	18.37	0.8	70.61	1.7	2.42	3.0	0.51	1.5	0.42	12.0	<0.000028	800.6	0.096	16.1
14/03/2022 16:42	30	23	68.58	1.0	149.45	1.1	17.42	2.2	67.11	1.5	2.32	3.0	0.48	2.9	0.38	8.7	<0.000028	N/A	0.075	40.4
14/03/2022 16:46	31	24	88.19	2.1	193.01	2.1	22.37	1.2	86.07	1.8	2.83	2.0	0.65	3.7	0.56	3.7	<0.000028	54748.3	0.070	23.6
14/03/2022 16:49	32	25	58.29	0.5	127.13	0.8	14.98	1.0	57.42	1.6	2.01	3.0	0.50	3.2	0.38	5.5	<0.000028	N/A	0.061	32.9
14/03/2022 16:53	33	26	76.18	0.8	164.31	0.7	19.20	1.5	74.97	1.5	2.49	4.0	0.59	4.4	0.47	5.0	<0.000028	N/A	0.10	11.0
14/03/2022 16:56	34	27	69.57	1.8	151.30	1.2	17.56	1.2	66.90	1.3	2.30	3.2	0.53	1.7	0.43	8.0	<0.000028	N/A	0.054	11.1
14/03/2022 17:00	35	28	112.34	0.8	244.44	0.5	28.59	0.8	109.91	0.8	3.72	1.3	0.76	3.5	0.65	11.4	<0.000028	N/A	0.076	16.2
14/03/2022 17:03	36	29	83.45	1.3	189.47	1.3	21.42	1.3	82.27	0.7	2.67	2.6	0.57	2.9	0.50	3.2	<0.000028	7692.7	0.12	2.9
14/03/2022 17:07	37	30	61.83	0.9	135.45	1.3	15.76	1.1	60.78	1.1	2.11	1.0	0.46	1.5	0.39	1.0	<0.000028	557.4	0.042	10.1
14/03/2022 17:11	38	31	72.39	0.2	157.02	0.8	18.17	0.8	70.37	0.8	2.32	3.8	0.50	2.6	0.45	8.5	<0.000028	N/A	0.081	17.1
14/03/2022 17:14	39	32	68.91	0.9	150.59	0.3	17.53	0.2	67.31	1.7	2.25	1.5	0.49	2.6	0.40	4.2	<0.000028	N/A	0.094	49.4
14/03/2022 17:18	40	33	62.58	0.4	138.52	0.9	16.06	1.2	61.14	0.4	2.06	2.4	0.51	3.8	0.42	7.7	<0.000028	N/A	0.11	15.6
14/03/2022 17:21	48	34	67.93	0.9	147.93	0.8	17.20	0.6	66.14	0.5	2.29	7.1	0.53	3.0	0.44	4.4	<0.000028	N/A	0.12	17.5
14/03/2022 17:25	49 rep1	35	66.08	0.5	144.07	0.3	16.45	0.3	63.72	1.6	2.23	0.1	0.57	1.6	0.45	7.8	<0.000028	N/A	0.051	31.5
14/03/2022 17:28	49 rep2	35	66.42	0.8	144.53	1.2	16.42	1.5	62.83	1.4	2.22	1.6	0.58	3.1	0.47	6.5	<0.000028	N/A	0.045	26.3
14/03/2022 17:32	50	36	52.54	0.5	109.92	0.7	13.14	0.1	49.91	1.1	1.74	3.5	0.44	4.3	0.43	3.3	<0.000028	N/A	0.094	20.8
14/03/2022 17:35	51	37	65.58	1.1	142.24	1.5	16.61	0.9	63.81	1.8	2.16	1.1	0.58	0.3	0.45	1.1	<0.000028	N/A	0.049	30.0
14/03/2022 17:39	52	38	46.36	0.6	98.62	1.2	11.65	0.7	44.37	0.8	1.59	0.9	0.40	4.2	0.36	7.5	<0.000028	N/A	0.068	6.0
14/03/2022 17:43	53	39	68.69	0.8	147.81	0.7	17.29	1.0	66.64	1.0	2.28	1.2	0.60	5.2	0.51	10.5	<0.000028	N/A	0.14	19.6
14/03/2022 17:46	54	40	58.45	0.6	124.09	0.8	14.51	0.8	55.99	1.2	1.97	1.0	0.47	7.1	0.40	1.5	<0.000028	N/A	0.081	20.9
14/03/2022 17:50	55	41	69.17	0.6	149.25	1.1	17.63	1.3	67.86	0.7	2.39	1.0	0.57	1.4	0.51	4.4	<0.000028	N/A	0.074	11.0
14/03/2022 17:53	56	42	71.47	2.0	153.23	2.2	18.10	2.4	70.28	1.9	2.33	6.0	0.67	1.3	0.58	5.5	<0.000028	N/A	0.12	9.7
14/03/2022 17:57	57	43	63.37	1.9	135.84	1.8	15.57	2.2	58.65	2.3	1.90	6.8	0.48	2.1	0.44	8.9	<0.000028	N/A	0.077	13.8
14/03/2022 18:00	58	44	98.47	1.1	214.41	1.2	24.81	1.1	94.56	1.4	3.09	2.7	0.69	2.1	0.56	2.3	<0.000028	N/A	0.091	8.7
14/03/2022 18:04	59	45	62.24	0.3	133.65	0.7	15.80	0.7	60.62	1.2	2.06	3.7	0.56	5.0	0.51	4.0	<0.000028	N/A	0.083	36.2
14/03/2022 18:07	60	46	59.60	0.6	128.54	0.9	15.09	0.7	58.77	0.8	2.02	0.2	0.54	2.7	0.48	8.6	<0.000028	N/A	0.076	13.1

Sample			195 -> 195 Pt [O2]		202 -> 202 Hg [O2]		205 -> 205 Tl [O2]		206 -> 206 [Pb] [O2]		207 -> 207 [Pb] [O2]		208 -> 208 Pb [O2]		209 -> 209 Bi [O2]		232 -> 248 Th [O2]		238 -> 238 U [H2]	
Acq. Date-Time	Sample Name	Comment	Conc. [ug/l]	Conc. RSD	Conc. [ug/l]	Conc. RSD	Conc. [ug/l]	Conc. RSD	Conc. [ug/l]	Conc. RSD	Conc. [ug/l]	Conc. RSD	Conc. [ug/l]	Conc. RSD	Conc. [ug/l]	Conc. RSD	Conc. [ug/l]	Conc. RSD	Conc. [ug/l]	Conc. RSD
14/03/2022 14:41	1	Blank 1	<0.00061	401.6	<0.0045	N/A	<0.00089	N/A	<0.0023	N/A	<0.00085	N/A	<0.0020	N/A	<0.00053	73.2	<0.00085	147.0	<0.000095	N/A
14/03/2022 14:45	2	Blank 2	<0.00061	397.6	<0.0045	N/A	<0.00089	N/A	<0.0023	N/A	<0.00085	N/A	<0.0020	N/A	<0.00053	135.2	<0.00085	N/A	<0.000095	N/A
14/03/2022 14:49	3	Blank 3	<0.00061	6.2	<0.0045	N/A	<0.00089	N/A	<0.0023	N/A	<0.00085	N/A	<0.0020	N/A	<0.00053	295.8	<0.00085	N/A	0.0010	127.0
14/03/2022 14:52	4	Ref. marine 1	<0.00061	133.6	<0.0045	N/A	1.38	0.2	41.63	1.1	38.09	2.2	40.18	0.3	0.63	3.6	14.96	1.1	3.18	2.2
14/03/2022 14:56	5	Ref. marine 2	<0.00061	174.4	<0.0045	N/A	1.63	5.4	50.65	1.7	46.25	2.7	48.41	1.9	1.01	9.6	18.49	4.9	4.28	0.7
14/03/2022 14:59	6	Ref. river 1	<0.00061	40.9	1.46	5.1	1.27	6.6	127.81	1.8	119.24	1.1	124.19	1.5	0.98	1.8	25.32	2.6	4.09	2.2
14/03/2022 15:03	7	Ref. river 2	<0.00061	468.0	1.18	17.0	1.21	3.4	101.35	0.9	95.74	0.5	99.26	0.8	0.90	4.2	21.65	1.1	4.02	1.9
14/03/2022 15:07	8	1	<0.00061	160.0	<0.0045	N/A	0.92	3.9	38.44	0.8	36.31	2.0	37.70	0.9	0.94	6.4	22.13	1.6	3.83	0.6
14/03/2022 14:31	9	2	<0.00061	60.0	<0.0045	N/A	0.99	3.7	46.21	0.4	44.17	0.5	45.57	0.3	0.83	3.2	25.06	1.5	4.01	2.6
14/03/2022 15:10	9 rep2	2	<0.00061	35.1	<0.0045	N/A	0.96	2.0	45.19	0.5	42.56	2.1	43.96	1.1	0.79	3.7	24.42	2.9	3.99	2.4
14/03/2022 15:14	10	3	<0.00061	244.4	<0.0045	N/A	0.82	5.3	38.94	1.6	36.53	0.7	38.00	1.0	1.23	4.3	26.02	1.0	4.39	0.5
14/03/2022 15:17	11	4	<0.00061	492.3	<0.0045	N/A	0.99	2.5	40.60	1.5	38.04	2.9	39.63	2.1	0.95	3.7	25.51	3.6	4.43	5.1
14/03/2022 15:21	12	5	<0.00061	95.9	<0.0045	N/A	0.86	2.0	36.44	1.6	34.14	0.4	35.63	0.7	1.21	3.3	22.27	1.2	3.56	1.1
14/03/2022 15:24	13	6	<0.00061	410.9	<0.0045	N/A	0.90	4.0	38.97	1.2	37.14	1.5	38.11	1.3	0.86	2.5	23.50	2.4	3.89	0.2
14/03/2022 15:28	14	7	<0.00061	142.6	<0.0045	N/A	0.96	2.9	40.27	1.3	37.95	1.2	39.43	1.0	0.95	4.4	25.88	1.2	4.01	2.1
14/03/2022 15:31	15	8	<0.00061	344.2	<0.0045	N/A	0.82	3.6	35.13	0.6	32.97	1.6	34.48	1.1	1.39	0.6	24.61	0.7	4.00	0.8
14/03/2022 15:35	16	9	<0.00061	122.2	<0.0045	N/A	0.58	6.3	28.93	1.5	27.05	1.1	28.15	0.9	2.16	4.0	16.84	1.0	2.89	2.5
14/03/2022 15:38	17	10	<0.00061	344.5	<0.0045	N/A	0.66	3.0	30.16	0.2	28.06	1.6	29.42	1.1	0.69	4.1	20.84	1.7	3.19	4.4
14/03/2022 15:42	18	11	<0.00061	N/A	<0.0045	N/A	0.83	3.5	37.17	0.9	35.08	0.8	36.20	0.6	1.14	4.0	23.89	0.7	3.62	3.5
14/03/2022 15:45	19	12	<0.00061	245.5	<0.0045	N/A	0.90	4.8	43.69	1.4	41.03	2.0	42.82	1.2	0.98	4.8	28.64	0.3	4.06	1.3
14/03/2022 15:49	20	13	<0.00061	333.8	<0.0045	N/A	0.66	3.0	33.35	1.4	31.61	0.4	32.76	1.3	1.22	2.7	21.31	0.7	3.54	1.0
14/03/2022 15:53	21	14	<0.00061	126.9	<0.0045	N/A	0.57	6.1	28.29	1.3	26.61	0.9	27.70	0.6	0.83	1.5	17.57	1.3	2.86	2.7
14/03/2022 15:56	22	15	<0.00061	58.8	<0.0045	N/A	0.55	5.7	25.53	1.2	24.09	1.4	25.15	0.7	0.62	3.8	18.12	0.0	3.08	1.5
14/03/2022 16:00	23	16	<0.00061	N/A	<0.0045	N/A	0.64	5.6	29.09	3.0	27.65	1.9	28.59	2.0	1.71	2.9	18.54	1.3	2.81	0.4
14/03/2022 16:03	24	17	<0.00061	N/A	<0.0045	N/A	0.73	5.5	31.74	1.9	30.16	1.9	31.26	2.1	0.71	6.8	19.71	2.3	3.09	3.1
14/03/2022 16:07	25	18	<0.00061	528.4	<0.0045	N/A	0.83	4.1	40.68	2.3	38.59	1.2	40.02	1.8	1.08	6.2	27.29	1.6	3.96	2.1
14/03/2022 16:10	26	19	<0.00061	62.1	<0.0045	N/A	0.83	3.5	35.47	2.2	33.41	1.7	34.46	1.5	1.55	4.1	22.91	1.3	3.68	4.0
14/03/2022 16:14	27	20	<0.00061	45.4	<0.0045	N/A	0.64	2.8	36.07	2.6	34.09	1.5	35.48	1.2	0.92	8.2	19.57	1.5	3.27	2.6
14/03/2022 16:35	28	21	<0.00061	25.5	<0.0045	N/A	0.66	6.7	31.65	1.6	30.00	0.9	31.12	0.5	1.58	2.3	21.69	2.1	3.38	4.7
14/03/2022 16:39	29	22	<0.00061	30.6	<0.0045	N/A	0.64	7.3	32.93	0.9	31.17	0.9	32.33	0.6	1.53	0.6	19.59	1.2	3.63	2.1
14/03/2022 16:42	30	23	<0.00061	76.4	<0.0045	N/A	0.64	4.8	30.72	1.2	29.03	0.9	30.20	1.1	1.13	1.9	18.99	2.4	3.16	1.6
14/03/2022 16:46	31	24	<0.00061	17.5	<0.0045	N/A	0.72	3.3	41.67	2.5	39.43	0.8	40.78	1.7	1.06	3.3	23.90	1.6	4.13	4.4
14/03/2022 16:49	32	25	<0.00061	263.5	<0.0045	N/A	0.52	7.5	25.52	2.6	24.16	0.8	25.11	1.9	0.75	12.1	18.14	1.9	4.04	2.2
14/03/2022 16:53	33	26	<0.00061	N/A	<0.0045	N/A	0.66	6.7	33.70	1.1	31.94	0.8	33.11	0.4	0.98	4.9	20.17	0.8	3.69	1.3
14/03/2022 16:56	34	27	<0.00061	371.7	<0.0045	N/A	0.61	13.0	29.10	3.0	27.28	1.3	28.33	1.9	1.05	5.2	18.66	5.1	3.48	4.5
14/03/2022 17:00	35	28	<0.00061	1499.0	<0.0045	N/A	1.07	1.0	44.97	1.3	42.41	0.6	44.27	0.7	1.21	4.2	29.56	1.0	4.58	0.7
14/03/2022 17:03	36	29	<0.00061	22.3	<0.0045	N/A	0.62	7.7	41.52	2.1	39.90	2.2	40.88	1.7	0.67	4.5	21.21	1.1	3.83	1.3
14/03/2022 17:07	37	30	<0.00061	61.3	<0.0045	N/A	0.62	2.7	25.92	3.2	24.73	0.9	25.41	1.9	0.78	4.9	17.37	1.7	2.73	1.7
14/03/2022 17:11	38	31	<0.00061	21.4	<0.0045	N/A	0.55	3.2	29.44	0.7	27.62	1.5	28.76	1.4	1.08	3.9	20.97	1.4	3.62	3.8
14/03/2022 17:14	39	32	<0.00061	N/A	<0.0045	N/A	0.65	7.0	30.24	1.2	28.02	1.6	29.36	0.7	0.86	0.7	18.75	0.4	3.09	1.8
14/03/2022 17:18	40	33	<0.00061	67.0	<0.0045	N/A	0.57	5.1	29.56	0.6	28.31	2.6	29.11	0.6	3.32	3.5	18.35	0.5	3.13	2.1
14/03/2022 17:21	48	34	<0.00061	121.7	<0.0045	N/A	0.64	1.8	29.60	1.1	27.74	0.5	28.67	0.9	0.74	16.6	17.91	1.3	3.07	3.2
14/03/2022 17:25	49 rep1	35	<0.00061	1140.3	<0.0045	N/A	0.80	7.2	30.13	1.1	27.55	1.2	28.90	0.9	0.71	3.9	18.12	1.2	4.05	1.9
14/03/2022 17:28	49 rep2	35	<0.00061	47.4	<0.0045	N/A	0.79	2.1	29.93	0.6	27.78	1.2	28.93	1.2	0.69	2.6	18.68	0.4	4.30	2.3
14/03/2022 17:32	50	36	<0.00061	N/A	<0.0045	N/A	0.55	3.2	22.11	1.4	20.48	1.7	21.49	0.8	1.09	3.3	14.43	1.8	3.88	0.5
14/03/2022 17:35	51	37	<0.00061	620.0	<0.0045	N/A	0.59	4.2	24.78	2.1	23.06	3.2	23.83	1.8	1.20	1.0	17.30	3.0	3.80	1.3
14/03/2022 17:39	52	38	<0.00061	N/A	<0.0045	N/A	0.50	6.3	24.12	2.0	21.64	1.9	22.83	1.4	0.70	7.3	13.16	1.1	3.60	0.2
14/03/2022 17:43	53	39	<0.00061	N/A	<0.0045	N/A	0.63	10.1	27.22	1.2	25.05	0.4	26.42	1.5	0.87	4.3	18.71	1.2	4.12	2.6
14/03/2022 17:46	54	40	<0.00061	28.9	<0.0045	N/A	0.67	5.0	27.94	0.6	26.28	0.7	27.36	0.7	0.63	3.3	16.51	1.2	3.59	3.3
14/03/2022 17:50	55	41	<0.00061	190.8	<0.0045	N/A	0.97	4.4	30.89	0.9	28.52	1.5	29.91	0.9	0.65	3.1	18.11	0.8	4.52	1.1
14/03/2022 17:53	56	42	<0.00061	N/A	<0.0045	N/A	0.56	6.6	23.63	2.0	21.73	1.7	22.80	2.5	0.96	0.6	18.73	1.8	4.08	1.3
14/03/2022 17:57	57	43	<0.00061	N/A	<0.0045	N/A	0.48	2.1	26.61	2.5	24.06	2.0	25.35	1.6	0.75	3.0	17.42	3.1	3.78	0.9
14/03/2022 18:00	58	44	<0.00061	366.1	<0.0045	N/A	0.83	5.4	37.05	1.2	33.94	0.7	35.73	0.6	1.35	3.3	23.99	3.3	4.85	2.2
14/03/2022 18:04	59	45	<0.00061	85.0	<0.0045	N/A	0.59	10.1	24.24	1.1	22.71	2.3	23.71	0.7	0.64	7.8	16.64	1.4	3.62	2.3
14/03/2022 18:07	60	46	<0.00061	95.4	<0.0045	N/A	0.60	4.4	23.42	1.5	21.45	1.7	22.62	1.0	0.68	1.9	16.06	1.0	3.52	2.8

Sample			7 -> 7 Li [No Gas]		9 -> 9 Be [H2]		11 -> 11 B [O2]		23 -> 23 Na [O2]		24 -> 24 Mg [O2]		27 -> 27 Al [H2]		28 -> 44 Si [O2]		31 -> 47 P [O2]		32 -> 48 S [O2]	
Acq. Date-Time	Sample Name	Comment	Conc. [ug/l]	Conc. RSD	Conc. [ug/l]	Conc. RSD	Conc. [ug/l]	Conc. RSD	Conc. [ug/l]	Conc. RSD	Conc. [ug/l]	Conc. RSD	Conc. [ug/l]	Conc. RSD	Conc. [ug/l]	Conc. RSD	Conc. [ug/l]	Conc. RSD	Conc. [ug/l]	Conc. RSD
16/03/2022 13:14	41	Blank 4	<0.00044	N/A	0.00	N/A	<0.08592	N/A	0.11	489.1	0.23	126.5	0.06	4.9	0.41	73.7	0.06	105.5	0.47	52.8
16/03/2022 13:17	42	Blank 5	<0.00044	N/A	0.00	N/A	<0.08592	N/A	<0.04421	N/A	0.044	4.0	0.055	7.2	0.71	7.7	0.045	18.3	<0.18470	N/A
16/03/2022 13:21	43	Blank 6	<0.00044	N/A	0.00	N/A	<0.08592	N/A	<0.04421	N/A	0.05	6.9	0.09	7.0	0.19	11.8	<0.02232	58.8	<0.18470	N/A
16/03/2022 13:24	44	Ref. marine 3	144.10	2.0	4.23	34.9	257.38	0.6	19234.39	2.1	29577.56	1.0	126445.66	3.5	7590.63	1.2	1985.13	1.5	3246.98	0.5
16/03/2022 13:28	45	Ref. marine 4	147.56	0.8	3.32	41.4	278.15	4.7	20663.71	2.4	31647.56	2.3	134490.83	0.8	8718.31	2.0	2137.90	4.3	3525.00	4.2
16/03/2022 13:32	46	Ref. river 3	64.75	0.7	3.09	60.6	85.52	3.5	1151.16	2.7	15252.02	1.1	66671.61	0.8	6553.20	0.6	4791.25	1.4	7652.19	1.9
16/03/2022 13:35	47	Ref. river 4	52.33	1.3	2.09	48.3	64.75	8.5	977.30	2.1	12226.83	0.6	55100.94	1.5	6978.15	0.7	3860.31	3.1	6223.83	1.8
16/03/2022 13:39	61	47	28.34	0.4	2.24	21.7	24.52	4.5	717.28	0.4	35526.19	0.4	44000.53	1.2	6119.30	0.6	1054.02	2.6	2912.81	0.8
16/03/2022 13:42	62	48	41.76	2.2	2.22	35.9	61.25	2.3	1046.47	1.9	36207.56	0.7	63210.05	1.0	6864.44	0.9	1221.91	2.3	1205.87	2.4
16/03/2022 13:46	63	49	36.49	1.8	2.32	30.1	46.71	5.1	1128.17	2.5	52953.63	1.1	58535.60	0.5	7740.49	0.8	1189.62	1.6	951.47	1.7
16/03/2022 13:49	64	50	31.82	2.0	2.54	65.6	27.13	4.2	824.29	1.4	40038.24	0.7	43984.41	0.5	6949.37	1.6	1024.33	1.5	746.53	1.7
16/03/2022 13:53	65	51 rep1	39.45	1.4	3.10	30.1	53.51	2.4	978.62	1.1	33315.10	0.4	57328.47	1.2	7201.95	1.6	1093.22	1.4	1567.58	1.9
16/03/2022 13:56	65	51 rep2	41.74	1.2	2.96	33.2	52.04	7.4	930.55	1.8	32403.82	0.5	56837.09	2.8	7020.03	1.4	1061.06	2.0	1522.45	0.9
16/03/2022 14:00	66	53	41.96	0.7	3.38	40.7	37.74	10.9	1172.69	1.4	48895.34	0.7	66228.07	0.6	6279.62	0.8	1340.21	0.2	1421.62	1.8
16/03/2022 14:03	67	54	35.04	1.5	2.65	48.9	29.68	9.8	884.74	4.6	43328.37	0.4	50355.03	3.0	6501.04	0.3	1104.37	1.7	2256.85	1.4
16/03/2022 14:07	68	55	28.49	2.9	2.43	29.7	29.17	4.4	693.00	0.8	37851.62	0.3	41954.36	1.1	6258.09	0.7	1096.71	1.1	2733.05	1.5
16/03/2022 14:11	69	56	46.38	1.4	2.53	10.8	67.56	10.6	1041.17	3.1	34220.38	1.2	63274.53	2.2	7022.71	1.2	1154.00	1.2	1032.90	1.3
16/03/2022 14:14	70	57	25.26	0.9	2.12	58.2	28.02	11.2	484.26	0.9	25231.27	1.1	33336.60	2.5	5521.87	1.2	783.86	2.5	1028.76	1.5
16/03/2022 14:18	71	58	25.62	1.4	1.40	33.4	26.57	7.5	572.47	2.9	33742.07	1.5	35816.82	1.8	5579.52	2.0	1069.24	3.1	894.06	3.8
16/03/2022 14:21	72	59	36.89	0.7	2.84	16.7	26.98	4.4	757.99	0.9	34705.29	0.5	47068.73	0.7	6280.51	0.8	1360.46	1.2	2623.79	0.9
16/03/2022 14:25	73	60	46.14	0.8	3.73	40.4	68.07	1.0	1103.75	0.0	37020.77	1.6	66871.22	0.7	7418.23	1.3	1278.99	2.4	1458.58	1.7
16/03/2022 14:28	74	61	50.81	1.7	3.48	4.1	64.25	6.1	1247.34	2.2	40785.66	1.1	76457.05	0.6	6828.16	1.1	1423.09	2.3	1448.41	1.9
16/03/2022 14:32	75	62	46.10	0.3	3.88	33.8	59.83	6.5	1122.63	3.3	39426.22	1.9	65145.01	0.7	7650.90	1.2	1417.25	1.7	1480.40	3.0
16/03/2022 14:35	76	63	35.06	0.6	2.67	35.6	34.84	6.4	915.14	1.0	38781.86	0.8	52053.16	1.1	6831.88	1.4	1093.86	2.0	1052.69	2.9
16/03/2022 14:39	77	64	29.85	1.8	1.11	24.6	26.31	9.8	521.49	1.6	31716.16	1.0	35246.55	0.8	5853.58	1.2	876.75	2.5	1544.06	3.1
16/03/2022 14:42	78	65	38.88	0.4	3.26	23.4	41.03	1.0	960.23	3.5	38448.51	0.1	56450.68	1.9	7068.66	3.5	1220.61	1.2	1542.24	1.0
16/03/2022 14:46	79	66	43.87	0.3	3.45	33.5	59.38	2.9	981.84	0.9	35649.01	0.3	60979.79	1.4	6353.31	0.4	1293.00	1.5	1559.51	1.3
16/03/2022 15:07	80	Blank 7	<0.00044	N/A	0.01	173.2	<0.08592	N/A	<0.04421	N/A	0.05	2.9	0.10	2.4	0.51	9.0	0.05	10.9	<0.18470	N/A
16/03/2022 15:11	81	Blank 8	<0.00044	N/A	0.00	N/A	<0.08592	N/A	<0.04421	N/A	0.06	6.9	0.28	4.6	0.80	3.5	0.19	6.7	<0.18470	N/A
16/03/2022 15:14	82	Blank 9	<0.00044	N/A	0.00	N/A	<0.08592	N/A	<0.04421	N/A	0.05	3.6	0.14	2.7	0.48	7.3	<0.02232	58.3	<0.18470	N/A
16/03/2022 15:18	83	Ref. marine 5	160.10	3.5	3.53	51.8	270.04	4.3	19472.36	1.0	29298.31	1.1	127106.77	3.1	6392.60	0.3	2030.36	1.8	3297.65	1.9
16/03/2022 15:22	84	Ref. marine 6	164.78	2.7	4.97	20.0	269.11	2.7	20154.79	1.3	30737.41	0.8	127278.73	2.4	7106.26	1.1	2142.43	1.0	3420.73	1.1
16/03/2022 15:25	85	Ref. river 5	59.34	2.0	1.86	40.0	74.33	3.1	1021.54	1.9	12918.10	1.7	58478.32	1.7	6897.49	2.1	4264.11	1.2	6758.04	1.1
16/03/2022 15:29	86	Ref. river 6	56.34	2.0	1.37	40.8	64.75	2.9	945.73	1.7	12138.12	0.8	53975.69	1.3	7174.13	2.5	3936.60	2.1	6187.62	1.9
16/03/2022 15:32	87	52	29.63	1.9	1.62	17.7	29.73	10.6	514.54	2.9	29430.62	1.2	36316.58	1.9	5197.57	1.7	882.74	3.1	2844.68	2.5
16/03/2022 15:36	88	67	50.25	3.0	2.67	50.9	66.93	9.2	1102.95	3.8	39215.27	1.6	65731.75	1.0	7827.11	1.2	1228.98	2.7	1240.74	3.2
16/03/2022 15:39	89	B1 2-1	49.46	1.6	2.32	21.8	23.28	11.9	1048.40	0.8	22096.07	0.2	67249.48	0.9	6850.89	1.0	1675.64	0.3	2276.09	0.9
16/03/2022 15:43	90	B1 3-1	47.82	0.7	3.24	31.1	22.85	4.1	1071.96	4.9	19773.02	1.3	68389.49	1.2	6500.99	0.4	1472.38	2.8	1663.46	1.7
16/03/2022 15:46	91	B1 4	40.05	0.9	4.35	43.3	24.31	11.3	1019.78	1.0	17825.95	0.7	62580.63	2.1	6720.17	0.9	1355.53	2.8	1783.05	1.9
16/03/2022 15:50	92	B1 5-1	34.79	2.0	1.69	93.7	19.78	4.7	837.51	2.6	17026.06	0.5	54663.85	2.2	7056.48	2.1	1390.13	1.6	1866.70	2.0
16/03/2022 15:53	93	B1 6	56.45	1.3	3.90	33.5	27.44	7.1	1116.52	4.4	22733.05	1.1	72794.07	0.6	6149.62	0.3	1705.72	1.0	2161.67	1.4
16/03/2022 15:57	94	B1 7	39.69	2.4	2.65	28.1	19.84	4.7	937.89	1.3	18345.88	0.5	57885.13	1.0	6410.41	0.5	1222.44	1.2	1821.31	1.7
16/03/2022 16:01	95	B2 2-1	35.98	0.8	2.08	34.9	18.12	1.6	678.85	1.4	16093.00	1.3	45836.50	1.7	6126.86	0.8	1230.44	2.2	1978.74	1.8
16/03/2022 16:04	96	B2 3-1	43.05	0.9	2.98	17.0	19.72	2.2	760.63	1.9	18974.05	2.0	54170.89	1.6	6241.95	1.2	1216.05	1.8	1837.70	3.0
16/03/2022 16:08	97	B2 4	35.42	0.5	2.76	36.1	18.29	6.4	735.50	1.2	16426.28	0.9	47669.22	1.3	6154.07	1.1	1307.54	2.9	2128.69	2.9
16/03/2022 16:11	98	B2 5 rep1	37.94	1.9	2.89	46.3	17.23	6.5	699.13	3.5	16422.81	2.2	49955.21	1.3	5721.25	2.3	1414.71	3.6	1798.45	3.9
16/03/2022 16:15	98	B2 5 rep2	38.34	1.9	2.50	56.9	18.58	8.5	749.55	2.2	17633.80	1.2	50541.17	2.7	6087.69	0.6	1526.12	2.9	1935.19	3.0
16/03/2022 16:18	99	B2 6	43.10	2.1	2.22	36.8	20.11	10.1	948.25	1.5	19772.84	1.4	57274.29	1.1	7160.88	1.9	1639.02	2.6	2136.45	2.1
16/03/2022 16:22	100	B3 2	42.83	1.2	3.08	30.8	25.62	5.4	1065.91	2.6	19302.90	0.7	65813.93	2.0	6526.03	1.0	1493.24	2.6	1695.11	2.0
16/03/2022 16:25	101	B3 3	37.18	2.0	1.93	12.5	18.55	4.8	714.53	1.6	16389.66	2.0	48717.63	2.4	7131.95	2.0	1168.34	1.1	1895.78	2.3
16/03/2022 16:29	102	B3 4	43.28	1.8	3.46	8.0	23.10	12.5	1020.35	1.0	20435.90	1.2	61169.09	1.2	6535.97	2.7	1468.00	1.0	1746.24	0.6
16/03/2022 16:33	103	B3 5	44.88	1.1	3.24	41.1	24.02	19.4	1026.88	0.4	19925.23	0.4	63917.14	0.8	6740.00	0.5	1551.97	0.7	1949.92	1.6
16/03/2022 16:36	104	B3 6	49.73	1.4	2.10	33.8	25.34	9.1	1083.42	1.5	21088.20	0.5	71945.78	1.7	6377.97	1.1	1709.12	1.6	1930.83	1.6
16/03/2022 16:40	105	B3 7	45.73	0.4	2.44	18.7	24.26	10.7	1081.17	1.7	20051.92	0.9	66870.44	1.4	6860.60	2.3	1543.80	1.9	1879.66	2.0
16/03/2022 16:43	106	Sars 1-1	109.63	0.2	6.73	32.9	57.97	2.0	1349.91	1.7	40434.76	0.6	137336.45	1.3	7501.69	1.0	1811.69	0.4	1876.95	0.1
16/03/2022 16:47	107	Sars 2-1	93.85	1.2	5.64	30.4	46.63	6.4	1380.20	2.4	37443.24	2.2	103051.48	3.2	6569.98	2.8	1511.58	1.8	830.59	1.8

Sample			39 -> 39 K [O2]		40 -> 40 Ca [H2]		45 -> 61 Sc [O2]		47 -> 63 Ti [O2]		51 -> 67 V [O2]		52 -> 52 Cr [O2]		55 -> 55 Mn [O2]		56 -> 56 Fe [H2]		59 -> 59 Co [O2]	
Acq. Date-Time	Sample Name	Comment	Conc. [ug/l]	Conc. RSD	Conc. [ug/l]	Conc. RSD	Conc. [ug/l]	Conc. RSD	Conc. [ug/l]	Conc. RSD	Conc. [ug/l]	Conc. RSD	Conc. [ug/l]	Conc. RSD	Conc. [ug/l]	Conc. RSD	Conc. [ug/l]	Conc. RSD	Conc. [ug/l]	Conc. RSD
16/03/2022 13:14	41	Blank 4	0.17	161.2	0.13	1.9	<0.00036	N/A	0.0045	112.4	0.00	171.1	0.00	146.6	0.02	219.8	0.038	8.9	0.00	282.6
16/03/2022 13:17	42	Blank 5	<0.05907	N/A	0.05	7.8	<0.00036	N/A	3.058	1.1	0.02	1.4	<0.00209	123.0	<0.01110	N/A	0.486	0.5	<0.00147	N/A
16/03/2022 13:21	43	Blank 6	<0.05907	N/A	0.04	8.1	<0.00036	N/A	0.0372	18.8	<0.00012	1105.1	<0.00209	313.5	<0.01110	N/A	0.06	1.4	<0.00147	N/A
16/03/2022 13:24	44	Ref. marine 3	40036.48	1.5	25858.66	2.6	23.12	1.3	373.04	1.7	388.52	1.3	173.90	1.1	565.19	1.2	69822.75	2.0	25.17	1.2
16/03/2022 13:28	45	Ref. marine 4	41748.32	2.7	27596.26	2.0	25.06	2.7	388.41	1.0	414.94	2.3	183.94	2.4	615.64	2.4	75233.13	0.3	27.28	3.0
16/03/2022 13:32	46	Ref. river 3	17676.83	0.9	160628.20	0.6	14.64	1.1	736.66	0.7	212.29	1.5	192.84	1.5	2857.34	1.0	66170.55	1.0	20.93	1.6
16/03/2022 13:35	47	Ref. river 4	14392.65	1.6	132737.19	0.7	12.06	0.6	592.59	0.8	169.86	1.1	157.40	1.0	2274.69	2.0	54415.74	1.0	16.98	1.0
16/03/2022 13:39	61	47	18276.73	1.1	74797.12	1.7	12.00	1.0	1280.89	0.5	75.79	0.6	56.72	0.8	744.28	0.9	44507.00	0.9	19.95	0.9
16/03/2022 13:42	62	48	24029.02	1.0	76236.89	1.1	14.25	3.3	1293.08	1.0	101.99	1.0	86.35	1.4	719.95	0.4	54733.24	1.1	20.99	0.8
16/03/2022 13:46	63	49	26014.18	0.6	96465.10	1.6	15.40	1.0	1462.39	0.9	101.26	1.0	83.93	1.5	876.01	1.9	47477.58	0.5	22.13	0.6
16/03/2022 13:49	64	50	18831.88	1.2	84919.95	0.5	11.84	1.5	1265.02	0.0	77.44	0.7	61.59	0.7	766.88	3.1	39771.39	1.5	17.78	0.8
16/03/2022 13:53	65	51 rep1	22482.59	1.1	68784.59	2.7	13.72	2.2	1283.05	0.3	96.80	0.3	78.05	0.8	725.43	0.4	53393.97	1.6	21.30	0.4
16/03/2022 13:56	65	51 rep2	21804.75	0.3	67239.95	1.3	13.41	0.1	1250.15	0.8	94.10	0.3	76.73	0.4	709.77	1.3	52611.13	2.0	20.59	1.0
16/03/2022 14:00	66	53	27863.04	0.3	96311.03	0.7	16.51	1.1	1484.84	0.9	104.97	1.4	81.49	1.5	914.00	1.0	56089.88	1.7	25.34	0.8
16/03/2022 14:03	67	54	19870.82	0.3	94585.46	2.2	12.94	2.0	1255.52	0.7	83.00	1.1	63.07	0.6	801.12	2.5	48935.67	2.3	21.86	0.6
16/03/2022 14:07	68	55	17559.73	1.0	81647.24	1.1	11.62	1.0	1181.91	0.8	75.02	0.4	56.16	0.3	743.24	1.2	42891.38	0.5	19.79	1.1
16/03/2022 14:11	69	56	24319.62	1.0	70813.03	1.8	14.54	2.7	1270.44	0.2	103.49	0.6	87.20	0.7	717.67	1.7	54205.20	2.3	22.01	0.9
16/03/2022 14:14	70	57	12670.36	0.9	58009.43	1.5	8.80	1.6	905.02	1.5	62.43	0.8	48.18	0.4	722.61	0.8	37909.03	1.3	16.46	0.3
16/03/2022 14:18	71	58	14469.94	2.0	71153.45	0.6	9.70	0.7	932.25	2.1	65.93	2.3	52.83	2.9	740.55	3.2	38198.79	1.6	17.29	1.4
16/03/2022 14:21	72	59	18127.09	1.2	77447.29	0.5	13.97	0.8	1442.70	1.3	90.75	1.1	64.13	1.1	899.70	1.0	55137.19	2.0	23.08	0.5
16/03/2022 14:25	73	60	26490.05	0.8	71962.36	0.9	15.94	0.3	1506.06	0.8	113.06	1.3	94.60	1.2	787.97	1.5	57951.86	0.5	23.97	0.6
16/03/2022 14:28	74	61	29410.99	0.5	77167.35	1.1	17.13	0.7	1544.95	0.9	118.09	1.0	101.94	1.2	843.89	1.5	62290.00	0.9	25.28	0.5
16/03/2022 14:32	75	62	26345.87	1.3	75530.83	0.9	15.98	1.7	1562.17	2.0	109.09	1.3	90.18	1.2	868.61	1.3	57696.01	0.9	25.15	1.8
16/03/2022 14:35	76	63	21125.63	0.8	78063.22	1.3	13.37	2.2	1326.21	0.5	89.66	0.5	70.61	1.4	859.74	1.6	48868.00	2.1	20.92	0.6
16/03/2022 14:39	77	64	13519.23	0.8	78749.91	0.6	9.41	1.7	1002.41	3.9	65.53	1.3	58.36	1.1	740.75	1.7	41153.44	0.7	18.35	1.4
16/03/2022 14:42	78	65	22756.48	0.6	74917.61	1.7	14.08	0.4	1485.86	0.8	93.33	0.1	74.60	1.3	848.01	0.6	52068.06	1.9	20.97	1.4
16/03/2022 14:46	79	66	22571.33	0.4	78247.61	1.7	14.14	1.2	1314.31	0.1	100.11	0.4	84.27	0.5	707.11	1.1	56443.63	0.9	22.02	0.5
16/03/2022 15:07	80	Blank 7	<0.05907	N/A	0.14	70.0	<0.00036	N/A	0.23	2.7	0.00	15.4	<0.00209	340.9	<0.01110	N/A	0.15	2.3	<0.00147	N/A
16/03/2022 15:11	81	Blank 8	<0.05907	N/A	<0.02983	31.4	<0.00036	N/A	3.16	1.1	0.02	5.3	<0.00209	92.6	<0.01110	N/A	0.70	1.8	<0.00147	N/A
16/03/2022 15:14	82	Blank 9	<0.05907	N/A	0.12	4.3	<0.00036	N/A	0.01	36.4	<0.00012	5867.0	<0.00209	369.0	<0.01110	N/A	0.12	4.6	<0.00147	N/A
16/03/2022 15:18	83	Ref. marine 5	39710.22	0.6	26167.61	2.7	23.36	0.3	366.70	1.2	389.28	1.1	173.34	0.6	570.23	0.8	70874.79	4.0	25.34	1.3
16/03/2022 15:22	84	Ref. marine 6	40940.81	1.1	26048.51	1.4	24.56	2.0	391.35	1.2	405.47	1.5	179.61	0.9	589.15	0.7	69710.63	2.3	25.99	0.7
16/03/2022 15:25	85	Ref. river 5	15239.69	0.1	140027.97	1.1	12.97	1.9	624.57	1.2	181.44	1.0	164.07	0.4	2460.38	0.3	57741.72	1.7	18.09	0.5
16/03/2022 15:29	86	Ref. river 6	14102.14	1.0	130879.68	0.6	11.90	2.0	608.01	1.1	168.66	0.6	152.63	0.9	2279.99	0.4	53685.56	0.4	16.61	1.6
16/03/2022 15:32	87	52	13407.46	1.5	70376.79	2.4	9.12	2.3	775.79	2.4	61.89	1.2	47.31	1.6	689.22	2.2	42368.90	0.7	18.03	1.7
16/03/2022 15:36	88	67	25102.20	1.5	85720.75	0.5	15.30	1.1	1401.47	1.3	107.13	1.0	86.40	1.3	813.13	0.2	57959.18	0.6	24.20	1.6
16/03/2022 15:39	89	B1 2-1	29897.74	1.1	28640.99	0.8	17.59	1.7	1826.32	0.7	103.22	0.8	80.46	0.5	1156.74	0.3	65470.47	0.5	31.87	0.8
16/03/2022 15:43	90	B1 3-1	31117.19	1.9	24198.02	1.4	17.19	2.5	1882.60	1.2	101.97	1.7	78.84	0.8	1018.92	1.4	59552.93	1.6	28.13	1.9
16/03/2022 15:46	91	B1 4	29641.78	1.2	23155.09	1.0	16.33	2.3	1791.75	0.3	96.54	0.9	74.98	1.0	940.13	1.7	52594.06	0.2	25.48	1.2
16/03/2022 15:50	92	B1 5-1	24760.59	0.4	20223.20	1.5	14.16	1.4	1696.68	0.7	84.06	1.1	63.00	0.7	886.94	2.7	49489.36	0.7	23.79	1.1
16/03/2022 15:53	93	B1 6	32804.79	1.5	25852.55	1.1	18.53	1.6	1986.46	0.8	111.66	0.3	86.86	0.9	1200.79	0.5	68205.19	0.8	32.43	1.0
16/03/2022 15:57	94	B1 7	27032.83	0.5	20179.87	0.5	14.97	1.0	1771.02	0.6	90.30	0.5	67.86	1.4	959.01	1.3	52705.05	0.2	26.35	0.8
16/03/2022 16:01	95	B2 2-1	20602.18	1.3	16406.06	0.9	12.18	3.1	1494.27	1.8	75.11	1.4	56.50	2.6	984.43	2.5	48317.75	0.8	22.75	1.8
16/03/2022 16:04	96	B2 3-1	22821.45	1.1	20386.88	0.3	13.93	2.0	1622.55	1.3	85.22	1.4	64.31	1.9	1109.91	1.6	57646.59	0.8	25.71	1.6
16/03/2022 16:08	97	B2 4	21286.62	1.0	18580.16	0.7	12.35	3.2	1574.13	1.0	75.19	0.8	55.94	0.9	947.58	2.4	48951.17	1.3	24.16	0.6
16/03/2022 16:11	98	B2 5 rep1	20889.66	2.8	18548.05	1.4	12.53	3.1	1479.55	2.9	74.96	2.8	56.96	2.8	962.69	3.0	51336.32	1.6	22.61	2.3
16/03/2022 16:15	98	B2 5 rep2	22214.78	0.9	18842.84	1.4	13.51	2.7	1581.88	0.5	80.02	0.3	61.00	1.2	1021.49	0.7	51470.33	1.2	24.08	0.4
16/03/2022 16:18	99	B2 6	26333.54	1.6	20247.28	0.6	15.32	0.5	1759.93	0.9	92.44	1.6	70.10	0.3	1110.95	1.4	56776.05	0.4	27.56	2.3
16/03/2022 16:22	100	B3 2	31282.01	1.4	19310.10	1.3	17.03	0.4	1916.53	0.4	101.93	1.0	76.64	1.4	992.06	2.3	56051.02	0.5	27.87	1.3
16/03/2022 16:25	101	B3 3	21737.15	1.3	20262.35	2.3	12.62	2.0	1587.16	1.6	76.63	1.0	56.52	2.6	875.93	1.1	47587.45	1.5	22.27	1.1
16/03/2022 16:29	102	B3 4	28822.58	1.3	21716.25	0.8	16.21	1.5	1860.12	1.1	97.85	0.9	73.99	1.2	1016.44	1.9	54820.07	1.5	26.50	0.8
16/03/2022 16:33	103	B3 5	30472.79	0.2	20239.65	1.6	16.86	2.0	1934.04	0.6	101.38	0.4	76.47	0.8	1023.29	2.0	57467.81	0.9	28.25	0.5
16/03/2022 16:36	104	B3 6	32213.31	0.8	21397.56	0.6	18.10	1.8	1940.19	0.9	107.18	0.7	81.61	1.1	1091.29	1.2	64315.35	0.2	30.80	0.4
16/03/2022 16:40	105	B3 7	31029.24	1.5	20296.47	1.6	17.24	1.6	1959.26	1.0	102.08	0.3	77.19	0.9	1024.46	1.5	59449.50	0.9	28.37	2.2
16/03/2022 16:43	106	Sars 1-1	49881.07	0.7	18195.06	0.9	36.26	0.9	3464.14	0.3	206.13	0.2	170.01	0.5	2069.53	1.0	127969.57	1.0	59.11	1.0
16/03/2022 16:47	107	Sars 2-1	37011.50	2.6	24205.55	2.1	26.20	1.5	3140.40	4.14	150.20	2.0	120.05	2.3	2395.79	2.0	92000.60	1.4	53.93	2.3

Sample			60 -> 60 Ni [O2]		63 -> 63 Cu [O2]		66 -> 66 Zn [H2]		71 -> 71 Ga [H2]		75 -> 91 As [O2]		78 -> 78 Se [H2]		85 -> 85 Rb [O2]		88 -> 88 Sr [H2]		89 -> 105 Y [O2]	
Acq. Date-Time	Sample Name	Comment	Conc. [ug/l]	Conc. RSD	Conc. [ug/l]	Conc. RSD	Conc. [ug/l]	Conc. RSD	Conc. [ug/l]	Conc. RSD	Conc. [ug/l]	Conc. RSD	Conc. [ug/l]	Conc. RSD	Conc. [ug/l]	Conc. RSD	Conc. [ug/l]	Conc. RSD	Conc. [ug/l]	Conc. RSD
16/03/2022 13:14	41	Blank 4	<0.00756	224.1	0.02	198.6	<0.00631	46.7	<0.00030	N/A	<0.00145	240.4	<0.00309	227.0	0.00	227.0	<0.00077	N/A	0.00	190.5
16/03/2022 13:17	42	Blank 5	<0.00756	N/A	<0.00637	N/A	<0.00631	605.9	<0.00030	N/A	<0.00145	22.5	<0.00309	136.2	<0.00022	N/A	<0.00077	N/A	<0.00017	55.3
16/03/2022 13:21	43	Blank 6	<0.00756	N/A	<0.00637	N/A	<0.00631	N/A	<0.00030	487.2	<0.00145	N/A	<0.00309	345.4	<0.00022	N/A	<0.00077	N/A	<0.00017	664.5
16/03/2022 13:24	44	Ref. marine 3	84.73	1.9	63.69	1.3	300.44	1.6	36.29	2.5	38.36	2.3	3.07	4.1	235.03	1.3	209.12	2.1	30.02	1.2
16/03/2022 13:28	45	Ref. marine 4	89.97	2.4	70.25	2.7	326.37	1.0	36.79	0.5	41.55	2.8	3.19	38.5	244.85	2.1	214.26	1.3	32.24	2.2
16/03/2022 13:32	46	Ref. river 3	102.19	2.2	89.49	1.5	789.46	0.8	21.95	1.2	19.91	2.9	4.35	6.2	130.55	1.2	456.61	1.6	35.24	1.2
16/03/2022 13:35	47	Ref. river 4	80.61	0.3	71.44	1.7	657.53	1.0	18.47	0.8	15.60	1.6	4.57	18.1	104.43	1.3	374.32	0.3	29.64	1.4
16/03/2022 13:39	61	47	33.40	0.9	28.56	1.8	88.08	0.3	18.86	1.7	6.30	10.6	1.88	10.7	105.65	0.4	81.94	0.9	41.56	0.7
16/03/2022 13:42	62	48	47.08	0.5	37.21	0.9	97.69	1.8	23.23	1.9	7.76	3.9	2.66	16.0	131.74	0.8	131.42	1.9	42.33	1.7
16/03/2022 13:46	63	49	45.92	2.0	29.16	1.0	106.47	2.1	22.74	1.7	6.06	7.8	2.04	19.0	137.95	0.8	95.95	0.3	43.98	0.6
16/03/2022 13:49	64	50	35.97	3.1	27.23	0.2	86.61	0.9	17.94	2.7	4.67	0.6	2.89	6.7	101.45	1.2	80.49	0.2	37.83	0.7
16/03/2022 13:53	65	51 rep1	44.52	1.3	32.27	0.2	94.55	0.8	22.57	2.3	7.73	7.1	2.51	11.9	127.67	0.7	108.03	0.7	41.99	0.8
16/03/2022 13:56	65	51 rep2	42.46	1.6	31.21	1.6	91.60	2.1	21.88	2.1	7.30	2.4	2.92	30.4	123.49	0.4	105.10	0.9	40.83	0.4
16/03/2022 14:00	66	53	44.48	2.4	37.34	0.5	125.00	1.8	26.95	1.4	6.69	3.3	3.21	24.4	155.29	0.6	89.70	1.2	48.72	0.3
16/03/2022 14:03	67	54	39.41	1.6	41.75	0.4	99.43	1.2	21.15	2.1	5.39	10.3	2.40	10.8	115.01	0.5	94.44	1.7	46.28	1.2
16/03/2022 14:07	68	55	35.02	1.7	33.61	0.9	86.66	2.0	17.20	0.5	6.10	5.5	1.82	34.9	104.72	0.8	91.69	0.7	40.73	0.5
16/03/2022 14:11	69	56	48.86	1.9	31.61	1.1	95.77	3.9	23.22	2.0	7.81	4.8	2.46	28.7	135.46	0.4	127.44	1.2	41.06	0.8
16/03/2022 14:14	70	57	32.26	1.8	25.10	0.8	74.39	0.5	13.55	0.4	6.42	8.7	1.61	30.9	73.09	0.7	78.16	1.0	31.88	0.5
16/03/2022 14:18	71	58	33.29	3.5	28.43	2.3	76.30	4.9	14.64	2.6	6.12	1.1	2.40	12.5	80.63	2.4	71.57	1.1	33.34	2.3
16/03/2022 14:21	72	59	39.20	1.6	37.37	1.1	90.41	1.2	20.53	0.9	5.33	4.6	2.30	27.5	112.56	1.0	117.95	0.7	49.01	0.8
16/03/2022 14:25	73	60	51.40	0.6	39.64	0.5	108.00	0.5	25.67	2.4	8.11	6.8	2.48	24.0	149.33	0.5	126.04	0.3	44.39	1.3
16/03/2022 14:28	74	61	53.01	1.1	35.91	2.5	117.39	2.0	27.98	2.0	7.96	6.7	2.25	18.4	160.66	0.3	137.94	1.6	52.59	0.6
16/03/2022 14:32	75	62	49.90	1.6	34.22	1.8	108.98	1.7	25.32	2.1	8.56	5.3	2.76	41.8	146.81	0.9	121.94	0.6	49.85	1.4
16/03/2022 14:35	76	63	42.10	0.9	46.90	1.7	99.50	1.0	21.25	2.9	6.52	1.5	2.67	11.1	113.81	0.6	93.15	1.4	44.10	0.7
16/03/2022 14:39	77	64	34.03	2.0	25.13	1.5	80.46	1.5	14.93	2.3	6.61	1.6	2.09	29.1	76.70	1.6	86.50	1.2	33.41	1.6
16/03/2022 14:42	78	65	41.98	0.4	30.24	1.1	120.66	0.7	21.96	1.2	6.38	3.3	2.73	30.7	127.15	0.9	103.58	0.7	43.97	0.1
16/03/2022 14:46	79	66	46.95	1.6	32.39	1.2	101.57	0.9	22.94	1.7	8.00	9.5	1.90	15.1	126.06	0.9	129.91	0.5	42.36	0.6
16/03/2022 15:07	80	Blank 7	<0.00756	N/A	<0.00637	N/A	<0.00631	N/A	<0.00030	N/A	<0.00145	N/A	<0.00309	278.5	<0.00022	N/A	<0.00077	N/A	<0.00017	97.9
16/03/2022 15:11	81	Blank 8	<0.00756	N/A	0.04	8.1	0.01	31.5	<0.00030	N/A	<0.00145	N/A	<0.00309	108.9	<0.00022	N/A	<0.00077	N/A	<0.00017	76.5
16/03/2022 15:14	82	Blank 9	<0.00756	1697.7	<0.00637	N/A	<0.00631	N/A	<0.00030	N/A	<0.00145	N/A	<0.00309	N/A	<0.00022	N/A	<0.00077	N/A	<0.00017	43.9
16/03/2022 15:18	83	Ref. marine 5	83.41	1.6	62.35	0.4	303.01	4.2	36.01	3.0	40.43	4.3	3.09	28.3	231.89	0.1	209.52	4.2	30.23	1.0
16/03/2022 15:22	84	Ref. marine 6	84.93	1.1	64.65	2.3	292.68	2.8	34.72	2.6	40.96	2.2	2.26	8.6	239.94	0.9	205.86	2.5	31.10	0.9
16/03/2022 15:25	85	Ref. river 5	85.33	0.1	76.40	0.8	681.56	1.7	19.07	2.4	18.02	5.6	4.23	29.4	111.46	0.6	392.01	1.0	30.89	0.2
16/03/2022 15:29	86	Ref. river 6	81.66	2.1	68.74	0.6	639.11	1.7	17.64	0.6	15.64	2.6	4.35	29.7	103.19	0.1	366.44	1.0	29.39	0.6
16/03/2022 15:32	87	52	34.55	0.6	43.65	2.9	83.15	2.4	15.12	0.5	5.70	10.2	1.98	12.1	80.98	1.5	75.96	0.7	32.02	0.9
16/03/2022 15:36	88	67	50.78	3.0	36.29	1.2	107.04	0.8	24.17	1.1	8.44	3.6	2.95	47.9	139.99	0.9	131.40	0.2	41.80	0.4
16/03/2022 15:39	89	B1 2-1	47.18	1.5	47.91	1.3	163.74	1.7	29.37	1.4	13.20	10.4	3.19	16.7	168.23	0.5	68.73	0.5	64.08	0.1
16/03/2022 15:43	90	B1 3-1	42.05	2.3	41.79	1.6	151.73	3.4	29.10	1.5	9.35	2.3	3.24	8.4	168.23	1.7	67.64	1.7	56.07	1.9
16/03/2022 15:46	91	B1 4	38.44	0.9	39.34	1.3	136.37	1.7	26.51	1.0	9.32	3.8	2.07	18.4	157.54	0.9	60.60	0.8	56.43	0.1
16/03/2022 15:50	92	B1 5-1	35.44	2.0	38.63	1.7	119.23	0.6	23.47	0.5	8.10	4.8	2.55	34.3	134.96	0.7	51.44	1.3	52.57	1.0
16/03/2022 15:53	93	B1 6	48.96	1.3	49.52	1.3	167.59	1.2	31.20	0.6	10.06	5.7	3.41	8.9	182.88	0.9	78.43	0.1	65.11	0.8
16/03/2022 15:57	94	B1 7	38.43	1.7	38.01	0.5	129.14	1.6	24.97	0.5	8.61	8.0	2.37	22.6	146.90	0.7	48.72	0.6	50.57	0.6
16/03/2022 16:01	95	B2 2-1	34.79	1.5	34.48	2.1	112.79	2.5	20.16	2.1	12.09	7.1	1.87	47.6	118.30	0.6	60.10	0.8	48.07	1.6
16/03/2022 16:04	96	B2 3-1	38.92	0.1	36.87	2.3	131.78	2.1	23.92	0.7	20.86	6.1	2.42	24.2	134.29	0.9	70.76	0.8	52.61	1.5
16/03/2022 16:08	97	B2 4	35.33	0.7	41.20	2.6	117.37	1.0	20.97	1.5	9.23	5.3	1.98	43.5	120.46	1.4	49.80	0.5	49.39	1.1
16/03/2022 16:11	98	B2 5 rep1	34.53	3.3	31.88	4.0	119.02	0.9	22.38	1.0	9.29	6.0	2.54	12.2	119.45	3.1	58.26	1.4	48.59	3.2
16/03/2022 16:15	98	B2 5 rep2	36.42	1.5	33.38	1.1	119.17	1.1	22.67	0.6	10.06	4.5	2.52	8.5	126.70	0.6	58.50	0.8	52.06	1.3
16/03/2022 16:18	99	B2 6	41.35	0.4	44.95	0.2	137.89	1.3	25.12	1.2	10.92	3.3	2.42	25.8	148.65	0.8	66.44	0.6	59.91	0.9
16/03/2022 16:22	100	B3 2	40.68	1.2	41.46	1.4	139.38	0.7	27.61	1.6	11.07	2.7	3.47	16.4	167.28	0.9	54.86	0.9	57.55	0.9
16/03/2022 16:25	101	B3 3	32.99	2.0	32.72	2.0	110.01	4.1	21.39	2.1	9.31	8.1	2.32	34.2	119.75	2.6	50.39	2.1	47.55	2.0
16/03/2022 16:29	102	B3 4	41.79	1.6	40.92	1.7	133.38	2.4	26.51	0.4	10.55	4.1	2.32	22.1	157.00	0.6	56.40	0.4	56.53	0.8
16/03/2022 16:33	103	B3 5	42.14	1.0	45.39	0.5	144.84	0.9	26.70	1.8	10.47	0.9	2.40	7.4	167.27	0.8	56.30	0.9	58.34	0.1
16/03/2022 16:36	104	B3 6	45.82	2.4	46.66	0.5	157.87	0.9	30.76	0.5	9.96	3.2	3.44	32.0	175.38	0.0	64.60	0.6	62.32	1.0
16/03/2022 16:40	105	B3 7	42.64	2.8	41.51	0.8	148.11	1.4	28.24	1.4	12.12	4.5	2.40	27.6	169.45	1.6	59.58	2.0	58.81	1.1
16/03/2022 16:43	106	Sars 1-1	97.30	1.4	109.84	0.6	336.25	0.9	48.88	0.3	139.73	2.1	4.16	4.7	401.76	0.7	48.42	1.5	51.43	0.2
16/03/2022 16:47	107	Sars 2-1	80.35	3.1	89.28	2.6	220.77	1.9	38.64	0.1	18.16	1.2	3.95	7.4	289.42	2.9	53.38	1.9	55.76	2.4

Sample			90 -> 106 Zr [O2]		93 -> 125 Nb [O2]		95 -> 127 Mo [O2]		111 -> 111 Cd [O2]		115 -> 115 In [O2]		118 -> 118 Sn [O2]		121 -> 137 Sb [O2]		133 -> 133 Cs [O2]		137 -> 137 Ba [O2]	
Acq. Date-Time	Sample Name	Comment	Conc. [ug/l]	Conc. RSD	Conc. [ug/l]	Conc. RSD	Conc. [ug/l]	Conc. RSD	Conc. [ug/l]	Conc. RSD	Conc. [ug/l]	Conc. RSD	Conc. [ug/l]	Conc. RSD	Conc. [ug/l]	Conc. RSD	Conc. [ug/l]	Conc. RSD	Conc. [ug/l]	Conc. RSD
16/03/2022 13:14	41	Blank 4	<0.00093	216.0	<0.00012	169.1	0.0078	174.2	0.00	198.2	0.00	130.2	0.00	52.5	<0.00044	224.8	0.00	207.1	<0.00234	986.0
16/03/2022 13:17	42	Blank 5	0.00	12.1	0.01	4.9	0.00	34.6	<0.00063	N/A	<0.00004	119.0	0.01	8.2	0.00	32.0	<0.00055	N/A	<0.00234	N/A
16/03/2022 13:21	43	Blank 6	<0.00093	N/A	0.00	44.7	<0.00069	N/A	<0.00063	266.9	<0.00004	N/A	<0.00084	61.4	<0.00044	54.5	<0.00055	N/A	<0.00234	N/A
16/03/2022 13:24	44	Ref. marine 3	32.26	1.4	0.039	18.4	1.98	9.5	0.43	22.9	0.19	10.4	1.27	8.5	0.185	64.1	15.37	0.6	1485.61	0.7
16/03/2022 13:28	45	Ref. marine 4	31.05	1.8	0.051	21.6	2.17	15.5	0.45	11.9	0.17	3.1	1.14	9.9	0.23	53.2	16.37	1.8	1577.30	1.9
16/03/2022 13:32	46	Ref. river 3	36.74	1.1	0.09	10.6	1.48	14.2	6.09	4.7	0.078	12.3	2.12	4.9	0.20	38.0	10.27	0.4	517.07	0.5
16/03/2022 13:35	47	Ref. river 4	31.68	1.0	0.12	12.2	1.31	5.9	4.81	5.0	0.071	15.3	1.83	4.2	0.26	14.0	8.33	3.8	422.80	0.9
16/03/2022 13:39	61	47	9.59	1.3	0.44	4.2	0.64	6.7	0.21	42.6	0.063	14.1	1.11	2.3	0.06	13.3	5.36	0.8	318.91	0.9
16/03/2022 13:42	62	48	14.57	2.1	0.41	4.7	0.97	2.8	0.44	5.8	0.07	10.1	1.23	4.1	0.09	59.7	9.67	1.3	397.26	0.8
16/03/2022 13:46	63	49	15.70	1.3	0.43	10.0	1.06	8.0	0.43	8.1	0.074	4.8	1.01	9.3	0.09	39.6	8.25	0.6	509.66	0.7
16/03/2022 13:49	64	50	11.82	1.5	0.43	5.5	0.77	15.0	0.32	35.9	0.056	12.7	0.99	4.4	0.045	75.7	5.45	0.9	385.36	0.9
16/03/2022 13:53	65	51 rep1	13.44	1.0	0.44	5.5	6.47	2.3	0.37	19.6	0.080	26.0	1.24	1.1	0.118	0.2	8.31	0.6	377.22	0.7
16/03/2022 13:56	65	51 rep2	13.24	1.3	0.42	8.3	6.05	3.4	0.27	11.7	0.067	5.6	1.22	9.3	0.15	36.1	8.21	0.9	366.36	1.3
16/03/2022 14:00	66	53	12.28	3.3	0.36	5.0	0.77	11.4	0.29	12.3	0.090	2.7	1.11	4.2	0.06	56.3	8.04	1.7	531.39	0.6
16/03/2022 14:03	67	54	10.92	0.5	0.42	9.1	0.84	4.3	0.26	22.9	0.072	10.4	1.15	3.6	0.060	35.6	6.02	1.5	333.19	1.1
16/03/2022 14:07	68	55	9.24	2.4	0.38	3.9	0.82	11.5	0.33	16.4	0.061	10.0	1.11	2.0	0.056	80.1	5.54	1.2	276.59	0.5
16/03/2022 14:11	69	56	13.86	1.2	0.40	4.4	1.19	8.9	0.36	10.0	0.078	14.4	1.29	3.2	0.14	38.5	9.88	1.4	378.46	0.5
16/03/2022 14:14	70	57	12.07	2.4	0.35	9.5	0.82	9.0	0.26	15.3	0.046	11.6	0.94	4.9	0.046	62.3	4.27	1.2	224.42	1.0
16/03/2022 14:18	71	58	10.39	1.4	0.40	10.2	0.69	14.2	0.24	28.4	0.062	24.6	0.88	3.5	0.064	42.7	4.50	1.2	278.98	0.9
16/03/2022 14:21	72	59	9.66	2.1	0.55	2.2	1.11	1.2	0.33	8.6	0.074	10.1	1.41	4.4	0.14	20.7	6.49	0.3	298.40	1.2
16/03/2022 14:25	73	60	15.10	2.7	0.44	3.7	1.23	9.1	0.50	5.4	0.081	6.3	1.29	6.2	0.070	30.2	10.61	1.2	434.28	1.2
16/03/2022 14:28	74	61	17.71	0.8	0.48	3.3	1.02	8.1	0.33	19.1	0.083	9.4	1.36	5.3	0.10	29.1	11.50	1.6	514.28	1.5
16/03/2022 14:32	75	62	17.32	2.8	0.53	4.3	1.00	8.7	0.60	9.4	0.085	7.0	1.27	1.0	0.093	44.6	9.89	0.5	445.40	0.4
16/03/2022 14:35	76	63	14.92	2.1	0.43	5.2	0.84	15.7	0.47	10.3	0.072	15.4	1.09	17.2	0.07	46.8	6.43	1.3	409.22	0.7
16/03/2022 14:39	77	64	13.30	1.6	0.41	3.0	0.72	17.1	0.25	18.6	0.052	10.5	0.93	7.1	0.093	76.7	4.28	0.3	240.39	1.0
16/03/2022 14:42	78	65	12.96	1.6	0.47	5.7	1.20	5.5	0.28	22.7	0.072	13.9	1.25	6.8	0.107	33.9	8.30	1.0	397.26	1.8
16/03/2022 14:46	79	66	14.36	1.6	0.48	6.2	1.44	2.9	0.34	23.1	0.076	10.6	1.32	0.9	0.14	60.0	8.90	1.6	373.85	0.8
16/03/2022 15:07	80	Blank 7	<0.00093	27.1	0.00	9.9	<0.00069	117.2	<0.00063	N/A	<0.00004	N/A	<0.00084	59.5	<0.00044	139.5	<0.00055	N/A	<0.00234	N/A
16/03/2022 15:11	81	Blank 8	0.01	15.9	0.01	3.9	0.00	12.8	<0.00063	1473.1	<0.00004	47.6	0.01	6.0	0.001	50.2	<0.00055	N/A	<0.00234	N/A
16/03/2022 15:14	82	Blank 9	<0.00093	182.2	<0.00012	N/A	<0.00069	N/A	<0.00063	1435.1	<0.00004	272.5	<0.00084	8.1	<0.00044	301.5	<0.00055	N/A	<0.00234	N/A
16/03/2022 15:18	83	Ref. marine 5	34.70	2.0	0.06	35.1	1.98	9.6	0.53	5.9	0.178	10.3	1.44	14.3	0.103	71.7	15.27	1.2	1470.11	1.1
16/03/2022 15:22	84	Ref. marine 6	37.22	2.4	0.08	4.6	2.33	3.1	0.52	32.7	0.196	8.3	1.60	10.3	0.22	0.6	16.08	1.2	1555.27	0.2
16/03/2022 15:25	85	Ref. river 5	34.56	1.6	0.15	7.0	1.33	14.2	5.04	5.5	0.081	1.5	2.11	4.1	0.311	15.4	8.96	1.7	443.15	1.3
16/03/2022 15:29	86	Ref. river 6	32.48	0.6	0.16	12.7	1.22	7.4	4.60	9.5	0.074	2.0	1.95	5.9	0.22	58.0	8.11	0.8	414.13	0.1
16/03/2022 15:32	87	52	7.94	2.3	0.40	7.8	0.91	12.8	0.38	15.6	0.050	10.1	0.95	9.7	0.094	30.5	4.65	0.7	190.72	0.9
16/03/2022 15:36	88	67	14.07	2.0	0.55	3.8	1.37	11.9	0.34	20.8	0.08	5.9	1.47	3.8	0.131	33.3	9.84	1.3	390.95	0.4
16/03/2022 15:39	89	B1 2-1	15.87	0.7	0.37	6.4	0.71	24.6	0.20	12.7	0.105	5.0	0.96	8.5	0.03	64.7	8.84	1.8	616.88	0.9
16/03/2022 15:43	90	B1 3-1	15.56	1.8	0.36	5.8	0.43	15.7	0.17	23.1	0.091	0.7	1.09	3.0	0.02	102.2	8.62	1.3	675.41	1.4
16/03/2022 15:46	91	B1 4	14.74	0.8	0.41	8.5	0.44	5.4	0.16	23.9	0.096	7.4	0.88	5.6	0.04	51.4	7.72	1.0	637.96	0.6
16/03/2022 15:50	92	B1 5-1	14.93	1.7	0.41	1.5	0.37	10.5	0.13	29.6	0.076	11.2	0.88	0.8	0.03	24.3	6.60	1.9	569.99	0.2
16/03/2022 15:53	93	B1 6	16.58	1.3	0.41	2.7	0.54	12.0	0.19	30.1	0.109	3.9	0.97	8.1	0.06	73.3	9.39	0.5	694.37	0.9
16/03/2022 15:57	94	B1 7	12.52	1.1	0.42	9.5	0.30	25.2	0.12	11.8	0.072	9.8	0.88	10.4	0.03	24.2	7.27	1.6	562.14	0.7
16/03/2022 16:01	95	B2 2-1	12.27	1.6	0.39	9.1	0.34	17.1	0.13	22.1	0.070	4.6	0.96	2.2	0.04	97.7	5.87	1.0	419.60	0.6
16/03/2022 16:04	96	B2 3-1	12.25	0.9	0.39	3.6	0.64	15.7	0.14	19.2	0.076	1.0	0.93	9.0	0.042	115.9	6.62	2.2	457.99	0.4
16/03/2022 16:08	97	B2 4	13.01	1.4	0.39	8.6	0.43	24.6	0.13	15.5	0.072	6.4	0.93	9.2	0.06	14.5	5.97	1.4	454.11	1.3
16/03/2022 16:11	98	B2 5 rep1	12.98	4.0	0.37	4.6	0.60	5.8	0.09	35.4	0.069	16.1	0.94	8.5	0.04	0.3	5.79	1.2	449.36	2.3
16/03/2022 16:15	98	B2 5 rep2	13.69	0.7	0.43	2.7	0.61	8.0	0.11	19.0	0.077	5.1	0.97	10.6	0.085	66.9	6.10	0.9	469.22	1.6
16/03/2022 16:18	99	B2 6	16.43	0.8	0.36	11.6	0.37	10.0	0.13	27.2	0.095	9.8	0.91	7.7	0.05	26.7	7.47	1.0	566.58	1.0
16/03/2022 16:22	100	B3 2	16.00	1.4	0.41	3.2	0.38	20.6	0.10	15.4	0.101	3.2	0.96	10.8	0.03	123.7	8.37	0.9	690.99	0.6
16/03/2022 16:25	101	B3 3	13.23	2.6	0.40	3.4	0.43	10.3	0.10	50.9	0.064	10.4	0.88	7.9	0.04	36.8	5.82	2.4	466.42	1.2
16/03/2022 16:29	102	B3 4	15.65	1.5	0.37	8.2	0.37	8.4	0.19	7.6	0.091	8.6	0.88	6.3	0.02	155.7	7.68	1.9	639.00	0.7
16/03/2022 16:33	103	B3 5	16.08	0.9	0.39	2.6	0.46	6.9	0.18	14.0	0.096	7.5	0.97	3.1	0.05	46.6	8.45	0.9	672.31	0.8
16/03/2022 16:36	104	B3 6	17.75	2.0	0.36	7.1	0.48	21.0	0.22	20.8	0.099	2.6	0.91	2.5	0.058	100.3	8.88	1.0	696.43	1.1
16/03/2022 16:40	105	B3 7	15.96	0.8	0.38	3.3	0.40	1.7	0.12	42.8	0.102	4.3	1.02	4.7	<0.02210	142.5	8.42	0.9	689.94	0.5
16/03/2022 16:43	106	Sars 1-1	27.10	1.9	0.53	7.9	0.67	16.3	0.27	19.8	0.186	4.7	1.07	4.0	0.09	46.0	29.14	0.9	763.58	0.5
16/03/2022 16:47	107	Sars 2-1	25.13	2.4	0.42	3.2	0.30	6.6	0.30	18.5	0.14	4.6	1.08	13.5	0.033	129.5	19.24	1.3	528.29	2.1

Sample			139 -> 155 La [O2]		140 -> 156 Ce [O2]		141 -> 157 Pr [O2]		146 -> 162 Nd [O2]		153 -> 153 Eu [O2]		169 -> 185 Tm [O2]		175 -> 191 Lu [O2]		181 -> 213 Ta [O2]		182 -> 214 W [O2]	
Acq. Date-Time	Sample Name	Comment	Conc. [ug/l]	Conc. RSD	Conc. [ug/l]	Conc. RSD	Conc. [ug/l]	Conc. RSD	Conc. [ug/l]	Conc. RSD	Conc. [ug/l]	Conc. RSD	Conc. [ug/l]	Conc. RSD	Conc. [ug/l]	Conc. RSD	Conc. [ug/l]	Conc. RSD	Conc. [ug/l]	Conc. RSD
16/03/2022 13:14	41	Blank 4	0.00	160.9	0.00	143.0	0.00	185.6	0.00	191.0	0.00	167.1	0.00	170.6	0.00	174.5	<0.00014	238.4	0.01	169.3
16/03/2022 13:17	42	Blank 5	<0.00002	334.4	0.00	85.7	<0.00006	N/A	<0.00027	N/A	<0.00008	N/A	<0.00004	0.0	<0.00009	161.7	<0.00014	124.3	0.00	25.8
16/03/2022 13:21	43	Blank 6	0.00	104.7	0.00	119.8	<0.00006	N/A	<0.00027	N/A	<0.00008	965.5	<0.00004	0.0	<0.00009	2618.8	<0.00014	572.4	0.00	78.5
16/03/2022 13:24	44	Ref. marine 3	53.70	0.1	104.71	1.1	12.87	0.5	49.79	1.0	2.24	1.6	0.38	5.0	0.25	10.7	<0.00014	N/A	0.03	122.3
16/03/2022 13:28	45	Ref. marine 4	53.19	0.9	104.82	1.4	12.88	1.1	50.32	1.3	2.35	1.7	0.39	4.2	0.33	10.7	<0.00014	N/A	0.03	65.3
16/03/2022 13:32	46	Ref. river 3	70.49	1.3	147.27	1.4	17.47	1.0	65.79	1.0	1.90	3.3	0.46	4.4	0.37	6.3	<0.00014	174.0	0.14	26.1
16/03/2022 13:35	47	Ref. river 4	63.85	1.7	132.02	1.4	15.60	1.9	58.96	1.9	1.59	3.3	0.40	6.4	0.33	12.5	<0.00014	N/A	0.16	4.5
16/03/2022 13:39	61	47	64.59	0.9	134.46	0.6	16.32	1.3	62.64	0.4	2.16	2.7	0.59	2.0	0.47	6.0	<0.00014	N/A	0.072	8.6
16/03/2022 13:42	62	48	66.18	0.9	136.03	0.8	16.36	0.5	62.50	0.5	2.23	3.3	0.56	1.4	0.44	5.5	<0.00014	N/A	0.10	24.3
16/03/2022 13:46	63	49	68.83	0.2	144.65	0.7	17.70	1.3	66.76	0.4	2.36	0.2	0.59	2.8	0.47	9.6	<0.00014	423.0	0.07	35.0
16/03/2022 13:49	64	50	59.91	0.5	124.87	0.9	15.23	1.8	58.66	0.7	2.01	3.6	0.53	2.5	0.42	3.0	<0.00014	N/A	0.081	9.5
16/03/2022 13:53	65	51 rep1	73.63	0.3	151.60	0.6	18.38	0.9	69.94	1.6	2.32	5.8	0.57	2.1	0.45	4.8	<0.00014	217.3	0.079	26.3
16/03/2022 13:56	65	51 rep2	71.54	1.0	146.66	1.0	17.76	1.0	67.23	1.6	2.29	2.2	0.55	2.4	0.46	2.0	<0.00014	N/A	0.08	26.1
16/03/2022 14:00	66	53	85.91	0.5	179.76	0.3	21.85	0.5	83.00	1.1	2.75	4.1	0.67	4.3	0.55	6.5	<0.00014	670.3	0.106	20.7
16/03/2022 14:03	67	54	76.03	1.0	157.86	0.7	19.16	1.6	73.00	1.2	2.46	1.9	0.63	0.8	0.54	4.7	<0.00014	355.8	0.078	25.3
16/03/2022 14:07	68	55	64.75	0.1	136.45	0.5	16.79	0.7	64.49	1.8	2.13	2.3	0.59	2.4	0.45	9.7	<0.00014	6431.8	0.07	23.1
16/03/2022 14:11	69	56	65.87	0.6	141.40	0.7	16.47	1.2	62.29	0.7	2.23	0.3	0.54	7.2	0.43	5.6	<0.00014	N/A	0.09	28.9
16/03/2022 14:14	70	57	56.61	0.7	117.12	0.6	14.21	1.0	54.06	0.7	1.78	3.9	0.44	3.0	0.36	5.4	<0.00014	203.8	0.109	35.7
16/03/2022 14:18	71	58	53.69	1.5	112.39	1.8	13.69	2.2	52.53	2.1	1.82	1.1	0.48	2.1	0.41	5.1	<0.00014	N/A	0.092	11.3
16/03/2022 14:21	72	59	71.29	1.5	148.11	1.4	18.14	0.9	69.66	0.4	2.40	5.0	0.71	0.7	0.62	3.8	<0.00014	176.5	0.12	20.9
16/03/2022 14:25	73	60	73.23	0.5	151.32	0.7	18.18	0.7	68.98	0.7	2.42	0.5	0.59	2.2	0.50	3.6	<0.00014	146.7	0.107	18.8
16/03/2022 14:28	74	61	84.21	1.3	174.88	1.3	21.12	1.5	80.25	0.8	2.80	2.3	0.73	2.9	0.55	6.5	<0.00014	N/A	0.080	1.0
16/03/2022 14:32	75	62	81.97	0.2	171.20	0.4	20.66	0.2	78.16	0.9	2.72	1.7	0.68	2.9	0.58	11.4	<0.00014	N/A	0.08	8.7
16/03/2022 14:35	76	63	78.52	0.8	163.69	0.6	19.83	0.5	75.30	0.1	2.51	1.9	0.60	1.1	0.50	7.0	<0.00014	N/A	0.095	20.1
16/03/2022 14:39	77	64	60.05	0.9	123.86	1.0	15.17	0.8	57.66	1.1	1.92	1.6	0.46	1.6	0.36	16.9	<0.00014	339.1	0.054	34.2
16/03/2022 14:42	78	65	69.17	0.8	144.53	0.9	17.48	0.7	66.78	1.0	2.31	3.6	0.63	3.6	0.53	9.4	<0.00014	N/A	0.09	16.1
16/03/2022 14:46	79	66	71.84	0.4	146.96	0.6	17.66	0.3	66.32	1.4	2.26	2.8	0.58	6.1	0.49	8.6	<0.00014	N/A	0.080	30.9
16/03/2022 15:07	80	Blank 7	0.00	134.5	0.00	108.2	<0.00006	N/A	<0.00027	143.6	<0.00008	9402.8	<0.00004	N/A	<0.00009	0.0	<0.00014	N/A	0.001	23.3
16/03/2022 15:11	81	Blank 8	0.00	30.3	0.00	35.7	<0.00006	N/A	<0.00027	N/A	<0.00008	N/A	<0.00004	N/A	<0.00009	0.0	<0.00014	66.5	0.002	2.5
16/03/2022 15:14	82	Blank 9	0.00	26.1	0.00	20.3	<0.00006	N/A	<0.00027	796.5	<0.00008	N/A	<0.00004	N/A	<0.00009	655.9	<0.00014	N/A	<0.00020	132.1
16/03/2022 15:18	83	Ref. marine 5	51.75	0.4	100.73	0.1	12.37	0.4	47.50	1.8	2.24	1.3	0.39	1.3	0.31	18.0	<0.00014	N/A	<0.00020	156.2
16/03/2022 15:22	84	Ref. marine 6	54.96	1.2	107.65	0.8	13.24	0.6	51.04	2.0	2.33	3.4	0.40	8.0	0.30	9.6	<0.00014	N/A	0.030	9.0
16/03/2022 15:25	85	Ref. river 5	64.65	0.9	133.95	1.6	15.83	0.9	59.52	2.2	1.65	3.7	0.40	5.8	0.34	6.6	<0.00014	219.4	0.218	12.8
16/03/2022 15:29	86	Ref. river 6	59.30	0.6	123.48	0.6	14.50	1.2	54.30	1.1	1.57	1.2	0.39	7.2	0.34	5.6	<0.00014	366.0	0.18	12.4
16/03/2022 15:32	87	52	53.46	1.9	114.22	1.4	13.36	1.3	50.86	2.7	1.73	4.5	0.42	2.5	0.35	6.4	<0.00014	227.6	0.093	22.6
16/03/2022 15:36	88	67	68.52	0.4	141.96	0.1	17.16	0.6	64.75	0.8	2.29	3.2	0.57	6.2	0.48	1.8	<0.00014	N/A	0.160	5.3
16/03/2022 15:39	89	B1 2-1	122.33	0.9	258.35	1.3	31.11	1.5	118.22	0.7	3.80	0.7	0.87	2.4	0.68	2.5	<0.00014	N/A	0.05	27.5
16/03/2022 15:43	90	B1 3-1	101.87	0.8	216.03	1.1	26.03	1.4	98.84	1.0	3.29	3.1	0.76	1.5	0.64	6.6	<0.00014	925.2	0.064	22.1
16/03/2022 15:46	91	B1 4	95.05	0.9	201.69	1.0	24.03	1.3	92.62	1.6	3.13	4.2	0.79	0.9	0.63	3.4	<0.00014	N/A	0.061	26.1
16/03/2022 15:50	92	B1 5-1	97.43	0.8	206.36	1.0	24.88	0.5	94.24	1.6	3.07	1.3	0.75	4.1	0.62	10.4	<0.00014	N/A	0.072	7.3
16/03/2022 15:53	93	B1 6	117.82	0.7	249.45	1.1	29.96	1.7	113.30	1.3	3.70	2.5	0.88	2.1	0.76	5.4	<0.00014	N/A	0.08	12.7
16/03/2022 15:57	94	B1 7	89.19	0.0	190.22	0.3	22.96	0.7	86.65	0.9	2.87	4.3	0.71	2.9	0.59	4.9	<0.00014	459.6	0.06	18.5
16/03/2022 16:01	95	B2 2-1	86.61	1.3	183.32	1.2	21.93	0.8	83.43	0.7	2.66	2.9	0.68	4.9	0.54	3.8	<0.00014	N/A	0.059	11.0
16/03/2022 16:04	96	B2 3-1	96.37	0.8	202.39	0.3	24.05	1.3	91.70	0.4	3.00	2.8	0.73	2.7	0.60	5.7	<0.00014	316.7	0.068	20.8
16/03/2022 16:08	97	B2 4	86.24	1.5	182.72	1.3	21.98	1.5	84.19	1.9	2.76	2.3	0.72	1.3	0.52	4.0	<0.00014	N/A	0.051	28.5
16/03/2022 16:11	98	B2 5 rep1	92.42	2.2	196.09	2.0	23.49	2.3	89.13	2.2	2.93	1.4	0.68	4.9	0.56	7.8	<0.00014	91.7	0.077	22.5
16/03/2022 16:15	98	B2 5 rep2	97.57	0.7	207.15	0.9	24.86	1.8	95.31	1.1	3.05	0.2	0.74	5.4	0.60	6.0	<0.00014	N/A	0.057	37.5
16/03/2022 16:18	99	B2 6	110.17	1.1	234.37	1.0	27.95	1.0	106.09	1.8	3.40	2.1	0.85	1.6	0.69	7.5	<0.00014	N/A	0.05	17.5
16/03/2022 16:22	100	B3 2	105.45	0.9	224.12	0.9	26.87	1.2	102.17	0.9	3.42	1.0	0.76	0.7	0.64	3.3	<0.00014	N/A	0.091	14.3
16/03/2022 16:25	101	B3 3	88.41	1.6	187.41	1.0	22.24	2.3	84.65	2.0	2.68	3.9	0.68	1.2	0.56	3.1	<0.00014	N/A	0.039	27.8
16/03/2022 16:29	102	B3 4	102.32	1.1	217.04	1.2	26.12	0.7	99.24	0.5	3.25	1.5	0.79	2.5	0.60	11.6	<0.00014	177.2	0.06	26.1
16/03/2022 16:33	103	B3 5	107.81	0.5	230.02	0.2	27.65	0.2	105.13	0.6	3.37	0.9	0.81	1.5	0.63	5.0	<0.00014	N/A	0.056	50.2
16/03/2022 16:36	104	B3 6	118.62	0.5	252.27	0.7	30.45	0.3	114.88	1.2	3.76	1.2	0.88	3.2	0.72	5.3	<0.00014	N/A	0.048	18.2
16/03/2022 16:40	105	B3 7	104.92	0.4	223.74	0.4	26.88	0.4	101.91	0.5	3.35	1.8	0.80	2.2	0.64	4.6	<0.00014	510.1	0.053	12.3
16/03/2022 16:43	106	Sars 1-1	126.88	0.7	254.79	0.4	32.08	0.8	121.99	1.2	3.56	1.6	0.63	4.9	0.55	1.6	<0.00014	569.3	0.061	21.7
16/03/2022 16:47	107	Sars 2-1	141.87	1.7	296.08	1.2	35.80	1.9	136.49	2.1	3.65	1.2	0.68	4.0	0.52	7.5	<0.00014	101.5	0.037	21.5

Sample			195 -> 195 Pt [O2]		202 -> 202 Hg [O2]		205 -> 205 Tl [O2]		206 -> 206 [Pb] [O2]		207 -> 207 [Pb] [O2]		208 -> 208 Pb [O2]		209 -> 209 Bi [O2]		232 -> 248 Th [O2]		238 -> 238 U [H2]	
Acq. Date-Time	Sample Name	Comment	Conc. [ug/l]	Conc. RSD	Conc. [ug/l]	Conc. RSD	Conc. [ug/l]	Conc. RSD	Conc. [ug/l]	Conc. RSD	Conc. [ug/l]	Conc. RSD	Conc. [ug/l]	Conc. RSD	Conc. [ug/l]	Conc. RSD	Conc. [ug/l]	Conc. RSD	Conc. [ug/l]	Conc. RSD
16/03/2022 13:14	41	Blank 4	0.00	91.9	0.01	40.4	<0.00070	N/A	<0.00097	1172.2	<0.00236	871.4	<0.00156	749.5	<0.00079	N/A	<0.00067	932.7	<0.00005	1183.2
16/03/2022 13:17	42	Blank 5	<0.00020	167.9	<0.00413	152.5	<0.00070	N/A	<0.00097	N/A	<0.00236	N/A	<0.00156	N/A	<0.00079	N/A	<0.00067	N/A	<0.00005	N/A
16/03/2022 13:21	43	Blank 6	<0.00020	181.0	<0.00413	110.3	<0.00070	N/A	<0.00097	N/A	<0.00236	N/A	<0.00156	N/A	<0.00079	N/A	<0.00067	N/A	<0.00005	N/A
16/03/2022 13:24	44	Ref. marine 3	0.05	79.6	<0.00413	N/A	1.35	7.9	40.74	1.0	38.70	0.2	39.76	0.4	0.62	0.6	15.42	1.3	3.44	3.1
16/03/2022 13:28	45	Ref. marine 4	<0.00020	N/A	<0.00413	N/A	1.41	4.4	44.96	1.6	41.03	1.6	43.13	1.0	0.71	2.9	16.59	1.8	3.62	6.6
16/03/2022 13:32	46	Ref. river 3	<0.00020	188.1	1.89	11.8	1.28	2.9	97.59	0.9	93.16	0.7	95.30	0.9	0.86	2.4	22.22	1.1	3.59	1.1
16/03/2022 13:35	47	Ref. river 4	0.02	55.5	1.39	21.7	1.07	3.0	81.13	1.9	77.71	1.6	79.35	1.7	0.70	3.6	19.43	3.1	3.20	1.8
16/03/2022 13:39	61	47	<0.00020	131.9	<0.00413	287.8	0.52	6.2	25.34	1.3	23.66	1.3	24.75	0.1	1.06	5.5	15.59	1.5	3.80	2.0
16/03/2022 13:42	62	48	<0.00020	128.6	<0.00413	N/A	0.65	4.1	27.81	1.4	25.66	1.8	26.68	1.5	0.59	1.8	17.55	4.2	3.80	1.8
16/03/2022 13:46	63	49	0.01	16.1	<0.00413	N/A	0.76	1.2	26.86	0.6	25.49	0.4	25.98	0.3	0.67	3.2	17.00	0.4	3.77	2.4
16/03/2022 13:49	64	50	<0.00020	96.4	<0.00413	N/A	0.50	4.8	22.21	1.0	20.84	0.5	21.52	0.6	0.59	7.8	14.57	1.1	3.43	2.0
16/03/2022 13:53	65	51 rep1	<0.00020	767.3	<0.00413	N/A	0.63	2.8	24.66	1.1	22.85	1.8	23.73	0.1	0.68	2.2	18.38	1.2	3.97	2.0
16/03/2022 13:56	65	51 rep2	<0.00020	206.7	<0.00413	N/A	0.58	3.7	23.80	1.1	22.17	1.2	23.13	0.8	0.62	2.4	17.96	3.0	3.95	4.4
16/03/2022 14:00	66	53	<0.00020	59.0	<0.00413	N/A	0.76	5.0	32.42	0.6	30.40	0.7	31.40	0.3	1.09	1.6	20.77	0.4	4.51	3.6
16/03/2022 14:03	67	54	0.01	67.7	<0.00413	N/A	0.53	3.5	25.06	1.5	23.47	1.9	24.12	1.4	0.70	1.5	18.03	2.2	3.85	1.7
16/03/2022 14:07	68	55	0.02	59.7	<0.00413	N/A	0.51	4.8	31.61	1.4	29.45	1.3	30.49	0.5	0.88	2.0	16.48	2.0	3.25	3.5
16/03/2022 14:11	69	56	0.01	99.3	<0.00413	N/A	0.72	6.3	27.72	2.1	26.00	0.3	26.78	1.3	0.57	6.7	17.39	0.3	4.08	2.3
16/03/2022 14:14	70	57	<0.00020	521.3	<0.00413	N/A	0.41	8.0	23.10	2.2	21.64	1.6	22.16	0.3	1.10	2.5	13.14	1.3	3.03	1.7
16/03/2022 14:18	71	58	0.02	53.4	<0.00413	N/A	0.43	7.5	21.04	1.2	19.99	1.7	20.48	0.6	0.97	2.9	13.28	2.5	2.88	1.7
16/03/2022 14:21	72	59	<0.00020	98.2	<0.00413	N/A	0.54	0.4	32.59	0.2	30.75	1.3	31.70	0.9	1.34	2.7	18.63	0.5	4.47	4.2
16/03/2022 14:25	73	60	0.01	34.1	<0.00413	N/A	0.76	5.0	29.25	0.9	27.13	1.2	28.04	0.5	0.72	3.6	18.96	2.2	4.17	2.4
16/03/2022 14:28	74	61	<0.00020	217.9	<0.00413	1127.0	0.82	2.7	31.65	1.0	29.62	1.4	30.90	1.7	0.81	2.1	21.02	2.3	4.08	1.7
16/03/2022 14:32	75	62	<0.00020	5400.0	<0.00413	N/A	0.74	8.2	30.27	0.8	28.03	0.8	29.13	0.2	1.25	1.6	20.74	0.6	4.34	0.5
16/03/2022 14:35	76	63	<0.00020	N/A	<0.00413	N/A	0.57	3.9	28.50	0.8	27.15	0.4	27.81	0.7	0.62	10.3	17.44	1.4	3.66	2.9
16/03/2022 14:39	77	64	<0.00020	47.1	<0.00413	N/A	0.40	3.9	32.68	0.7	30.71	0.8	31.62	0.5	6.30	0.3	14.16	0.4	3.14	1.8
16/03/2022 14:42	78	65	0.01	236.2	<0.00413	N/A	0.64	3.2	25.77	1.6	23.96	2.1	25.02	1.6	0.71	2.4	17.58	1.8	3.51	2.4
16/03/2022 14:46	79	66	0.01	116.0	<0.00413	N/A	0.64	5.1	28.62	0.2	26.44	1.4	27.57	0.3	0.66	3.3	17.91	0.7	3.93	1.2
16/03/2022 15:07	80	Blank 7	0.00	59.6	<0.00413	N/A	<0.00070	N/A	<0.00097	N/A	<0.00236	N/A	<0.00156	N/A	<0.00079	N/A	<0.00067	552.9	<0.00005	N/A
16/03/2022 15:11	81	Blank 8	<0.00020	N/A	<0.00413	N/A	<0.00070	N/A	<0.00097	N/A	<0.00236	N/A	<0.00156	N/A	<0.00079	N/A	<0.00067	210.8	<0.00005	153.6
16/03/2022 15:14	82	Blank 9	<0.00020	298.9	<0.00413	31.6	<0.00070	N/A	<0.00097	N/A	<0.00236	N/A	<0.00156	N/A	<0.00079	N/A	<0.00067	N/A	<0.00005	1355.1
16/03/2022 15:18	83	Ref. marine 5	0.03	86.2	<0.00413	300.4	1.36	7.4	41.75	1.1	38.54	1.9	39.95	0.3	0.68	4.8	15.25	0.8	3.33	2.4
16/03/2022 15:22	84	Ref. marine 6	0.02	31.3	<0.00413	766.7	1.39	2.6	43.31	2.1	40.30	0.5	41.44	1.1	0.72	6.8	16.32	3.0	3.31	4.4
16/03/2022 15:25	85	Ref. river 5	<0.00020	77.5	1.89	17.9	1.06	3.4	88.86	1.5	85.49	0.6	87.32	1.0	0.73	5.1	19.58	2.6	3.01	5.1
16/03/2022 15:29	86	Ref. river 6	<0.00020	161.2	1.63	4.4	0.99	1.4	74.80	0.3	70.52	0.4	72.83	0.3	0.65	4.8	17.28	0.6	2.94	1.1
16/03/2022 15:32	87	52	<0.00020	282.2	<0.00413	N/A	0.38	5.0	22.24	1.7	20.85	2.4	21.32	1.9	3.60	1.8	14.90	3.3	3.14	1.7
16/03/2022 15:36	88	67	<0.00020	432.1	<0.00413	869.7	0.73	7.1	28.76	1.2	26.89	1.4	27.79	0.8	1.10	4.2	18.00	1.5	4.07	2.0
16/03/2022 15:39	89	B1 2-1	<0.00020	153.4	<0.00413	N/A	0.79	2.3	38.80	2.8	36.23	1.8	37.62	1.1	0.85	4.1	28.87	0.6	3.87	3.4
16/03/2022 15:43	90	B1 3-1	0.02	71.7	<0.00413	N/A	0.76	2.6	34.31	1.8	32.40	0.7	33.52	1.3	0.77	1.6	24.78	2.0	3.77	4.6
16/03/2022 15:46	91	B1 4	0.02	46.7	<0.00413	412.2	0.73	0.4	31.96	2.1	30.10	2.1	31.03	1.7	0.71	4.4	22.65	0.5	3.32	2.8
16/03/2022 15:50	92	B1 5-1	<0.00020	93.9	<0.00413	N/A	0.60	9.6	28.40	1.6	26.75	1.6	27.61	1.9	0.69	8.9	22.32	0.6	3.13	2.8
16/03/2022 15:53	93	B1 6	<0.00020	N/A	<0.00413	N/A	0.84	6.2	38.72	0.8	36.13	1.2	37.53	0.8	1.19	2.9	28.44	0.8	4.16	3.5
16/03/2022 15:57	94	B1 7	<0.00020	43.1	<0.00413	N/A	0.67	4.8	30.94	0.5	29.39	1.1	30.22	0.1	0.68	5.2	21.86	2.3	3.08	2.4
16/03/2022 16:01	95	B2 2-1	<0.00020	233.2	<0.00413	N/A	0.57	3.0	26.04	1.4	25.15	1.6	25.64	1.2	0.59	8.2	20.88	0.4	2.94	2.6
16/03/2022 16:04	96	B2 3-1	0.01	147.4	<0.00413	N/A	0.59	3.8	28.72	0.5	27.39	1.0	28.18	0.5	0.84	3.1	22.97	1.2	3.38	3.2
16/03/2022 16:08	97	B2 4	<0.00020	N/A	<0.00413	N/A	0.57	1.9	28.18	1.7	26.24	0.9	27.25	1.3	0.63	3.6	20.96	0.9	3.13	4.1
16/03/2022 16:11	98	B2 5 rep1	<0.00020	N/A	<0.00413	N/A	0.54	3.0	27.85	1.8	26.63	3.1	27.22	2.2	0.65	6.1	21.35	1.9	3.50	3.7
16/03/2022 16:15	98	B2 5 rep2	0.02	18.8	<0.00413	N/A	0.58	3.9	29.33	1.1	27.96	1.7	28.54	0.7	0.65	2.9	22.73	1.9	3.49	2.9
16/03/2022 16:18	99	B2 6	0.01	25.7	<0.00413	N/A	0.70	5.8	32.00	0.4	30.16	1.7	31.44	1.3	0.70	3.1	25.91	1.0	3.67	3.3
16/03/2022 16:22	100	B3 2	<0.00020	184.2	<0.00413	250.9	0.78	4.4	35.13	0.5	33.13	1.0	34.07	0.3	1.02	7.8	25.09	1.9	3.60	1.6
16/03/2022 16:25	101	B3 3	<0.00020	222.9	<0.00413	N/A	0.54	9.6	24.92	0.1	23.80	1.8	24.59	1.2	0.79	6.5	20.54	1.6	2.97	2.5
16/03/2022 16:29	102	B3 4	<0.00020	3.5	<0.00413	N/A	0.75	2.3	32.69	0.7	31.26	0.7	31.98	0.4	0.71	4.0	24.08	2.2	3.39	1.2
16/03/2022 16:33	103	B3 5	<0.00020	294.1	<0.00413	N/A	0.83	4.0	34.77	0.2	32.59	1.5	33.96	0.5	0.83	4.7	25.52	1.0	3.59	2.9
16/03/2022 16:36	104	B3 6	<0.00020	250.5	<0.00413	N/A	0.81	0.7	38.53	0.4	36.41	0.5	37.82	1.4	0.86	5.6	27.68	0.5	3.95	1.3
16/03/2022 16:40	105	B3 7	<0.00020	195.1	<0.00413	N/A	0.80	2.6	40.25	1.1	38.13	2.1	39.28	0.9	1.45	2.7	24.99	1.1	3.68	1.2
16/03/2022 16:43	106	Sars 1-1	<0.00020	163.0	<0.00413	346.7	2.44	0.6	61.08	0.4	57.25	1.2	59.18	0.5	1.45	2.8	32.66	0.6	6.09	3.5
16/03/2022 16:47	107	Sars 2-1	0.010	159.6	<0.00413	N/A	1.87	3.2	46.75	2.6	43.86	2.8	45.47	2.1	0.74	7.7	31.17	3.0	5.15	5.9

Table B.3: Detection limits for the ICP-MS analysis.

Tune Mode	Scan Type	Q1	Q2	Name	R	DL	BEC	Units
No Gas	MS/MS	7	7	Li	1.000	2.58E-03	1.79E-02	ug/l
H2	MS/MS	9	9	Be	1.000	0.00E+00	0.00E+00	ug/l
O2	MS/MS	11	11	B	1.000	4.69E-02	6.46E-01	ug/l
O2	MS/MS	23	23	Na	1.000	2.56E-01	1.63E+00	ug/l
O2	MS/MS	24	24	Mg	1.000	7.86E-02	4.93E-02	ug/l
H2	MS/MS	27	27	Al	0.999	1.21E-03	2.49E-02	ug/l
O2	MS/MS	28	44	Si	1.000	8.78E-02	1.37E+00	ug/l
O2	MS/MS	31	47	P	1.000	1.39E-02	5.39E-02	ug/l
O2	MS/MS	32	48	S	1.000	2.24E-01	1.35E+00	ug/l
O2	MS/MS	39	39	K	1.000	1.10E-01	6.80E-01	ug/l
H2	MS/MS	40	40	Ca	1.000	4.39E-03	1.24E-01	ug/l
O2	MS/MS	45	61	Sc	1.000	7.22E-04	3.45E-03	ug/l
O2	MS/MS	47	63	Ti	1.000	1.44E-03	6.82E-04	ug/l
O2	MS/MS	51	67	V	1.000	1.26E-03	1.11E-03	ug/l
O2	MS/MS	52	52	Cr	1.000	4.25E-03	1.65E-02	ug/l
O2	MS/MS	55	55	Mn	1.000	1.69E-02	1.27E-02	ug/l
H2	MS/MS	56	56	Fe	1.000	7.40E-03	8.97E-02	ug/l
O2	MS/MS	59	59	Co	1.000	7.92E-04	4.86E-03	ug/l
O2	MS/MS	60	60	Ni	1.000	1.56E-03	7.07E-03	ug/l
O2	MS/MS	63	63	Cu	1.000	1.89E-02	2.85E-02	ug/l
H2	MS/MS	66	66	Zn	1.000	1.12E-02	1.79E-02	ug/l
H2	MS/MS	71	71	Ga	1.000	3.91E-04	4.13E-04	ug/l
O2	MS/MS	75	91	As	1.000	2.34E-03	5.86E-04	ug/l
H2	MS/MS	78	78	Se	0.998	6.90E-03	1.33E-03	ug/l
O2	MS/MS	85	85	Rb	1.000	2.50E-03	4.68E-03	ug/l
H2	MS/MS	88	88	Sr	1.000	9.98E-04	4.01E-03	ug/l
O2	MS/MS	89	105	Y	1.000	2.21E-04	5.54E-05	ug/l
O2	MS/MS	90	106	Zr	1.000	4.61E-04	6.64E-04	ug/l
O2	MS/MS	93	125	Nb	1.000	1.23E-04	7.69E-05	ug/l
O2	MS/MS	95	127	Mo	1.000	3.80E-04	6.92E-04	ug/l
O2	MS/MS	111	111	Cd	1.000	6.30E-04	1.21E-04	ug/l
O2	MS/MS	115	115	In	1.000	3.49E-05	2.31E-05	ug/l
O2	MS/MS	118	118	Sn	1.000	8.60E-04	1.88E-03	ug/l
O2	MS/MS	121	137	Sb	1.000	7.63E-04	2.55E-04	ug/l
O2	MS/MS	133	133	Cs	1.000	5.30E-04	1.06E-03	ug/l
O2	MS/MS	137	137	Ba	1.000	2.27E-03	1.97E-03	ug/l
O2	MS/MS	139	155	La	1.000	7.77E-05	7.11E-05	ug/l
O2	MS/MS	140	156	Ce	1.000	1.50E-04	7.59E-05	ug/l
O2	MS/MS	141	157	Pr	1.000	4.26E-04	1.19E-04	ug/l
O2	MS/MS	146	162	Nd	1.000	1.73E-04	6.68E-05	ug/l
O2	MS/MS	153	153	Eu	1.000	5.57E-05	7.31E-05	ug/l
O2	MS/MS	169	185	Tm	1.000	2.76E-04	8.41E-05	ug/l
O2	MS/MS	175	191	Lu	1.000	4.27E-05	4.16E-05	ug/l
O2	MS/MS	181	213	Ta	1.000	2.85E-05	4.66E-05	ug/l
O2	MS/MS	182	214	W	1.000	2.63E-04	3.57E-04	ug/l
O2	MS/MS	195	195	Pt	1.000	6.13E-04	6.03E-04	ug/l
O2	MS/MS	202	202	Hg	1.000	4.54E-03	2.92E-02	ug/l
O2	MS/MS	205	205	Tl	1.000	8.93E-04	2.06E-03	ug/l
O2	MS/MS	208	208	Pb	1.000	2.02E-03	5.79E-03	ug/l
O2	MS/MS	209	209	Bi	1.000	5.31E-04	9.91E-04	ug/l
O2	MS/MS	232	248	Th	1.000	8.55E-04	5.69E-04	ug/l
H2	MS/MS	238	238	U	1.000	9.49E-05	3.15E-05	ug/l
No Gas	MS/MS	7	7	Li	0.9999	4.36E-04	1.58E-02	ug/l
H2	MS/MS	9	9	Be	1.0000	0.00E+00	0.00E+00	ug/l

Tune Mode	Scan Type	Q1	Q2	Name	R	DL	BEC	Units
O2	MS/MS	11	11	B	0.9998	8.59E-02	5.94E-01	ug/l
O2	MS/MS	23	23	Na	1.0000	4.42E-02	1.47E+00	ug/l
O2	MS/MS	24	24	Mg	1.0000	4.57E-03	3.76E-02	ug/l
H2	MS/MS	27	27	Al	1.0000	7.45E-03	6.34E-02	ug/l
O2	MS/MS	28	44	Si	1.0000	8.31E-02	1.15E+00	ug/l
O2	MS/MS	31	47	P	1.0000	2.23E-02	3.69E-02	ug/l
O2	MS/MS	32	48	S	1.0000	1.85E-01	9.88E-01	ug/l
O2	MS/MS	39	39	K	1.0000	5.91E-02	6.80E-01	ug/l
H2	MS/MS	40	40	Ca	1.0000	2.98E-02	1.33E-01	ug/l
O2	MS/MS	45	61	Sc	1.0000	3.64E-04	2.29E-03	ug/l
O2	MS/MS	47	63	Ti	1.0000	2.49E-03	2.07E-03	ug/l
O2	MS/MS	51	67	V	1.0000	1.24E-04	7.02E-04	ug/l
O2	MS/MS	52	52	Cr	1.0000	2.09E-03	1.80E-02	ug/l
O2	MS/MS	55	55	Mn	1.0000	1.11E-02	9.35E-03	ug/l
H2	MS/MS	56	56	Fe	1.0000	7.85E-03	8.65E-02	ug/l
O2	MS/MS	59	59	Co	1.0000	1.47E-03	3.84E-03	ug/l
O2	MS/MS	60	60	Ni	1.0000	7.56E-03	7.64E-03	ug/l
O2	MS/MS	63	63	Cu	1.0000	6.37E-03	3.12E-02	ug/l
H2	MS/MS	66	66	Zn	0.9999	6.31E-03	2.42E-02	ug/l
H2	MS/MS	71	71	Ga	1.0000	3.04E-04	4.07E-04	ug/l
O2	MS/MS	75	91	As	1.0000	1.45E-03	5.56E-04	ug/l
H2	MS/MS	78	78	Se	1.0000	3.09E-03	2.31E-03	ug/l
O2	MS/MS	85	85	Rb	1.0000	2.17E-04	4.24E-03	ug/l
H2	MS/MS	88	88	Sr	1.0000	7.69E-04	3.06E-03	ug/l
O2	MS/MS	89	105	Y	1.0000	1.70E-04	5.97E-05	ug/l
O2	MS/MS	90	106	Zr	1.0000	9.33E-04	9.71E-04	ug/l
O2	MS/MS	93	125	Nb	1.0000	1.23E-04	6.50E-05	ug/l
O2	MS/MS	95	127	Mo	1.0000	6.88E-04	6.95E-04	ug/l
O2	MS/MS	111	111	Cd	1.0000	6.27E-04	1.21E-04	ug/l
O2	MS/MS	115	115	In	1.0000	3.98E-05	1.92E-05	ug/l
O2	MS/MS	118	118	Sn	1.0000	8.38E-04	1.27E-03	ug/l
O2	MS/MS	121	137	Sb	1.0000	4.42E-04	8.51E-05	ug/l
O2	MS/MS	133	133	Cs	1.0000	5.48E-04	9.83E-04	ug/l
O2	MS/MS	137	137	Ba	1.0000	2.34E-03	8.54E-03	ug/l
O2	MS/MS	139	155	La	1.0000	1.94E-05	3.04E-05	ug/l
O2	MS/MS	140	156	Ce	0.9999	1.02E-06	4.73E-05	ug/l
O2	MS/MS	141	157	Pr	1.0000	5.77E-05	4.99E-05	ug/l
O2	MS/MS	146	162	Nd	1.0000	2.68E-04	5.17E-05	ug/l
O2	MS/MS	153	153	Eu	1.0000	8.43E-05	4.28E-05	ug/l
O2	MS/MS	169	185	Tm	1.0000	4.36E-05	1.26E-05	ug/l
O2	MS/MS	175	191	Lu	1.0000	8.58E-05	1.65E-05	ug/l
O2	MS/MS	181	213	Ta	1.0000	1.43E-04	4.94E-05	ug/l
O2	MS/MS	182	214	W	1.0000	2.03E-04	2.06E-04	ug/l
O2	MS/MS	195	195	Pt	1.0000	2.02E-04	5.56E-04	ug/l
O2	MS/MS	202	202	Hg	1.0000	4.13E-03	2.10E-02	ug/l
O2	MS/MS	205	205	Tl	0.9998	6.97E-04	2.89E-03	ug/l
O2	MS/MS	206	206	[Pb]	1.0000	9.71E-04	6.93E-03	ug/l
O2	MS/MS	207	207	[Pb]	1.0000	2.36E-03	8.71E-03	ug/l
O2	MS/MS	208	208	Pb	1.0000	1.56E-03	7.10E-03	ug/l
O2	MS/MS	209	209	Bi	1.0000	7.91E-04	1.30E-03	ug/l
O2	MS/MS	232	248	Th	1.0000	6.67E-04	4.95E-04	ug/l
H2	MS/MS	238	238	U	1.0000	5.33E-05	2.05E-05	ug/l

Table B.4: General detection limits for pre-treated samples in the ICP-MS analysis.

Content this sheet: Detection limits (DL) various material, witch has to bee pre-treated (digestion, dilution e.g.), prior to analyses

Detection limits is calculated from QL-25% values in column F (details in sheet QL-1).
Checking if Blank DL (BDL) defined as 3*std of method blanks versus QL-25%, is verified for each individually project.
Sample amount and final volume after digestion, used calculating DL in solid material.
Formulas is still active, so putting in new sample amount or final volume, will automatically recalculate the detection limits for you

Density data used calculating sample volume from sample weight given by Tore Syversen. Values in () used in calculations.
Whole blood females 1.05-1.056, males 1.055-1.064 (1.058) Plasma 1.025-1.029 (1.027) Serum 1.024-1.028 (1.026), Urine 1.01

Ranges of sample amount and final volumes used for analyzes
Cells with parameters included in formulas/formulas themselves, are marked with this background colour

Material	Sample amount (g)		Final volume (ml)	
	In formula	Range	In formula	Range
Blood, Serum, CSF	1,00	0.3-2	12	3-24
Urine	5,00	1-6	50	10-60
Organics	0,25	0.001-1	60	(3 - unlimited)
Sediments	0,02	0.01-2	50	(3 - unlimited)

Table 1 - detection limits, counting digits = 3 — Sorting Key : Ele

Abbreviations: NC = not checked, <QL = no signal at all

Sorting key: Element
Lr, Mr, Hr = Low, Medium and High Resolution

Sign	Isotope	Element	Resolution	QL-25% (µg/l)	DL in original sample: Blood/ Serum, CSF µg/kg	Urine µg/kg	Organics µg/g	Sediments µg/g	unit
Al	27	Aluminium	Mr	0,20	2,40	2,00	0,05	0,50	
Sb	121	Antimony	Mr	0,0020	0,0240	0,0200	0,0005	0,0050	
As	75	Arsenic	Hr	0,025	0,300	0,250	0,006	0,063	
Ba	137	Barium	Mr	0,013	0,156	0,130	0,003	0,033	
Be	9	Beryllium	Lr	0,0020	0,0240	0,0200	0,0005	0,0050	
Be	9	Beryllium	Mr	0,0080	0,0960	0,0800	0,0019	0,0200	
Bi	209	Bismuth	Lr	0,0010	0,0120	0,0100	0,0002	0,0025	
B	11	Boron	Lr	0,050	0,600	0,500	0,012	0,125	
B	11	Boron	Mr	0,080	0,960	0,800	0,019	0,200	
Br	81	Brom	Hr	3,0	36,0	30,0	0,7	7,5	
Cd	111/114	Cadmium	Lr	0,0020	0,0240	0,0200	0,0005	0,0050	
Cd	111/114	Cadmium	Mr	0,0100	0,1200	0,1000	0,0024	0,0250	
Ca	44	Calcium	Mr	2,0	24,0	20,0	0,5	5,0	
Ce	140	Cerium	Lr	0,0002	0,0024	0,0020	0,0000	0,0005	
Cs	133	Cesium	Lr	0,0005	0,0060	0,0050	0,0001	0,0013	
Cl	35	Chlorine	Mr	100	1 200	1 000	24	250	
Cr	53	Chromium	Mr	0,0200	0,2400	0,2000	0,0048	0,0500	
Co	59	Cobalt	Mr	0,0040	0,0480	0,0400	0,0010	0,0100	
Cu	63/65	Cupper	Mr	0,030	0,3600	0,3000	0,0072	0,0750	
Dy	163	Dysprosium	Lr	0,0008	0,0096	0,0080	0,0002	0,0020	
Er	166	Erbium	Lr	0,0003	0,0036	0,0030	0,0001	0,0008	
Eu	153	Europium	Lr	0,0008	0,0096	0,0080	0,0002	0,0020	
Gd	155	Gadolinium	Mr	0,020	0,240	0,200	0,005	0,050	
Ga	69	Gallium	Mr	0,0070	0,0840	0,0700	0,0017	0,0175	
Ge	72	Germanium	Hr	0,020	0,240	0,200	0,005	0,050	
Au	197	Gold	Lr	0,0002	0,0024	0,0020	0,0000	0,0005	
Hf	178	Hafnium	Lr	0,0010	0,0120	0,0100	0,0002	0,0025	
Ho	165	Hollium	Lr	0,0002	0,0024	0,0020	0,0000	0,0005	
In	115	Indium	Lr	0,0005	0,0060	0,0050	0,0001	0,0013	
I	127	Iodide	Mr	1,0	12,0	10,0	0,2	2,5	
Fe	56	Iron	Mr	0,020	0,240	0,200	0,005	0,050	
Ir	193	Iridium	Lr	0,0005	0,0060	0,0050	0,0001	0,0013	
La	139	Lantan	Lr	0,0005	0,0060	0,0050	0,0001	0,0013	
La	139	Lantan	Mr	0,0020	0,0240	0,0200	0,0005	0,0050	
Pb	208	Lead	Lr	0,0020	0,0240	0,0200	0,0005	0,0050	
Li	7	Lithium	Lr	0,005	0,060	0,050	0,001	0,013	
Li	7	Lithium	Mr	0,030	0,360	0,300	0,007	0,075	
Lu	175	Lutetium	Lr	0,0002	0,0024	0,0020	0,0000	0,0005	
Mg	24	Magnesium	Mr	0,10	1,20	1,00	0,02	0,25	
Mg	25	Magnesium	Mr	0,50	6,00	5,00	0,12	1,25	
Mn	55	Manganese	Mr	0,0060	0,0720	0,0600	0,0014	0,0150	
Hg	202	Mercury	Lr	0,0020	0,0240	0,0200	0,0005	0,0050	
Mo	98	Molybdenum	Mr	0,020	0,240	0,200	0,005	0,050	
Nd	146	Neodymium	Lr	0,0002	0,0024	0,0020	0,0000	0,0005	
Ni	60	Nikkel-60	Mr	0,015	0,180	0,150	0,004	0,038	
Nb	93	Niob	Lr	0,001	0,012	0,010	0,000	0,003	
Nb	93	Niob	Hr	0,025	0,300	0,250	0,006	0,063	
Pd	104	Palladium	Hr	0,050	0,600	0,500	0,012	0,125	
P	31	Phosphor	Mr	0,40	4,80	4,00	0,10	1,00	
Pt	195	Platinum	Lr	0,0010	0,0120	0,0100	0,0002	0,0025	
K	39	Potassium	Mr	1,0	12,0	10,0	0,2	2,5	
Pr	141	Praseodymium	Lr	0,0003	0,0036	0,0030	0,0001	0,0008	
Re	185	Rhenium	Hr	0,04	0,48	0,40	0,01	0,10	
Rh	103	Rhodium	Lr	0,0005	0,0060	0,0050	0,0001	0,0013	
Rh	103	Rhodium	Hr	0,0100	0,1200	0,1000	0,0024	0,0250	
Rb	85	Rubidium	Mr	0,012	0,144	0,120	0,003	0,030	
Ru	85	Ruthenium	Lr	0,0010	0,0050	0,030	0,050	0,300	
Sm	147	Samarium	Lr	0,0005	0,0060	0,0050	0,0001	0,0013	
Sc	45	Scandium	Mr	0,0040	0,0480	0,0400	0,0010	0,0100	
Se	82	Selenium	Lr	0,05	0,60	0,50	0,01	0,13	
Se	78	Selenium	Hr	0,150	1,800	1,500	0,036	0,375	
Si	29	Silisium	Mr	10,0	120,0	100,0	2,4	25,0	
Ag	109	Silver	Mr	0,020	0,240	0,200	0,005	0,050	
Na	23	Sodium	Mr	10,0	120,0	100,0	2,4	25,0	
Sr	88	Strontium	Mr	0,025	0,300	0,250	0,006	0,063	
S	32	Sulphur	Mr	5,0	60,0	50,0	1,2	12,5	
S	34	Sulphur	Mr	20	240	200	5	50	
Ta	181	Tantalum	Lr	0,0002	0,0024	0,0020	0,0000	0,0005	
Te	125	Tellur	Mr	0,100	1,200	1,000	0,024	0,250	
Tb	159	Terbium	Lr	0,0002	0,0024	0,0020	0,0000	0,0005	
Tl	205	Thallium	Lr	0,0003	0,0030	0,0025	0,0001	0,0006	
Th	232	Thorium	Lr	0,0005	0,0060	0,0050	0,0001	0,0013	
Tm	169	Thulium	Lr	0,0005	0,0060	0,0050	0,0001	0,0013	
Sn	118	Tin	Lr	0,001	0,012	0,010	0,000	0,003	
Sn	118	Tin	Mr	0,010	0,120	0,100	0,002	0,025	
Ti	47	Titanium	Mr	0,020	0,240	0,200	0,005	0,050	
U	238	Uranium	Lr	0,0003	0,0030	0,0025	0,0001	0,0006	
V	51	Vanadium	Mr	0,0030	0,0360	0,0300	0,0007	0,0075	
W	182	Wolfram	Lr	0,0010	0,0120	0,0100	0,0002	0,0025	
Yb	172	Ytterbium	Lr	0,0004	0,0048	0,0040	0,0001	0,0010	
Yb	89	Yttrium	Lr	0,0004	0,0048	0,0040	0,0001	0,0010	
Zn	66	Zink-66	Mr	0,025	0,300	0,250	0,006	0,063	

Table B.5: Tuning parameters for the ICP-MS analysis.

	Scan Type	Q1	Q2	ISTD	R	a	b (blank)	Name	DL	BEC	Units	cps/ppb	Heading results
Start statistical calculations													
O2	MS/MS	11	11	103 -> 103 Rh [O2]	1.000	0.001	0.001	**B**	0.057	0.171	ug/l	**285**	11 -> 11 B [O2]
H2	MS/MS	23	23	103 -> 103 Rh [H2]	0.99998	0.047	0.100	**Na**	0.093	2.105	ug/l	**12,282**	23 -> 23 Na [H2]
O2	MS/MS	23	23	193 -> 193 Ir [O2]	0.99992	0.196	0.292	**Na**	0.142	1.485	ug/l	**15,081**	23 -> 23 Na [O2]
H2	MS/MS	24	24	103 -> 103 Rh [H2]	0.99999	0.034	0.003	**Mg**	0.021	0.081	ug/l	**8,716**	24 -> 24 Mg [H2]
O2	MS/MS	24	24	103 -> 103 Rh [O2]	0.99996	0.035	0.003	**Mg**	0.021	0.076	ug/l	**12,907**	24 -> 24 Mg [O2]
H2	MS/MS	27	27	103 -> 103 Rh [H2]	0.99997	0.039	0.004	**Al**	0.018	0.113	ug/l	**10,004**	27 -> 27 Al [H2]
H2	MS/MS	28	28	103 -> 103 Rh [H2]	1.00000	0.009	0.018	**Si**	0.248	1.979	ug/l	**2,385**	28 -> 28 Si [H2]
O2	MS/MS	28	44	185 -> 185 Re [O2]	0.99994	0.111	0.176	**Si**	0.220	1.588	ug/l	**3,588**	28 -> 44 Si [O2]
O2	MS/MS	29	45	193 -> 209 Ir [O2]	0.99999	0.003	0.006	**Si**	0.472	2.254	ug/l	**193**	29 -> 45 Si [O2]
O2	MS/MS	31	47	193 -> 209 Ir [O2]	0.99999	0.021	0.003	**P**	0.131	0.130	ug/l	**1,524**	31 -> 47 P [O2]
O2	MS/MS	32	48	193 -> 209 Ir [O2]	0.99998	0.034	0.058	**S**	0.059	1.679	ug/l	**2,461**	32 -> 48 S [O2]
H2	MS/MS	39	39	103 -> 103 Rh [H2]	0.99995	0.086	0.126	**K**	0.114	1.459	ug/l	**22,300**	39 -> 39 K [H2]
O2	MS/MS	39	39	103 -> 103 Rh [O2]	0.99998	0.148	0.169	**K**	0.077	1.141	ug/l	**54,015**	39 -> 39 K [O2]
H2	MS/MS	40	40	103 -> 103 Rh [H2]	0.99999	0.131	0.059	**Ca**	0.019	0.448	ug/l	**33,820**	40 -> 40 Ca [H2]
O2	MS/MS	44	60	185 -> 185 Re [O2]	0.99992	0.007	0.003	**Ca**	0.103	0.496	ug/l	**228**	44 -> 60 Ca [O2]
O2	MS/MS	45	61	193 -> 209 Ir [O2]	0.99992	1.109	0.000	**Sc**	0.0001	0.0000	ug/l	**79,116**	45 -> 61 Sc [O2]
O2	MS/MS	47	63	103 -> 103 Rh [O2]	0.99998	0.014	0.000	**Ti**	0.005	0.0029	ug/l	**5,202**	47 -> 63 Ti [O2]
O2	MS/MS	51	67	103 -> 103 Rh [O2]	0.99990	0.193	0.000	**V**	0.0007	0.0015	ug/l	**70,314**	51 -> 67 V [O2]
O2	MS/MS	52	52	103 -> 103 Rh [O2]	0.99999	0.124	0.015	**Cr**	0.010	0.122	ug/l	**45,600**	52 -> 52 Cr [O2]
O2	MS/MS	55	55	185 -> 185 Re [O2]	0.99975	2.462	0.014	**Mn**	0.0026	0.006	ug/l	**79,828**	55 -> 55 Mn [O2]
H2	MS/MS	56	56	103 -> 103 Rh [H2]	1.00000	0.219	0.023	**Fe**	0.008	0.103	ug/l	**56,549**	56 -> 56 Fe [H2]
O2	MS/MS	59	59	103 -> 103 Rh [O2]	0.99998	0.135	0.001	**Co**	0.0021	0.009	ug/l	**49,393**	59 -> 59 Co [O2]
H2	MS/MS	60	60	103 -> 103 Rh [H2]	0.99991	0.009	0.000	**Ni**	0.018	0.022	ug/l	**2,325**	60 -> 60 Ni [H2]
O2	MS/MS	60	60	103 -> 103 Rh [O2]	0.99992	0.034	0.001	**Ni**	0.0022	0.019	ug/l	**12,476**	60 -> 60 Ni [O2]
O2	MS/MS	63	63	103 -> 103 Rh [O2]	0.99984	0.093	0.003	**Cu**	0.0030	0.028	ug/l	**33,916**	63 -> 63 Cu [O2]
H2	MS/MS	66	66	103 -> 103 Rh [H2]	0.99998	2.379	0.001	**Zn**	0.0002	0.0004	ug/l	**614,717**	66 -> 66 Zn [H2]
H2	MS/MS	71	71	103 -> 103 Rh [H2]	0.99999	0.163	0.000	**Ga**	0.0005	0.0004	ug/l	**41,999**	71 -> 71 Ga [H2]
O2	MS/MS	75	91	193 -> 209 Ir [O2]	0.99989	0.091	0.000	**As**	0.0005	0.0004	ug/l	**6,513**	75 -> 91 As [O2]
H2	MS/MS	78	78	103 -> 103 Rh [H2]	0.99998	0.005	0.000	**Se**	0.0025	0.0010	ug/l	**1,415**	78 -> 78 Se [H2]
O2	MS/MS	78	94	193 -> 209 Ir [O2]	0.99991	0.010	0.000	**Se**	0.010	0.0019	ug/l	**700**	78 -> 94 Se [O2]
H2	MS/MS	85	85	103 -> 103 Rh [H2]	0.99996	0.345	0.002	**Rb**	0.0020	0.007	ug/l	**89,080**	85 -> 85 Rb [H2]
O2	MS/MS	85	85	103 -> 103 Rh [O2]	0.99990	0.293	0.002	**Rb**	0.0015	0.007	ug/l	**106,669**	85 -> 85 Rb [O2]
H2	MS/MS	88	88	103 -> 103 Rh [H2]	0.99999	0.453	0.001	**Sr**	0.0010	0.0020	ug/l	**117,050**	88 -> 88 Sr [H2]
O2	MS/MS	89	105	185 -> 233 Re [O2]	0.99993	2.300	0.000	**Y**	0.0001	0.0000	ug/l	**170,622**	89 -> 105 Y [O2]
O2	MS/MS	90	106	193 -> 209 Ir [O2]	0.99991	0.798	0.000	**Zr**	0.0006	0.0006	ug/l	**56,990**	90 -> 106 Zr [O2]
O2	MS/MS	93	125	193 -> 209 Ir [O2]	1.00000	1.527	0.000	**Nb**	0.0001	0.0000	ug/l	**108,917**	93 -> 125 Nb [O2]
O2	MS/MS	98	130	193 -> 193 Ir [O2]	0.99990	0.306	0.001	**Mo**	0.0011	0.0017	ug/l	**23,514**	98 -> 130 Mo [O2]
H2	MS/MS	107	107	103 -> 103 Rh [H2]	0.99995	0.112	0.000	**Ag**	0.0026	0.0015	ug/l	**28,955**	107 -> 107 Ag [H2]
O2	MS/MS	107	107	103 -> 103 Rh [O2]	0.99999	0.114	0.000	**Ag**	0.0004	0.0015	ug/l	**41,559**	107 -> 107 Ag [O2]
O2	MS/MS	114	114	193 -> 193 Ir [O2]	0.99990	0.258	0.000	**Cd**	0.0005	0.0001	ug/l	**19,808**	114 -> 114 Cd [O2]
O2	MS/MS	118	118	185 -> 185 Re [O2]	0.99991	0.955	0.003	**Sn**	0.0023	0.0032	ug/l	**31,002**	118 -> 118 Sn [O2]
O2	MS/MS	121	121	103 -> 103 Rh [O2]	0.99998	0.032	0.000	**Sb**	0.0017	0.0003	ug/l	**11,805**	121 -> 121 Sb [O2]
O2	MS/MS	121	137	103 -> 103 Rh [O2]	0.99997	0.042	0.000	**Sb**	0.0007	0.0001	ug/l	**15,253**	121 -> 137 Sb [O2]
H2	MS/MS	133	133	185 -> 185 Re [H2]	0.99984	0.384	0.000	**Cs**	0.0002	0.0010	ug/l	**145,882**	133 -> 133 Cs [H2]
O2	MS/MS	133	133	103 -> 103 Rh [O2]	0.99991	0.428	0.000	**Cs**	0.0003	0.0011	ug/l	**155,983**	133 -> 133 Cs [O2]
O2	MS/MS	137	137	185 -> 185 Re [O2]	0.99983	0.424	0.001	**Ba**	0.0016	0.0032	ug/l	**13,739**	137 -> 137 Ba [O2]
O2	MS/MS	139	155	193 -> 193 Ir [O2]	0.99961	0.023	0.000	**La**	0.009	0.0042	ug/l	**1,734**	139 -> 155 La [O2]
O2	MS/MS	140	156	185 -> 233 Re [O2]	0.99993	2.102	0.000	**Ce**	0.0001	0.0001	ug/l	**155,914**	140 -> 156 Ce [O2]
O2	MS/MS	141	157	185 -> 233 Re [O2]	0.99986	2.697	0.000	**Pr**	0.0000	0.0000	ug/l	**200,060**	141 -> 157 Pr [O2]
O2	MS/MS	146	162	185 -> 233 Re [O2]	0.99993	0.450	0.000	**Nd**	0.0002	0.0000	ug/l	**33,397**	146 -> 162 Nd [O2]
O2	MS/MS	147	163	185 -> 233 Re [O2]	0.99998	0.351	0.000	**Sm**	0.0001	0.0000	ug/l	**26,008**	147 -> 163 Sm [O2]
O2	MS/MS	153	153	185 -> 185 Re [O2]	0.99994	1.947	0.000	**Eu**	0.0001	0.0000	ug/l	**63,119**	153 -> 153 Eu [O2]
O2	MS/MS	157	173	185 -> 233 Re [O2]	0.99995	0.368	0.000	**Gd**	0.0001	0.0000	ug/l	**27,305**	157 -> 173 Gd [O2]
O2	MS/MS	159	175	185 -> 233 Re [O2]	0.99999	2.418	0.000	**Tb**	0.0000	0.0000	ug/l	**179,388**	159 -> 175 Tb [O2]
O2	MS/MS	163	179	185 -> 233 Re [O2]	0.99995	0.603	0.000	**Dy**	0.0002	0.0000	ug/l	**44,697**	163 -> 179 Dy [O2]
O2	MS/MS	165	181	193 -> 209 Ir [O2]	0.99998	2.378	0.000	**Ho**	0.0000	0.0000	ug/l	**169,665**	165 -> 181 Ho [O2]
O2	MS/MS	166	182	193 -> 209 Ir [O2]	0.99997	0.774	0.000	**Er**	0.0000	0.0000	ug/l	**55,217**	166 -> 182 Er [O2]
O2	MS/MS	169	185	185 -> 233 Re [O2]	0.99996	1.943	0.000	**Tm**	0.0000	0.0000	ug/l	**144,147**	169 -> 185 Tm [O2]
O2	MS/MS	172	172	193 -> 193 Ir [O2]	0.99994	0.211	0.000	**Yb**	0.0002	0.0000	ug/l	**16,187**	172 -> 172 Yb [O2]
O2	MS/MS	175	191	193 -> 209 Ir [O2]	0.99998	2.038	0.000	**Lu**	0.0000	0.0000	ug/l	**145,422**	175 -> 191 Lu [O2]
O2	MS/MS	178	194	193 -> 209 Ir [O2]	1.00000	0.328	0.000	**Hf**	0.0002	0.0001	ug/l	**23,429**	178 -> 194 Hf [O2]
O2	MS/MS	181	213	103 -> 103 Rh [O2]	0.99996	0.312	0.000	**Ta**	0.0001	0.0000	ug/l	**113,559**	181 -> 213 Ta [O2]
O2	MS/MS	182	214	185 -> 233 Re [O2]	0.99992	0.281	0.000	**W**	0.0004	0.0004	ug/l	**20,879**	182 -> 214 W [O2]
O2	MS/MS	202	202	193 -> 193 Ir [O2]	1.00000	0.097	0.000	**Hg**	0.0024	0.0016	ug/l	**7,504**	202 -> 202 Hg [O2]
H2	MS/MS	205	205	193 -> 193 Ir [H2]	0.99996	0.179	0.000	**Tl**	0.0008	0.0014	ug/l	**52,271**	205 -> 205 Tl [H2]
H2	MS/MS	208	208	193 -> 193 Ir [H2]	0.99994	0.219	0.002	**Pb**	0.0005	0.007	ug/l	**63,621**	208 -> 208 Pb [H2]
O2	MS/MS	208	208	193 -> 193 Ir [O2]	0.99996	0.628	0.005	**Pb**	0.0011	0.008	ug/l	**48,229**	208 -> 208 Pb [O2]
H2	MS/MS	232	232	193 -> 193 Ir [H2]	0.99999	0.157	0.000	**Th**	0.0000	0.0000	ug/l	**45,444**	232 -> 232 Th [H2]
O2	MS/MS	232	248	103 -> 103 Rh [O2]	0.99994	0.057	0.000	**Th**	0.0000	0.0000	ug/l	**20,925**	232 -> 248 Th [O2]
H2	MS/MS	238	238	193 -> 193 Ir [H2]	1.00000	0.159	0.000	**U**	0.0001	0.0000	ug/l	**45,949**	238 -> 238 U [H2]
Stop statistical calculations													
Average									0.0271	0.2226			
Min									0.0000	0.0000			
Max									0.4722	2.2536			
Number									70	70			

C Chromatograms

This section contains the chromatograms of the following samples in this order:

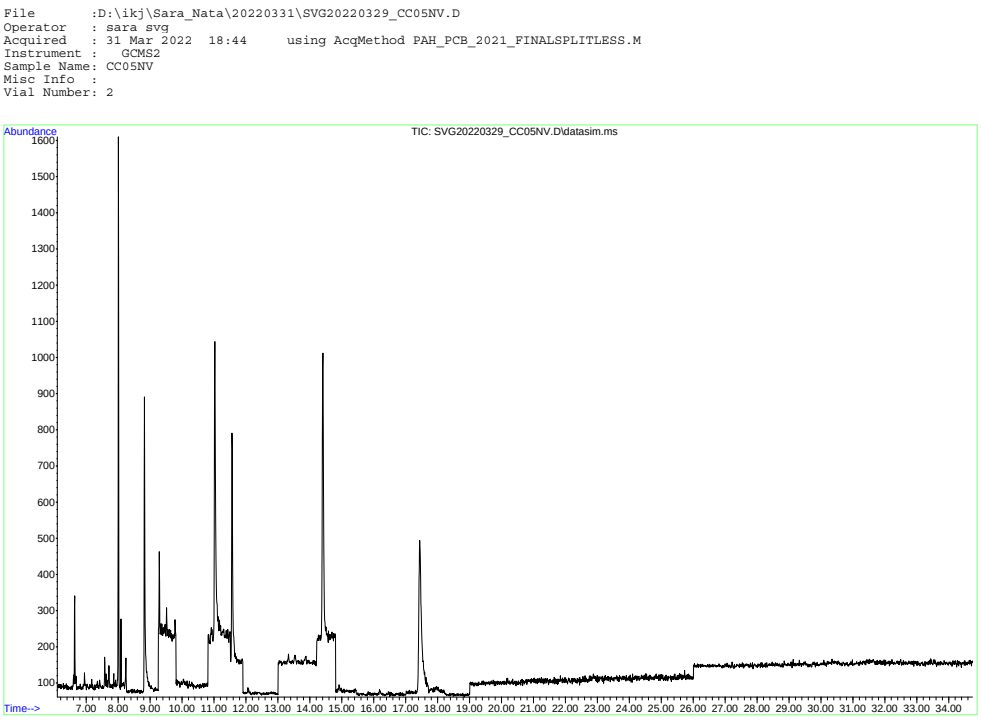

Figure C.1: Chromatogram of calibration curve sample with 0.5 ng/g of ES. The peaks have the following retention times: PCB-28 = 11.627, PCB-52 = 12.059, PCB-101 = 13.532, PCB-118 = 14.915, PCB-138 = 16.182, PCB-153 = 16.182, PCB-180 = 18.198.

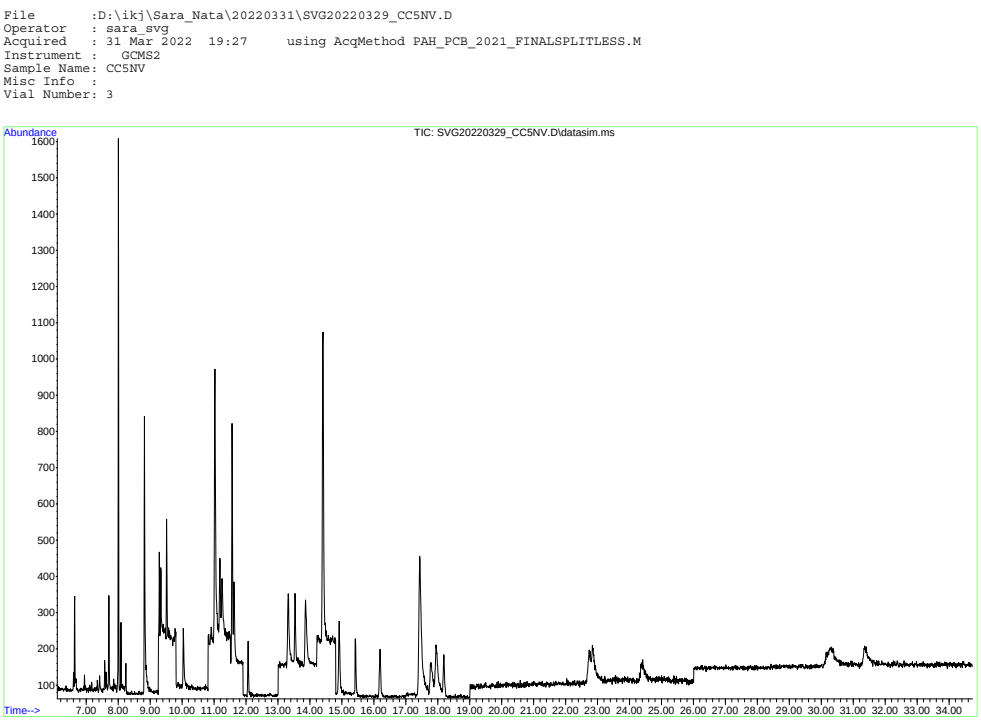

Figure C.2: Chromatogram of calibration curve sample with 5 ng/g of ES. The peaks have the following retention times: PCB-28 = 11.627, PCB-52 = 12.066, PCB-101 = 13.532, PCB-118 = 14.915, PCB-138 = 16.196, PCB-153 = 16.182, PCB-180 = 18.190.

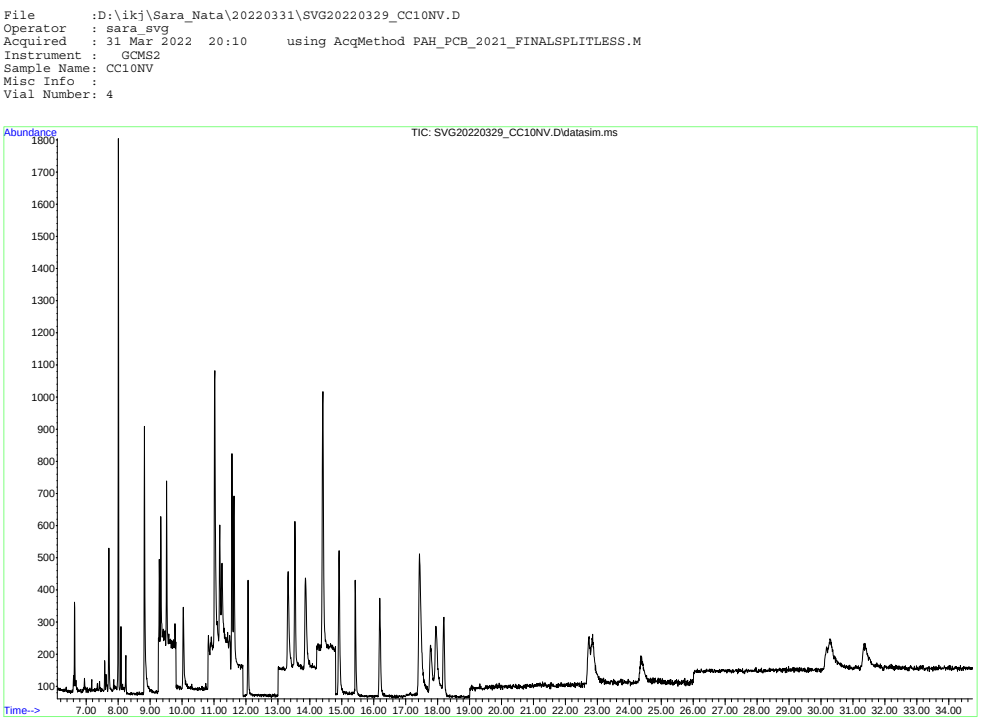

Figure C.3: Chromatogram of calibration curve sample with 10 ng/g of ES. The peaks have the following retention times: PCB-28 = 11.627, PCB-52 = 12.059, PCB-101 = 13.532, PCB-118 = 14.916, PCB-138 = 16.189, PCB-153 = 16.189, PCB-180 = 18.198.

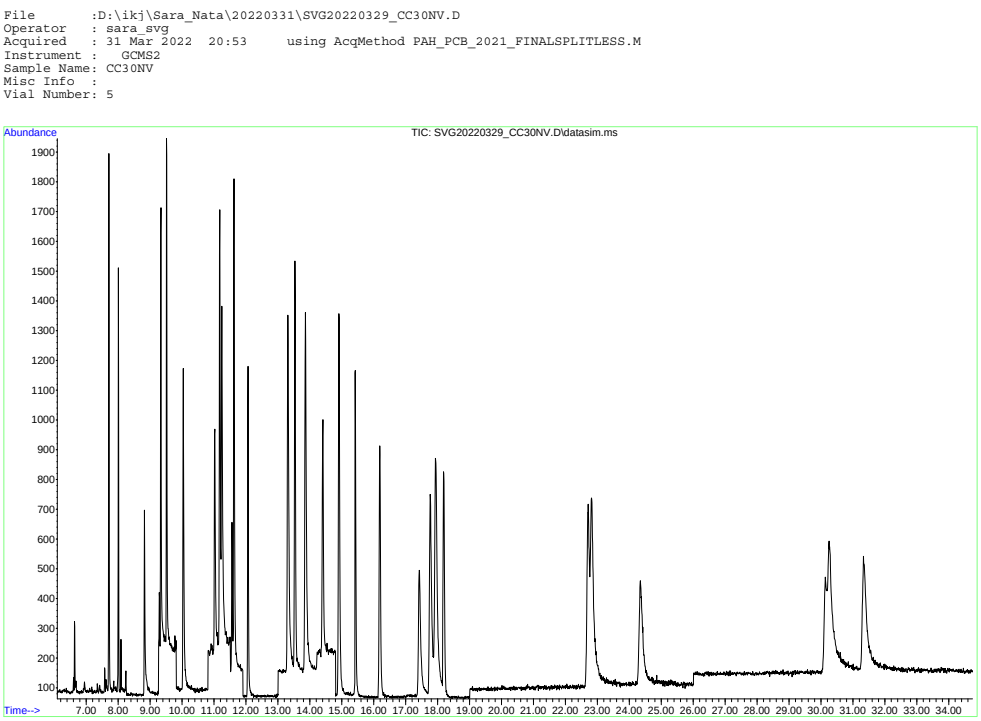

Figure C.4: Chromatogram of calibration curve sample with 30 ng/g of ES. The peaks have the following retention times: PCB-28 = 11.627, PCB-52 = 12.059, PCB-101 = 13.532, PCB-118 = 14.908, PCB-138 = 16.189, PCB-153 = 16.189, PCB-180 = 18.183.

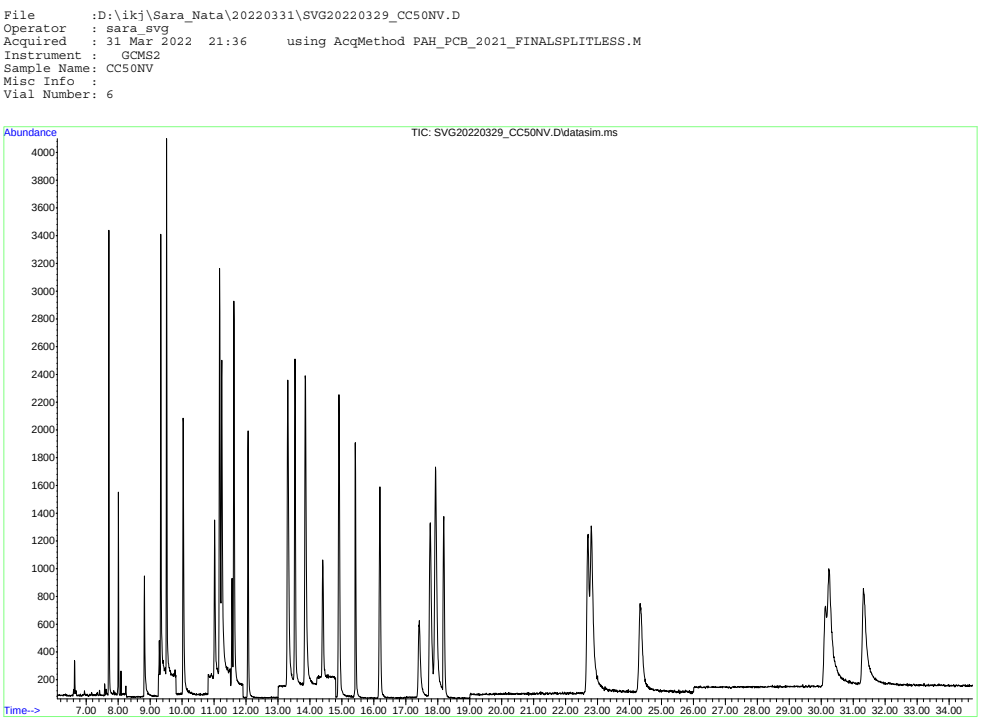

Figure C.5: Chromatogram of calibration curve sample with 50 ng/g of ES. The peaks have the following retention times: PCB-28 = 11.618, PCB-52 = 12.059, PCB-101 = 13.532, PCB-118 = 14.916, PCB-138 = 16.189, PCB-153 = 16.189, PCB-180 = 18.190.

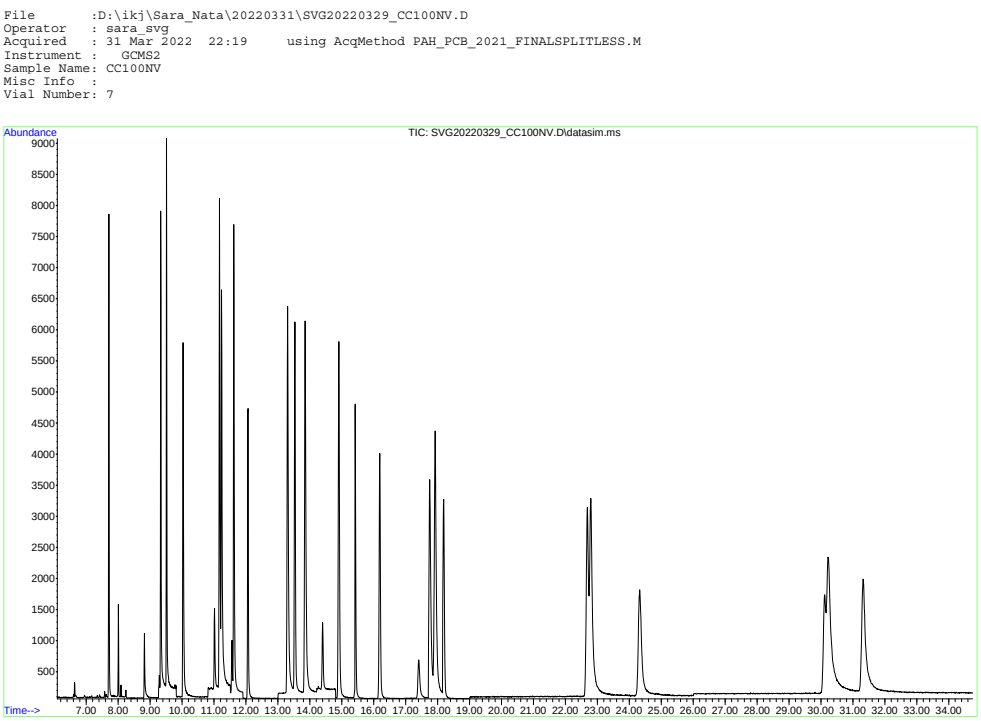

Figure C.6: Chromatogram of calibration curve sample with 100 ng/g of ES. The peaks have the following retention times: PCB-28 = 11.618, PCB-52 = 12.059, PCB-101 = 13.532, PCB-118 = 14.916, PCB-138 = 16.189, PCB-153 = 16.189, PCB-180 = 18.190.

```
File       :D:\ikj\Sara_Nata\20220331\SVG20220329_S1_TW.D
Operator   : sara svg
Acquired   :  1 Apr 2022  10:30     using AcqMethod PAH_PCB_2021_FINALSPLITLESS.M
Instrument :   GCMS2
Sample Name: S1_TW
Misc Info  :
Vial Number: 44
```

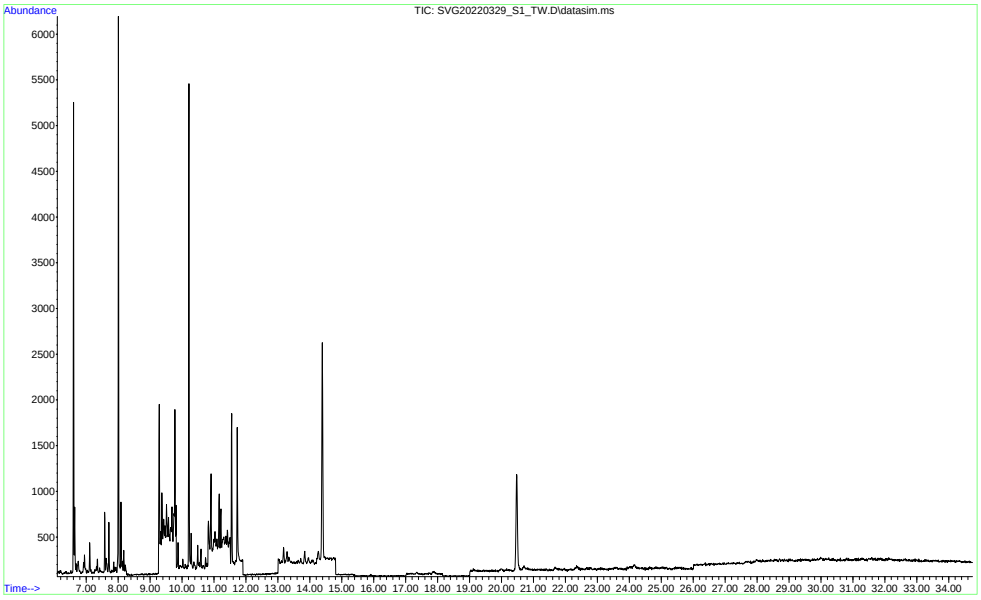

Figure C.7: Chromatogram of sample 1.

```
File       :D:\ikj\Sara_Nata\20220331\SVG20220329_S2_TW.D
Operator   : sara svg
Acquired   :  1 Apr 2022  11:12     using AcqMethod PAH_PCB_2021_FINALSPLITLESS.M
Instrument :   GCMS2
Sample Name: S2_TW
Misc Info  :
Vial Number: 45
```

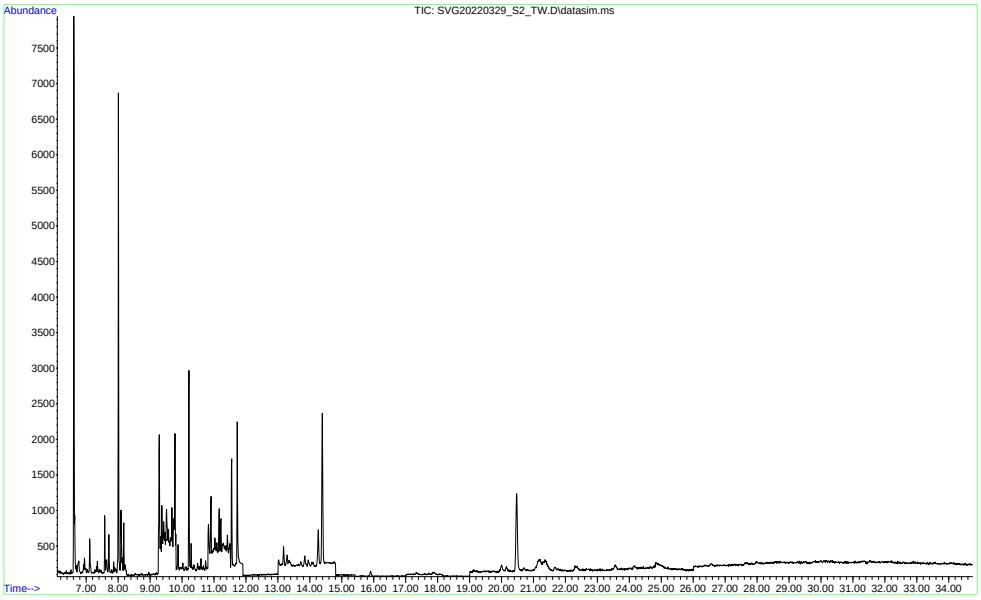

Figure C.8: Chromatogram of sample 2.

```
File       :D:\ikj\Sara_Nata\20220331\SVG20220329_S3_TW.D
Operator   : sara svg
Acquired   :  1 Apr 2022  11:55     using AcqMethod PAH_PCB_2021_FINALSPLITLESS.M
Instrument :   GCMS2
Sample Name: S3_TW
Misc Info  :
Vial Number: 46
```

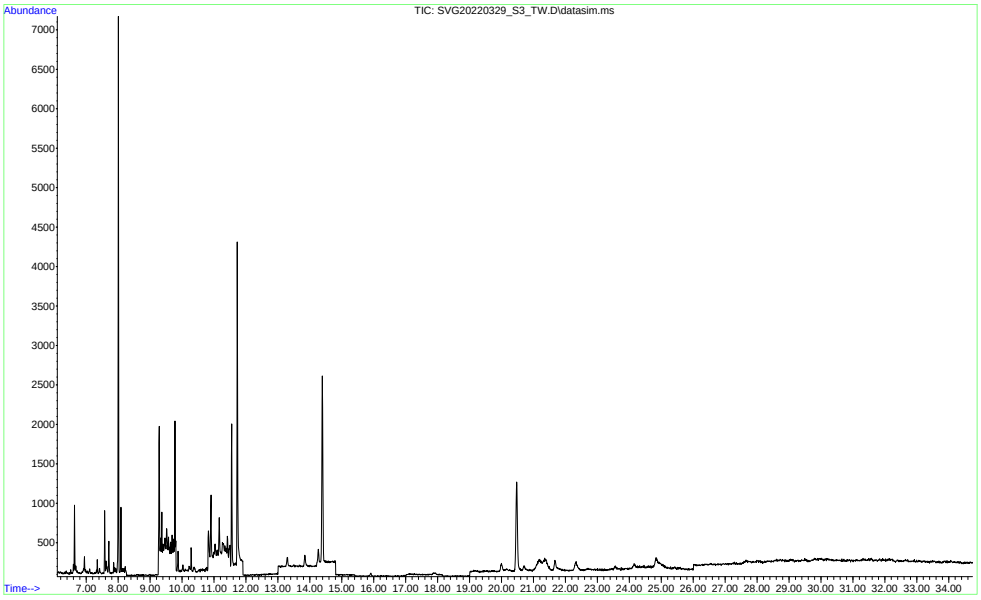

Figure C.9: Chromatogram of sample 3.

```
File       :D:\ikj\Sara_Nata\20220331\SVG20220329_S4_TW.D
Operator   : sara svg
Acquired   :  1 Apr 2022  12:38     using AcqMethod PAH_PCB_2021_FINALSPLITLESS.M
Instrument :   GCMS2
Sample Name: S4_TW
Misc Info  :
Vial Number: 47
```

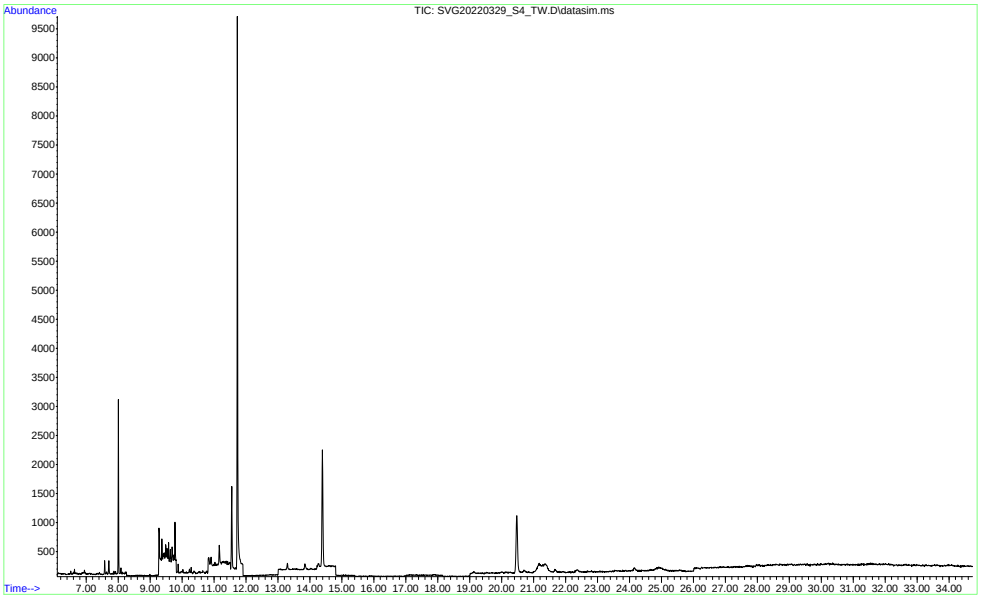

Figure C.10: Chromatogram of sample 4.

```
File       :D:\ikj\Sara_Nata\20220331\SVG20220329_S5_TW.D
Operator   : sara svg
Acquired   :  1 Apr 2022  13:21     using AcqMethod PAH_PCB_2021_FINALSPLITLESS.M
Instrument :   GCMS2
Sample Name: S5_TW
Misc Info  :
Vial Number: 48
```

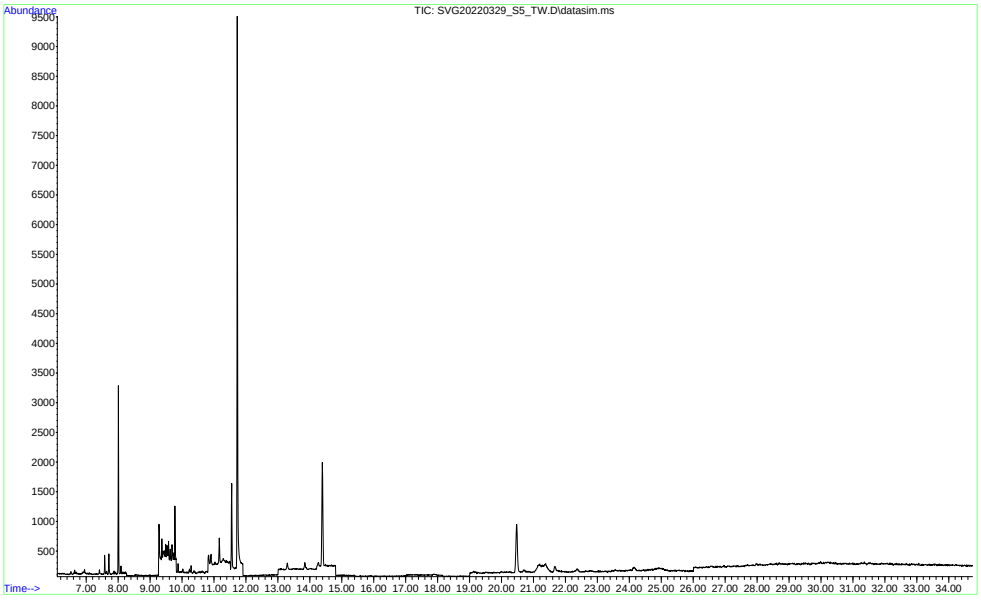

Figure C.11: Chromatogram of sample 5.

```
File       :D:\ikj\Sara_Nata\20220331\SVG20220329_S6_TW.D
Operator   : sara svg
Acquired   :  1 Apr 2022  14:04     using AcqMethod PAH_PCB_2021_FINALSPLITLESS.M
Instrument :   GCMS2
Sample Name: S6_TW
Misc Info  :
Vial Number: 49
```

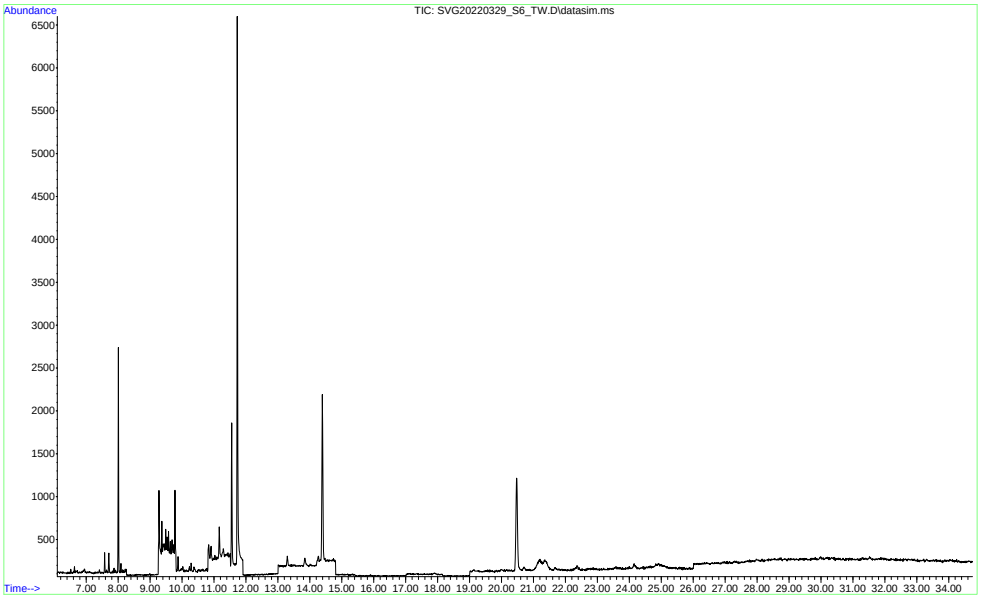

Figure C.12: Chromatogram of sample 6.

```
File       :D:\ikj\Sara_Nata\20220331\SVG20220329_S7_TW.D
Operator   : sara svg
Acquired   :  1 Apr 2022  14:47     using AcqMethod PAH_PCB_2021_FINALSPLITLESS.M
Instrument :   GCMS2
Sample Name: S7_TW
Misc Info  :
Vial Number: 50
```

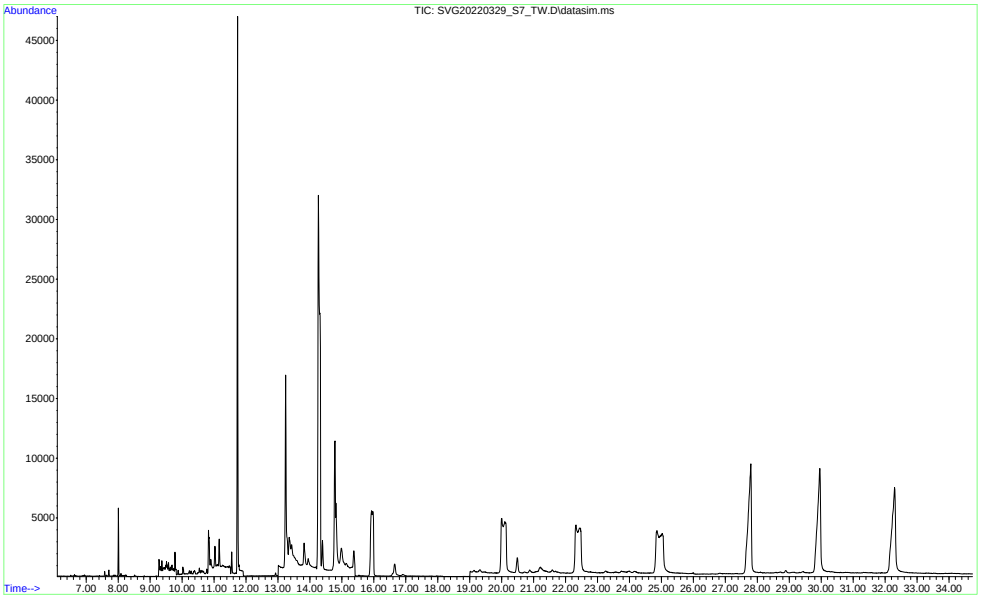

Figure C.13: Chromatogram of sample 7.

```
File       :D:\ikj\Sara_Nata\20220331\SVG20220329_S8_TW.D
Operator   : sara svg
Acquired   :  1 Apr 2022  15:30     using AcqMethod PAH_PCB_2021_FINALSPLITLESS.M
Instrument :   GCMS2
Sample Name: S8_TW
Misc Info  :
Vial Number: 51
```

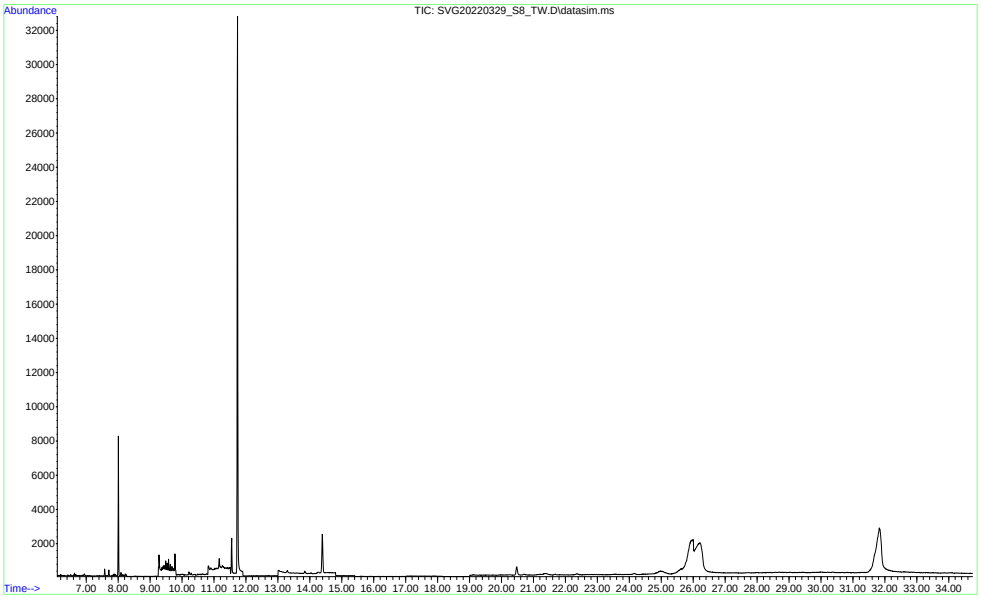

Figure C.14: Chromatogram of sample 8.

```
File       :D:\ikj\Sara_Nata\20220331\SVG20220329_S9_TW.D
Operator   : sara svg
Acquired   :  1 Apr 2022   4:46     using AcqMethod PAH_PCB_2021_FINALSPLITLESS.M
Instrument :   GCMS2
Sample Name: S9_TW
Misc Info  :
Vial Number: 39
```

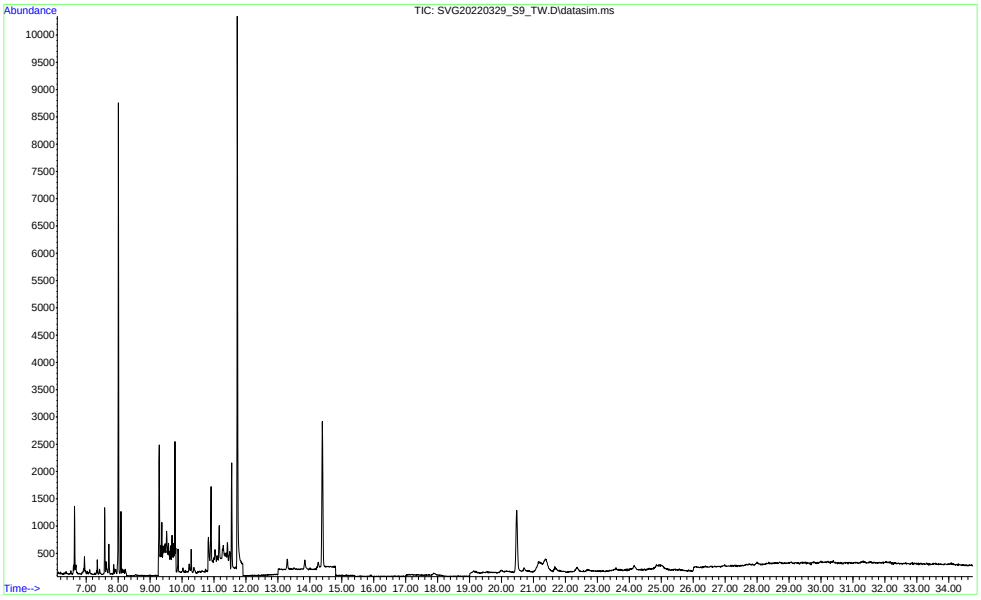

Figure C.15: Chromatogram of sample 9.

```
File       :D:\ikj\Sara_Nata\20220331\SVG20220329_S10_TW.D
Operator   : sara svg
Acquired   :  1 Apr 2022   5:29     using AcqMethod PAH_PCB_2021_FINALSPLITLESS.M
Instrument :   GCMS2
Sample Name: S10_TW
Misc Info  :
Vial Number: 40
```

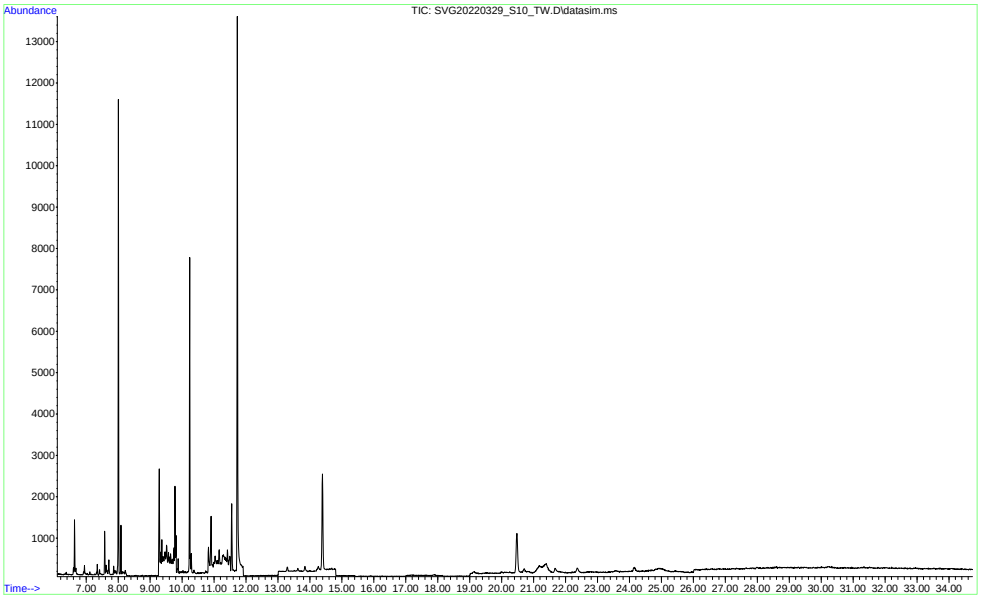

Figure C.16: Chromatogram of sample 10.

```
File       :D:\ikj\Sara_Nata\20220331\SVG20220329_S11_TW.D
Operator   : sara svg
Acquired   :  1 Apr 2022   6:12     using AcqMethod PAH_PCB_2021_FINALSPLITLESS.M
Instrument :   GCMS2
Sample Name: S11_TW
Misc Info  :
Vial Number: 41
```

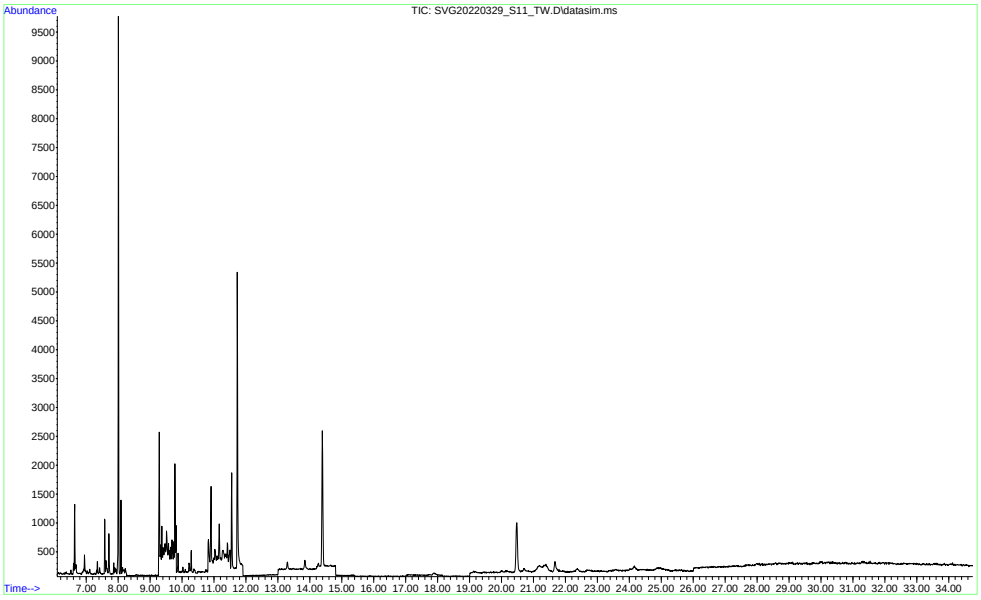

Figure C.17: Chromatogram of sample 11.

```
File       :D:\ikj\Sara_Nata\20220331\SVG20220329_S12_TW.D
Operator   : sara svg
Acquired   :  1 Apr 2022   6:55     using AcqMethod PAH_PCB_2021_FINALSPLITLESS.M
Instrument :   GCMS2
Sample Name: S12_TW
Misc Info  :
Vial Number: 42
```

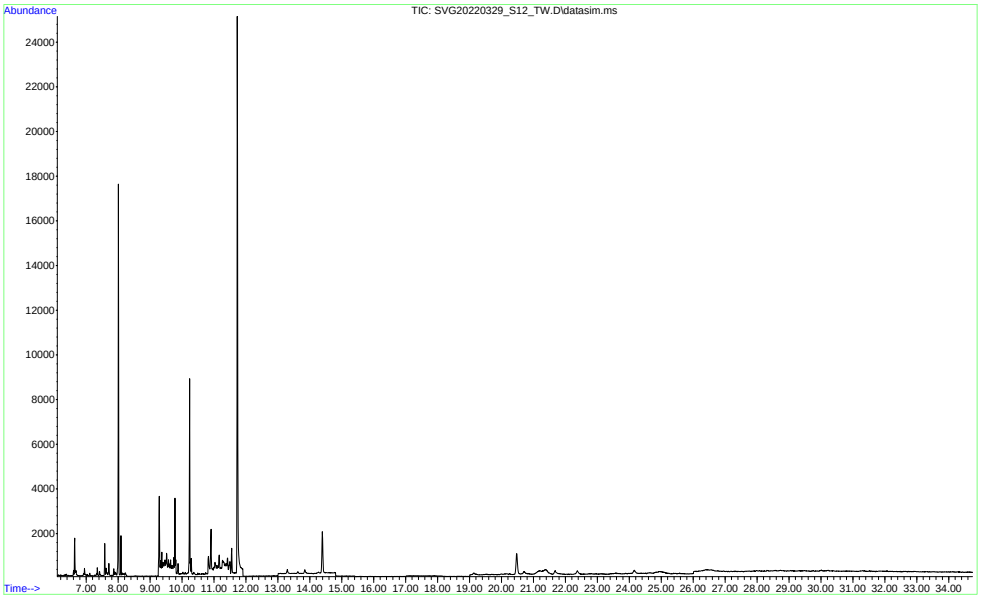

Figure C.18: Chromatogram of sample 12.

D Calibration curves

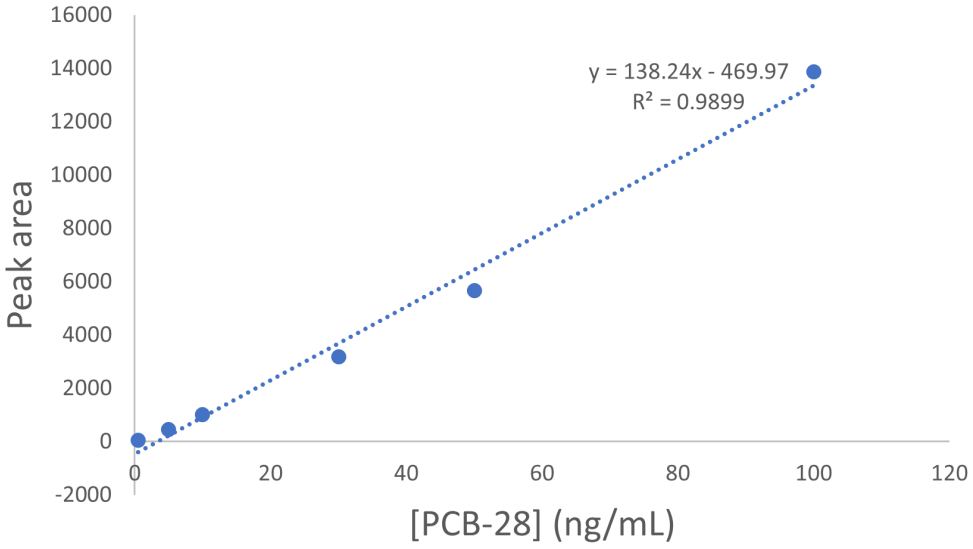

Figure D.1: Calibration curve for PCB-28 plotting concentration against peak area.

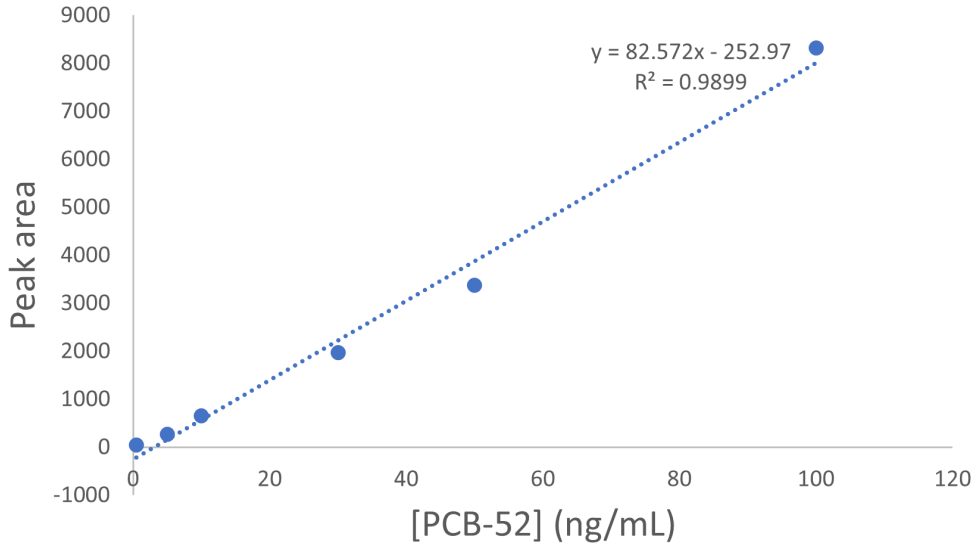

Figure D.2: Calibration curve for PCB-52 plotting concentration against peak area

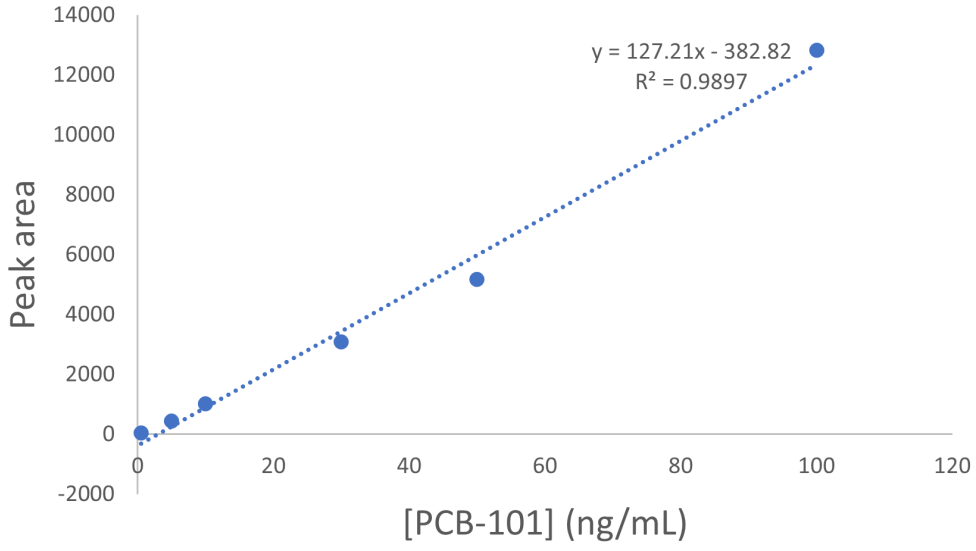

Figure D.3: Calibration curve for PCB-101 plotting concentration against peak area

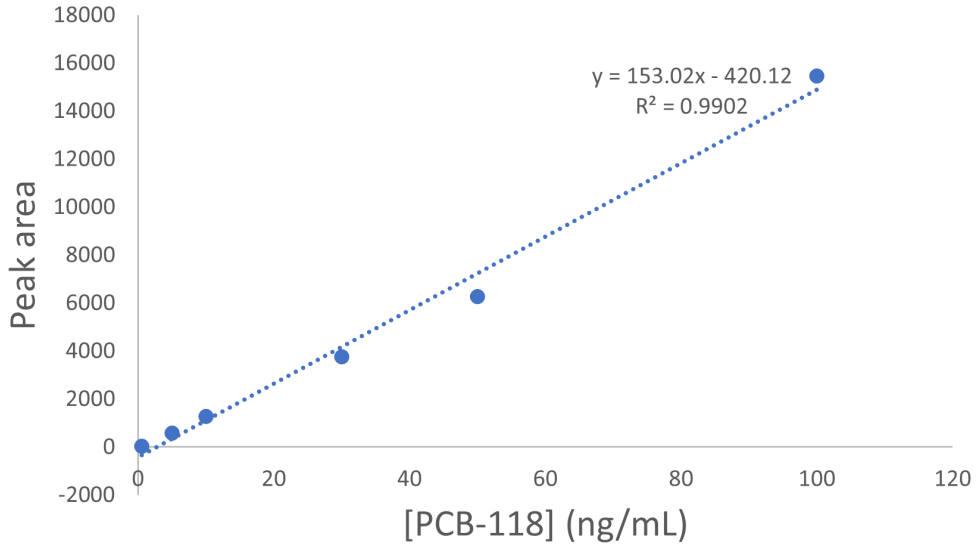

Figure D.4: Calibration curve for PCB-118 plotting concentration against peak area

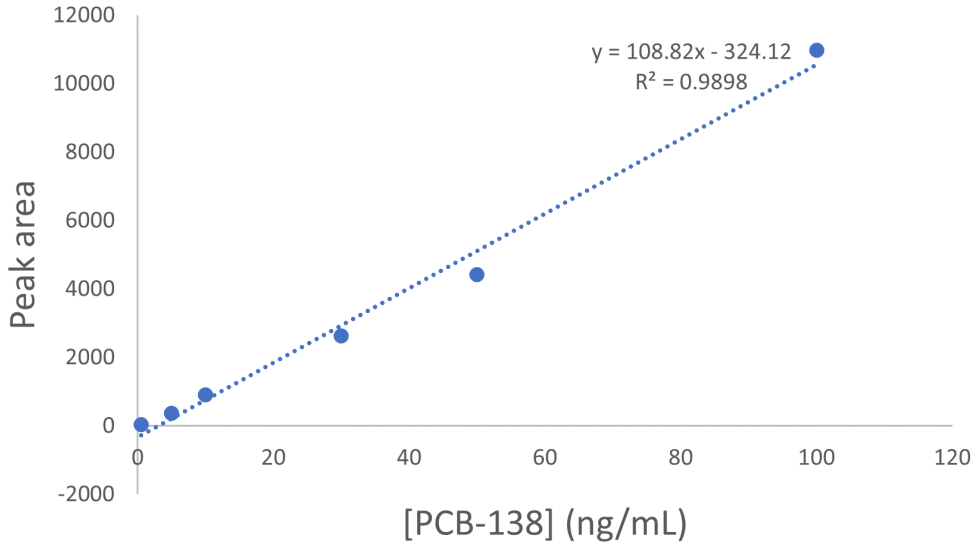

Figure D.5: Calibration curve for PCB-138 plotting concentration against peak area

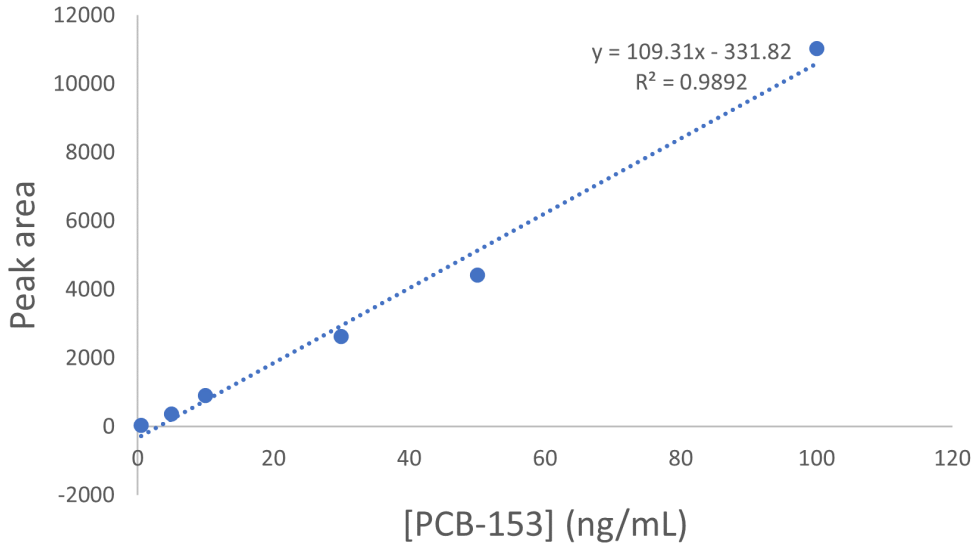

Figure D.6: Calibration curve for PCB-153 plotting concentration against peak area

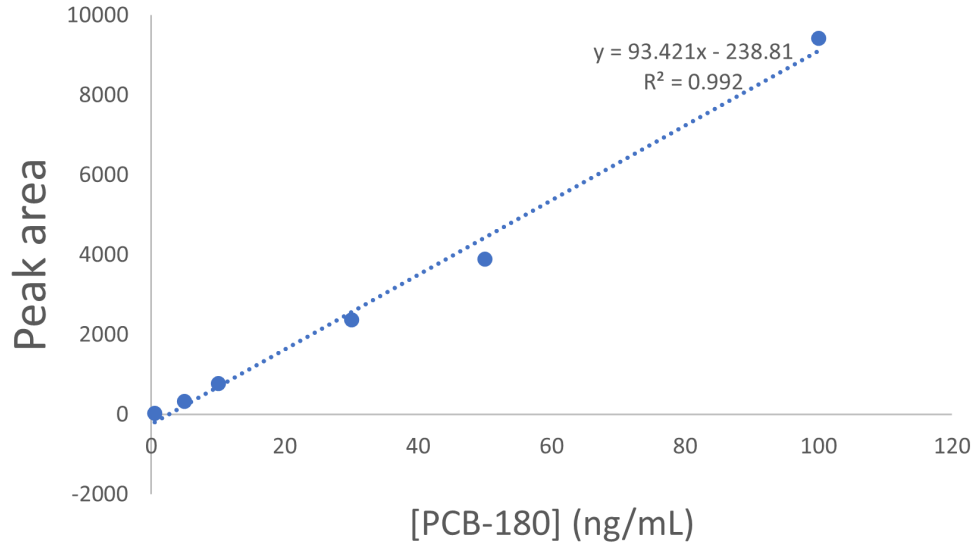

Figure D.7: Calibration curve for PCB-180 plotting concentration against peak area

E Statistical tests

The following tables E.1-E.13 show the results of the Shapiro-Wilks test applied to the groups of data for the selected trace elements. Group A denoted BIA A, group B denotes BIA B, and group K denotes data collected by Kveli in 2015 [106].

Table E.1: Results from the Shapiro-Wilk test applied to the Cd data.

Group	N	Significance	Conclusion
A	33	.974	Normal
B	33	.007	Non-normal
K	11	.774	Normal

Table E.2: Results from the Shapiro-Wilk test applied to the Fe data.

Group	N	Significance	Conclusion
A	34	.238	Normal
B	33	.162	Normal
K	11	.358	Normal

Table E.3: Results from the Shapiro-Wilk test applied to the Pb data.

Group	N	Significance	Conclusion
A	34	.118	Normal
B	33	.386	Normal
K	11	.268	Normal

Table E.4: Results from the Shapiro-Wilk test applied to the As data.

Group	N	Significance	Conclusion
A	34	.285	Normal
B	33	.417	Normal
K	11	.514	Normal

Table E.5: Results from the Shapiro-Wilk test applied to the Al data.

Group	N	Significance	Conclusion
A	34	.200	Normal
B	33	.032	Non-normal
K	11	.118	Normal

Table E.6: Results from the Shapiro-Wilk test applied to the Ti data.

Group	N	Significance	Conclusion
A	34	.491	Normal
B	33	.471	Normal
K	11	.272	Normal

Table E.7: Results from the Shapiro-Wilk test applied to the Li data.

Group	N	Significance	Conclusion
A	34	.164	Normal
B	33	.064	Normal
K	11	.029	Non-normal

Table E.8: Results from the Shapiro-Wilk test applied to the Cu data.

Group	N	Significance	Conclusion
A	33	.432	Normal
B	33	.045	Non-normal
K	11	.459	Normal

Table E.9: Results from the Shapiro-Wilk test applied to the Zn data.

Group	N	Significance	Conclusion
A	33	.468	Normal
B	33	.048	Non-normal
K	11	.516	Normal

Table E.10: Results from the Shapiro-Wilk test applied to the Sn data.

Group	N	Significance	Conclusion
A	33	.983	Normal
B	33	.025	Non-normal
K		.505	Normal

Table E.11: Results from the Shapiro-Wilk test applied to the Co data.

Group	N	Significance	Conclusion
A	34	.500	Normal
B	33	.204	Normal
K	11	.737	Normal

Table E.12: Results from the Shapiro-Wilk test applied to the Mg data.

Group	N	Significance	Conclusion
A	34	.224	Normal
B	33	.003	Non-normal
K	11	.006	Non-normal

Table E.13: Results from the Shapiro-Wilk test applied to the Be data.

Group	N	Significance	Conclusion
A	34	.048	Non-normal
B	33	.082	Normal
K	11	.076	Normal

Thomas Walmsley

Studies of environmental footprint in Brøggerdalen after rocket launching in Ny-Ålesund

NTNU
Norwegian University of
Science and Technology